NASA Technical Memorandum 4312

AD-A241 256
||||| || ||| ||||| || ||||| ||

NASA Aerodynamics Program
Annual Report 1990

DTIC
ELECTE
S OCT 0 2 1991 D
D

Louis J. Williams, Kristin A. Hessenius,
Michael Dudley, Pamela F. Richardson,
George Unger, and Steve Wander

AUGUST 1991

NASA

91-12087
||||| ||||| ||| |||| |||

91 10 1 067

NASA Technical Memorandum 4312

NASA Aerodynamics Program
Annual Report 1990
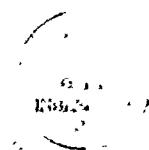
Louis J. Williams, Kristin A. Hessenius,
Michael Dudley, Pamela F. Richardson,
George Unger, and Steve Wander
*NASA Office of Aeronautics,
Exploration and Technology*
Washington, D.C.

Accesion For	
NTIS CRA&I	☑
DTIC TAB	☐
U..a:::ou:·ced	☐
Justification	
By	
Dist.ibution /	
Availability Codes	
Dist	Avail a:.d / or Special
A-1	

NASA

National Aeronautics and
Space Administration

Office of Management

Scientific and Technical
Information Program

1991

Preface

This annual report contains information describing highlighted accomplishments for the past year from NASA's Aerodynamics Research and Technology Program.

The Aerodynamics Research and Technology Program is conducted as part of the response to NASA's charter to: (1) Preserve the role of the United States as a leader in aeronautical science and technology, and the application thereof; (2) Improve the usefulness, performance, speed, safety, and efficiency of aeronautical vehicles; (3) Supervise and direct the scientific study of the problems of flight with a view to their practical solution; and (4) Ensure the timely provision of a proven technology base for a safe, efficient, and environmentally compatible air transportation system.

Last year celebrated the 75th anniversary of the establishment of NASA's predecessor agency, the National Advisory Committee for Aeronautics (NACA). Aerodynamics research was the primary focus of the NACA and continues today as an essential element of NASA's program.

The Aerodynamics Research and Technology Program is managed by the Aerodynamics Division, which is one of five divisions in the Office of Aeronautics, Exploration and Technology in NASA Headquarters. The program includes both fundamental and applied research directed at the full spectrum of aerospace vehicles, from rotorcraft to planetary entry probes. The program encompasses analytical, computational, and experimental efforts conducted using the world's best wind tunnel, computational, and flight research facilities at NASA's Ames and Langley Research Centers.

It is impossible to do justice to the breadth and depth of this comprehensive research program in a single document. The intent of this report is to render a balanced view of NASA's Aerodynamics Program by presenting accomplishment highlights from fiscal year 1990. Other documents and conferences provide a more extensive forum for detailed coverage of a given area. For brevity, we have not included all of the highlights that were submitted for consideration, and we apologize to those whose submissions were not incorporated. We deferred reporting on ongoing activities until a subsequent edition of this document.

This report is arranged in chapters which outline the applied research and technology programs by vehicle type and the fundamental research by subject area. Each chapter includes an introduction by the appropriate Aerodynamics Division program manager, and each accomplishment highlight identifies the responsible researcher at the field centers. To facilitate communication, the address and phone numbers are also listed.

Mr. Louis J. Williams   Dr. Kristin A. Hessenius
Director   Deputy Director

Aerodynamics Division, Code RF
National Aeronautics and Space Administration
Washington, DC 20546

Table of Contents

Chapter Five Numerical Aerodynamics Simulation (NAS) 65

Chapter Six Rotorcraft 83

Chapter Eleven Aerothermodynamics Research and Technology 181

Chapter Twelve Aerobraking 203

List of Figures

Chapter Five   Numerical Aerodynamics Simulation (NAS)...........................65

Chapter Six   Rotorcraft 83

Chapter Seven   Fighter/AttackAircraft 113

Chapter Eight Hypersonic Aerodynamics 129

Chapter Nine Aeroacoustics Research and Technology 145

Chapter Ten High Speed Research 155

Chapter Eleven Aerothermodynamics Research and Technology 181

Chapter Twelve Aerobraking 203

Chapter 1

Subsonic Aerodynamics

The objective of the Subsonic Aerodynamics Program is to provide the technology to improve the performance, efficiency, and economics of future transport aircraft. To accomplish this objective, the program currently is focusing on the areas of hybrid laminar flow technology and the reduction of aerodynamic interference between major aircraft components.

A hybrid laminar flow control system has been installed on the wings of a Boeing 757 transport to investigate the effectiveness, maintainability, and costs of applying this technology to subsonic transports.

Computational design tools are being developed that will specify optimum aerodynamic contours in the vicinity of the juncture of major aircraft components, such as wing/engine nacelle, to minimize interference and reduce drag.

Program Manager: Michael Dudley
                     OAET/RF
                     Washington, DC 20546
                     (202) 453-2795
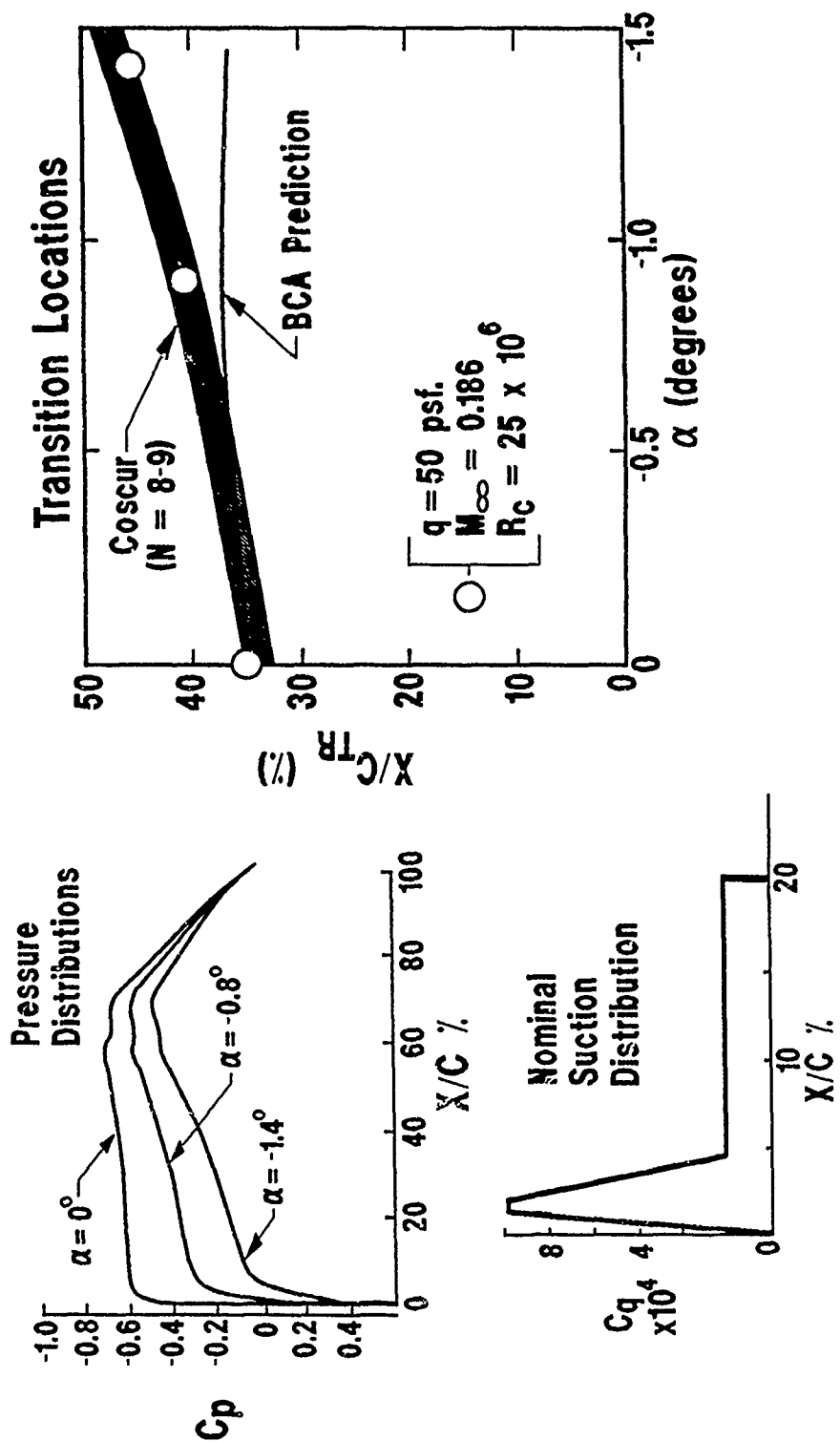
Figures 1-1. 20 Foot Chord HLFC Wind Tunnel Model Test

2

1-1 20-Foot Chord HLFC Wind Tunnel Model Test

Objective. To perform basic research on Hybrid Laminar Flow Control (HLFC) in the controlled wind tunnel environment.

Approach. Under a NASA contract, Boeing Commercial Airplanes has fabricated a 20-foot chord model and installed it in their 5-foot by 8-foot research wind tunnel. Wind tunnel sidewall fairings produce an infinite sweep-wing flow over the model at the test conditions. The model is swept 30° and has a section with a pressure distribution representative of a high subsonic speed, HLFC transport wing with suction to 20% chord. The large chord allows achievement of Reynolds numbers typical of the midspan region of a large transport at unit Reynolds numbers typical of transport cruise conditions.

Accomplishments. The initial tests of the model were performed in the fall of 1989. These tests revealed that Boeing aerodynamic design criteria for boundary layer transition are conservative (i.e., more extensive laminar flow was achieved than predicted). NASA predictions employing curvature effects in stability theory were consistent with observations. The tests also indicated a possible effect of suction hole induced disturbances.

Significance. These tests provided the first confirmation of HLFC at a Reynolds number representative of commercial transports: 25 million. The first data concerning potential suction hole induced disturbances on a swept wing were also obtained.

Status/Plans. The model has been placed in temporary storage, pending provision of additional funds to complete the research test program.

Richard D. Wagner
Flight Applications Division
Langley Research Center
(804) 864-1903
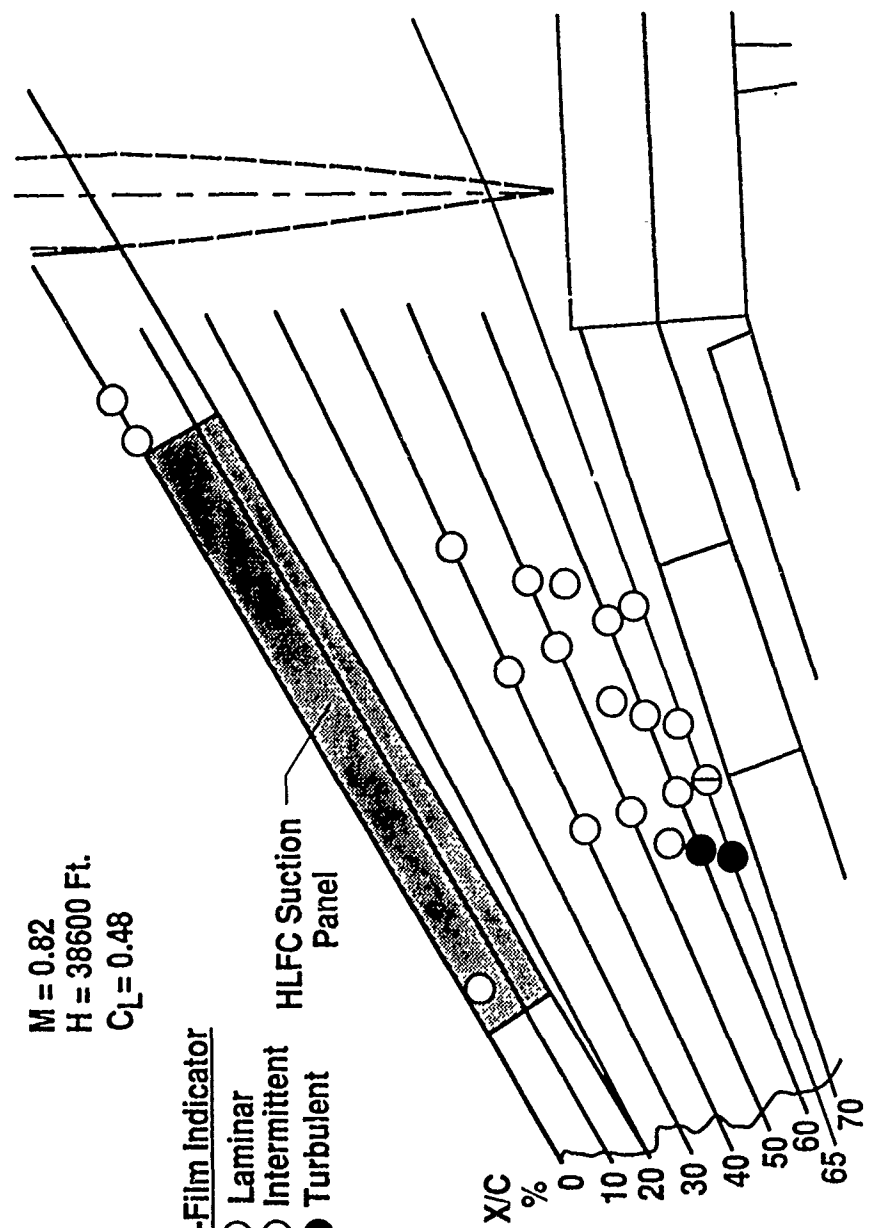
Figure 1-2. High Reynolds Number HLFC Flight Experiment

4

1-2 High Reynolds Number HLFC Flight Experiment

Objective. To evaluate Hybrid Laminar Flow Control (HLFC) for application to commercial and military transports.

Approach. A cooperative program was established between NASA, the U.S. Air Force, and Boeing Commercial Airplanes (BCA) to perform the research. A contract was awarded to BCA in November 1987, with cost to be shared 34% by BCA and 66% by NASA and the U.S. Air Force (the latter equally divided). Under the contract, Boeing was to modify a Boeing 757 aircraft with a partial span HLFC system and flight test the aircraft at cruise conditions up to chord Reynolds number of about 30 million.

Accomplishments. Last year the flight test hardware was fabricated and then installed on the 757 during the first and second quarter of FY 1990. Measurements of the surface smoothness and fairness revealed that the installed HLFC test surfaces surpassed laminar flow surface quality requirements. Flight testing began in March 1990. Extensive laminar flow was attained on the first flight utilizing suction.

Significance. The results of this program have shown that
- practical production-line techniques are adequate for the manufacture of transport aircraft wings to laminar flow surface quality criteria;
- a practical HLFC system (including suction, anti-icing, insect protection, high-lift, and purge systems) can be integrated into the leading edge of a modern transport;
- HLFC can be used to obtain extensive laminar flow on the wing of a high subsonic speed transport.

Status/Plans. Flight testing is continuing. Some operational experience will be gained to assess the in-service operation features of the technology.

Richard D. Wagner
Flight Applications Division
Langley Research Center
(804) 864-1903
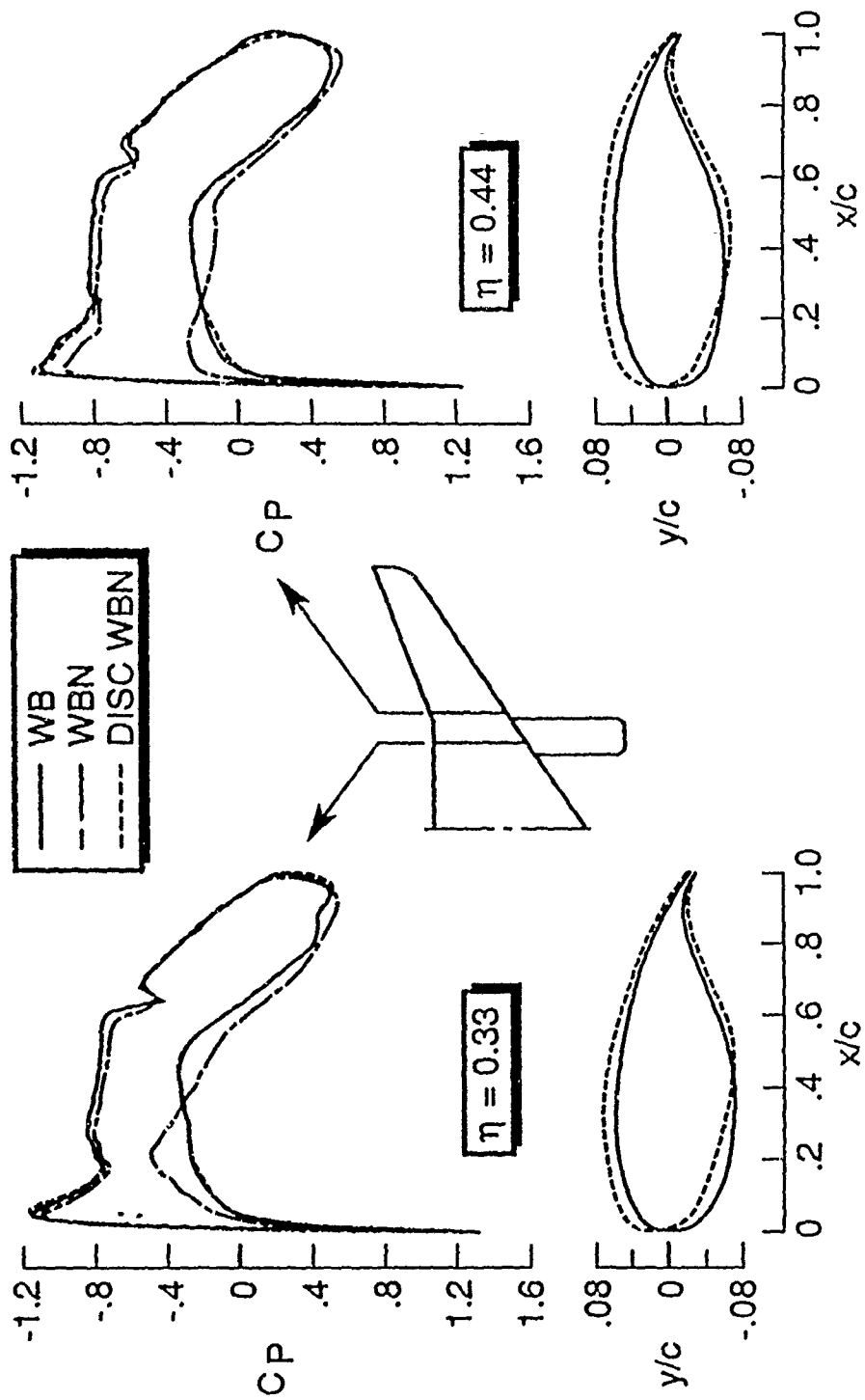
Figure 1-3. Elimination of Nacelle Interference Using the DISC Design Method

6

1-3 Elimination of Nacelle Interference Using the DISC Design Method

Objective. To recontour an existing wing for a military transport-type model to eliminate nacelle interference by use of the Direct Iterative Surface Curvature (DISC) method.

Approach. The DISC design method is a technique that modifies surface curvatures and slopes of an initial geometry so that a target pressure distribution is matched. This method has been coupled with various codes, including the Wing/Body/Pod/Pylon/Winglet (WBPPW) code by Charles Boppe. For this exercise, DISC and the Boppe method were applied to a high-wing transport configuration with nacelles. By specifying wing/body only pressures as target pressure distributions, a new wing shape was obtained for the nacelle-on case.

Because of problems computing the pylon flow with the WBPPW code, the pylon was left out of the solution, and the nacelle shape itself was modified to simulate the pylon effect. When analyzed, the configuration with the new nacelle shape yielded pressures comparable to wind tunnel data. This modified nacelle was used for all design calculations.

Accomplishments. A new wing shape for the High-Wing Transport Model has been computed. To accomplish this, the existing configuration was analyzed with the nacelles off, and the results were used as target pressure distributions. The DISC method was then applied to the existing wing/body with nacelles on to produce a new wing design. When analyzed, the new design with nacelles yields pressures very similar to the original design without nacelles.

The figure shows pressure distributions and airfoils for stations both slightly inboard and slightly outboard of the nacelle centerline at cruise Mach number. Computed pressures are shown for the original wing and body, and the original wing/body with the nacelle added. The DISC curve shows the results for the new wing coupled with the body and nacelle. Thus, the finished wing design when analyzed with nacelles on yields the previous clean wing pressures. This holds true for both design and off-design Mach numbers.

Reproducing nacelle-off pressures with the nacelle-on configuration required moderate twist and thickness changes. The DISC designed airfoil sections each show an increase in twist of approximately 1 percent. The inboard and outboard section thicknesses increase 0.5% and 2.0%, respectively.

Significance. This exercise demonstrates the ability of the DISC design method to eliminate nacelle interference. The ability to design to a specific pressure distribution with nacelles on should help maintain elliptical spanloads for reduced induced drag and limit other undesirable effects of nacelle-on wing performance, such as earlier separation and lift loss.

Status/Plans. Wind tunnel tests are planned to verify the design results. Future plans also include coupling the DISC method with more advanced codes to better define the flow in the wing/nacelle/pylon area.

Leigh Ann Smith
Transonic Aerodynamics Branch
Langley Research Center
(804) 864-2878

Chapter 2

Test Techniques and Instrumentation

Technology is being provided for critical experimental research ... ...lity required to improve the measurement of the fundamental flow properties of fluids and the ..veral ... ..., ...mic performance of aircraft components and configurations. The primary testing errors due to ... ... and support interference for both static and dynamic ...sting are being analyzed and the developmen... ... .strumentation and measurement techniques for real-time, flow diagnosis is being performed with emphasi... ...n nonintrusive method.. These developments occur across the range of conditions from cryogenic to high te...p...t..te and from low subsonic to hypersonic speeds.

Research areas being addressed are (1) heavy gas wind tunnel t sting to operate at high Reynolds numbers, (2) solid-state camera /optical image correction techniques to correlate flight test data of aircraft encounters with wing tip vortices generated by large aircraft; (3) nonintr...ive Rayleigh-Raman multi-point measurements of gas density in hypersonic flow; (4) liquid crystal skin friction sensors capable of high-frequency response in high-speed flows; and (5) non intru. ive infrared thermography of global heat transfer rates or wind tunnel models in hypersonic flow.

Program Manager: . Michael Dudley
OAET/RF
Washington, DC 20546
(202) 453-2795

M = 0.60 C_L = 1.26   RN = 500,000

- - - - - - α = 4.669, γ = 1.40 C_d = .0187
——————— α = 6.236, γ = 1.09 C_d = .0283

Near maximum lift

Laminar bubble

Separation

Cp

X/C
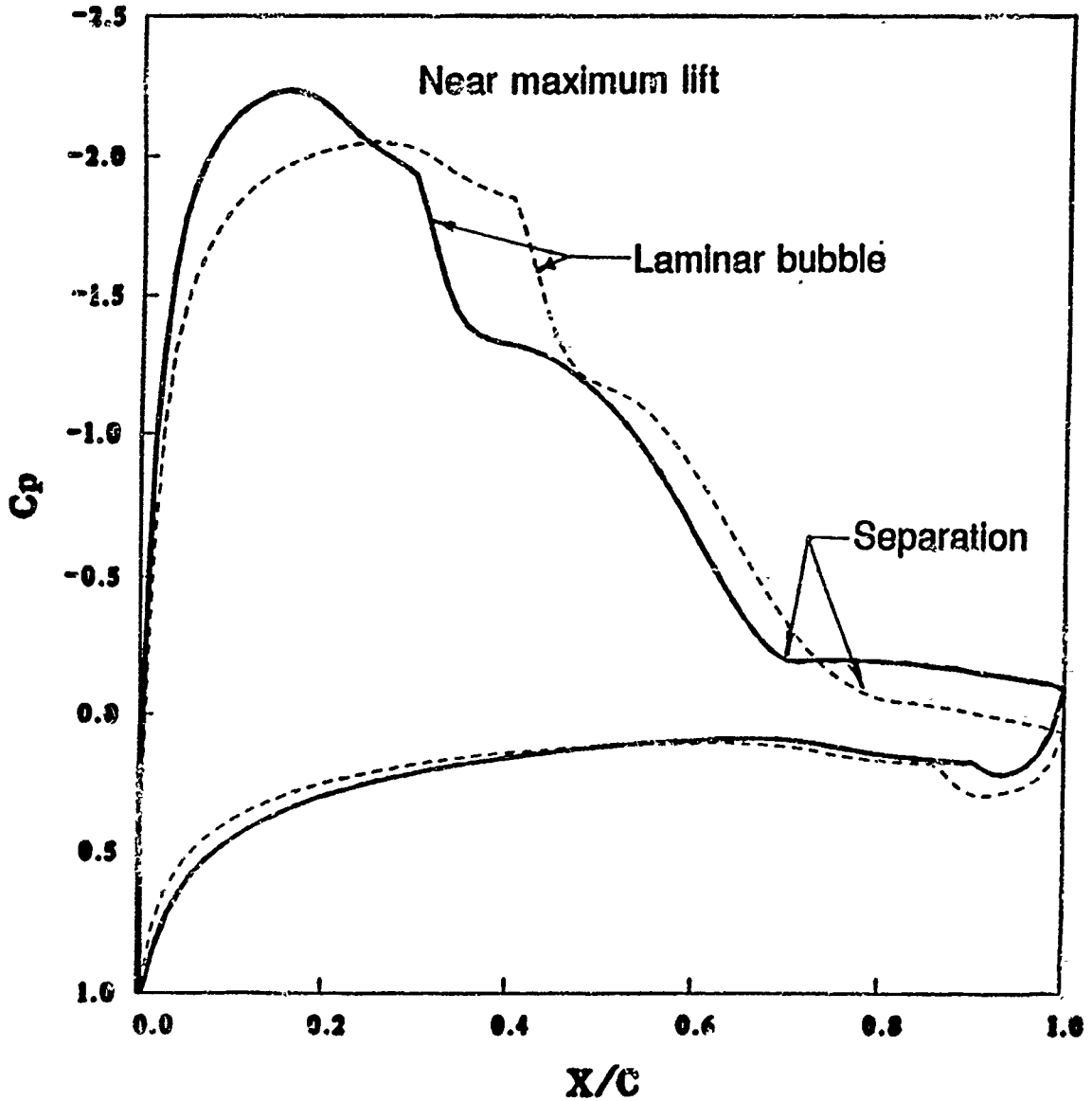
Figure 2-1. Ryan Airfoil ISES Computation, 2-D Analysis High Altitude
Reconnaissance Airplane

10

2-1 Analysis of Heavy Gas Effects on Shock Position

Objective. To determine the accuracy of wind tunnel data obtained from heavy gas testing.

Approach. Euler and Navier-Stokes CFD codes will be used to examine the effects of heavy gas on the aerodynamic characteristics of aircraft components. The project will begin with a study of single-element airfoil sections operated in a heavy gas. This will be followed by studying the effects of heavy gas on multi-element airfoils. Experiment/CFD correlations will be undertaken when wind tunnel data from heavy gas testing are available.

Accomplishments. Initial CFD calculations with Euler and Navier-Stokes codes have been performed to evaluate the effects of gamma on surface pressures for selected airfoil sections and flow conditions. Preliminary calculations have shown that the aerodynamic characteristics of airfoil sections are independent of gas properties for incompressible flow. When the flow is compressible the surface pressure distributions are affected by gamma. In particular, the shock position is a function of gamma but may be correctable by transonic similarity parameters.

Significance. Heavy gas testing will permit a significant increase in Reynolds number compared with that of air. This will give more accurate data for aircraft configurations that operate at high Reynolds numbers.

Status/Plans. The initial phase of the study has been to study the effects of gamma on the aerodynamic characteristics of airfoils. Future computations will be undertaken to determine the effect of heavy gas on boundary layer development in both compressible and incompressible flow for single- and multi-element airfoils.

Raymond M. Hicks, James J. Reuther
Advanced Aerodynamic Concepts Branch
Ames Research Center
(415)604-5656
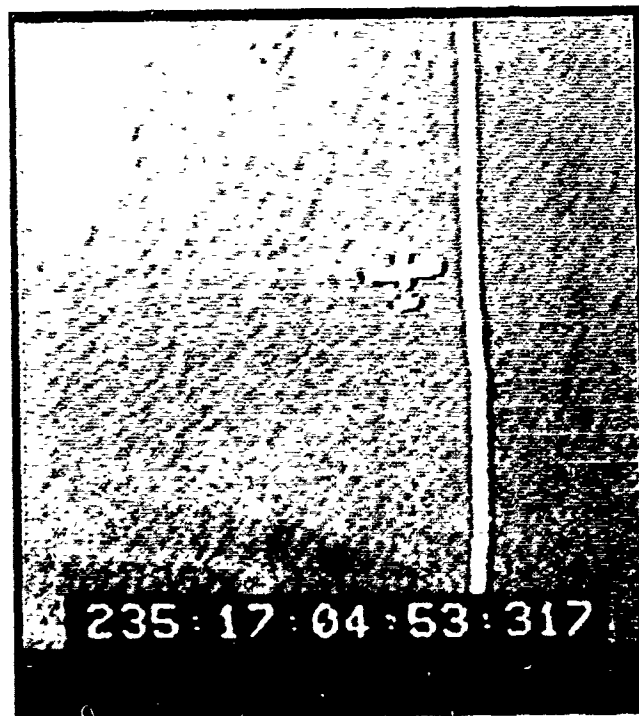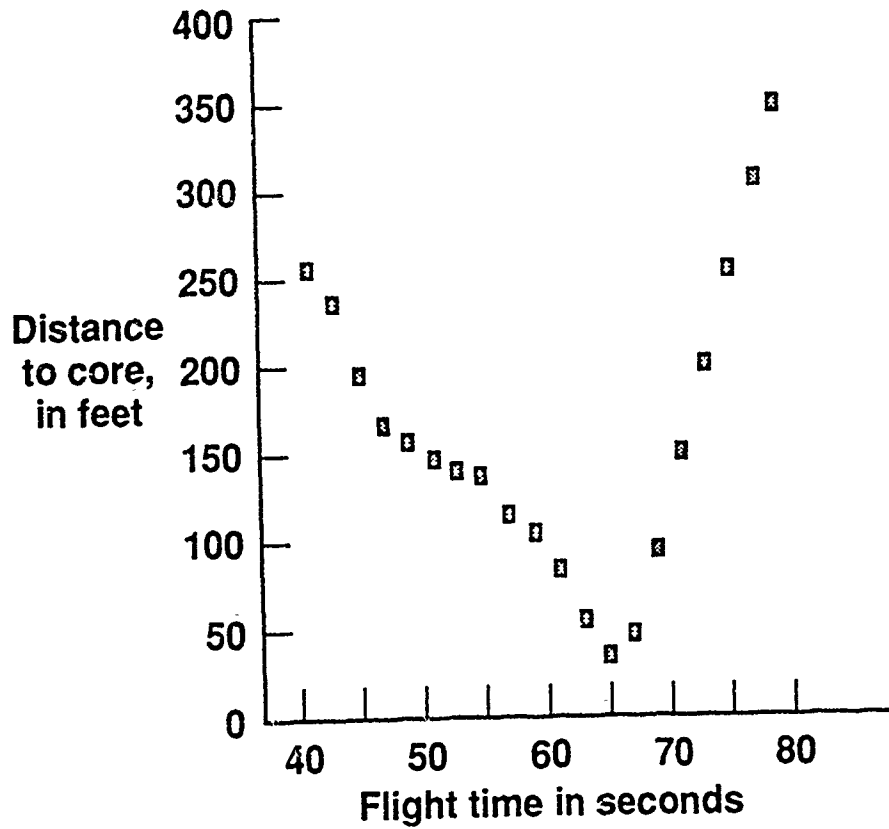
Figure 2-2. Video Support of Vortex Interaction Studies

2-2 Video Support of Vortex Interaction Studies

Objective. To extend the use of solid-state camera systems together with optical element corrections and image acquisition and processing techniques to a flight application for experimentally testing a theoretical model of a proposed on-board, vortex avoidance system. This system would utilize state-of-the-art sensors (e.g., flow direction, accelerometers, and roll rate gyros) to detect the proximity to a wing tip trailing vortex.

Approach. In a collaborative effort with FAA's Langley Engineering Field Office, Wallops Flight Facility, and Langley Research Center, a Lockheed P-3, equipped with wing tip smokers, served to generate wing tip vortices. An instrumented Piper PA-28 aircraft continuously recorded on-board sensor data as the pilot varied the distance to the disturbance. A Beech T-34 aircraft overflying the scene with miniature, wing tip mounted solid-state cameras monitored the encounters. The video frames were time coded to correlate with the on-board sensor data. A typical frame is shown in the photo. The video cameras were calibrated using analytical photogrammetry techniques to recover distortion-free imagery. The wingspan of the probe aircraft on the corrected image data was used to scale the photograph and allow accurate measurements of the distance between the PA-28 and the core. Imagery was recorded at 30 Hz video rates.

Accomplishments. A PC-controlled frame grabber system with customized software was used to acquire and process selected frame sequences for which flight sensor data were available. The system employed experience gained in developing the LaRC Video Model Deformation system. The accompanying plot depicts a typical reduced image data set. Core distance measurements are estimated to have an accuracy of 5%.

Significance. If an effective warning system to detect the proximity of a vortex were found, then the conservative longitudinal landing separation between aircraft required to ensure vortex dissipation could be relaxed with consequent increase of airport traffic throughput.

Status/Plans. The video image data analysis is reported in NASA TM 102691. The reduced data obtained with this technique are merged with flight data and reported in NASA TM 102672, which is in final review. The FAA will use this documentation to decide future action.

Walter L. Snow, Brooks A. Childers
Instrument Application Branch
Langley Research Center
(804) 864-4636

20 INCH MACH 6 TUNNEL

Experiment schematic
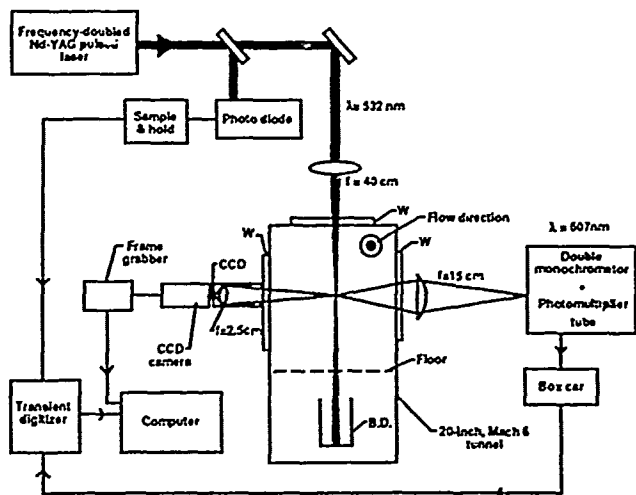
Rayleigh measurements
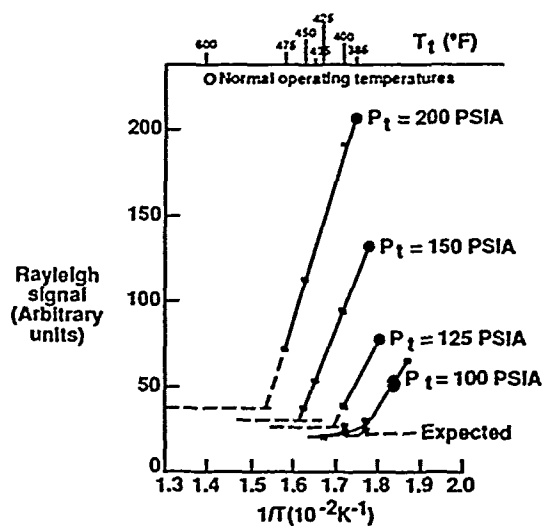
Figure 2-3. Rayleigh-Raman Scattering Measurements

2-3 Local Gas Density Measurements by Rayleigh-Raman Scattering

Objective. To investigate Rayleigh-Raman scattering for nonintrusive, simultaneous, multipoint measurements of local gas density along a line in hypersonic facilities at Langley.

Approach. Raman scattering provides a reliable, well-understood method for measuring both partial specie density and temperature. Rayleigh scattering can provide total gas density measurement in particulate-free gases with substantially enhanced signals over Raman. Since the Langley 20-inch Mach 6 wind tunnel is a relatively particle-free test environment, Rayleigh scattering was considered a high-priority candidate technique for flow field density mapping for CFD validation tests. Raman scattering is also considered a viable candidate for both density and temperature measurement but with reduced signal-to-noise ratio.

Accomplishments. An evaluation system was developed and used for simultaneous, multipoint measurements in the laboratory and at the Langley 20-inch Mach 6 tunnel. The experiment schematic shows the apparatus used in these tests. The Raman free-stream measurements agreed with expectations; however, the Rayleigh signals were too large. Interestingly, the Rayleigh data show clear trends when related to facility operating conditions (the accompanying figure shows one example). These trends suggest that the signals are probably reflecting a free-stream nucleation process and that small increases in local temperature reduce nucleation significantly.

Significance. Instrumentation capable of simultaneous, multipoint measurements of local gas density has been developed. Nucleation interferes with the interpretation; however, single-point measurements based on the Raman approach are possible, and a small increase in local temperature may allow Rayleigh measurements. The data indicate that free-stream nucleation is probably present over most of the operating regime of the 20-inch, Mach 6 facility.

Status/Plans. The results were published in a NASA TMX, also, a follow-up article has been accepted by the AIAA Journal for future publication. Model flow field measurements with the addition of local temperature, an evaluation at the 31-inch Mach 10 facility, and an investigation of UV scattering for planar measurements are planned.

B. Shirinzadeh, M. E. Hillard, R. J. Exton
Measurement Physics Branch
Langley Research Center
(804) 864-4604
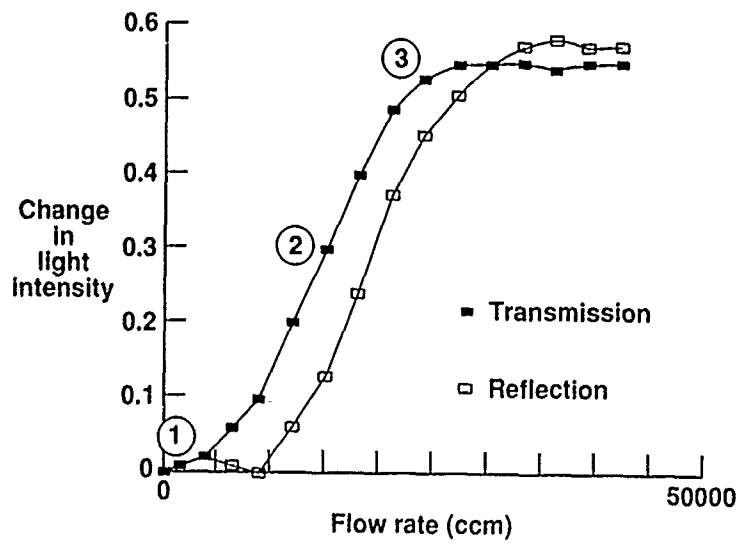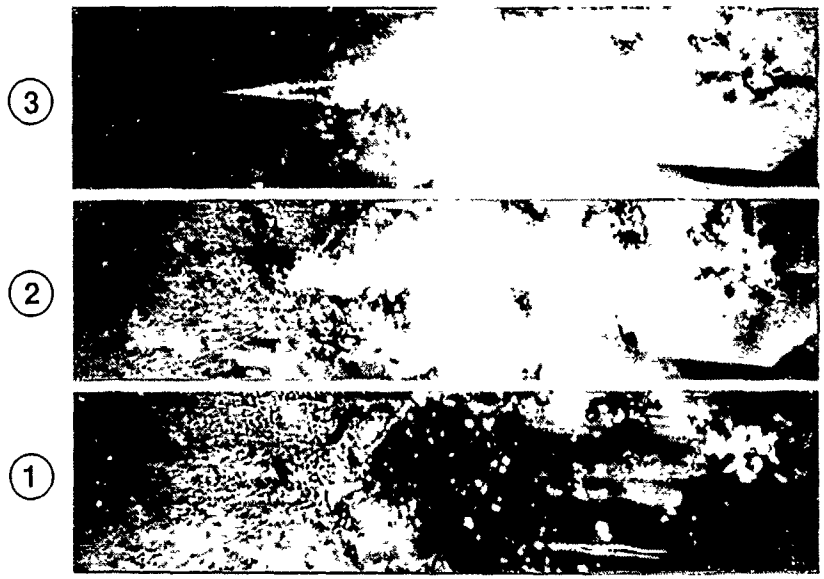
Figure 2-4. Liquid Crystal Skin Friction Sensor

2-4 Liquid Crystal Skin Friction Sensor

Objective. To investigate the use of liquid crystals as a quantitative sensor of aerodynamic phenomena occurring at the solid surface/fluid interface.

Approach. Ferro-electric liquid crystals will be used both as a single element, liquid crystal layer only, and in a dual element, liquid crystal/piezoelectric polymer, sandwich configuration. Polarization rotation in the liquid crystals caused by aerodynamic interaction with the molecular alignment, in the single element case, and with mechanically generated piezoelectric forces in the sandwich configuration, will be studied.

Accomplishments. A thin layer, 1 to 2 microns thick, of ferro-electric liquid crystal material was applied to a glass plate and subjected to a controlled shear flow parallel to the surface. Initial tests with the single element configuration have shown measurable changes in both transmission and reflection of light as a function of flow velocity.

Significance. Because the liquid crystal layer is so thin, it is very robust and should not be blown off in even high speed flows. Secondly, because it has one surface free and a low orientational viscosity, relatively high frequency phenomena should be visible.

Status/Plans. A report of the initial findings is currently awaiting publication. Piezoelectric polymer interactions, free surface dynamics, and structural and birefringent properties with respect to the substrate surface will be examined

Devendra S. Parmar
Electro-Mechanical Instrumentation Branch
Langley Research Center
(804) 864-4744

17

Air m=10 a=15° t=3 sec Re/ft=2.0X10^6
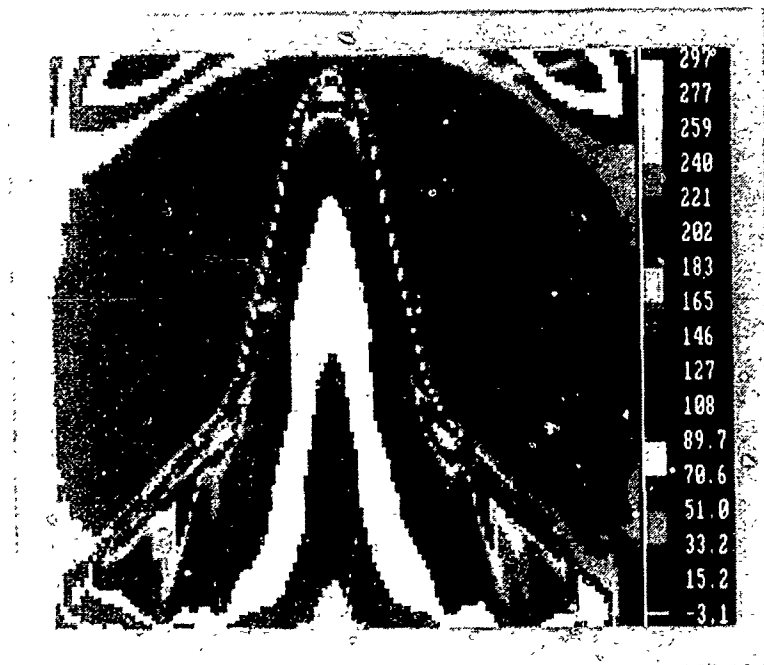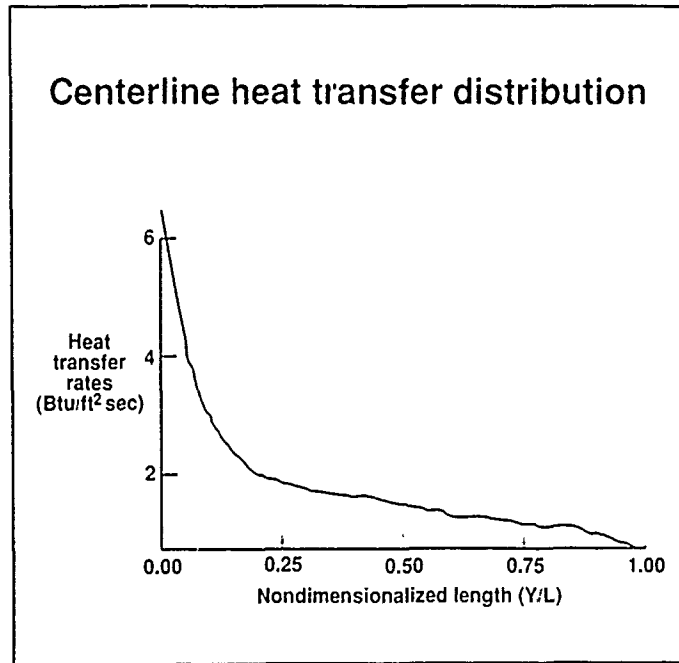
Figure 2-5. Heat Transfer Measurements on a Generic Orbiter Model Using IR Thermography

18

2-5 Evaluation of IR Thermography for Hypersonic Heat Transfer Measurements

Objective. To evaluate infrared (IR) thermography for providing nonintrusive global heat transfer rate measurements on wind tunnel models in hypersonic flow.

Approach. Because of recent advances in infrared technology and image processing, a program was initiated to compare IR with other techniques for providing surface temperature/heat transfer measurements on various aerodynamic geometries at hypersonic speeds. A commercial infrared imaging system with an 8- to 12-micrometer wavelength bandpass and video rates of 6.25 frames per second were used. A PC-based image processing system capable of real-time digitization, processing, and displaying data was used. A zinc selenide window, optimized for 98% transmission in the 8- to 12-micrometer range, was used for optical access to the wind tunnel test section. The spectral emittance of wind tunnel model material was measured using spectrophotometric techniques.

Accomplishments. The temperature measurement accuracy of the system was determined to be ± 3% of reading in the range of 0-1000° F. A series of tests were conducted on a generic orbiter model at the Langley 31-inch Mach 10 wind tunnel for model angles-of-attack of 0, 15, and 30, and Reynolds numbers of 0.5 and 2 million per foot. The IR images provided real-time qualitative heating patterns such as effects of shock/shock interaction on the model. The time variation of measured surface temperature distributions was used for calculating heat transfer rates based on the one-dimensional semi-infinite heat transfer principle.

Significance. Over the past 1-1/2 years, IR thermographic measurement capability has been developed and applied in three hypersonic wind tunnels-31-inch Mach 10, 20-inch Mach 6, and Mach 20 high Reynolds number

helium tunnel. The results from these initial tests demonstrated the capability for providing nonintrusive heat transfer measurements in hypersonic facilities using IR thermography.

Status/Plans. Wind tunnel tests on various aerodynamic geometries will be conducted, and data will be compared with other heat transfer measurement techniques and CFD predictions.

Kamran Daryabeigi, David W. Alderfer
General Research Instrumentation Branch
Gregory M. Buck
Experimental Hypersonics Branch
Langley Research Center
(804) 864-4745

Chapter 3

Transition and Turbulence Physics

The objective of the Transition and Turbulence Physics Program is to develop a fundamental understanding of flow structures relating to transition and turbulence and to incorporate these flow structures into sophisticated flow models for use with computational methods. Extensive efforts are being developed within the program to solve the full Navier-Stokes equations, which include transitioning and turbulent flows. However, the realities of todays supercomputer limitations in terms of memory and speed make it impractical to consider full Navier-Stokes solutions for all but the simplest problems. Practically speaking, research in transition and turbulence modeling with various levels of approximation is providing the bridge for the gap until the computer power is available. The understanding of the physical flow structures of transitioning and turbulence flows is being examined from two directions, computational and experimental. Extensive advancements in test instrumentation being developed within other discipline programs is enhancing transitional and turbulence experimental research. Observations being made experimentally are providing insight to computational efforts for understanding and advanced computational techniques. Likewise, understanding of flow physical behavior is providing mechanisms for advanced experimental research. Both the computational and experimental efforts are vital to the advancement of this technology. The program supports the Center for Turbulence Research which assembles world renowned experts in the field to generate new concepts regarding turbulence. A similar effort is being established for fluid mechanics research emphasizing transition.

Program Manager: Pamela F. Richardson
                   OAET/RF
                   Washington, DC 20546
                   (202) 453-9857
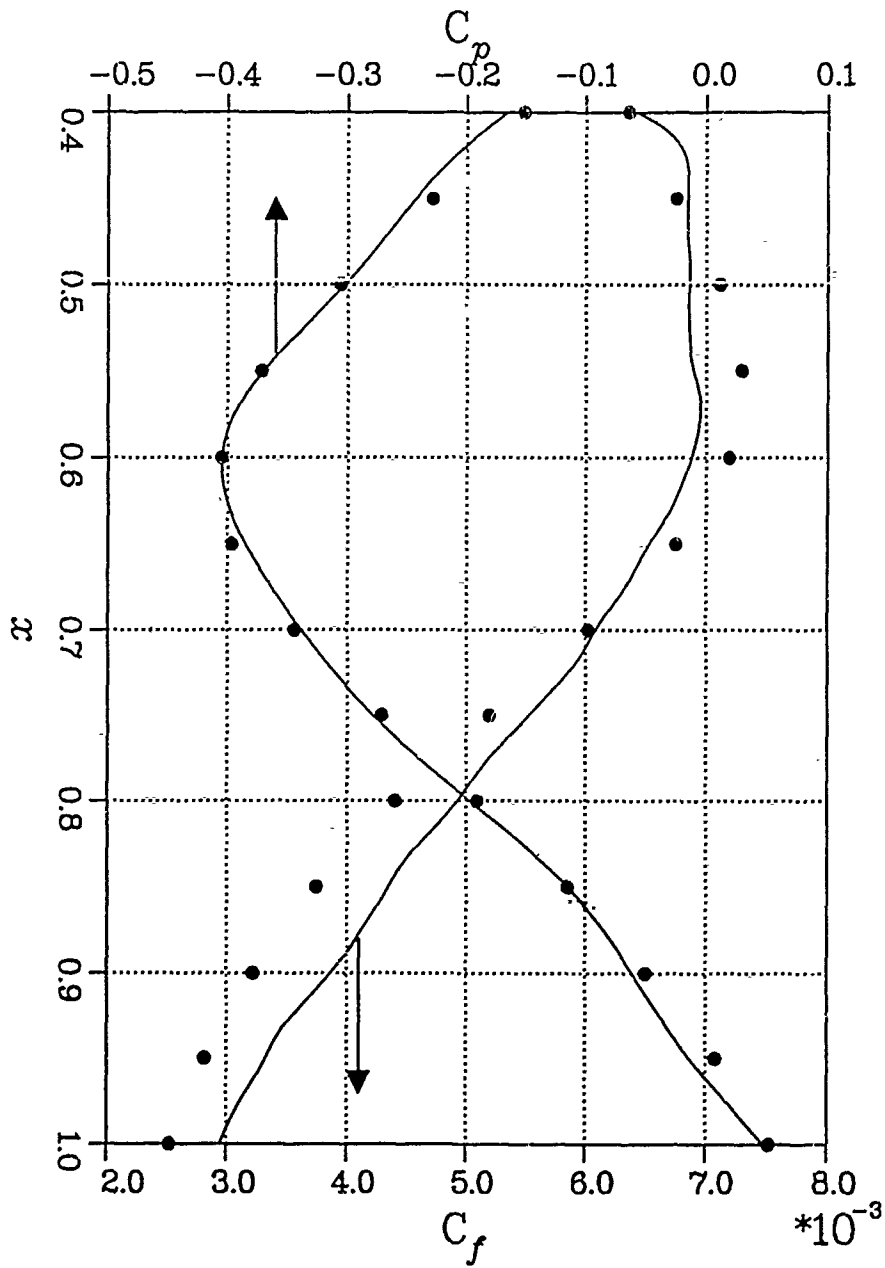
Figure 3-1. Pressure and Skin Friction

3-1 A Turbulent Boundary Layer with Pressure Gradients

Objective. To conduct the direct numerical simulation of a turbulent boundary layer with favorable then adverse pressure gradient, treating the flow as truly spatially developing (earlier studies relied on approximations that required the flow to develop slowly). The flow was designed in collaboration with Drs. Westphal and Watmuff of the Fluid Mechanics Laboratory. Watmuff made the measurements.

Approach. We used a well-established spectral solver of the incompressible, three-dimensional, time-dependent, unaveraged Navier-Stokes equations over a flat plate. It can now treat spatially developing flows thanks to the "fringe" method.

Accomplishments. This is a solution of the full NSE with very-high-quality turbulent inflow conditions and "soft" outflow conditions. Frequent interaction with the experimenters was maintained, and in-depth comparisons are being made leading to high confidence (see figure; 1 experiment; —simulation).

Significance. Boundary layers are interesting only with pressure gradients. This gradient is moderate (the flow does not separate), but it is enough to make the log law fail, as well as the current turbulence models (Cebeci-Smith, Baldwin-Lomax). This gives much food for thought. On the other hand the Reynolds number is too low for a straightforward calibration of the models. We need more ideas in that area.

Status/Plans. We need to obtain smooth statistics, analyze the results in full detail from a theoretical land modeling point of view, publish, and store averaged data and field for CTR use.

P. R. Spalart
Computational Dynamics Branch
Ames Research Center
(415) 604-5867

MEASURED DISTURBANCE GROWTH RATES
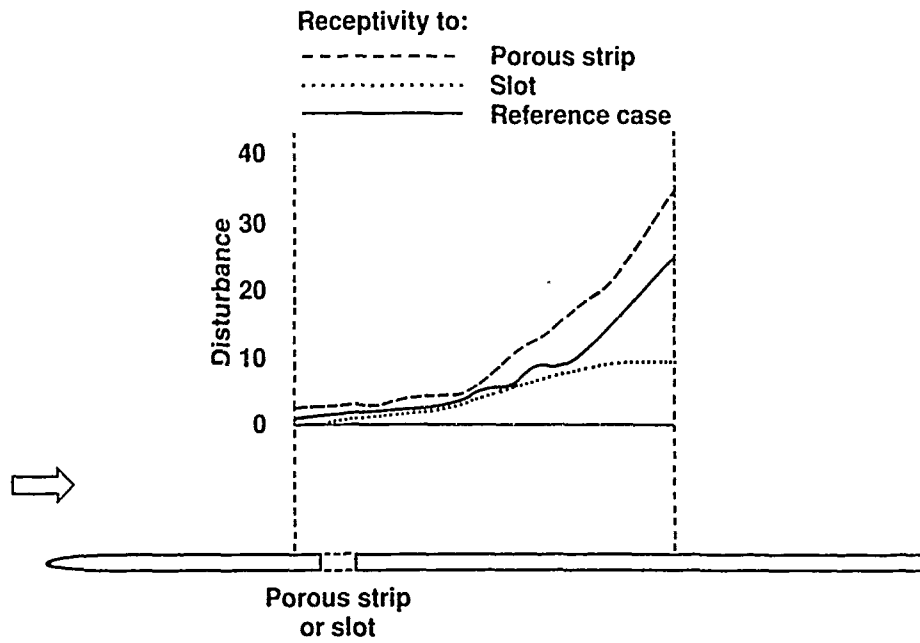
Figure 3-2. Measured Disturbance Growth Rates

24

3-2 Receptivity of Boundary Layers to Acoustic Disturbances

Objective. Transition control is most effective at the early stages before nonlinear amplification effects take hold. The motivation of the present work - a cooperative program between McDonnell Douglas Research Laboratory and Ames Fluid Mechanics Laboratory (FML) - was to examine the earliest stage of transition by measuring the receptivity of laminar boundary layers to external disturbances in FML wind tunnels.

Approach. The experiment was conducted in two low-speed FML wind tunnels on geometrically similar flat plate models. The first experiment was run in the FML Smoke Tunnel, a 40 x 40 cm Blower-Driven Indraft Wind Tunnel and the second in a newly constructed 120-cm x 80-cm Indraft Tunnel powered by the FML Compressor System. Two facilities were used to cover a wider range of Reynolds numbers. In each case, the receptivity to acoustic signal was generated by a speaker radiating into the test section. The flat plate model has an elliptic nose and a screened slot to promote disturbance growth.

Accomplishments. The feasibility of measuring receptivity to acoustic disturbances was demonstrated by decomposing the signal into separate acoustic and instability waves. The receptivity site may be either the leading edge or the slot location, depending on the fineness of the leading-edge fairing.

Significance. Questions always arise concerning the use of wind tunnel facilities for transition research. These preliminary experiments show that carefully designed wind tunnels with conventional aerodynamic lines can be used for analyzing transitional flows.

Status/Plans. Future receptivity studies will focus on other disturbance sources and means of controlling wave growth.

G. Zilliac, S. Davis
Fluid Dynamics Research Laboratory
Ames Research Center
(415) 604-4197
R. Wlezian, D. Parekh,
McDonnell Douglas Research Laboratory
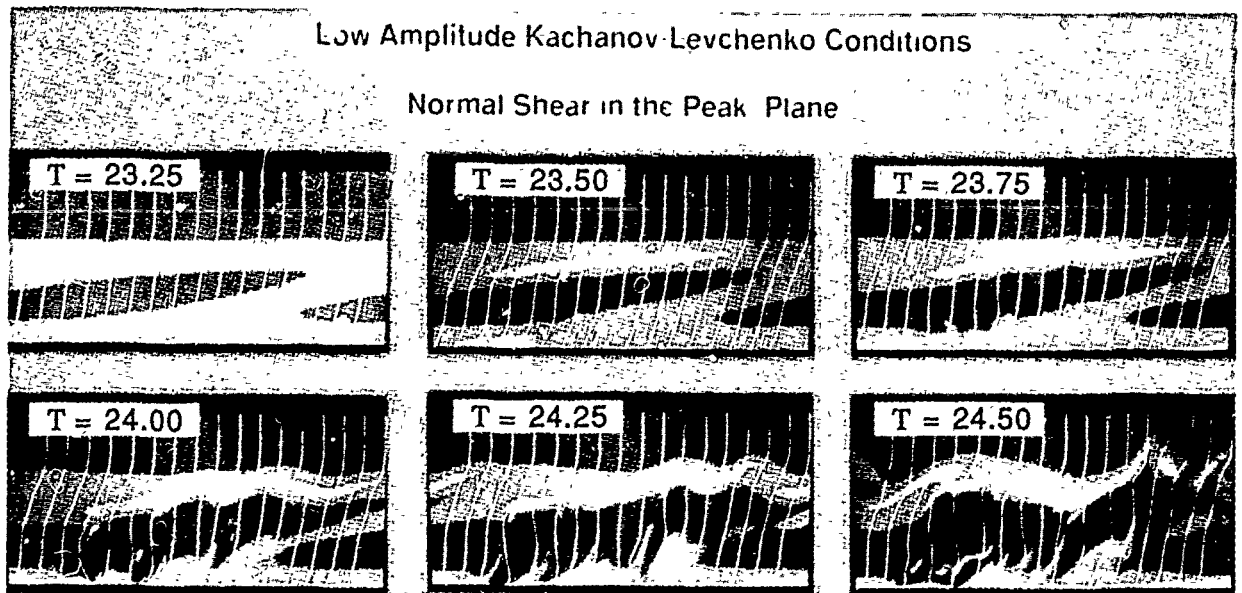
Figure 3-3. Subharmonic Small-Scale Laminar Breakdown

26

3-3 Multiple Paths to Laminar Breakdown in a Boundary Layer

Objective. The classical boundary-layer transition experiments of the early 1960s led to a scenario for the breakdown of laminar flow in which large-scale detached shear layers, induced by a nonlinear instability of the primary Tollmien-Schlichting waves, played a leading role. The roll-up of the detached shear layers is distinguished experimentally by sharp velocity "spikes." However, several recent experiments are indicative of transition to turbulence via laminar breakdown in which spikes are not at all apparent. The present study aimed to clarify the distinctions between these two experimentally observed types of laminar breakdown.

Approach. High resolution numerical simulations have been employed to study the laminar breakdown stage of boundary-layer transition to turbulence. These allow precise control of initial conditions and provide full flow-field information.

Accomplishments. These numerical simulations have focused on laminar breakdowns induced by a subharmonic secondary instability. No experimental evidence yet exists for a subharmonic breakdown driven by detached shear layers; the classical experiments all pertained to the fundamental secondary instability. Nevertheless, some of the numerical simulations have reproduced the classical type of breakdown in which the detached shear layers appear. The laminar breakdown process in other simulations has been characterized by much weaker detached shear layers but with very strong wall bursts. The simulations indicate that the key parameters determining the type of breakdown are the initial amplitudes of the disturbances: large initial amplitudes produce large-scale detached shear layers, whereas small initial amplitudes are associated with small-scale vortices.

Significance. These simulations indicate that subharmonic secondary instabilities (at sufficiently large amplitudes) can also produce "spikes": these are not merely the province of the fundamental instability. They also are indicative of the richness of the boundary-layer transition process, with at least two different, but probably not mutually exclusive, routes to turbulence available.

Status/Plans. A large numerical data base for subharmonic laminar breakdowns is now available. These data can be correlated with nonlinear theories of the transition region and carefully interrogated to reveal the relative importance of vortex stretching, vortex diffusion, and other nonlinear phenomena to laminar breakdown. The data will also be analyzed to determine how the type of laminar breakdown influences the choice of model for the transition zone. The laminar breakdown resulting from yet a third type of secondary instability (called the de-tuned instability) is also worth further study.

T. A. Zang , M. Y. Hussaini,
Theoretical Flow Physics Branch
Langley Research Center
(804) 864-2307
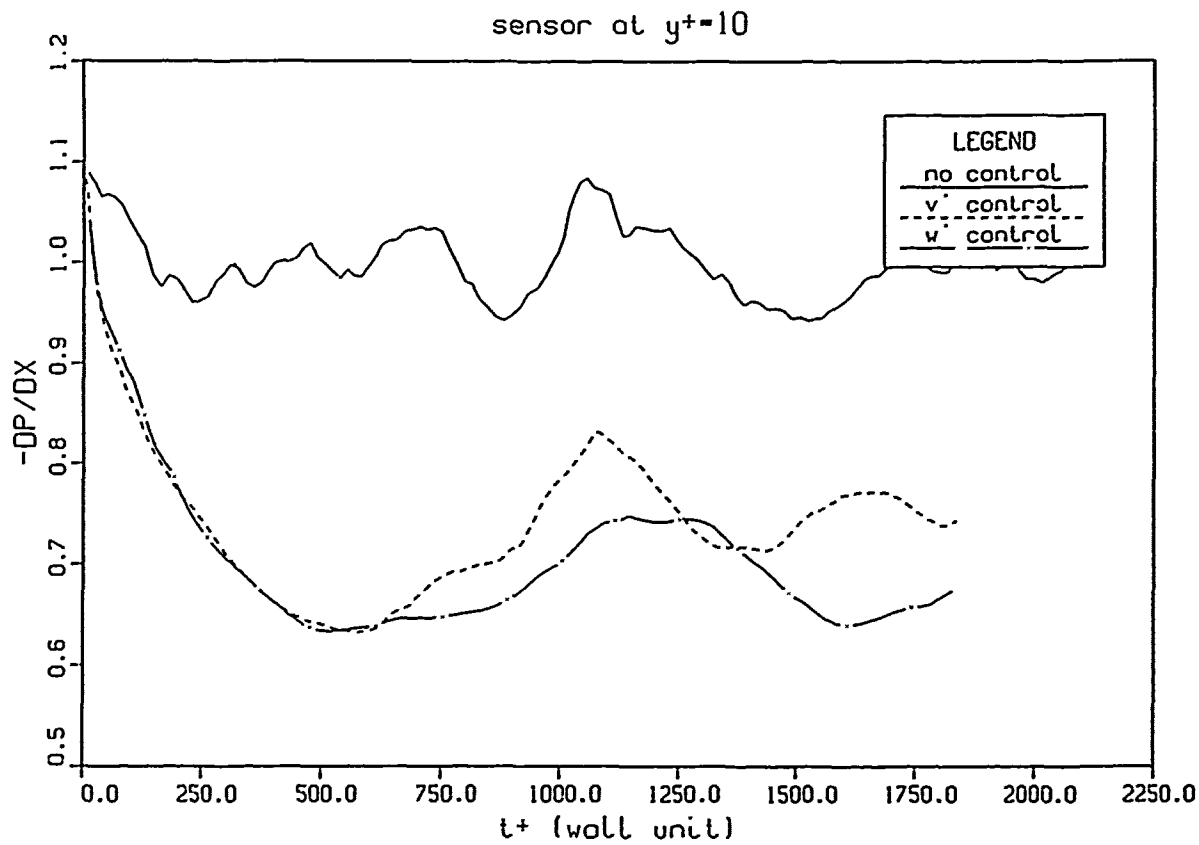
Figure 3-4. History of Pressure Gradient

28

3-4 Active Control of Turbulence Through Direct Numerical Simulations

Objective. To develop an active control strategy for manipulation of turbulent flows to achieve a significant drag reduction.

Approach. Physical algorithms that can suppress the coherent structures in turbulent flows with subsequent net skin-friction reduction was sought. A direct numerical simulation technique was used to explore new concepts for active control of turbulent flows. Owing to the availability of all flow variables at many spatial locations, and the ability to readily alter flow boundary conditions, this numerical simulation technique provides a unique laboratory for testing and design of turbulence control concepts.

Accomplishments. An active control algorithm based on blowing and suction at the wall exactly opposite to the instantaneous wall-normal velocity at a location near the wall was developed. It was found that the optimum location for matching the transpiration velocity was at $y^+=10$. Approximately 20% reduction in skin friction was achieved. It was also found that the same control strategy was able to delay (or suppress) transition to turbulence.

Significance. It is shown that one can achieve a substantial drag reduction by manipulating the large-scale structures in turbulent flows. Although the control strategy developed in this study may not turn out to be feasible for implementation, it will be a guide to developing other control strategies that can be implemented in real applications.

Status/Plans. For practical considerations it is essential that the sensor for the active control be confined to the wall. Control strategies based on the surface variables alone will be explored. Combined active and passive control using a riblet surface will be explored.

H. Choi, J. Kim, P. Moins
Center for Turbulence Research
Ames Research Center
(415) 604-5867

SKIN FRICTION

* * * Computation (Instantaneous)

◇ ◇ ◇ Experiment

White (Turbulent)

Blasius (Laminar)
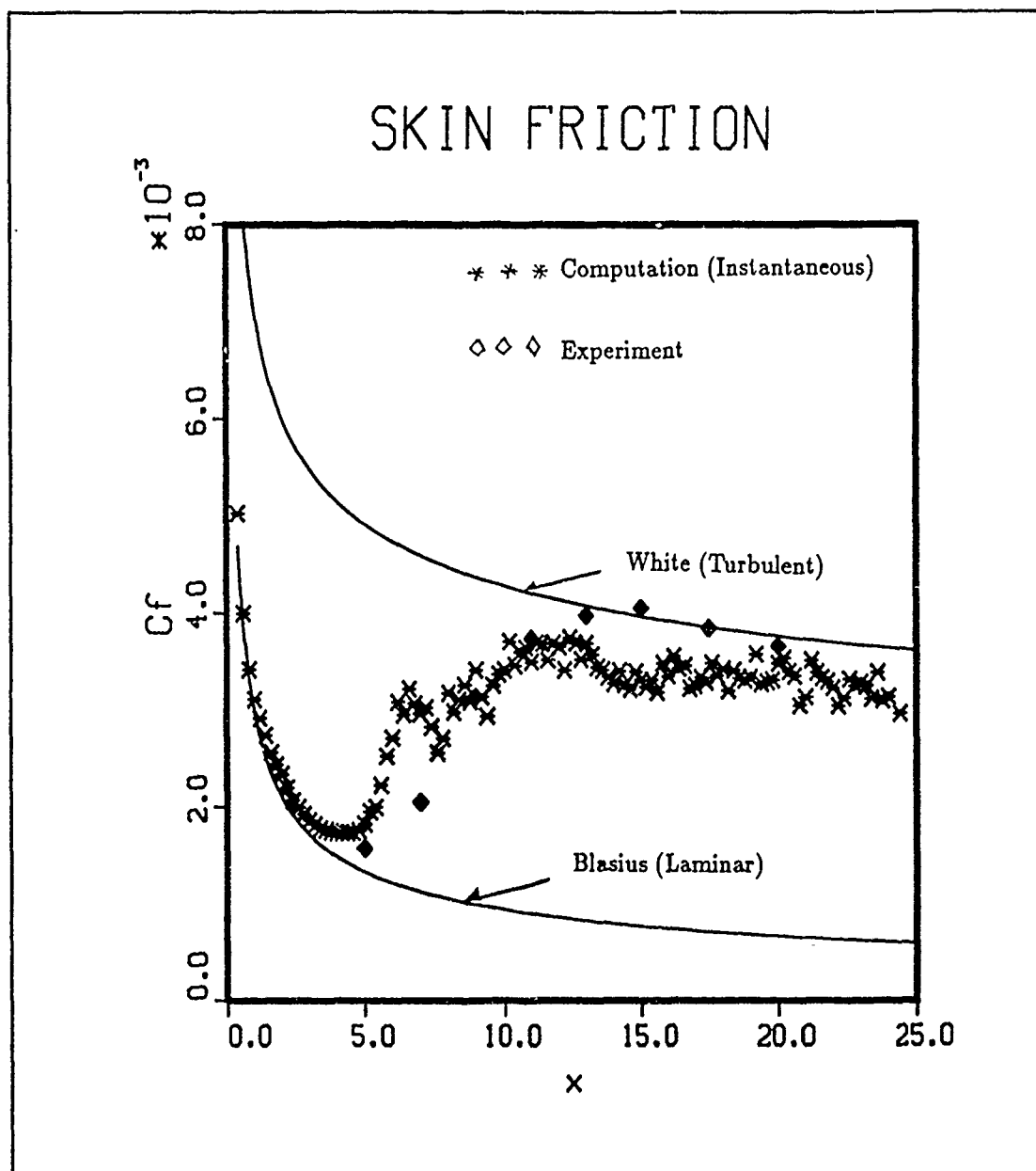
Figure 3-5. Finite-Difference Approach to Direct Simulations of Turbulent/Transitional Flow

30

3-5 Finite-Difference Approach to Direct Simulations of Turbulent/Transitional Flow

Objective. To develop finite-difference methods that can be used for direct simulations of compressible turbulent/transitional flow.

Approach. The principal obstacle to using existing finite-difference schemes for direct simulations of turbulent/transitional flow is the inadequate accuracy levels of such schemes. In this study the use of high-order accurate finite-difference methods was investigated.

Accomplishments. A fifth-order accurate, upwind-biased, finite-difference method has been developed for direct simulations of compressible, turbulent, and transitional flow. The truncation error of this scheme is sufficiently small to yield accurate simulations of turbulent flow with a reasonable number of grid points. A variant of this method that is applicable to incompressible flows has been used to simulate low Reynolds number, fully developed, turbulent channel flow. The results thus obtained compare well with results of earlier simulations using the spectral method. The version of the method for compressible flows has been used to develop a code to compute transitional/turbulent flow over a flat plate. Preliminary results have been obtained on a coarse grid for a freestream Mach number of 0.1 and Reynolds number of 50000.0/inch. The accompanying figure shows the skin friction distribution on the plate as a function of the distance along the plate. The computed data appears "noisy" because they have not been averaged in time. The transition region compares well with the experimental data. The skin friction values in the turbulent region are a little lower than the data. Grid refinement studies indicate that a computation on a finer grid will yield the right distribution of skin friction.

Significance. To date the most successful direct simulations have been performed with spectral methods because of the very high accuracies that these methods possess. However, spectral methods are difficult to use for complex geometries. The high-order accurate finite-difference method developed in this study can, with modifications, be used in a straightforward manner for complex geometries. In addition, the direct simulation of transition on a flat plate being attempted in this study represents a first-of-a-kind effort in CFD.

Status/Plans. The flat-plate computation is being performed on a more refined mesh with 16.8 million grid points.

Man Mohan Rai, Parviz Moin
Fluid Dynamics Division
Ames Research Center
(415) 604-4499
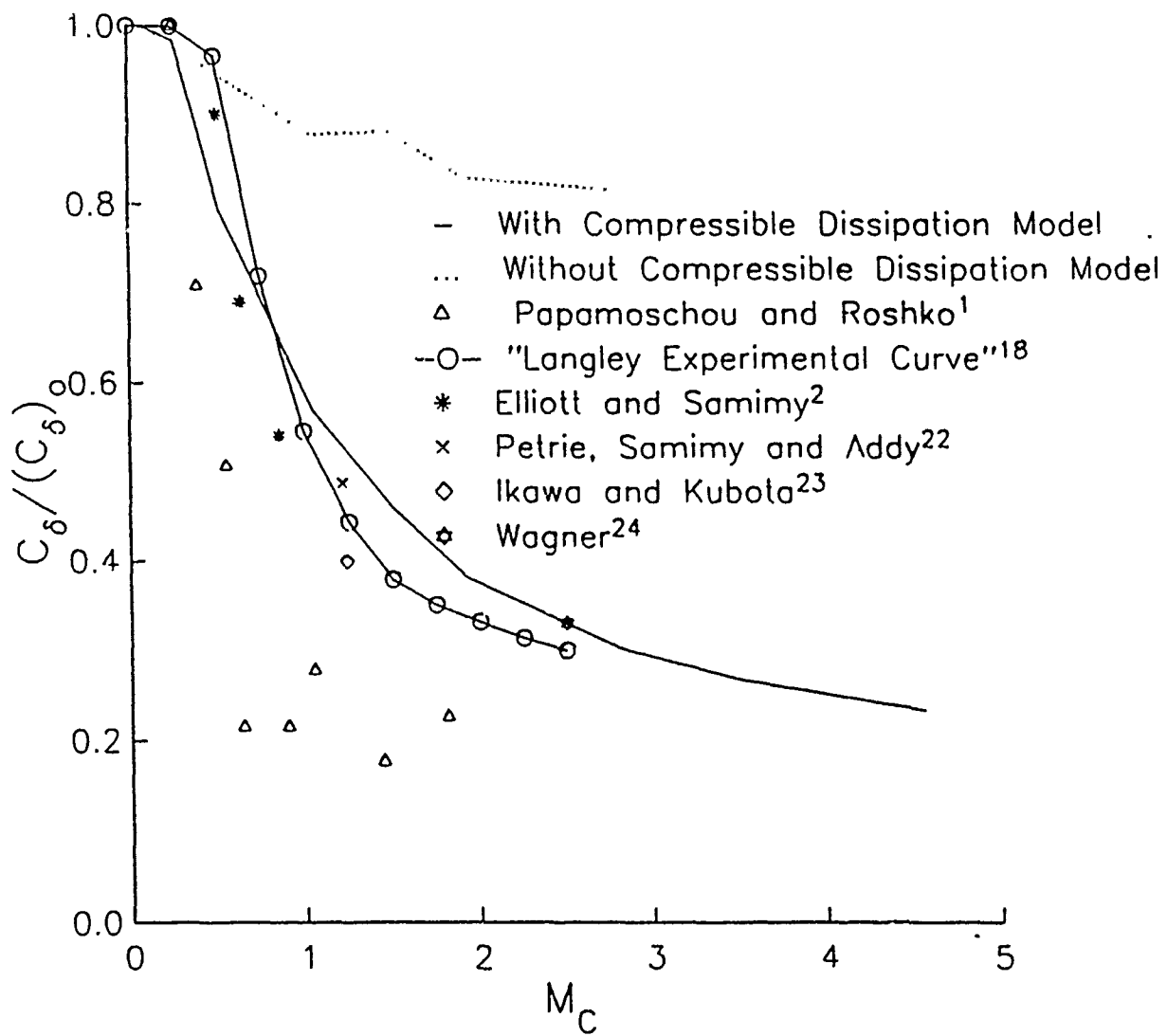
Figure 3-6. Variation of Normalized Spreading Rate of a Compressible Shear Layer with Relative Mach Number

32

3-6 Reynolds Stress Modeling for Compressible Turbulence

Objective. To develop and implement a Reynolds stress turbulence closure model for high-speed compressible flows.

Approach. Both a theoretical analysis and direct simulations of compressible, homogeneous turbulence were used to develop a turbulence model applicable to supersonic and hypersonic flows. A program of turbulence model testing was initiated on the compressible shear layer.

Accomplishments. Transport equations were formulated for the Favre-averaged Reynolds stress tensor and the turbulent dissipation rate. The turbulence dissipation rate was further decomposed into a solenoidal (incompressible) part, ε_s, and a compressible part, ε_c. Both an asymptotic analysis and a direct simulation of homogeneous turbulence showed that the compressible dissipation depended on the turbulent Mach number, M_t. This information was used to develop the following model for the compressible dissipation rate: $\varepsilon_c = \alpha_1 \varepsilon_1 M^2_t$, where the model constant $\alpha_1 = 1$. The figure shows the results, for the normalized spreading rate $C_\delta/(C_\delta)_0$ of a compressible shear layer, using this new closure model. The poor performance of a variable-density generalization of a standard incompressible closure (see figure) indicated the need for explicitly incorporating the mechanisms associated with turbulence compressibility. The figure shows that inclusion of the new model for ε_c into the Reynolds stress closure leads to agreement with the following critical trends in the experimental data: first, the significant decrease in the spreading rate with Mach number, and second, the relative insensitivity of the spreading rate, after its initial decrease, to further increases in the relative Mach number.

Significance. The need for incorporating the physics of compressible turbulence in order to capture strong compressibility effects such as the dramatic reduction of high-speed shear layer growth has been unequivocally established. A turbulence model based on an asymptotic analysis and validated against direct numerical simulations, has successfully captured the reduction in growth rate of the compressible shear layer.

Status/Plans. This new closure model will be applied to other compressible flows such as perturbed and unperturbed turbulent boundary layers. Additional compressibility effects such as strongly nonisentropic thermodynamic fluctuations will be modeled.

Sutanu Sarkar, Gordon Erlebacher
ICASE, Langley Research Center,
(804) 864-2194
L. Balakrishnan
Old Dominion University

33

- Rotating Disk Model Flow -
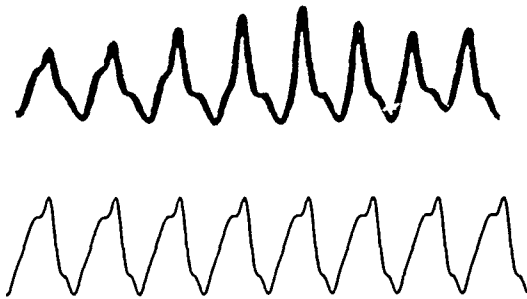
Top: Hot-wire history;
        (Wilkinson, et al)
Bottom: Streamwise velocity vs.-θ,
          secondary instability theory
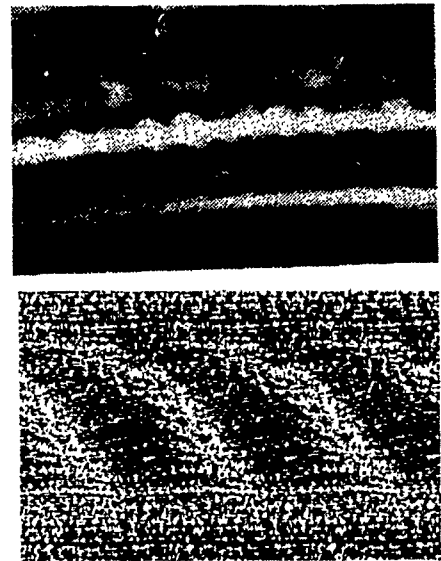
Top: Smoke flow visualization;
        (Kohama)
Bottom: Lagrangian particle distribution,
          secondary instability theory

Figure 3-7. Secondary Parametric Instability of Crossflow Disturbance

34

3-7 Secondary Instability of Cross-Flow Disturbances

Objective. To clarify the role of instability-wave interactions in the later stages of transition in three-dimensional boundary layers.

Approach. The similarity solution for the boundary layer flow on a rotating disk is used as a prototype for three-dimensional boundary layers, which exhibit inflectional instabilities known as crossflow modes. These low-frequency disturbances are observed on swept wings as vortices nearly aligned with the potential-flow direction, and are a mechanism for transition in favorable pressure gradient regions on such wings. The rotating-disk model flow has been investigated through hot-wire and flow-visualization experiments and using linear stability theory. It has been conjectured in the literature that the breakdown of these disturbances comes about as the result of nonlinear interaction of these linear modes; this interaction was to be elucidated via direct simulation and weakly nonlinear theory.

Accomplishments. Direct numerical simulations were carried out using a distribution of primary linear disturbances as initial condition; the expected nonlinear interactions were not observed. Parametric secondary instability analysis revealed a robust, broad-band instability, appearing at a threshold primary amplitude of about 8%. The accompanying graphic shows a comparison of experimental and theoretical time histories and flow-field visualizations. In the experimental hot-wire time histories, taken by Wilkinson and Malik, the feature of the additional "bump" was difficult to explain using wave interaction theories. This feature is apparent in the time history for temporal secondary instability theory; exact details of the histories do not correspond, since assumptions are made in the theory that do not correspond preciesely

with the experimental wave evolution. The convected-particle flow-field visualizations (right) show the appearance of small-scale vortices, angled with respect to the original crossflow vortex; this feature was interpreted from the experimental visualizations to be helical structures.

Significance. Understanding of the stages of breakdown of crossflow disturbances is crucial for developing engineering criterion for transition in flows dominated by these disturbances.

Status/Plans. The secondary instability theory is being applied to the nonsimilar three-dimensional boundary layer computed for the swept-wing experiment in the Arizona State University transition wind tunnel; comparisons will be made with detailed hot-wire measurements taken there. Spatial simulations are planned to assess the effects of pressure gradient and nonparallel mean flow on the present (temporal) simulations.

S. Balachandar, Craig L. Streett
Theoretical Flow Physics Branch,
Langley Research Center
(804) 864-2230

Neutral Curves

Sharp Cone

$(\mathrm{Re}_x)_{crit} \approx 2.25 \times 10^6$

Blunt Cone ($R_n = 31250$)

$(\mathrm{Re}_x)_{crit} = 3.3 \times 10^6$

$(x_{blunt}/x_{sharp})_{crit} = 14$

N Factor Calculations

Sharp Cone

	$N = 10$	$N = 5.5$
$(\mathrm{Re}_x)_{tr}$	14.8×10^6	6.5×10^6

$(\mathrm{Re}_x)_{crit} = 2.25 \times 10^5$
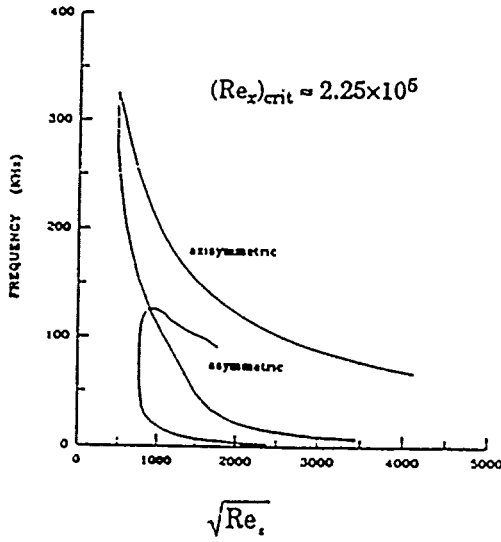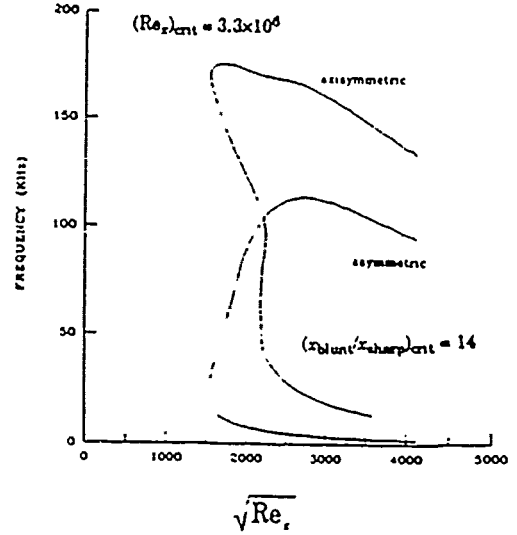
Blunt Cone ($R_n = 31250$)

	$N = 10$	$N = 5.5$
$(\mathrm{Re}_x)_{tr}$	19.3×10^6	11×10^6

$(\mathrm{Re}_x)_{crit} = 3.3 \times 10^6$
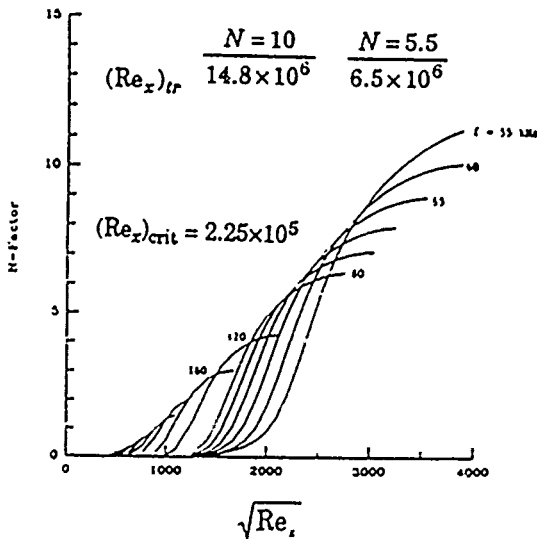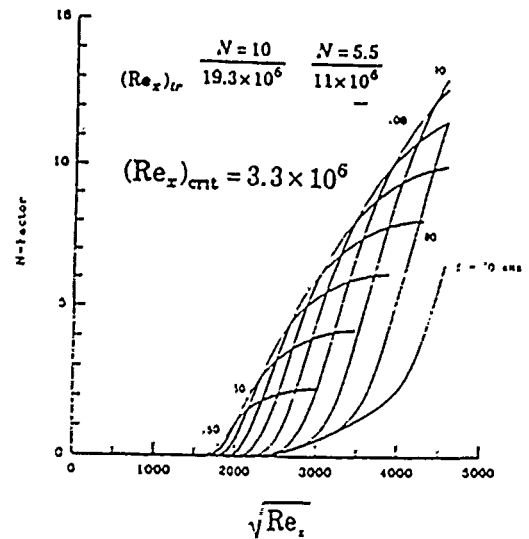
Figure 3-3. Stability of Mach 8 Flow Past a 7° Semivertex Cone

36

3-8 Bluntness Effects on Hypersonic Boundary Layer Transition

Objective. To understand the process of boundary layer transition in high-speed and three-dimensional boundary layers. This understanding and modeling and prediction capability can be achieved only through various studies involving internalization of disturbances (receptivity), linear and nonlinear development of various disturbances (Tollmein-Schlicting (TS), crossflow, Gortler), and their possible interaction.

Approach. Navier-Stokes and Parabolized Navier-Stokes (PNS) codes are used to accurately compute the basic flow and its first and second derivatives, which are then analyzed using linear stability theory. For a blunt cone, a compressible Navier-Stokes code was used to compute the basic flow in the nose region, which provided initial conditions for the subsequent PNS solution. About 200 grid points were used across the shock layer in the PNS calculation. Linear stability calculations were performed by using a fourth-order accurate two-point compact scheme.

Accomplishments. Linear stability analysis of the Mach 8 flow past a 7° semivertex blunt cone (nose Reynolds number = 31250) was performed. Results indicated that due to nose bluntness the critical Reynolds number for the onset of instability increased by an order of magnitude (from about 2.25×10^5 for the sharp cone to 3.3×10^6 for the blunt cone). The predicted critical Reynolds number, the disturbance frequency and the growth rates are in agreement with the experiments of Stetson et al. (1984) at $M_\infty = 8$. N factor calculations show that estimated transition Reynolds number increases due to small nose bluntness. The stabilizing effect of bluntness can be characterized by the free stream nose Reynolds number (R_n) which also explains the "apparent" unit Reynolds number effect found in the ballistic range data of Potter (1974). Calculations were also performed for reentry-F cone data ($M_\infty = 20$, 5° semi-vertex cone) using equilibrium gas model. The results suggest that second mode disturbances were responsible for transition in this high Mach number boundary layer.

Significance. Transition prediction is crucial for the design of aerospace vehicles, such as NASP, and supersonic laminar flow control for High Speed Civil Transport (HSCT). The agreement of our stability results for hypersonic flow with experimental data gives some confidence in the theory and its usefulness for transition prediction.

Status/Plans. The codes will be used to study instabilities in 3-D boundary layers at supersonic and hypersonic Mach numbers for bodies at angle of attack.

M. R. Malik, C.-L. Chang, R. E. Spall
High Technology Corporation
Langley Research Center
(804) 864-5564
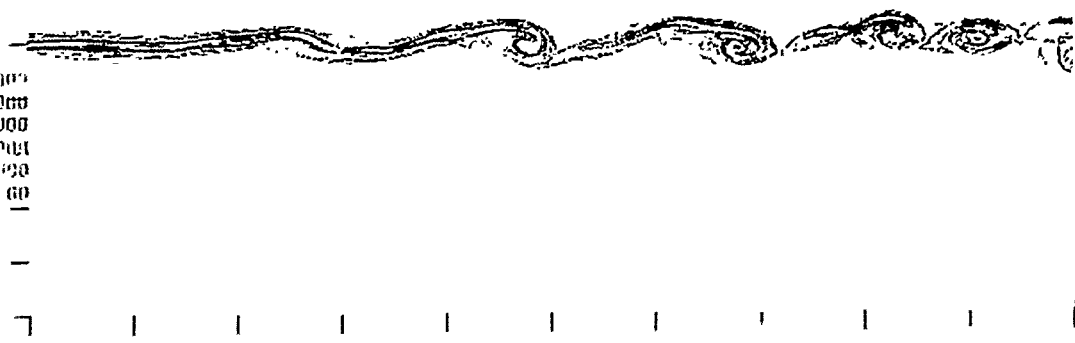
Figure 3-9. Studies in Direct Simulation of High-Speed Mixing Layers With and Without Chemical Heat Release

3-9 Studies in Direct Simulation of High-Speed Mixing Layers With and Without Chemical Heat Release

Objective. To examine the effects of convective Mach number, disturbance levels, initial profiles, Reynolds number, and chemical heat release on the structure of a high-speed mixing layer.

Approach. The SPARK2D code is used to perform a direct numerical simulation of the high-speed two-dimensional mixing-layer. The numerical algorithm used is the Dissipative Compact Parameter Scheme (DCPS), which has a formal accuracy of $O(\Delta t^2, \Delta x^4)$.

Accomplishments. High-speed mixing-layer calculations were made at convective Mach numbers (M_c) of 0.38 and 0.76 for a number of initial disturbance levels, for two initial profiles, and for a range of Reynolds numbers using the SPARK2D code. Fine grids were used to ensure that all the relevant length-scales were resolved. From the calculations, the following conclusions have been made: (1) Assumed hyperbolic tangent profiles need large disturbance levels to make the flow transitional. (2) The growth rates obtained from the time-averaged data compare reasonably well with existing experimental data, illustrating the compressibility effects. (3) The role of heat release is to reduce the growth rate of the mixing layer by about 5-7% and to reduce the convective speed of the structures by about 10% at $M_c = 0.38$. Preliminary results indicate that increasing the convective Mach number will reduce the effect of heat release. (4) Changes in density in the flow result from temperature, pressure, and composition variations in the compressible case, unlike in incompressible flows, where temperature and composition are the dominating factors. (5) The reduction in Reynolds stresses and kinetic energy of fluctuations, as well as the reduction of entrainment with heat release, are akin to those in incompressible flows, but to a much lesser extent. In view of the weaker role of heat release, it is reasonable to conclude that it is useful to concentrate on nonreacting flows for the mixing-related issues. Heat release is likely to provide only a small perturbation to many nonreacting flows.

Significance. Direct numerical simulation of high-speed mixing layers have improved the understanding of fuel-air mixing in scramjet combustors. Current studies have enabled determination of several important techniques for producing high levels of mixing and combustion efficiency in a scramjet combustor.

Status/Plans. Flow conditions exist in which the above conclusions may be only partially valid. Further study of these issues as well as a complete study of three-dimensional nonreacting and chemically reacting mixing-layers is necessary.

Balu Sekar, H. S. Mukunda,
Mark H. Carpenter
Theoretical Flow Physics Branch
Langley Research Center
(804) 864-2318

Vorticity Contours

Array of Vortex Generators

Mixing Layer Wind Tunnel

Effect on Turbulent Energy

Effect on Growth Rate
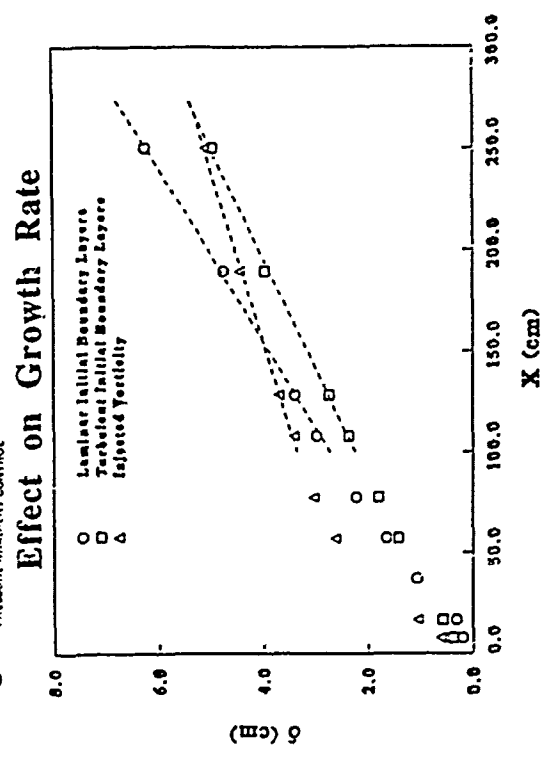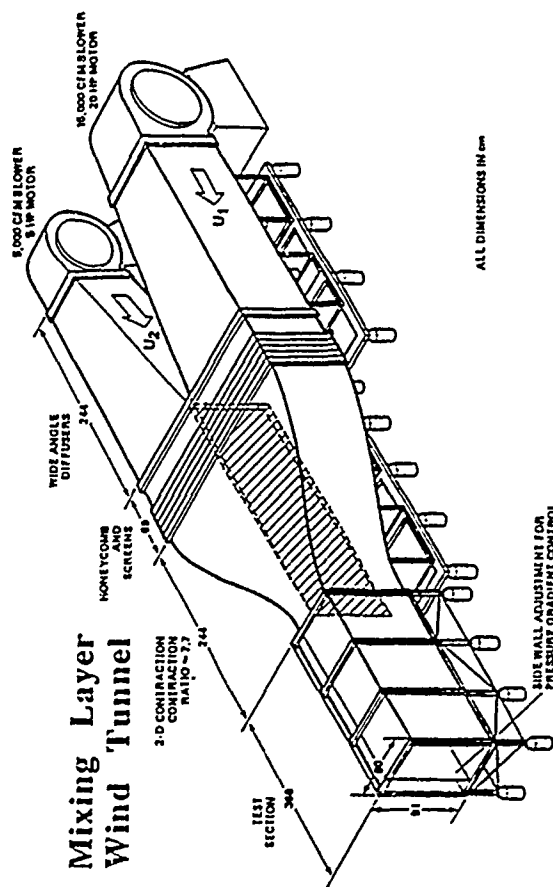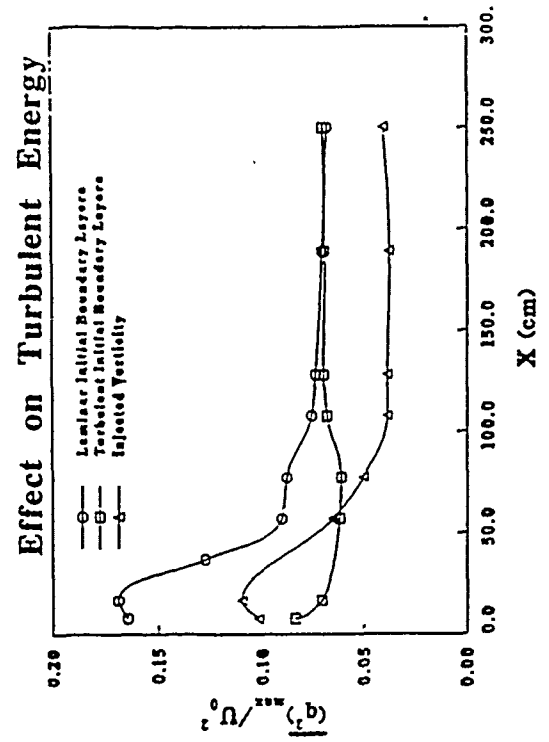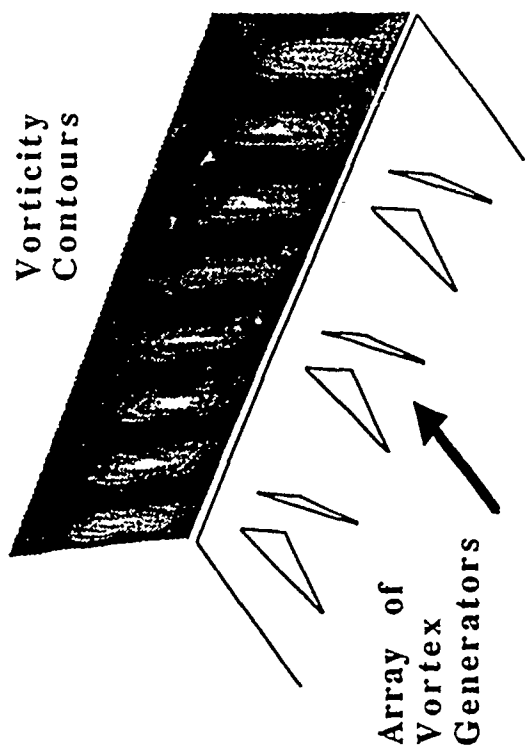
Figure 3-10. Mixing Layer Control Through Vorticity Injection

40

3-10 Experimental Studies of Plane Mixing Layer Structure

Objective. Past flow visualization studies of mixing layers have shown the presence of streamwise vortical structures riding among the primary spanwise vortices. The current research objective is to first establish, through direct measurements, the presence and role of the streamwise structures in plane mixing layers at high Reynolds numbers. Once this has been established, the objective is to investigate ways of controlling the structure and hence the growth and mixing properties of the mixing layer.

Approach. A new wind tunnel facility was designed and built specifically for free-shear layer research. The unique feature of this facility, with two independent drive systems, is the ability to easily generate mixing layers at various Reynolds numbers and velocity ratios, with a wide variety of initial and operating conditions. Measurement of the mean flow and turbulence statistics are obtained on fine cross-plane grids at several streamwise locations using hot-wire anemometry. The evolution of the streamwise structures is studied by examining contours of the mean vorticity and Reynolds stresses generated on IRIS workstations.

Accomplishments. The origin, reorganization, and evolution of the streamwise vortical structures in a plane mixing layer has been measured for the first time. The effects of tripping the initial boundary layers and those of triggering and injecting streamwise vorticity into the mixing layer have also been investigated.

Significance. The results show that the streamwise vortical structures have a significant effect on the mixing layer two-dimensionality in the near-field, although their strengths and effects were found to diminish with increasing downstream distance. The structures also have a strong effect on the mixing layer entrainment and hence its growth and mixing properties. It has been demonstrated that the growth rate of the mixing layer can be effectively controlled for relatively long portions of its development by injecting streamwise vorticity using passive devices installed in the upstream boundary layers.

James H. Bell, Rabindra D. Mehta
Fluid Dynamics Research Branch
Ames Research Center
(415) 604-4141

Chapter 4

Computational Methods and Validation

The objective of the Computational Methods and Validation Program is to develop and apply advanced analysis and computational methods for solving complex, fluid dynamics problems and to perform detailed, benchmark experiments using redundant facilities and instrumentation to produce high-quality archival data sets to which CFD solutions can be compared. Areas of interest include modeling turbulence and transition and computing complex flows (steady and unsteady, inviscid and viscous) over two-and three-dimensional geometries ranging in speed from zero to hypersonic and including such effects as mass injection and withdrawal. Additional objectives are to (1) demonstrate proof-of-concept computations for pioneering applications, (2) disseminate validated computer codes to the aerospace community and provide maintenance and consultation on their use, (3) develop innovative techniques for scientific visualization of flow-field solutions, and (4) provide an experimental data base that is taken in the form and detail consistent with CFD modeling requirements and that has documented accuracy and limitations of the experimental data.

The Computational Methods Program is focused on the present and future technology needs of the aerospace community. These needs include (1) developing faster and more efficient numerical algorithms to facilitate solutions of the full Navier-Stokes equations by large-eddy, simulation/small-scale turbulence modeling, (2) developing advanced geometric modeling and grid generation techniques for complex, three-dimensional configurations, (3) improving understanding of the effects of grid characteristics on solution accuracy, convergence, and stability, (4) enhancing computational capabilities through development and use of advanced computer architectures and expert systems concepts, and (5) developing improved methods for numerical simulation of aerothermodynamic flow phenomena associated with hypersonic cruise and maneuver vehicles, including real-gas chemistry.

Experiments are designed for comparison with numerical CFD results in order to (1) understand flow physics, (2) develop physical models for CFD codes, (3) calibrate CFD codes, and (4) validate CFD codes. The experiments range in speed from subsonic to hypersonic and include a variety of configurations including generic, fighter/attack, subsonic transport, rotorcraft, ASTOVL, and propulsion systems. Work continues in developing high-quality data bases for several classes of flows, including (1) high-and low-aspect ratio wings in subsonic and transonic flows, (2) simple 3-D turbulent flows, including time histories; (3) flow fields about aircraft components, (4) propulsive lift flow interactions in ground effect, and (5) unsteady flow interaction in rotor flow fields.

Program Manager: Pamela F. Richardson
                    OAET/RF
                    Washington, DC 20546
                    (202) 453-9857

43

$$\left(M_\infty = 0.84, \ \alpha = 3.06^0, \ Re_{\bar{c}} = 11.7\text{x}10^6\right)$$

97x25x17 grid computations
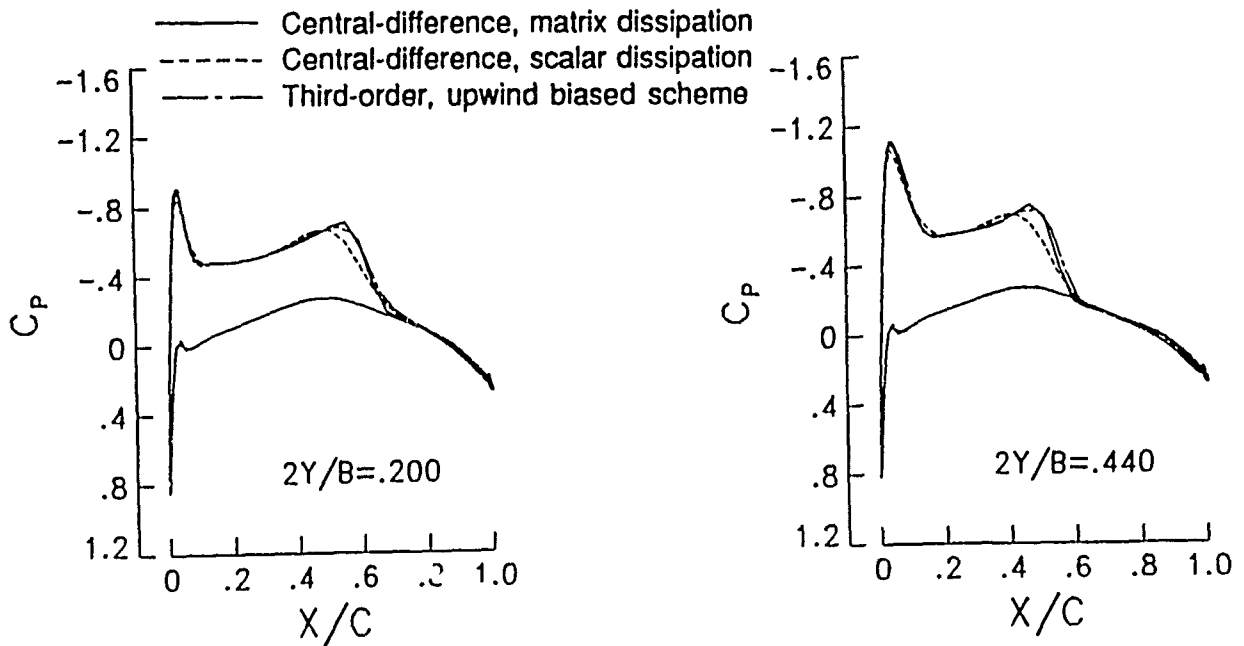
Figure 4-1. Comparison of Central- and Upwind- Difference Results for ONERA M6 Wing

4-1 Development of a Matrix-Valued Dissipation Model for Central-Difference Schemes

Objective. To develop an efficient and accurate numerical solution procedure for three-dimensional high Reynolds number viscous flows.

Approach. Using concepts from upwind schemes, a matrix-valued dissipation model was formulated which gives appropriate dissipation for each wave component and hence reduces the overall levels of artificial dissipation.

Accomplishments. A matrix-valued dissipation model has been incorporated in a multigrid, central-difference, time-marching, Thin-Layer Navier-Stokes code, TLNS3D, which was developed for solving high Reynolds number, viscous flow problems of aerodynamic interests. The accuracy of the TLNS3D code is enhanced significantly, especially in the vicinity of shock-waves, through the use of a matrix dissipation model. Based on computations of transonic flow over transport and fighter wings, the proposed scheme is found to be more cost effective than the original scheme using a scalar dissipation model and appears to be comparable to upwind biased schemes in accuracy.

Significance. Overall efficiency of the central-difference scheme is improved due to matrix dissipation, and the new scheme provides engineering accuracy on coarser grids.

Eli Turkel, Veer N. Vatsa
Computational Aerodynamics Branch
Langley Research Center
(804) 864-2236

OM6 Wing, $M_\infty = 0.84$, $\alpha = 3.06°$
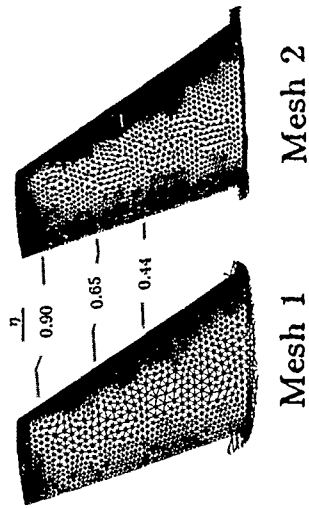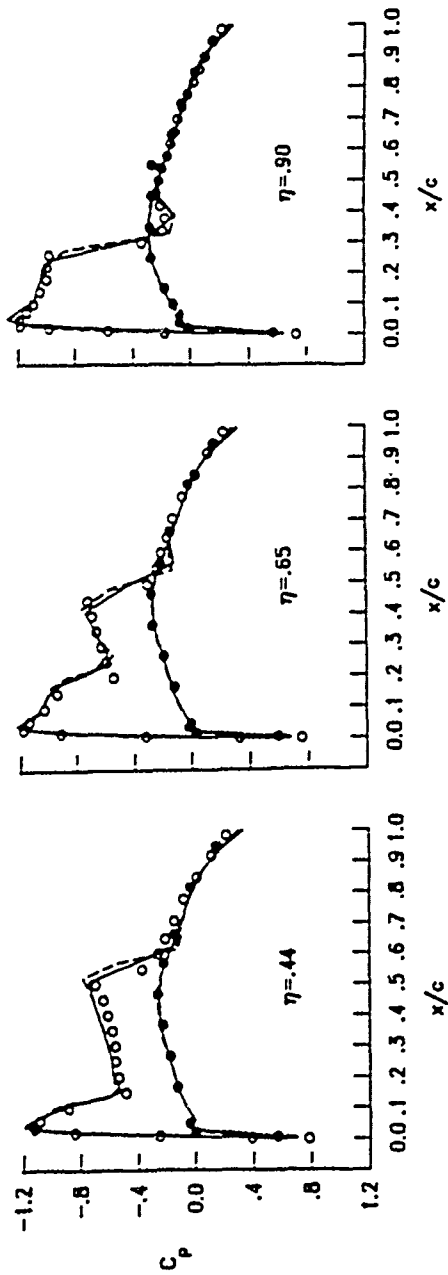
Figure 4-2. Chordwise Surface Pressure Distributions

46

4-2 A Fast Upwind Solver for the Euler Equations on Three-Dimensional Unstructured Meshes

Objective. To construct an efficient upwind code for accurately solving the 3-D Euler equations on unstructured tetrahedral meshes.

Approach. Proven technologies used in 3-D structured upwind codes were extended into the 3-D unstructured environment. An explicit cell-centered finite-volume flow solver was developed which utilizes flux-difference splitting and a simple new method for efficiently constructing the higher-order differences.

Accomplishments. Solutions were computed for the ONERA M6 wing on two tetrahedral meshes at transonic conditions: $M_\infty = 0.84$, and $\alpha = 3.06°$. This represents a generally accepted difficult test case. Mesh 1 contained 108,755 cells, and Mesh 2 consisted of 231,507 cells. The surface meshes are depicted on the figure. The solution was advanced in time by a 3-stage Runge-Kutta time-stepping scheme with a Courant-Friedrichs-Lewy (CFL) number of 4.0. Convergence to steady state was accelerated with local time stepping and implicit residual smoothing. No explicit form of limiting was applied during calculations as is commonly needed with upwind flow solvers.

The figure shows the effect of mesh size on the streamwise surface C_p distribution at three span stations. The results are plotted in comparison to experimental data at a Reynolds number of 11.7 million, corresponding to conditions for which viscous effects are relatively small. The computations on both meshes agree well with experiments for each spanwise location. The primary effect of mesh size is confined to the resolution of the leading-edge suction peak and the shock width, with the finer Mesh 2 yielding slightly better resolution. The accuracy of these solutions is typical of that obtained with current structured upwind codes.

The calculations required 73 words per cell for both meshes. Structured codes generally require around 40 to 50 words per cell. The solutions were computed on a single processor of the NASA Langley Research Center Cray-2s Voyager and required 35×10^{-6} sec/cycle/cell, which is comparable to that of structured codes. Total run times were approximately 1 hour/40 minutes for Mesh 1 and 4 hours/30 minutes for Mesh 2.

Significance. The presented results represent a significant advance in both accuracy and code efficiency compared with other available 3-D unstructured methods. The geometrical flexibility associated with tetrahedral meshes coupled with an accurate and efficient flow solver provide a substantial new capability for solving geometrically complex flow problems.

Status/Plans. Additional calculations are planned to further assess grid sensitivities on the M6 wing and to evaluate the method on more complex geometries. Planned extensions to the basic flow solver include adding the viscous terms, implicit time integration, and solution-adaptive mesh and moving mesh capabilities. Mesh-sequencing is presently being investigated for accelerating convergence.

Neal T. Frink
Transonic Aerodynamics Branch
Langley Research Center
(804) 864-2864

A BOEING 747 CONFIGURATION

Surface Mach Number

Surface Triangulation
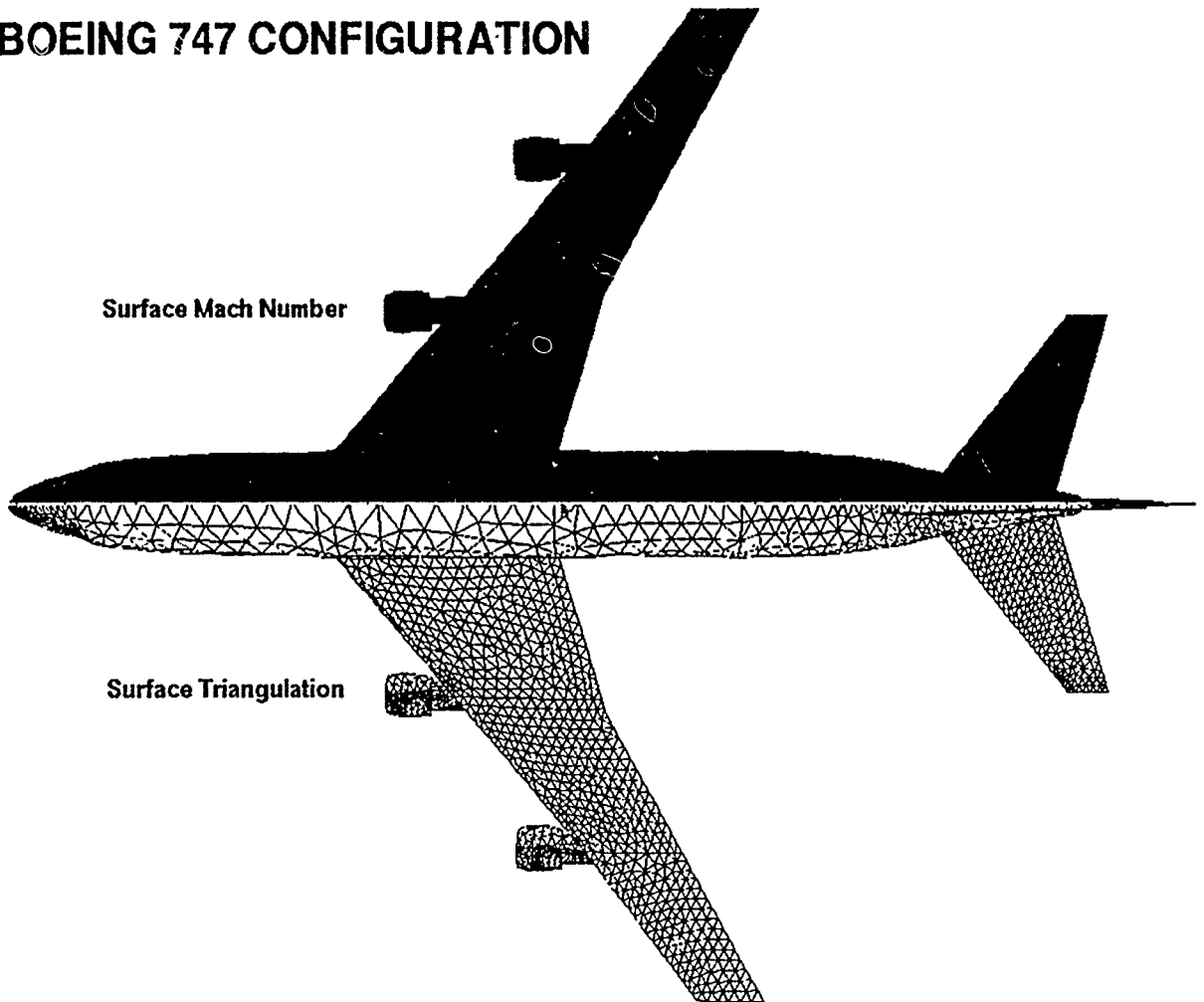
Figure 4-3. Transonic Euler Solution About a Full Aircraft Configuration
Using Unstructured Grid

48

4-3 Transonic Euler Solution About a Full Aircraft Configuration Using Unstructured Grid

Objective. To develop a reliable package containing an unstructured grid generator, a Euler equation solver, and a post-processor graphics visualization program.

Approach. The "advancing front technique" is employed to generate and refine an unstructured, tetrahedral grid (VGRID3D). This technique concurrently defines new points and generates the grid connectivity. Efficient data structures such as octrees and heap lists have been used to perform many search operations associated with unstructured grid generation. A transonic inviscid flow solution is obtained on the grid using a new, efficient upwind flow solver, USM3D. The results are analyzed and plotted using an interactive, graphics post-processor program, VPLOT3D.

Accomplishments. A tetrahedral grid has been generated from the surface patch definition of the Boeing 747-200 with flow-through nacelles using VGRID3D. The grid consists of 105,372 cells, 19,698 nodes, 8402 boundary faces, and 4195 boundary nodes. An inviscid solution has been obtained on this grid using USM3D. The converged result is portrayed in the accompanying figure, which shows both the surface grid as well as shaded Mach contours for $M_\infty = 0.84$ and $\alpha = 2.73°$. The red contours on the wing indicate a region of supersonic flow, which is terminated by a shock wave where the contours transition to yellow. This solution was obtained with a Courant-Friedrichs-Lewy (CFL) number of 3 in 1600 cycles for a decrease in the residual error of 3.7 orders of magnitude. The solution required about 1 hour/40 minutes of Cray-2s Voyager time and used less than 8 megawords of memory.

Significance. Besides their inherent capability of handling complex configurations with ease, unstructured grids offer better control over the grid size and point clustering and are apt to efficiently incorporate adaptive refinement techniques. The presented results were readily obtained on the first attempt and thus demonstrate the robustness of the code in computing a complex flow field about a full aircraft configuration.

Status/Plans. Work is presently under way for making a quantitative calibration of the VGRID3D/USM3D package for a range of geometries and flow regimes to further assess accuracy and robustness. Future plans include assessing the usefulness of this package as a design tool.

Paresh Parikh, Shahyar Pirzadeh,
Neal T. Frink
Transonic Aerodynamics Branch
Langley Research Center
(804) 864-2864
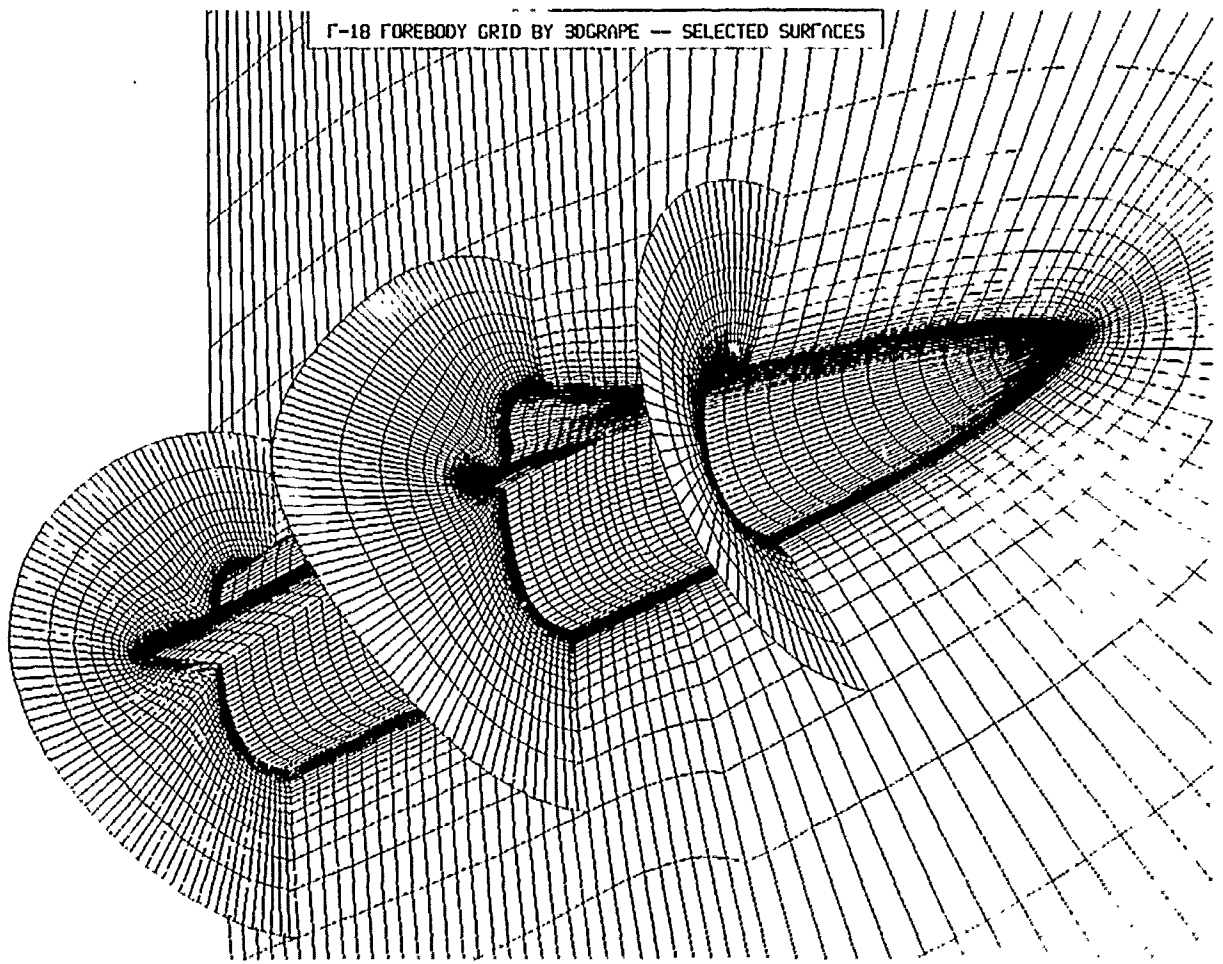
Figure 4-4. F-18 Forebody Grid By 3DGRAPE — Selected Surfaces

50

4-4 3DGRAPE Code and User Guide Released for Distribution

Objective. To make available to the computational fluid dynamics (CFD) community a computer program that generates three-dimensional volume grids for a variety of applications, including realistic aerodynamic configurations.

Approach. A FORTRAN computer program was written that allows complex physical domains to be divided into blocks. Grids in the blocks fit together to make a grid filling the entire physical domain, and the grid in each block is relatively simple to generate and use. Grids are produced by numerical solution of Poisson's equation. Right-hand-side terms are designed to automatically provide arbitrary control of grid cell size and skewness near boundary surfaces.

Accomplishments. This program, called 3DGRAPE, has been written. It was tested by approximately 50 users on problems as diverse as viscous flow about fighter aircraft and the fluid dynamics of molten steel. It has been transferred to the Computer Software Management and Information Center (COSMIC) for distribution. A 119-page Technical Memorandum (TM) has been written to serve as a users' manual for the program. The TM contains a mathematical derivation of the method, a description of the input data, and sample cases.

Significance. Grid generation has emerged as a major pacing item in the progress of CFD. It is expected that this program will significantly reduce the time and effort required for grid generation and enhance the capability to treat realistic problems.

Status/Plans. The initial release version of the program and its accompanying documentation are complete. Continued interaction with the user community will lead to enhanced versions with even greater capability. 3DGRAPE is being integrated with powerful graphical workstations, further reducing the time required for grid generation.

Reese L. Sorenson
Applied Computational Fluids Branch
Ames Research Center
(415) 604-4471
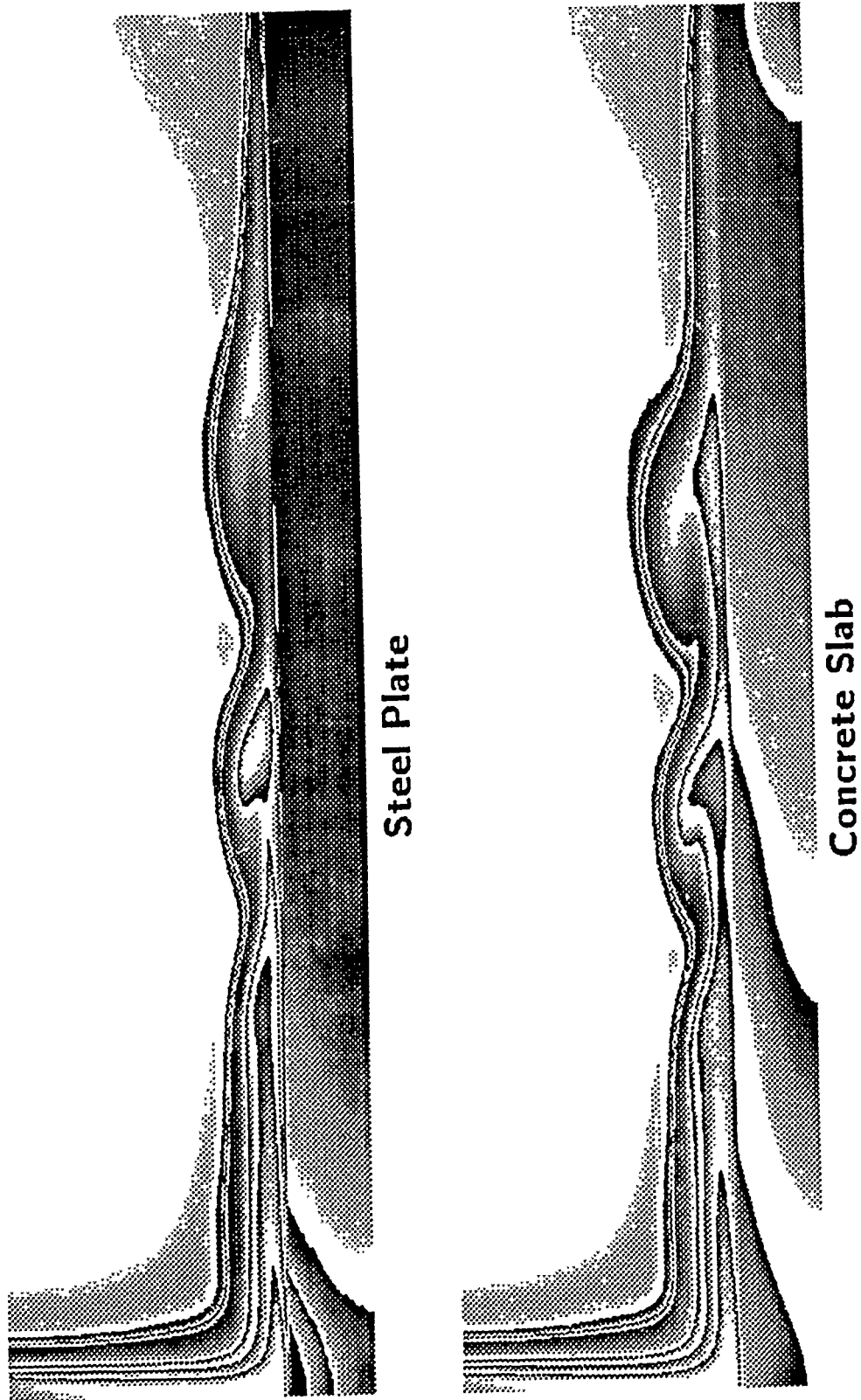
Figure 4-5. Hot Jet Temperature Profiles ($T_{jet}/T_{\infty} = 5.6$, Time ~ 0.1 sec.)

4-5 CFD Thermal Ground Environment Program

Objective. To develop and validate coupled CFD/thermal prediction capability for runway failure due to propulsive jet impingement.

Approach. Unsteady three-dimensional Navier-Stokes and thermal conduction solvers were coupled, and the resultant multidisciplinary *HOTJET* code was validated by comparison with experimental and flight data.

Accomplishments. Time-accurate, arbitrary three-dimensional geometry thermal conduction code was completed (implicit approximate-factorization scheme) and coupled to multiple overset/patched block time-accurate Navier-Stokes code via iterative fluid/solid interface boundary condition. Single-discipline (e.g., flow simulation or conduction prediction) validation was completed. Multidisciplinary coupled flow/solid thermal conduction validation is in progress.

Significance. This capability will allow cost-effective analysis of runway failure resulting from exposure to hot propulsive jets. At present, costly test-to-failure full-scale jet engine experimental studies are required. Technology was developed applicable to a broad range of nonadiabatic aero-heating problems.

Status/Plans. We plan to complete validation of coupled fluid/solid thermal conduction prediction capability, and include developed technology into complete powered-lift aircraft prediction software (see Harrier AV-8B Computation-to-Flight Program) to allow prediction of runway failure modes for a specific aircraft concept.

Patricia A. Abeloff, William R. Van Dalsem
Applied Computational Fluids Branch
Ames Research Center
(415) 604-3983
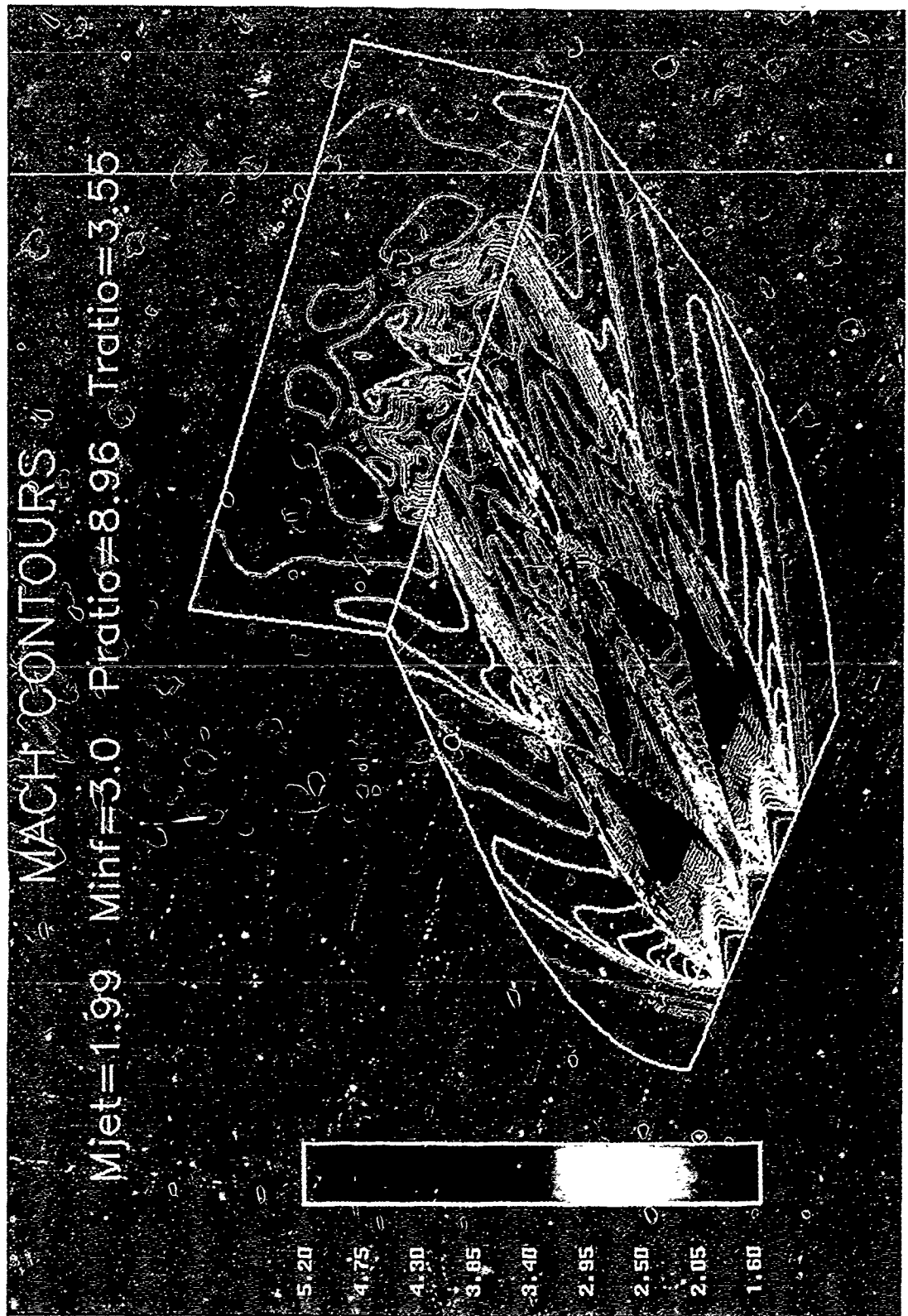
Figure 4-6. Interaction of Multiple Plumes Mach Contours

54

4-6 Multiblock Multigrid Euler Calculations of Three-Dimensional Plume Flows

Objective. To develop a computational tool to aid in the study of rectangular nozzle flows.

Approach. An explicit upwind method was used to solve the finite volume formulation of the Euler equations. Multigrid acceleration was implemented to increase the rate of convergence. A multiblock data structure was used to provide geometric flexibility for the analysis of complex nozzle configurations.

Accomplishments. Two types of upwind methods were investigated: van Leer's Flux-Vector-Splitting and Roe's Flux-Difference-Splitting. Both used MUSCL-type differencing and a modified Runge-Kutta time-stepping scheme. The program was used to compute the two-nozzle flow shown in the accompanying figure. The flow conditions were M_∞ = 3.0, M_{jet} = 1.99, P_{jet}/P_∞ = 8.96, T_{jet}/T_∞ = 3.55. The nozzles' exit is at the left with flow from left to right across a symmetry plane. The Mach contours of the predicted flow field are shown on the symmetry plane and the outflow boundary of the computational domain.

Significance. The multiblock structure provides a computer program that is independent of grid topology. This allows the same computer program to be used to solve internal flows (such as nozzle flows that may be an H-H grid topology) and external flows (such as flow over a wing that may be a C-H, C-O, or an O-O grid topology) without making changes to the program. This provides sufficient flexibility to calculate geometrically complex nozzle flow configurations.

Status/Plans. Future plans include improving the computational efficiency of the computer program by investigating various types of residual smoothing and the inclusion of viscous terms in the governing equations.

Frank E. Cannizzaro (ODU), Alaa Elmiligui (ODU), N. Duane Melson
Computational Aerodynamics Branch
Langley Research Center
(804) 864-2227
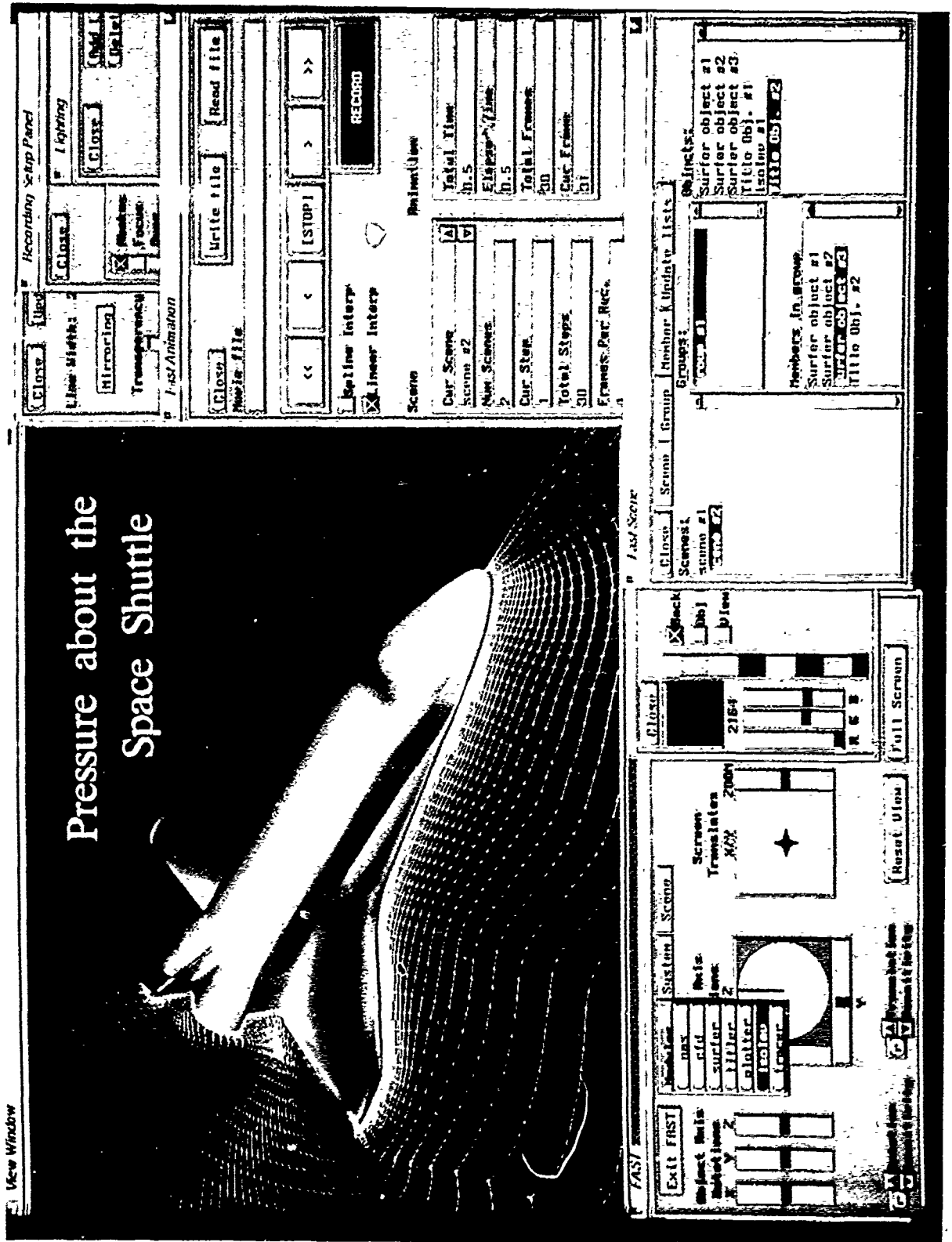
Figure 4-7. Pressure About the Space Shuttle

4-7 Development of a New Generation of Fluid Flow Visualization Software: Flow Analysis Software Toolkit (FAST)

Objective. Current visualization software consists of separate programs for the different functions of visualization which were developed over a period of years. Some of the older programs were not designed to be highly interactive, none takes advantage of the new features of the new workstations, and each has a different user interface. The objective of this project is to create a single program designed to be highly interactive, to take advantage of the new features of the workstations, to have a consistent interface for all of the visualization functions, and to distribute the computing across processors where appropriate.

Approach. A totally new visualization program was designed based on modern interactive interface principles and on distributed computing principles. After the framework of the new program was completed, the functionality of all the previous programs was added to the new program. Then new functionality based on new technology was added.

Accomplishments. A new visualization program has been developed that permits much more effective visual analysis of fluid flows. The interface facilitates highly interactive analysis and is consistent for all visualization functions. More visualization techniques are possible with this new software than were available on all the previous programs combined. The program is extensible, therefore modules with new functions can be easily added.

Significance. The large improvements in visual analysis capability will significantly enhance our capabilities to study complex fluid flows using computers. This software is expected to replace the previous programs, which are used at more than 500 sites across the country.

Status/Plans. The beta version of the program has been released to 30 sites that have requested to work with us on this preliminary version. Initial beta-test codes have been released to approximately 200 sites.

Val Watson
Fluid Dynamics Division
Ames Research Center
FTS 464-6421
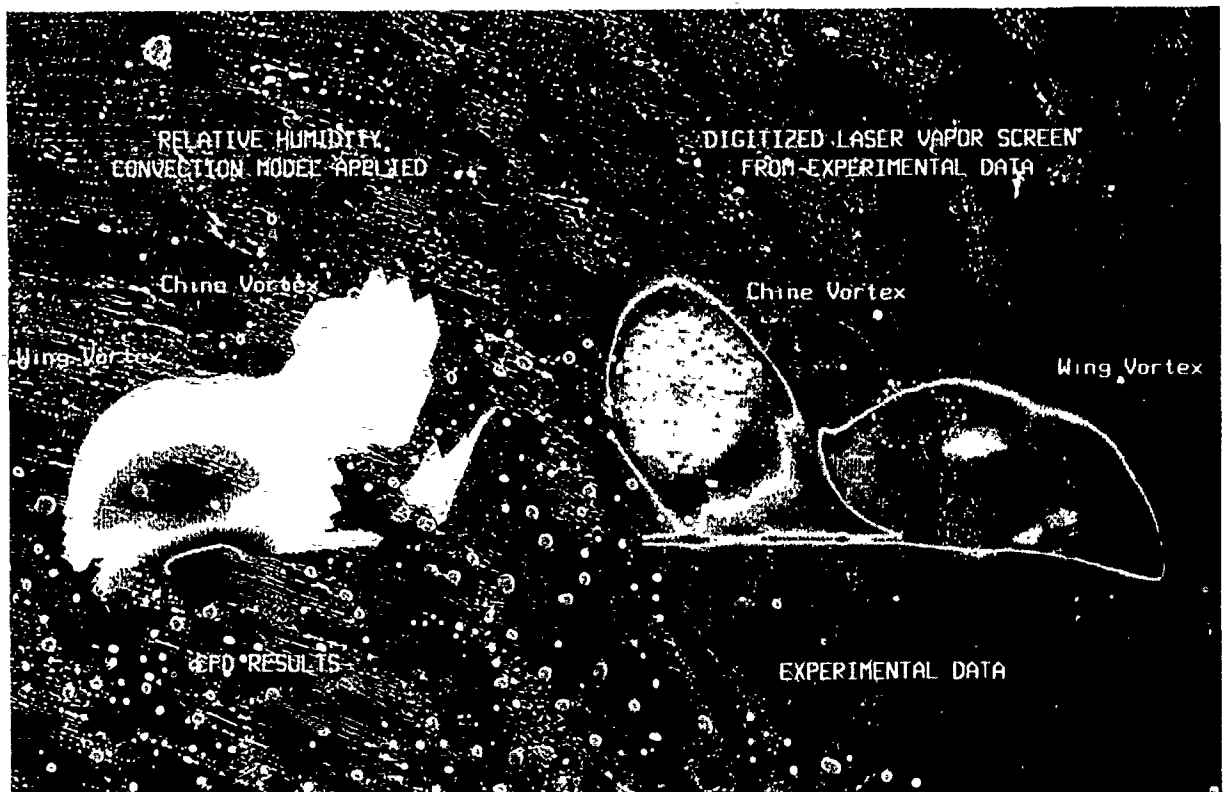
Figure 4-8. Digitized Laser Vapor Screen From Experimental Data and Condensation
Model From Euler Results

58

4-8 Advanced Quantifiable Vapor Screen and CFD Prediction Validation Technique for High-Speed Wind Tunnels

Objective. To develop a technique for using experimental vapor screen images of off-body flow fields about advanced aircraft configurations in transonic wind tunnels to quantitatively validate computational fluid dynamics (CFD) predictions.

Approach. A 3-year research program was established in 1989 with funding provided by the Ames Directors' Discretionary Fund. In this program, existing CFD results (both Euler and Navier-Stokes) will be post processed to yield predicted condensation structures throughout the off-body flow field. The predicted structures will undergo detailed comparison with digitized laser vapor screen images using advanced workstation image analysis techniques. As the condensation model and workstation comparison technique are developed, an improved high productivity method for CFD validation will be created.

Accomplishments. A relative humidity model has been applied to Euler results and shows good contour comparisons but weak persistence of the vortex downstream. Accordingly, a convection model is being developed with first results being produced as of this writing.

Significance. Previous work by Campbell and Chambers (Langley) has shown that for certain cases, there is a correlation between CFD predicted relative humidity and free flight conditions. The present study has shown that the correlation can be observed over a wide range of wind tunnel test conditions using the laser vapor screen technique. By improving the correlation over a wider range of test conditions we create the option for using vapor screen data as a reliable means of validating CFD results yielding tremendous savings in time .

Status/Plans. Development of the convection model will continue. Pending comparison of results, work may begin on a particle growth model, which will also provide for inclusion of light-scattering information for correlation of the vapor screen image intensity.

John A. Schreiner
Advanced Aerodynamic Concepts Branch
Ames Research Center
(415) 604-5860

Rearward Facing Step Investigation
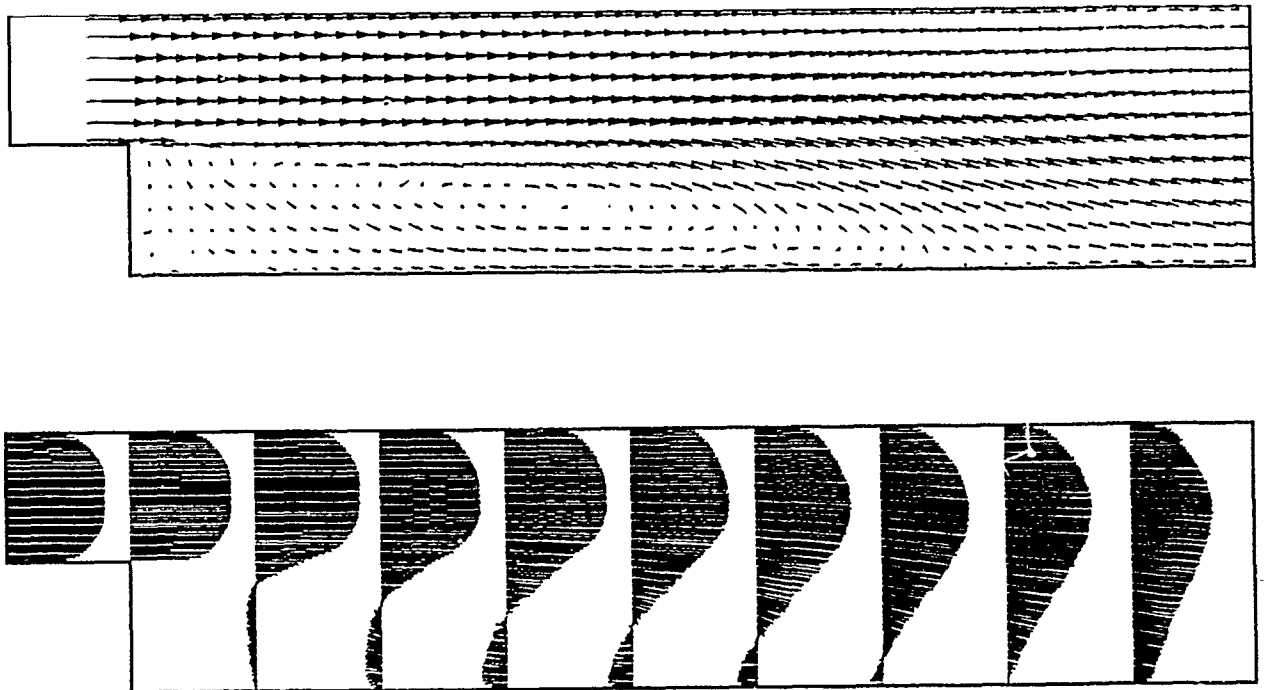
Figure 4-9. Rearward Facing Step Investigation

4-9 Three Component Laser Velocimeter Surveys of the Flow Over a Rearward Facing Step

Objective. To provide detailed flow-field measurements of the flow over a rearward facing step for the development and validation of Direct Turbulence Simulations (DTS), Large Eddy Simulations (LES), and Reynolds-Averaged Navier-Stokes closure models.

Approach. A cooperative program was established between Ames and Langley to perform the research. The Langley investigation focused on the measurement of the three components of velocity throughout the flow over the rearward facing step. These data would be used to obtain the mean velocities and the normal and Reynolds stresses in the flow.

Accomplishments. The phase I investigation of the flow over the step was conducted from January through June. Two 700-point flow-field surveys were conducted along the centerline of the facility, and detailed boundary layer surveys were made at 27 locations. Over 6 million individual measurements of velocity were made at 4000 locations in the flow.

Significance. These data are the first three component measurements of the flow over a rearward facing step and provide a unique data base for the development and validation of DTS, LES, and closure models.

Status/Plans. Testing in the new facility will begin in January 1991 with an expanded test matrix.

Scott O. Kjelgaard
Experimental Methods Branch
Langley Research Branch
(804) 864-1289

61

Figure 4-10. One-Equation Turbulence Transport Model

62

4-10 A One-Equation Turbulence Transport Model for High Reynolds Number Flows

Objective. To develop new turbulence models based on differential equations that easily retrofit existing Navier-Stokes solvers without compromising efficiency or robustness of solver.

Approach. New turbulence model equations were derived using specially designed variables. The choice of solution variables vastly improves the robustness of numerical solution schemes and significantly reduces the grid requirements near solid walls without sacrificing accuracy.

Accomplishments. In the course of this study, a turbulence transport model based on a single partial differential equation was developed. The model easily retrofits existing Navier-Stokes solvers using algebraic models. Numerical computations and subsequent comparison with experiments indicate high numerical robustness and superior predictive capability of the one-equation model over algebraic models. For several transonic flow fields involving shock waves interacting with boundary layers, the one-equation model yielded significant improvement over algebraic models.

Significance. The study indicates that turbulence models based on differential equations can be used in current generation Navier-Stokes solvers without sacrificing efficiency, accuracy, or robustness.

Status/Plans. Results for the one-equation model have been submitted for publication as a NASA Technical Memorandum. A two-equation model with similar numerical benefits is under development.

Barrett S. Baldwin, Timothy J. Barth
Computational Fluid Dynamics Branch,
Ames Research Center
(415) 604-6740

Chapter 5

Numerical Aerodynamics Simulation (NAS)

The Numerical Aerodynamic Simulation (NAS) program provides readily accessible supercomputing capability to the United States' top aeronautical researchers in Government, industry, and academia. The NAS program also includes research and technology development to ensure application of emerging technologies to computational fluid dynamic and other computational sciences. Specifically, the current research involves the enhancement of software and hardware technology for parallel computer architectures.

The objectives of NAS are (1) to maintain a pathfinding role in providing leading-edge supercomputing capabilities to NASA, DoD, and other Government agencies, industry, and universities as a critical element for continued leadership in computational aeronautics and related fields; (2) to stimulate the development of state-of-the-art, large-scale, computer systems and advanced computational tools for pioneering research and development; and (3) to provide a strong research tool for OAET.

To maintain the lead in large-scale computing capability, NAS is implementing a strategy of installing, at the earliest possible opportunity, the most powerful high-speed processor (HSP) available. NAS maintains at least two HSPs, one of which is fully operational and represents more mature technology, and the other, which is a higher performance prototype or early production model. The current HSP configurations are a Cray-2 installed in January 1988 and a Cray Y-MP installed in November 1988. The Cray Y-MP is the first computer to sustain a computation rate of a billion floating point operations per second (GFLOP). Current plans are to replace the Cray-2 with a new processor (HSP-3) in 1992.

NAS was the first supercomputing facility to install a standard operating system (UNIX) and communication software on all processors. UNIX offers the flexibility of both batch and interactive computing and provides a common user interface on all user-visible subsystems. NAS is linked to 35 remote locations nationwide by NASnet, a unique, high-performance communication network, allowing researchers at remote locations to have similar interactive capability as local users at the NAS facility.

The vision for the NAS program is to provide by the year 2000 an operational computing system capable of simulating an entire aerospace vehicle system within a computing time range from one to several hours. It is estimated that a computing time rate of one trillion floating point operations per second (TFLOPS) is required to accomplish this goal.

Program Manager: Pamela F. Richardson
                            OAET/RF
                            Washington, DC 20546
                            (202) 453-9857
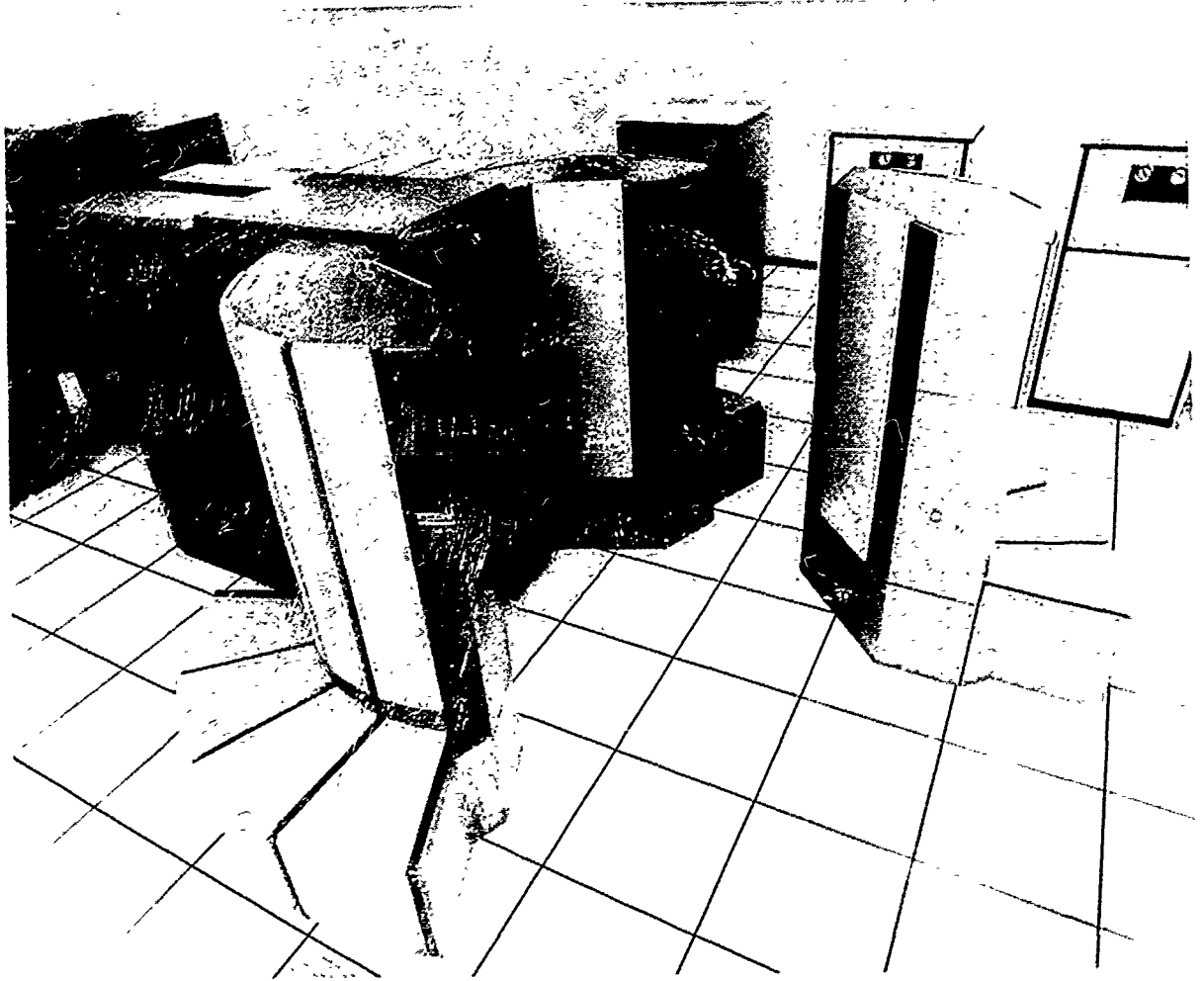
Figure 5-1. Y-MP Upgrade

5-1 Y-MP Upgrade

Objective. To provide a substantial increase in the amount of central memory available to NAS Cray Y-MP users.

Approach. The contract with Cray Research Incorporated for lease of the Y-MP provided NAS with various options for engineering upgrades. An option was selected that would increase the central memory of the Y-MP by a factor of four, from 32 million (64-bit) words to 128 million words. In addition to increasing the central memory, the eight central processing units (CPUs) of the Y-MP were replaced by new CPUs which operate at 5% faster clock speeds.

Accomplishments. The original Y-MP was removed and replaced with the upgraded version on January 22, 1990. A period of extensive electrical and software checkout was followed by a successful installation demonstration on February 10 and a stringent 30-day acceptance test, during which time the machine's performance under a production workload was closely monitored. The upgraded Y-MP passed the acceptance test and was turned over to normal production status on March 12. The cumulative uptime during the test was 94.4%, which exceeded the test requirement of 90%.

Significance. This memory upgrade provides NAS with the largest memory Y-MP in the world. The upgrade greatly enhances the capabilities of the Y-MP. CFD codes, which formerly could run only on the larger (but slower) Cray-2 at NAS, can now take advantage of the speed of the Y-MP. In addition, the larger memory allows more efficient use of the available CPUs and produces a significant increase in the overall throughput of the Y-MP. System monitoring before and after the upgrade shows a 29% reduction in the CPU cycles needed by UNICOS to service the workload as well as a 13% increase in the average FLOP (floating point operation) rate of the computer.

Status/Plans. The upgrade is complete and there are no plans to enhance the current Y-MP hardware. Future improvements to the NAS supercomputing environment will be made through planned acquisitions of new hardware.

John T. Barton
NAS Systems Development Branch
Ames Research Center
(415) 604-4409
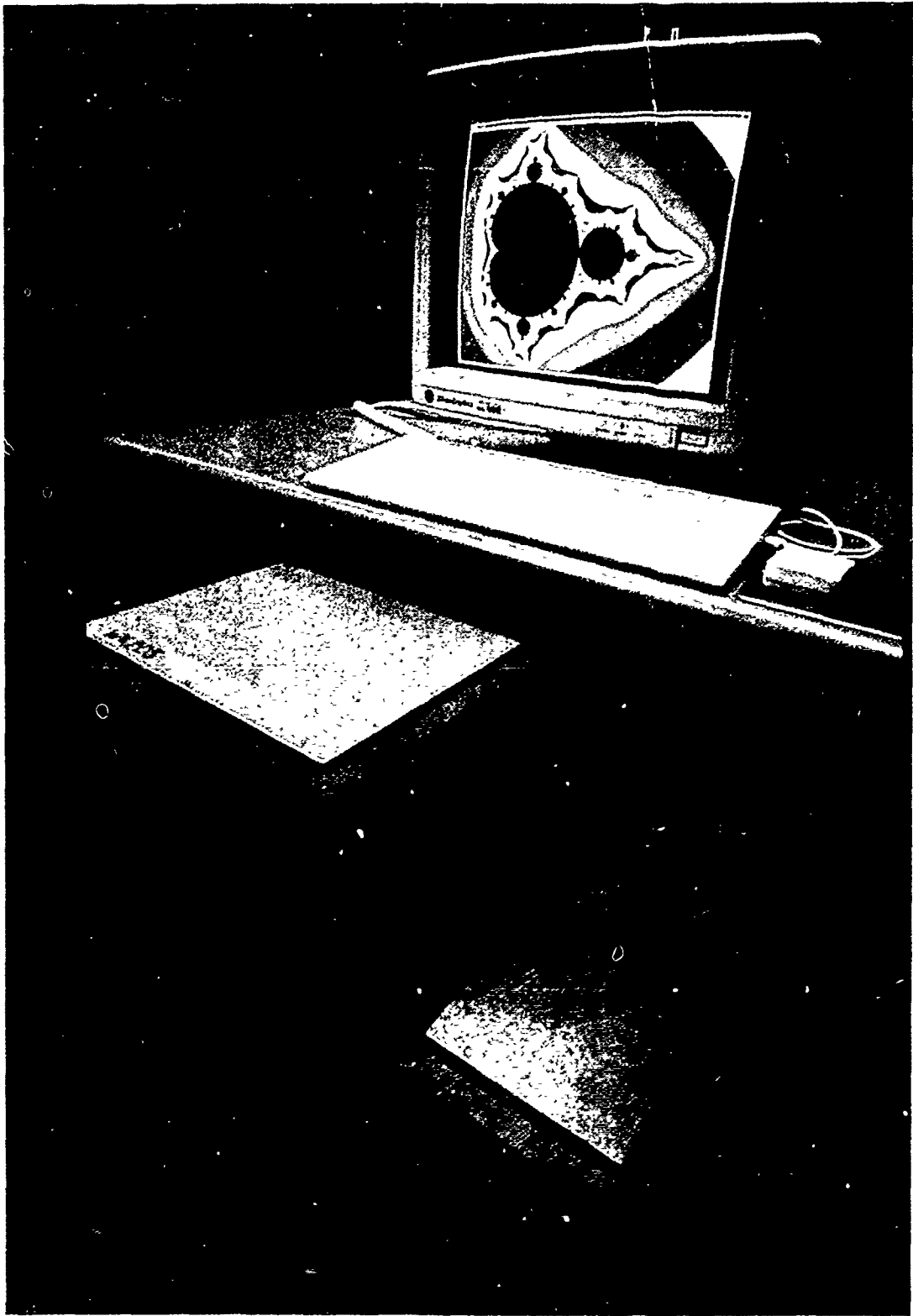
Figure 5-2. SGI 4D/320 VGX Graphics Workstation

5-2 Award of Second Generation Graphics Workstation Contract

Objective. To provide scientific users of the Numerical Aerodynamic Simulation (NAS) Facility with state-of-the-art graphics workstations for supercomputer simulations.

Approach. A full and open competitive procurement was undertaken. A Request for Information was released in April 1987. After extensive discussions with prospective vendors and the development of both compute-intensive and graphics benchmarks, the Request for Proposals for a requirements-type contract was released in January 1989.

Accomplishments. Proposal evaluation, best-and-final evaluation, selection, and negotiations led to the contract award (NAS2-13222) to Silicon Graphics Incorporated (SGI) on June 21, 1990. Contract modifications to incorporate the latest SGI technology and an initial order were made on June 22, 1990. The contract is open to all NASA scientists (whether users of the NAS Facility or not) and to other Government scientists who use the NAS Facility. The system selected was an SGI 4D/320VGX, which includes two general purpose processors, powerful 3-D graphics engines, 140-bits-per-pixel graphics, 48 megabytes of memory, a 780-megabyte disk drive, a 1/4-inch tape drive, and a high-performance I/O (input/output) channel. The firm fixed price is considerably less than the current GSA discount. Other high-end SGI systems and support peripherals are also available through this contract.

Significance. This workstation will increase the computational scientist's productivity in visualizing and understanding computational fluid dynamics or other simulation results. The current NAS workstation is the SGI 4D/70G. In comparison, the 4D/320VGX has 5 times the computing power and 10 times the graphics power as measured by NAS benchmarks.

Status/Plans. The NAS Program will provide, as budget permits, 12 of these systems to each of the OAET centers (ARC, LaRC, LeRC) for users of the NAS Facility. The intent is to use this contract for 3 years, after which a new competitive procurement will be undertaken.

Thomas Lasinski
NAS Applied Research Office
Ames Research Center
(415) 604-4405
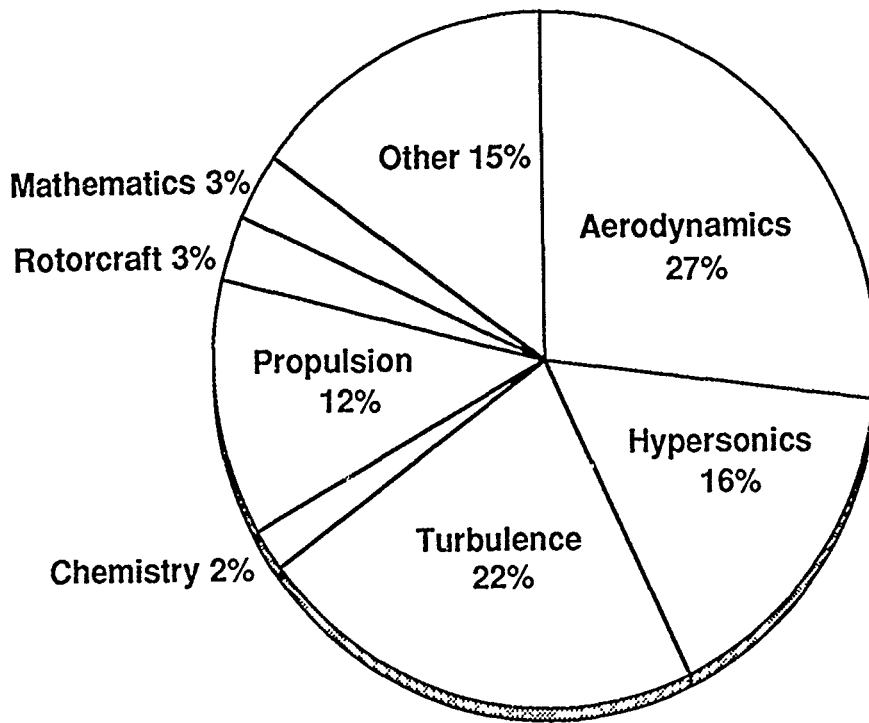
by discipline
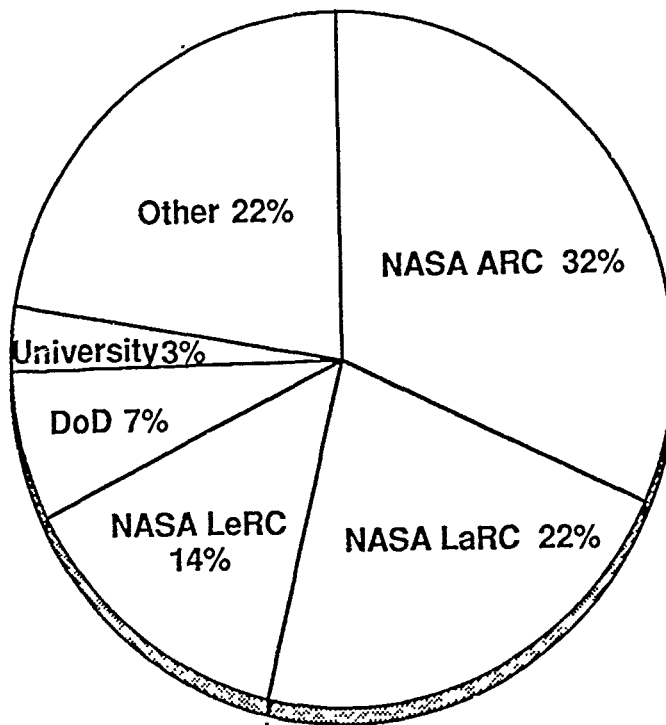
by location

Figure 5-3. NAS HSP Utilization 89/90 Operations Year

5-3 Service and Support of NAS

Objective. To provide a national computational capability to NASA, Department of Defense, industry, other Government agencies, and universities as a necessary element in ensuring continuing leadership in computational fluid dynamics and related computational aerospace disciplines.

Approach. A stable, state-of-the-art supercomputer environment will be maintained for NAS clients by managing NAS production systems, providing around-the-clock operations and client services, and incorporating new technology into the production system in an aggressive manner. NAS's primary computational resources are a Cray-2 and a Cray Y-MP.

Accomplishments. For the 89/90 Operational Period (March 1, 1989 to March 3, 1990), over 1600 scientific users worked on more than 450 scientific projects from over 130 locations nationwide. A total of 119,000 Cray-2 equivalent CPU (central proce unit) hours were used by scientific wc In addition, processing priority was provided to projects of special importance. The Cray-2 had an availability of 96%, and the newly installed Y-MP had an availability of 95%. The Y-MP statistic is particularly significant since this period includes the early operational use of the first customer shipped Y-MP, and the Y-MP upgrade to 128 megawords. Multi-user support systems had a composite availability of 97%. The systems were utilized more than 98% throughout the year. In addition, the interconnection between the Cray-2 and Y-MP was upgraded to 800 megabits per second, and NAS served as an alpha or beta test site for each major new UNICOS release.

Significance. The NAS Processing System Network has been constantly enhanced with leading edge technology while maintaining its production availability to NAS users. This early introduction of new technology has resulted in significant improvements in computing performance and functionality.

Status/Plans. We will continue to provide support to the NAS client community by improving service and incorporating new technology.

William T.C. Kramer
NAS Computational Services Branch
Ames Research Center
(415) 604-4600

UTS/580 version 1.2.4

```
┌─────────────────────────────────────────────────────────────┐
│                    ┌──────────────────────────────────────┐  │
│                    │   Rapid Access Storage Hierarchy     │  │
│                    └──────────────────────────────────────┘  │
│                          ▲              ▲                     │
│   ┌──────────────┐                 ┌──────────┐              │
│   │  Bulk File   │                 │  Volume  │              │
│   │  Transfer    │                 │  Manager │              │
│   └──────────────┘     ┌────────┐  └──────────┘              │
│                        │  File  │       ▲                    │
│        ┌─────────┐     │ System │  ┌──────────────┐          │
│        │ rcp/ftp │     │Utilities│  │  STK 4400    │          │
│        └─────────┘     └────────┘  │  Repository  │          │
│                                     │  Controller  │          │
│                                     └──────────────┘          │
```

User Space
- -
Kernel Space

```
┌─────────────────────────────────────────────────────────────┐
│        ┌─────┐  ┌───────────────────────────────┐           │
│        │     │  │       UTS File System         │           │
│        │  S  │  │  (includes file system switch) │           │
│        │  o  │  └───────────────────────────────┘           │
│        │  c  │        ┌──────────────────┐                  │
│        │  k  │        │       RAID       │      Kernel       │
│        │  e  │        └──────────────────┘      Routines     │
│        │  t  │                                               │
│        └─────┘                                               │
│                     Device Drivers                            │
└─────────────────────────────────────────────────────────────┘
```

```
┌──────────┐   ┌──────────┐   ┌──────────┐
│ Non-MSS  │   │ STK 4400 │   │          │
│  DASD    │   │   (2)    │   │          │
└──────────┘   └──────────┘   │          │
┌──────────┐   ┌──────────┐   ┌──────────┐
│HYPERchannel│ │ MSS DASD │   │3480 Tape │
│Interfaces │  │ 240 GB   │   │ Operator │
└──────────┘   └──────────┘   │ Console  │
                               └──────────┘
```
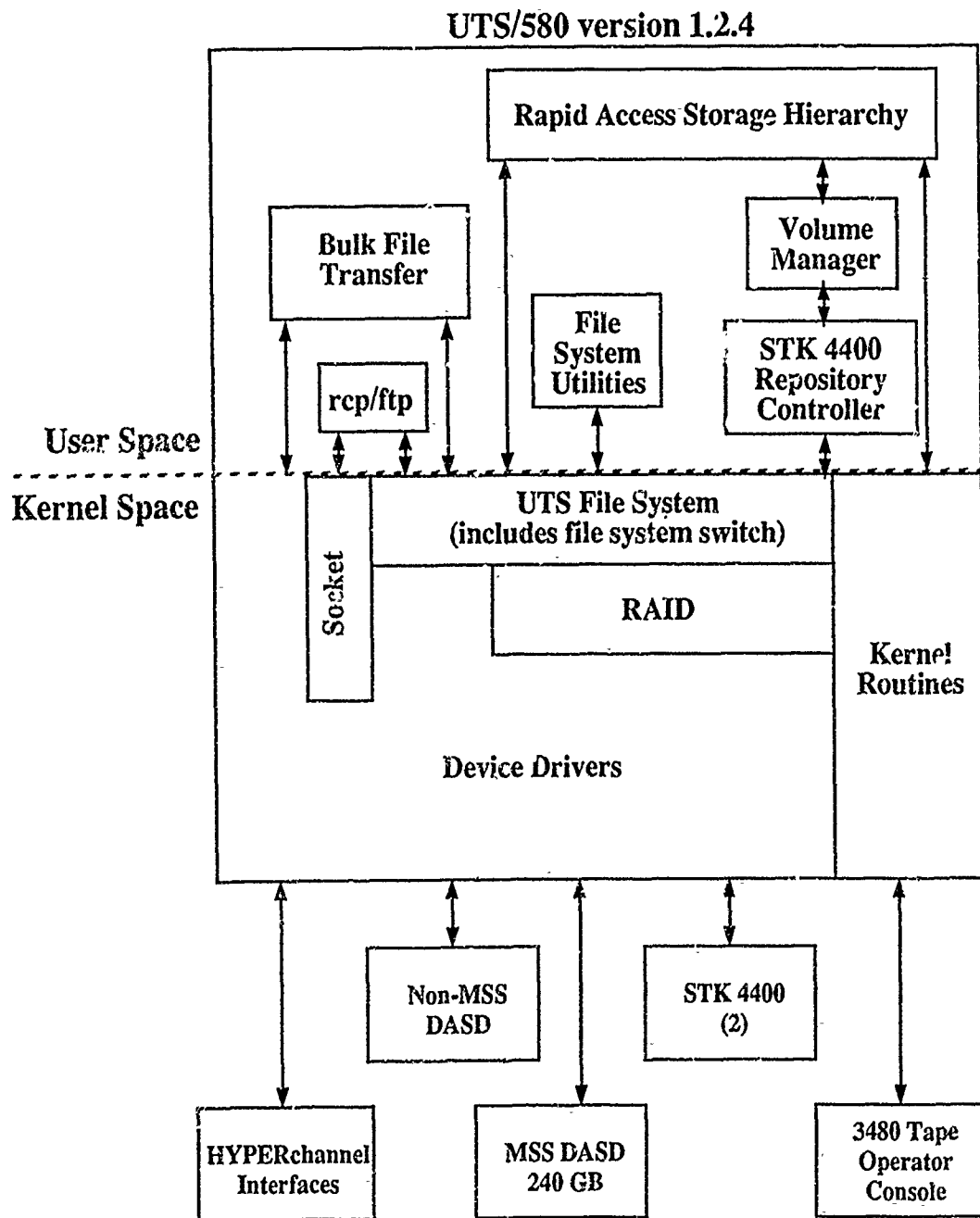
Figure 5-4. MSS 2 Software Configuration

72

5-4 Mass Storage System Version 2.0

Objective. To provide a high-performance, highly reliable, user-transparent Mass Storage System (MSS) for integration into the UNIX and TCP/IP (Transmission Control Protocol/Internet Protocol) open systems architecture environment.

Approach. MSS 2 is designed to appear to users as a normal UNIX system with a large complement of very fast, very reliable disks. This has been accomplished by incorporating three separate changes into Amdahl's UTS 1.2 implementation of UNIX. The first is the High Performance File System, a fault-tolerant parallel-access disk file system, which provides rapid access to large files while eliminating system interruptions for backups. The second is the Rapid Access Storage Hierarchy, through which all files appear to be on disk, despite the fact that infrequently used files are actually stored on less expensive tape. The third is the Volume Manager, which controls automated and manual volume mounts and dismounts. To make the system's file transfer capabilities available to the supercomputers on the network, a high-performance parallel network access method was also incorporated.

Accomplishments. Release 2.0 was delivered to the NAS Systems Development Branch for testing in January 1990. Maintenance release 2.0.1 (April 1990) included an interim striping network utility, an MSS 1 to MSS 2 file conversion utility, and a delayed file hardening feature.

Significance. MSS 2 offers NAS users the best file transfer performance (10 megabytes per second) of any Mass Storage System of which we are aware. It is also the MSS most suited for use in the UNIX and TCP/IP environment. It is able to survive any single hardware or media failure without data loss. Its automatic restoration of archived files upon demand allows users to direct access their files, regardless of whether they are on disk or tape.

Status/Plans. A second maintenance release, 2.0.2, is planned for the first week in July, immediately prior to the production debut of MSS 2. There are plans for further enhancement releases, culminating with release 2.4. At that point, MSS 2 will be ported to the next major release of UTS, will have a transfer rate of 20 to 30 megabytes per second, and will no longer have the current maximum file size limit of 2 gigabytes.

David Tweten
NAS Systems Development Branch
Ames Research Center
(415) 604-4416
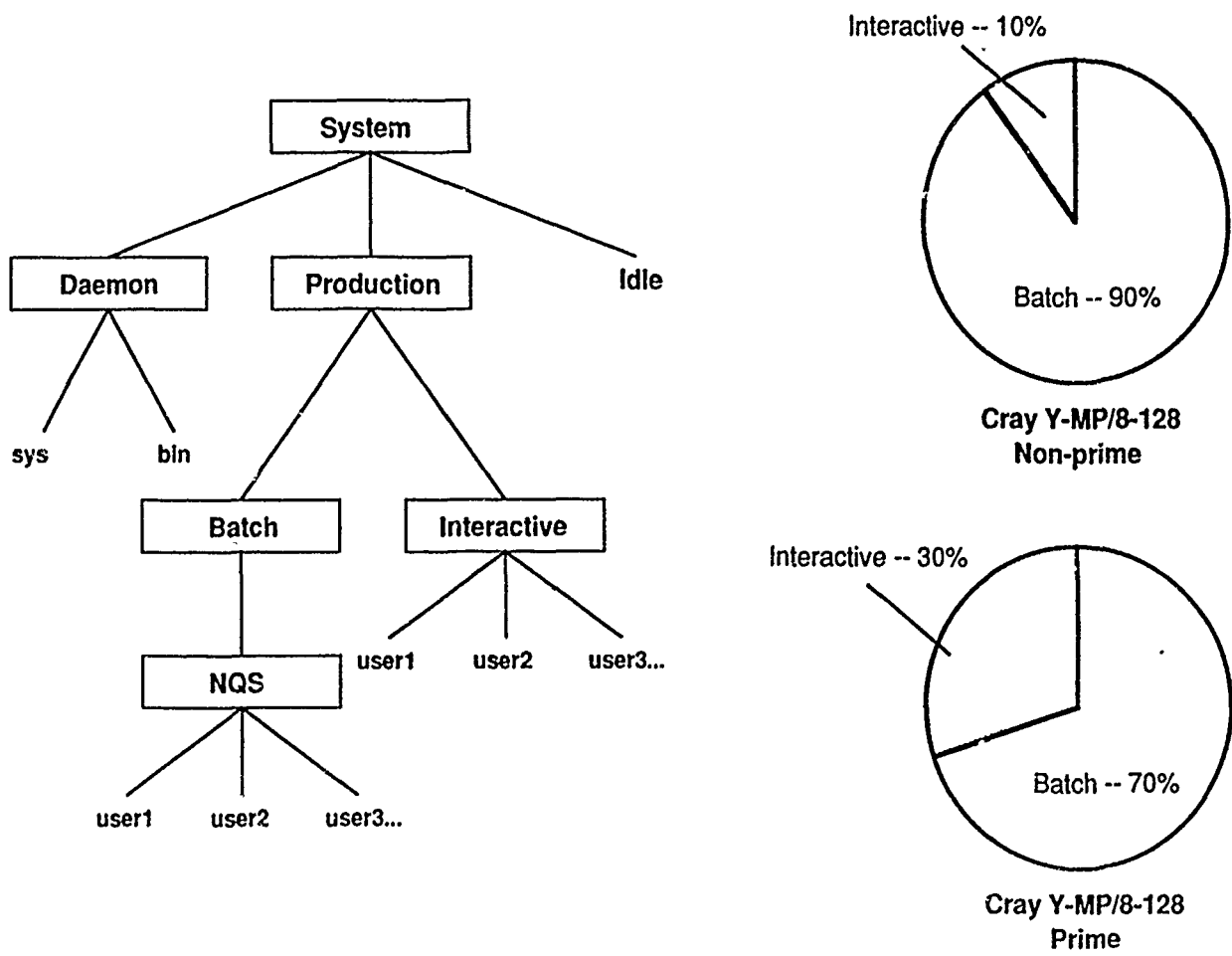
Figure 5-5. The Fair Share Scheduler

5-5 Installation of the Fair Share Scheduler

Objective. To better manage the daytime High-Speed Processor interactive workloads that were interfering with batch (NQS) throughput and causing high levels of swapping.

Approach. The Fair Share Scheduler was selected as a mechanism to distribute system resources more equitably among interactive users and to provide a guaranteed percentage of CPU (central processing unit) cycles to NQS jobs. It was configured to support different resource allocations for interactive and batch processes. In addition, suitable modifications were made to the Network Queuing System so that it could interact properly with the Scheduler. Bugs and limitations in the Fair Share Scheduler and related tools as provided by Cray Research Inc. were rectified, while the additional tools needed were identified and written.

Accomplishments. The Fair Share Scheduler was enabled on both the Cray-2 and Cray Y-MP in early December 1989. Swapping was reduced dramatically, and NQS throughput improved and became more predictable.

Significance. NAS became one of the first supercomputer centers to run the Fair Share Scheduler. In addition to solving the immediate problems in a direct and efficient manner, the Fair Share Scheduler provided NAS with new functionality and flexibility. For example, during the Y-MP memory upgrade acceptance period, up to 90% of system resources were made available for acceptance tests without reconfiguration. This allowed rapid isolation of problems and accelerated corrective action.

Status/Plans. The Fair Share Scheduler is in production. NAS has met several times with the developers and plans to evaluate a new and more comprehensive version called Share.

Toby Harness
NAS Computational Services Branch
Ames Research Center
(415) 604-4310
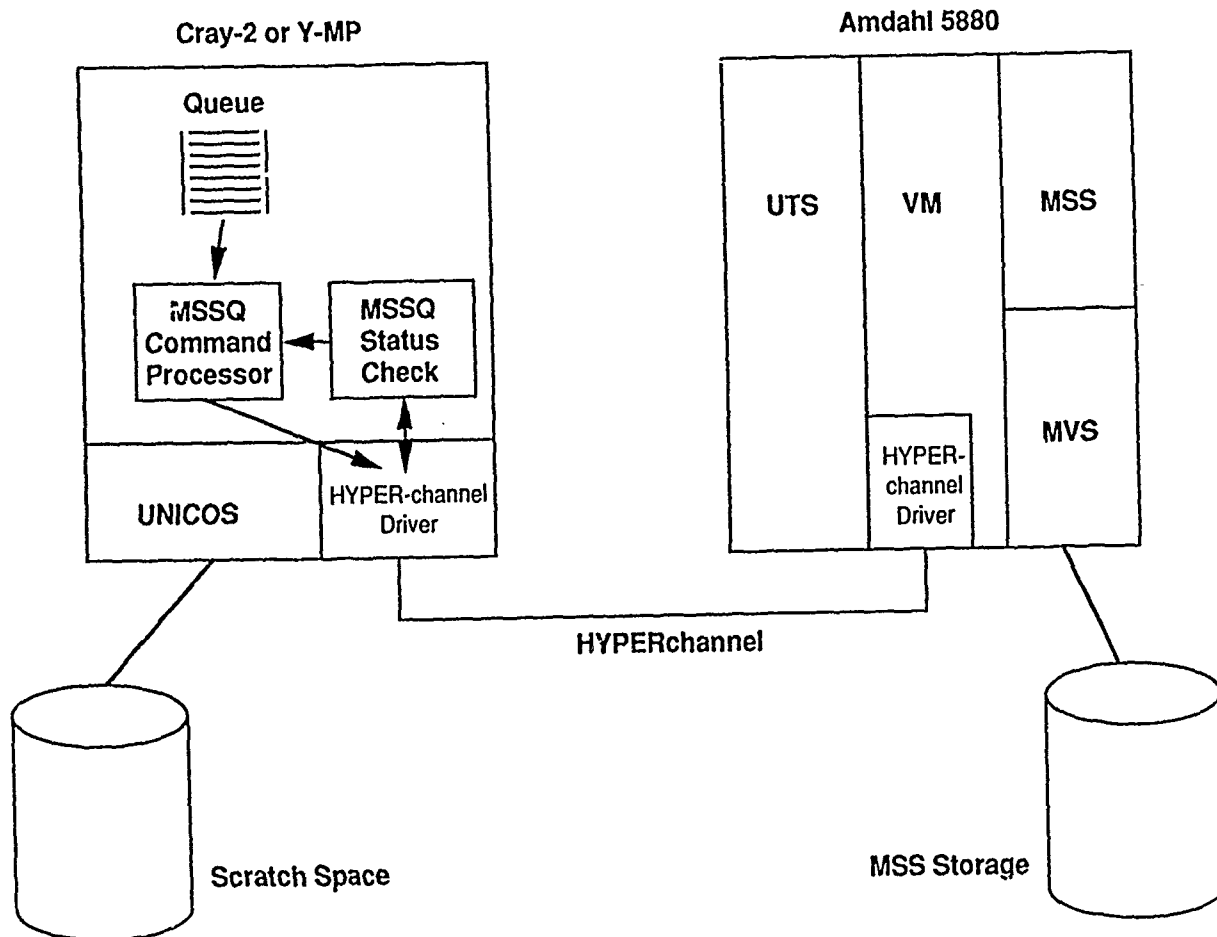
Figure 5-6. MSSQ Component Diagram

76

5-6 MSSQ

Objective. To eliminate the need for Mass Storage System (MSS) users to be aware of MSS system availability before submitting transmission commands and to ensure that every MSS transmission command is executed, regardless of MSS system condition when the command is submitted by the user.

Approach. Because the UTS, MVS, and VM operating system components of MSS are not accessible from UNICOS on the Crays, MSS commands issued during scheduled or unscheduled MVS or VM outages failed without notification to the user. This required the user to constantly check for successful transmission, and resubmit the commands if they failed. The approach was to develop an MSS interface (MSSQ) to hold user commands in a queue on the Crays and automatically issue them based upon MSS resource availability. An MSSQ process reporting utility was developed to inform users of the status of their commands.

Accomplishments. A set of MSSQ commands was implemented in September 1989.

Significance. User inconvenience and time consumption was reduced in accordance with the objective. The user is now shielded from both scheduled and unscheduled MSS outages while being given current status on MSSQ processes. NAS MSS transmission volume has increased from 2 gigabytes per day in September 1989 to 8 gigabytes per day in June 1990, partly as a result of MSSQ.

Status/Plans. Since installation, MSSQ has been a stable and indispensable part of the Mass Storage System. Plans are to leave it in place without enhancement during the installation of MSS 2.

Julian Richards
NAS Computational Services Branch
Ames Research Center
(415) 604-46119
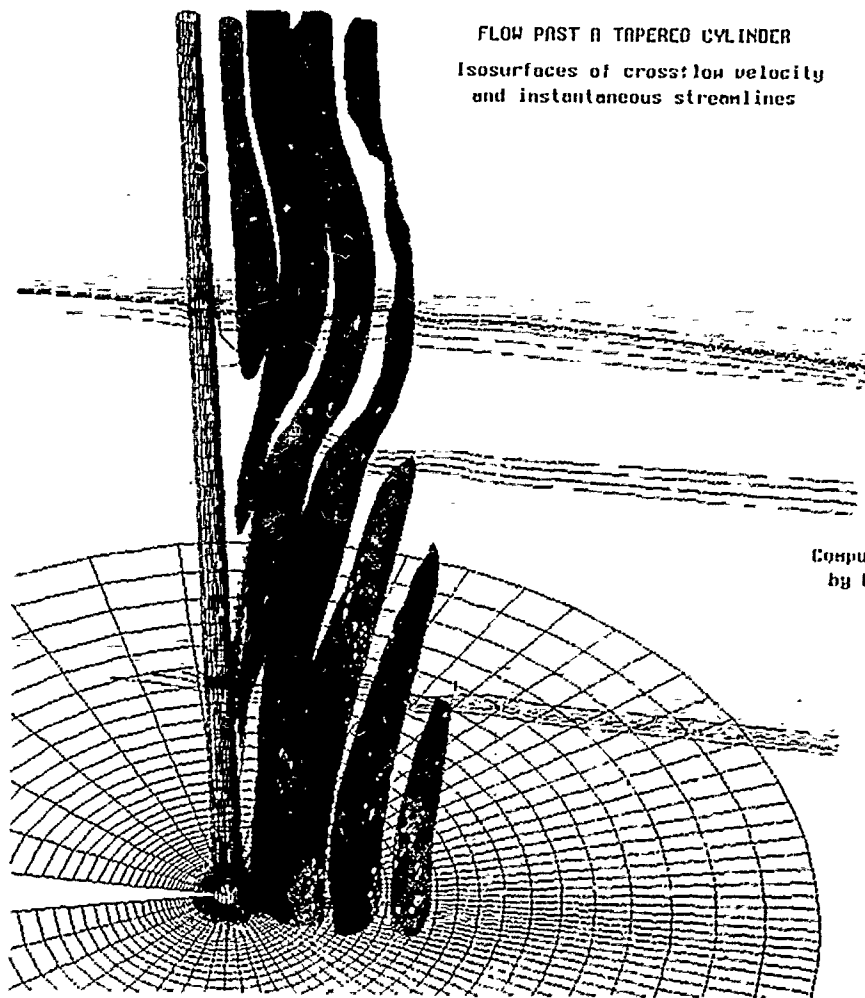
FLOW PAST A TAPERED CYLINDER

Isosurfaces of crossflow velocity
and instantaneous streamlines

0.200	MACH
0.00 DEG	ALPHA
1.23x10**2	Re
1.15x10**4	TIME
64x64x32	GRID

Computed on the NAS Connection Machine
by Dennis Jespersen and Creon Levit
NASA/Ames Research Center

Figure 5-7. Solution of 3-D Unsteady Flows on the Connection Machine Using Explicit and Factored Implicit Methods

78

5-7 Solution of 3-D Unsteady Flows on the Connection Machine Using Explicit and Factored Implicit Methods

Objective. To design, implement, verify, and utilize a three-dimensional full Navier-Stokes solver on the Connection Machine (CM).

Approach. A 3-D full Navier-Stokes solver was implemented from scratch on the CM-2 in the starlisp language. Thin layer diagonal implicit options were verified using ARC3D on the Cray Y-MP.

Accomplishments. The code has been completed. The 3-D unsteady cylinder flow problems were solved for code RFAF. The 3-D unsteady slender cone flows have been solved, visualized, and compared with the ongoing wind tunnel experiments of Van Atta and Picarillo at UC-San Diego.

Significance. This code demonstrates that unsteady viscous compressible flow about three-dimensional bodies can be efficiently solved on large curvilinear grids using the massively parallel SIMD (single instruction stream, multiple data stream) Connection Machine.

Status/Plans. Performance of the implicit option on 8K CM processors is comparable to a one-processor Y-MP. Performance of the explicit option is even better. We are currently running a variety of unsteady tapered cylinder flows. We will rewrite the code in CM Fortran, tune its performance, and implement additional factored and unfactored implicit solution methods.

Creon Levit
NAS Applied Research Office
Ames Research Center
(415) 604-4403
Dennis Jespersen
Comp. Fluid Dynamics Branch
Ames Research Center
(415) 604-6742
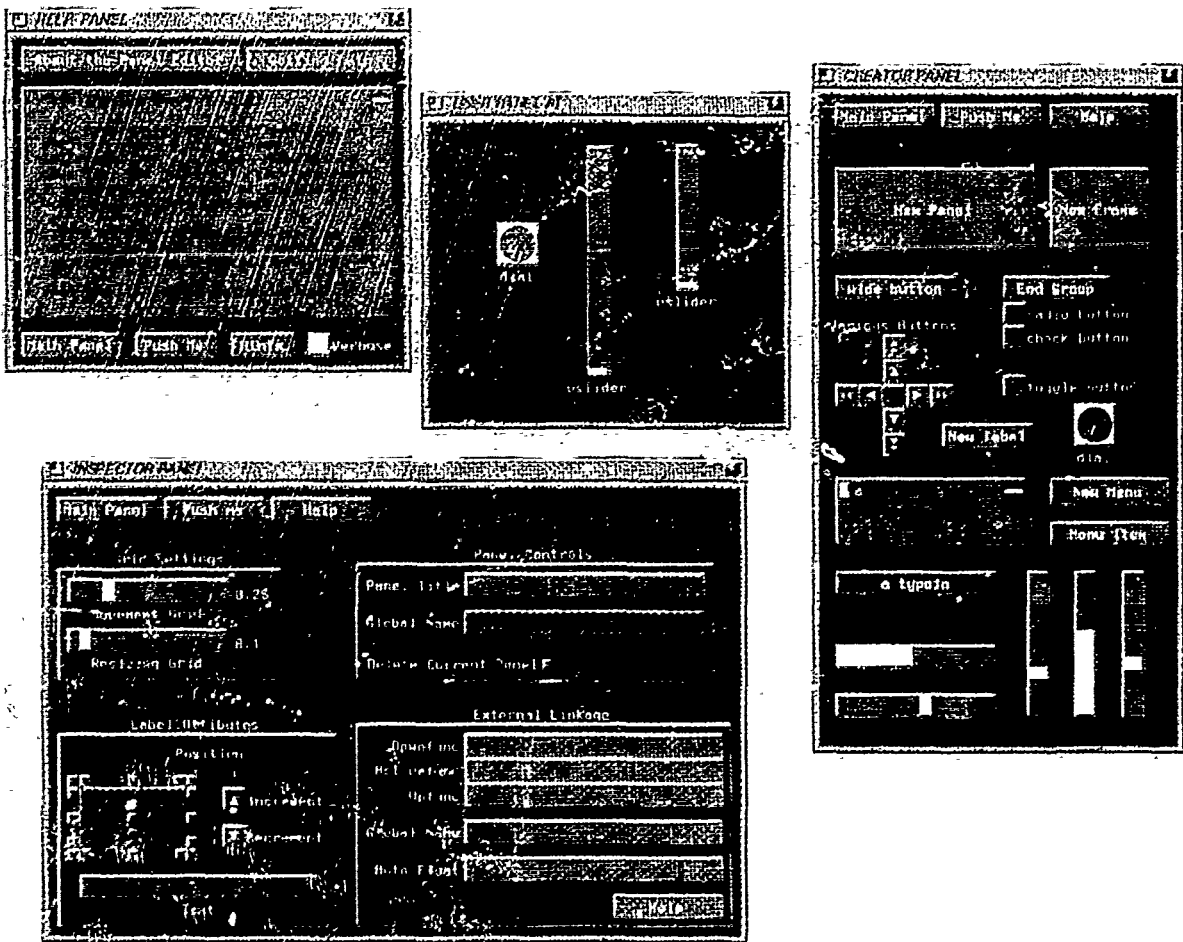
Figure 5-8. The Panel Editor

5-8 The Panel Editor

Objective. To produce a program that allows anyone to create Panel Library-based graphical user interfaces with minimal effort. If possible, it is desirable for the final program to be easily optimized by the knowledgeable end-user.

Approach. The Panel Library itself is used for the basic mouse interaction. A public domain Scheme interpreter was extended to allow calling access to Panel Library functions and data. The bulk of the Panel Editor was then written in Scheme.

Accomplishments. The Panel Editor is a fast, extensible, stand-alone program that can construct entire user interfaces with the point-and-click paradigm. Since it generates Scheme or C code that exactly reproduces the user interface as it appears on the screen, it was used to create its own interface. It is possible to escape to the underlying Scheme interpreter at any time to debug or modify its behavior. In practice, it is an extremely reliable program.

Significance. Using this tool, Panel Library user interfaces can be generated extremely quickly in C code form. This research also shows that a mixed language approach can sometimes be used to solve interesting problems, and that it is possible to have most of the advantages of both languages with almost none of the disadvantages of either.

Status/Plans. The Panel Editor is currently in beta test. Although it is definitely useful in its present form, it is being enhanced in response to user feedback.

Eric Raible
NAS Applied Research Office
Ames Research Center
(415) 604-4405

Chapter 6

Rotorcraft

The objective of the Rotorcraft Program is to provide the technologies for helicopters and other rotor-borne aircraft to achieve quiet, low-vibration operation with increased performance, agility, maneuverability, and stability, all with acceptable handling qualities. Much of the work is done in conjunction with the U.S. Army and the FAA and in cooperative programs with industry.

Improved analysis can now handle many local aerodynamic phenomena, but the transonic, unsteady, complex wake interaction flow requires another generation of codes. Therefore, much of the rotorcraft program still is empirically based, with validation of analysis as a goal. This approach requires new test techniques, upgraded test facilities, carefully instrumented models, sophisticated simulation, and increased use of the latest generation of computers. New ideas also are part of the program, since the complexity of rotorcraft makes it a fertile area for innovative approaches.

The heart of the aerodynamic portion of the program is airloads research. Small scale, pressure-tapped blade data have become available with the full-scale results due in 1991. Complimentary efforts are under way in component, interference, and wake testing and prediction. These databases are used in acoustic and vibration research, which constitutes more than half of the program resources. The airload models also will be used for rotor state control and higher harmonic control to suppress noise or vibration or to enhance maneuverability.

Handling qualities research in the Aerodynamics Division is based on vehicle flight dynamics, with emphasis on simulation and eventually flight test using a variable stability UH-60. New flight test capability is planned, with research challenges in integrated control, automation, and higher-frequency control a focus.

Higher speed rotorcraft will continue to be dominated by tiltrotor efforts. Certification issues are being addressed on the simulator and in noise testing and prediction. Also under way are improvements in performance, interior noise, vibration, and stability. The importance of these research opportunities for civil applications will be reported in 1991 under contract to Boeing Commercial Airplane Company.

Program Manager: Mr. George Unger
                     OAET/RF
                     Washington, DC 20546
                     (202) 453-5420

CIVIL TILT-ROTOR II SIMULATION
NASA VERTICAL MOTION SIMULATOR

Motivation
Civil certification of V-22 tilt-rotor will introduce a new aircraft configuration into national airspace

Objectives
- Investigate steep approaches in instrument meterological conditions for V-22-class transport tilt-rotors
- Investigate use of conversion aids
- Develop a flight path director display
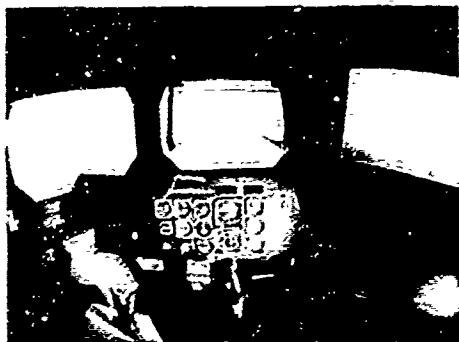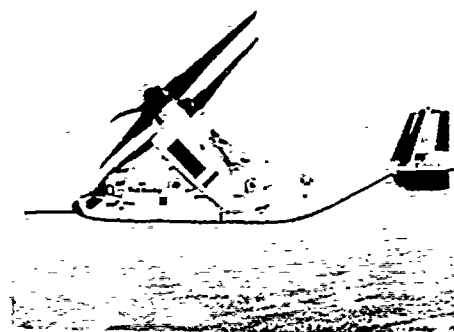
Approach
- Compare alternate glide slope angles in I.M.C.
- Government pilots (NASA, DoD, FAA)

Payoff
Civil certification criteria developed with minimum impact on V-22 test program

Figure 6-1. Civil Tilt-Rotor II Simulation
NASA Vertical Motion Simulator

84

6-1 Civil Tilt-Rotor II VMS Simulation Experiment

Objectives. The Civil Tilt-Rotor II (CTR-2) experiment continued investigation of issues facing civil certification of transport-category tiltrotor aircraft. Specific to the CTR-2 experiment was an investigation of steep approaches to short landings in instrument meteorological conditions using "raw data" instrument guidance. This represents a worst case scenario of minimal instrument flight equipment. Supplemental investigations included an initial evaluation of aids for reconversion (from airplane-mode to helicopter-mode flight) and development of a flight path display as an alternative to a flight director. Previous civil tiltrotor experiments rated the level flight tiltrotor reconversion as a Level 2 handling qualities task, hence requiring improvement for routine operations.

Approach. The test matrix for the principal investigation of steep glide slopes included six glide slope angles (6° to 25°) and six atmospheric conditions. Eight government pilots evaluated their task performance and workload for the reconversion from airplane-mode flight at 180 knots to the approach configuration, glide slope tracking on the approach, and the landing.

Accomplishments. Over 400 evaluation runs were made by eight government pilots. Using raw data instrument guidance, fundamental design issues were raised for instrument approaches on steep glide slopes. The 6° glide slope was flown at a speed at or above the "power bucket" speed. Hence pilots used the more familiar "front-side" control technique, keeping pilot workload manageable for marginal Level I handling qualities. All of the steeper approach angles suffered from the need for the less familiar "back-side" control technique. Pilot ratings for the steeper approaches were solidly Level II, making them undesirable even as a back-up mode.

Significance. The simulation experiment and its results helped focus the FAA on requirements for certification of tiltrotors using steep approaches. The poor pilot ratings and task performance for glide slopes of 9° and higher suggests minimum equipment lists requiring more than raw data instrumentation for those approaches in Instrument Meteorological Conditions (IMC) conditions. Both the conversion aids and the flight path vector display point the way toward technology that can achieve the desired performance in IMC operations.

Status/Plans. Having bounded the problem of steep approaches with minimum instrument equipment, and finding it unsatisfactory for the task, the next step is to evaluate technology that might provide desired performance. A simulation experiment planned for winter 1990-91 will evaluate the use of a three- or four-cue flight director or the flight-path-vector display to assist such approaches. Similarly, the reconversion problem will be addressed by improvements to the conversion aid concepts and displays.

William A. Decker
Flight Dynamics and Controls Branch
Ames Research Center
(415) 604-5007
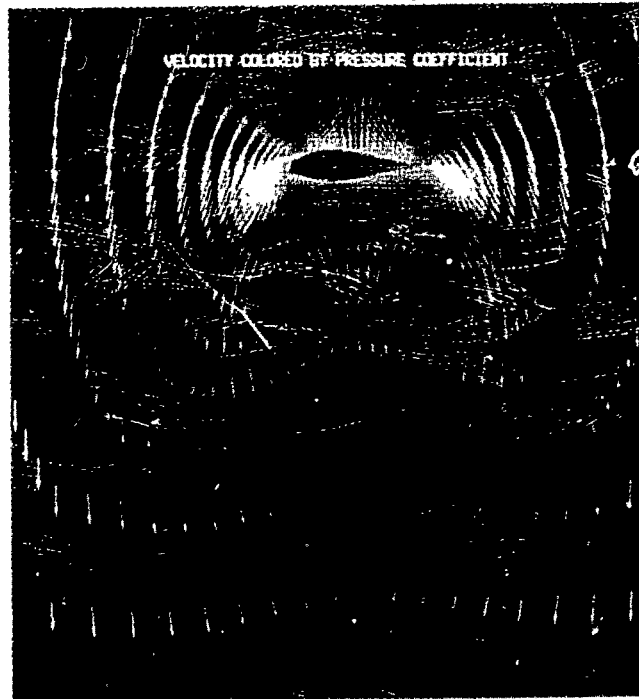
2-D NAVIER STOKES MODEL
OF V-22 WING IN HOVER
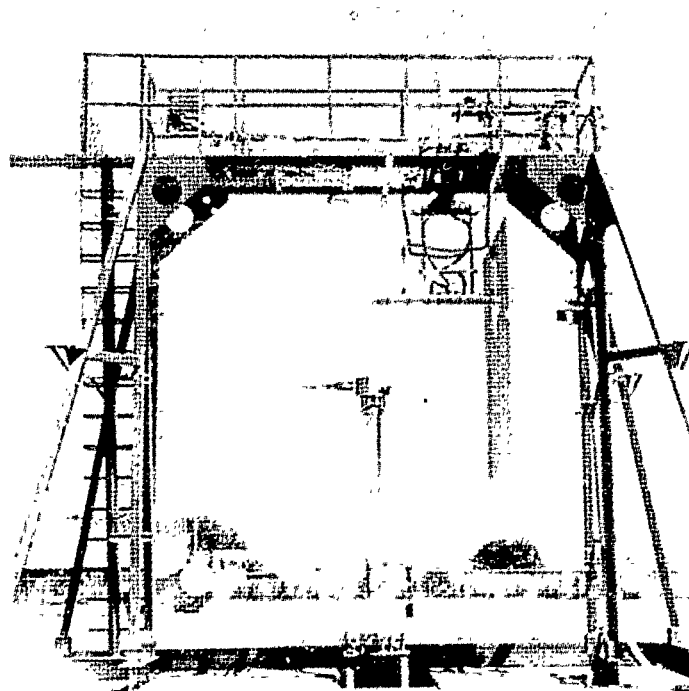
NEW HOVER TEST RIG
WITH SEMI-SPAN WING

Figure 6-2. Tiltrotor Download Reduction Program

6-2 Tiltrotor Download Reduction Program

Objective. To develop validated analyses and evaluate tiltrotor download concepts to minimize the download experienced by the hovering tiltrotor aircraft. Accurate viscid analysis methods will be developed to understand the fundamental fluid behavior of rotor wake/wing interaction and significant reductions in tiltrotor download will be demonstrated to increase the hover load capability of the aircraft or increase useful mission range.

Approach. We plan to develop accurate numerical prediction techniques concurrently and conduct experimental investigations to demonstrate download reduction. Full three-dimensional unsteady thin layer Navier-Stokes and unsteady panel models of the rotor wake/wing/fuselage interaction will also be developed, and the new Ames Hover Test Rig (HTR) will be developed and tested for evaluating promising concepts for download reduction in small scale at the NFAC Outdoor Aerodynamics Research Facility (OARF).

Accomplishments. The unsteady loading and vortical shedding of a V-22 wing in a downwash field was calculated in two-dimensions. Coherent, oscillating shed vortical structures in the wing wake was captured. Test preparations were completed for the new HTR with a 7-foot diameter V-22 scaled rotor system at the OARF. Scaled wing with upper surface blowing for download reduction was tested. Together with Continuum Dynamics, Inc., we identified new upper surface modification to reduce download.

Significance. First successful calculation of tiltrotor wing wake in two dimensions using Navier-Stokes model which can be used to investigate various parameters influencing tiltrotor download. HTR is a new national research capability for hover tiltrotor studies, and it can be used for aerodynamic performance and acoustics research.

Status/Plans. Extend Navier-Stokes model to three dimensions and include realistic rotor wake model and experimentally investigate various download reduction devices on two different wings at the OARF. We will acquire wide-field shadowgraphs for the model tiltrotor system together with full rotor performance documentation and will correlate small-scale and large-scale semi-span tiltrotor and wing download performance data to determine scaling effects.

Jeffrey Light , Alexandra Frerking
Rotorcraft Aeromechanics Branch
Ames Research Center
FTS 464-4881 or FTS 464-6856

OASPL, dB

65° NACELLE TILT
130 KNOTS
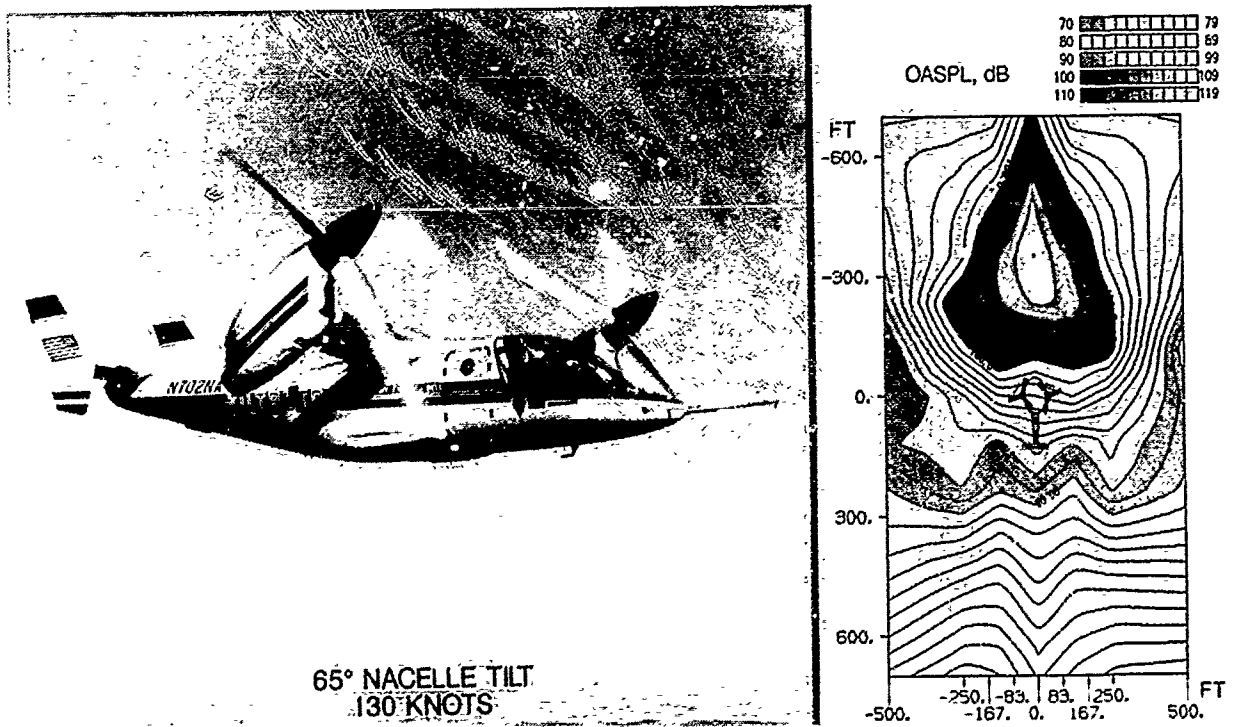
Figure 6-3. XV-15 Tiltrotor Far Field Acoustics Flight Test Ground Contour Generation

88

6-3 XV-15 Tiltrotor Far-Field Acoustics Flight Test Ground Contour Generation

Objective. To measure the far-field acoustics from the current tiltrotor configuration and to establish a high-confidence level (90%), accurate (±1.5 dB) far-field acoustics data base for validation of ROTONET and other noise prediction codes.

Approach. Langley Research Center entered into a joint agreement with Bell Helicopter Textron Incorporated to conduct noise tests on the XV-15 tiltrotor aircraft. Level flyover tests were conducted for a range of velocities, altitudes, and nacelle tilt angles.

Accomplishments. The tiltrotor flight test program was conducted during September 1988. The aircraft was repeatedly flown over a 20-element microphone array to provide ensemble-averaged sideline acoustic measurements, as well as direct overhead measurements. Acoustic data were obtained for 29 different flyover conditions. The aircraft flew the same trim conditions at both 250-foot and 750-foot altitudes, which yielded a total of nine ensembled average data points beneath the aircraft. The 750-foot measurements were corrected to a 250-foot propagation distance. This highly accurate data set was then used to produce ground contour of the acoustic far-field footprint.

Significance. The tiltrotor aircraft is relatively quiet when operating in the airplane mode; however, when operating in a typical approach configuration, the noise level increases significantly due to the impulsive content of the acoustic signal. Since the approach configuration is most critical to community acceptance, the high noise levels could present problems at proposed heliports.

Status/Plans. The data are being analyzed using the Langley refined ensemble-averaging technique for an improved confidence interval. These results have been incorporated into the ROTONET data base and are being used to validate ROTONET predictions.

Robert A. Golub
Aeroacoustics Branch
Langley Research Center
(804) 864-5281

PORT SIDE

STARBOARD SIDE
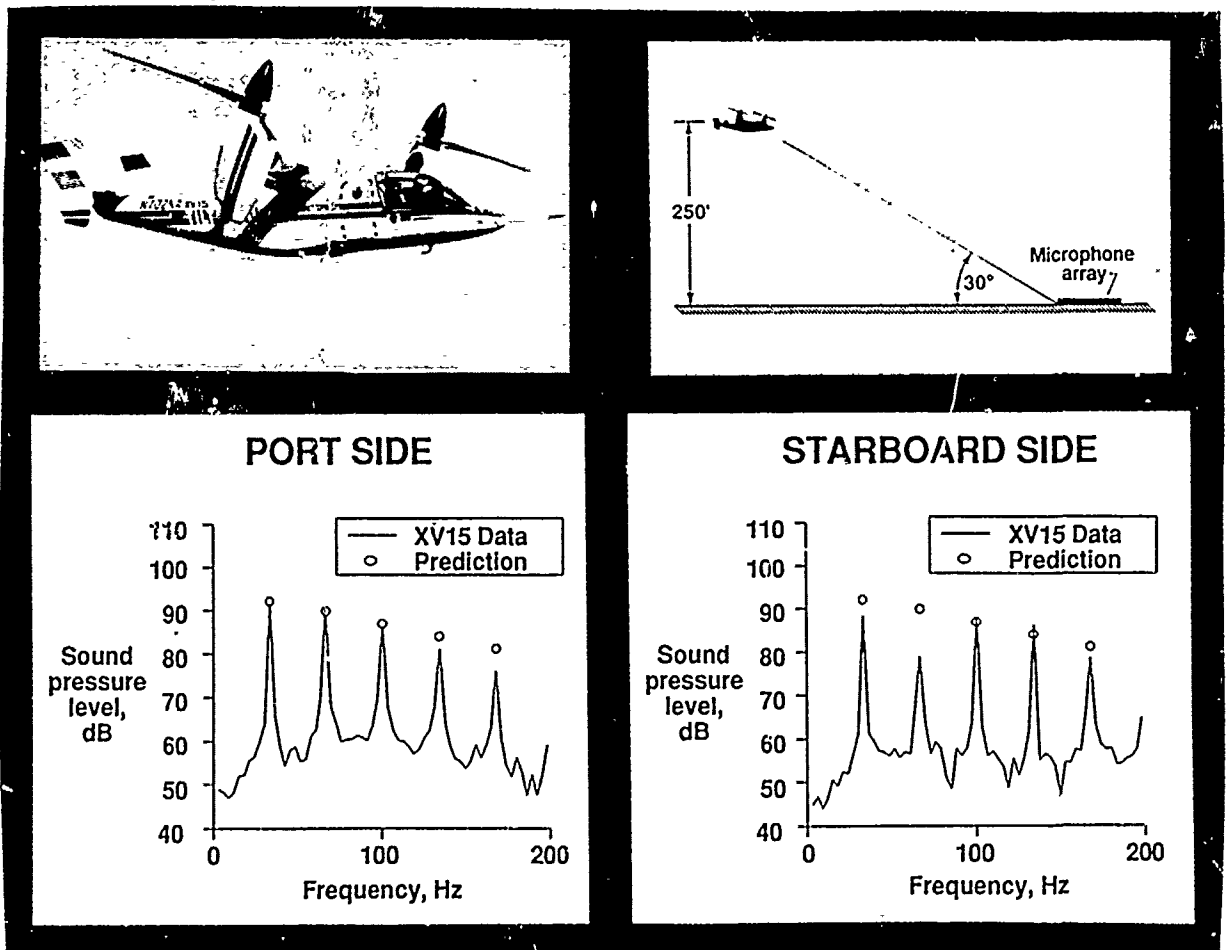
Figure 6-4. XV-15 Tiltrotor Noise Prediciton Validation

6-4 ROTONET Predictions of XV-15 Tiltrotor Far-Field Acoustics

Objective. To use the high confidence level (90%), accurate ($\pm$1.5 dB) XV-15 far-field acoustics data base to validate ROTONET predictions.

Approach. LaRC entered a joint agreement with Bell Helicopter to conduct noise tests on the XV-15 tiltrotor aircraft. Level flyover tests were conducted for a range of velocities, altitudes, and nacelle tilt angles. The data have been installed into an ANOPP data base for comparison with ROTONET predictions.

Accomplishments. The tiltrotor flight test program was conducted during September 1988. The aircraft was repeatedly flown over a 20-element microphone array to provide ensemble-averaged acoustic measurements. Acoustic data were obtained for 29 different flyover conditions. For the data shown in the figure, the aircraft was at an altitude of 250 feet and approximately 30° above the horizon with respect to the microphone position, as shown in the upper right of the figure. The lower half of the figure presents experimental data (solid lines) for the port and starboard aircraft sides corresponding to narrowband analyses for the aircraft traveling at 90 knots in an approach configuration (nacelle tilt = 85°). The ROTONET predictions for this configuration were performed using the Multirotor Source Noise module (MSN). The tiltrotor aircraft blade passage frequency and its harmonics are shown by the small round circles. This prediction comparison with the experimental data is considered to be quite good and is typical of all the measured positions (5) for this particular configuration and emission angle.

Significance. These results show that the use of the ROTONET Multirotor Source Noise module to predict for the XV-15 tiltrotor aircraft yields good prediction results for the far-field rotor blade passage frequency and its harmonics.

Status/Plans. More prediction comparisons at other angles are being examined.

Robert A. Golub
Aeroacoustics Branch
Langley Research Center
(804) 864-5281

Figure 6-5. Trailed Rotor Model Ames Low-Speed Wind Tunnel Test

6-5 Fifteen Percent Scale Trailed Rotor Concept Low-Speed Wind Tunnel Test

Objective. To research the low-speed aerodynamic performance of the Trailed Rotor high-speed rotorcraft concept in the cruise configuration. A secondary objective was to make a qualitative performance comparison of the Trailed Rotor and Folding Tilt Rotor concepts.

Approach. The small-scale Trailed Rotor test was a joint program between NASA Ames, McDonnell Douglas Helicopter Company, and the Naval Air Development Center. The model was a 15% scale semi-span wing with pod and trailing blades. The model allowed for adjustments in ailerons, flaps, spoiler, wing-pod angle, the number of trailed blades, blade twist, and blade azimuth. The approach used was a component build-up of the model from a clean wing to the Trailed Rotor configuration. Additionally, modifications to the baseline five-bladed Trailed Rotor model were studied to evaluate the aerodynamic sensitivity of the concept to aircraft design issues.

Accomplishments. Low-speed testing of the Trailed Rotor model was conducted in the NASA Ames 7-by 10-foot wind tunnel. Baseline aerodynamic performance was determined through model component build-up. Test results showed only a minimal effect of the pod and trailed blades on wing aerodynamic performance as compared to the clean wing. Tradeoffs in overall wing/pod aerodynamics due to model configuration changes were identified. Test results showed qualitatively the advantages of the Trailed Rotor concept over the Folding Tilt Rotor concept in cruise performance.

Significance. Results from this research demonstrated the low-speed performance characteristics of a Trailed Rotor. Evaluations of various model configurations and trailed blade changes identified technical areas that need further study to optimize wing, pod, and trailed blades integration.

Status/Plans. The current test has been completed. Future plans include a high-speed cruise performance test and a large-scale trailed rotor conversion test.

Jeffrey Johnson, Stephen Swanson, Larry Young
Rotorcraft Aeromechanics Branch
Ames Research Center
(415) 464-6976, (415) 464-4565
or (415) 464-4022
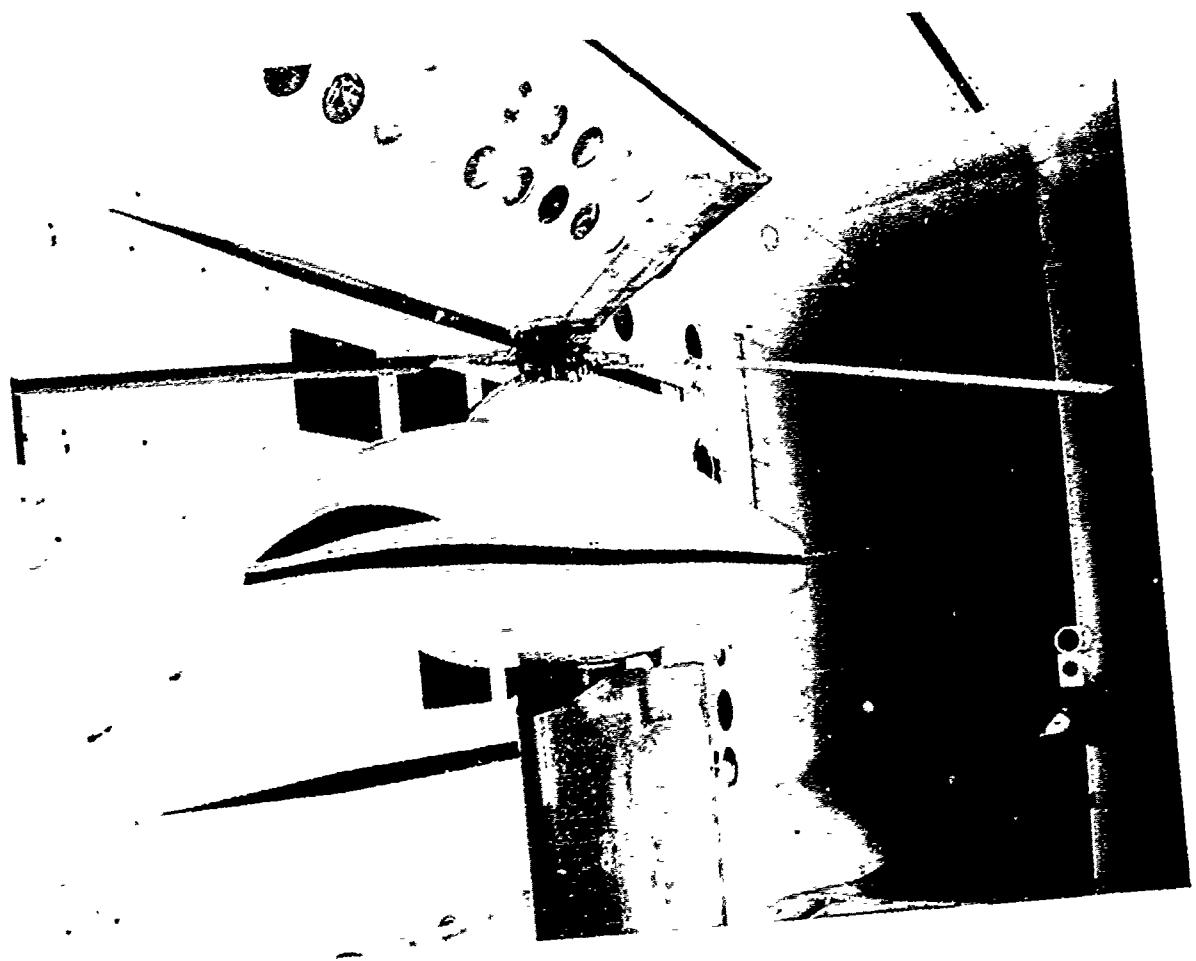
Figure 6-6. Extension-Twist Coupling Concept Demonstrated in TDT

94

6-6 Extension-Twist Coupling Concept Demonstrated in TDT

Objective. Tiltrotor aircraft are designed to operate in both helicopter and airplane modes of flight. This operational flexibility results in several conflicting design requirements. One such design requirement, which has significant effects on aerodynamic performance, is blade twist. Typically, the twist employed is a compromise between that required in the two different modes of flight. Performance could be improved if it were possible to vary the blade twist between the two flight modes. Tiltrotor aircraft typically vary rotor speed by about 20% between the two flight modes. This change in rotor speed induces a rather substantial change in the centrifugal force along the blade, which could be used to passively change the twist of an extension-twist-coupled composite blade. Thus, the objective is to design an extension-twist-coupled composite blade to have optimum twist distributions in both airplane and helicopter flight modes.

Approach. Analytical and experimental studies have been designed to demonstrate the improvements in tiltrotor blade performance. These studies include whirl tests and wind tunnel tests conducted on a set of model-scale blades, with the primary goal of measuring blade twist as a function of rotor speed. Results from this experimental phase will be compared with those obtained from analytical studies using companion finite-element analysis models of the rotor blade.

Accomplishments. The set of composite model rotor blades used in this research investigation was manufactured from existing blade molds for a low-twist metal helicopter rotor blade, and was designed with a view towards establishing a preliminary "proof of concept" for extension-twist-coupled rotor blades. Wind tunnel testing of the set of extension-twist-coupled rotor blades was re-cently completed in the NASA Langley Transonic Dynamics Tunnel, following an abbreviated initial entry in the hover test facility. Data were obtained in hover for both a ballasted and unballasted configuration in ambient air conditions, and a ballasted configuration (only) in near-vacuum conditions. The blades were mounted on the Aeroelastic Research Experimental System (ARES) helicopter model and were spun through the 100-800 rpm range, with a corresponding sweep of collective pitch at 100 rpm intervals. While preliminary results indicate a maximum twist of approximately 5° was obtained with the ballasted blades, yielding good preliminary agreement with analysis, further and more comprehensive data reduction is currently under way.

Significance. This task has demonstrated the feasibility of changing blade twist as a function of rotor speed using an extension-twist-coupled composite blade design.

Status/Plans. As discussed above, comprehensive data reduction shall be performed and compared with results obtained from finite-element analyses of the model blade. The comparison of these results will provide a basis for the design of a highly twisted extension-twist-coupled model blade for tiltrotor aircraft.

Renee C. Lake, Mark W. Nixon
Configuration Aeroelasticity Branch
Langley Research Center
(804) 864-1226

ROTONET PHASE IV SYSTEM MULTIROTOR SOURCE NOISE MODULE

NASA/MDHC FLIGHT TEST
500E EXPERIMENTAL HELICOPTER

ROTOR HEAD TELEMETRY

5 - BLADED MAIN ROTOR

BLADED TAIL ROTOR

MUFFLER

105°
75°
θ
Observation angle

HARMONICS: 1/2   1st
DATA
ROTONET

Sound pressure level, dB

θ, deg
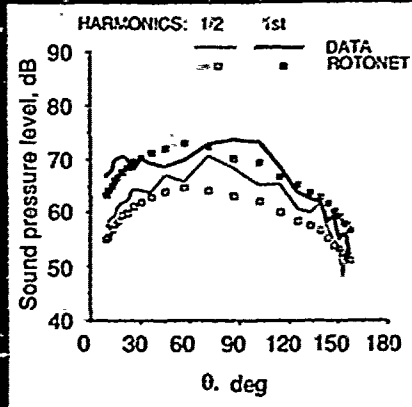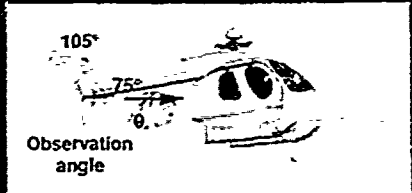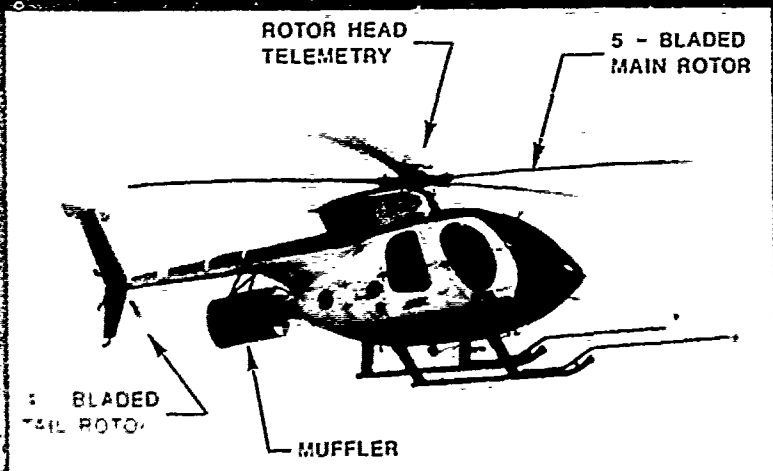
Figure 6-7. ROTONET Phase IV System Multirotor Source Noise Module

6-7 ROTONET Phase IV System
Multirotor Source Noise Module

Objective. To predict and analyze the acoustic interaction effects of multiple rotor systems on high-speed rotorcraft with application to tiltrotor and tandem-rotor systems.

Approach. The ROTONET system was used to predict the acoustic time history for two isolated rotor systems and compute the acoustic interaction between them, accounting for the relative position and phase of the two rotor systems.

Accomplishments. An examination of the MDHC 500E four-blade tail rotor with nonorthogonal blades was chosen as the first study to be performed. The tail rotor was modeled as two-blade rotors rotating in the same direction. Each two-blade rotor was loaded with one-half of the required thrust. Predictions were made of the in-plane radiated noise for each rotor and summed to produce the four-blade rotor signature. The case predicted was for a level flyover at 250 foot altitude at 72 knots speed.

The figure on the left is a photograph of the highly instrumented 500E helicopter as it was outfitted to fly the far-field acoustics test with the four-blade tail rotor. The figure on the right shows comparisons between ROTONET predicted SPL time history for the 1/2 and 1st harmonic of the tail rotor. The predictions agree reasonably well with the measured data throughout the flyover. The accuracy of the predictions for the four-blade configuration is comparable with the accuracy of the ROTONET predictions for the standard two-blade configuration.

Significance. The demonstrated capability of ROTONET to predict the acoustic interaction of two rotor systems is directly applicable to the design evaluation of tiltrotor, tandem-rotor, and coaxial-rotor systems.

Status/Plans. The Multirotor Source Noise Module will be applied to evaluate spectral and directional acoustic radiation patterns for tiltrotor aircraft.

Robert A. Golub
Aeroacoustics Branch
Langley Research Center
(804) 864-5281

Sikorsky S-76A Helicopter
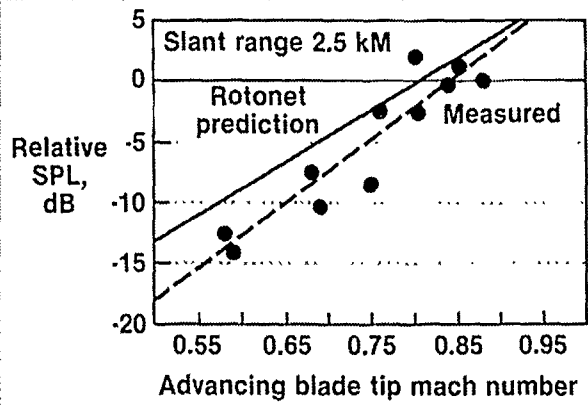
Comparison of Results

Figure 6-8. Effects of Reduced Advancing Blade-Tip Mach Number

6-8 Acoustic Results of the Sikorsky S-76 Variable Rotor-Speed Tests

Objective. To investigate helicopter noise reduction as a function of advancing blade-tip Mach number.

Approach. The Sikorsky S-76A helicopter, with an operations weight of 4,400 Kg, is the only helicopter certified by the FAA to operate at more than one main-rotor speed during flight. It is known analytically that as the main-rotor blade advancing tip Mach number, M_{AT}, is reduced, its associated noise is reduced. To study this noise reduction potential, a flight experiment was designed whereby the helicopter noise would be measured as the helicopter operated at several different flight speeds and main-rotor speeds. This produced a wide range of advancing blade-tip Mach numbers to which the noise could be related. A time signal was recorded simultaneously with measurements of the helicopter noise, operations parameters, position along its flight track, and weather data located at two sites separated by a distance of 8 km and to the side of the helicopter flight track. Ground impedance at five sites over which the acoustic signals were propagated were also measured.

Accomplishments. Shown in the figure is a view of the S-76 helicopter along with some predicted and measured noise results as a function of the measured M_{AT}. The predictions were obtained from the helicopter noise prediction program ROTONET. Measured narrowband sound pressure levels were obtained with the helicopter at a slant range of 2.5 km. The SPLs, measured at the main-rotor fundamental acoustic frequency, are related to the sound pressure level measured at the largest M_{AT}. The data show that at the larger M_{AT} numbers, agreement with ROTONET predictions is good with a divergence from theory as the lower values of M_{AT} are reached.

Significance. Previous to the S-76 test, data available to study the far-field noise generated by reducing the rotor speed of a helicopter were limited to recorded noise for an experimental version of the McDonnell Douglas 500E. Data obtained from this S-76 test have significantly enlarged the data base for research on the effects of reducing helicopter main-rotor advancing blade-tip Mach numbers on the far-field noise of operational commercial helicopters.

Status/Plans. The data will be used to study the predicted results made from advanced formulations in computer codes (ROTONET, ICHIN, and ARCAS) as they relate to measured field results.

Arnold W. Mueller
Applied Acoustics Branch
Langley Research Center
(804) 864-5277

40% Model BO-105; $\mu=.114$; $\alpha_{TPP}=3.1°$

Prediction Method

FLOW

Measurement plane

CAMRAD/JA → lift → FPR → blade → WOPWOP

distribution   pressures

unsteady C_l

Acoustic field

DNW Wind Tunnel Data

Upstream   Downstream

Prediction

Upstream   Downstream
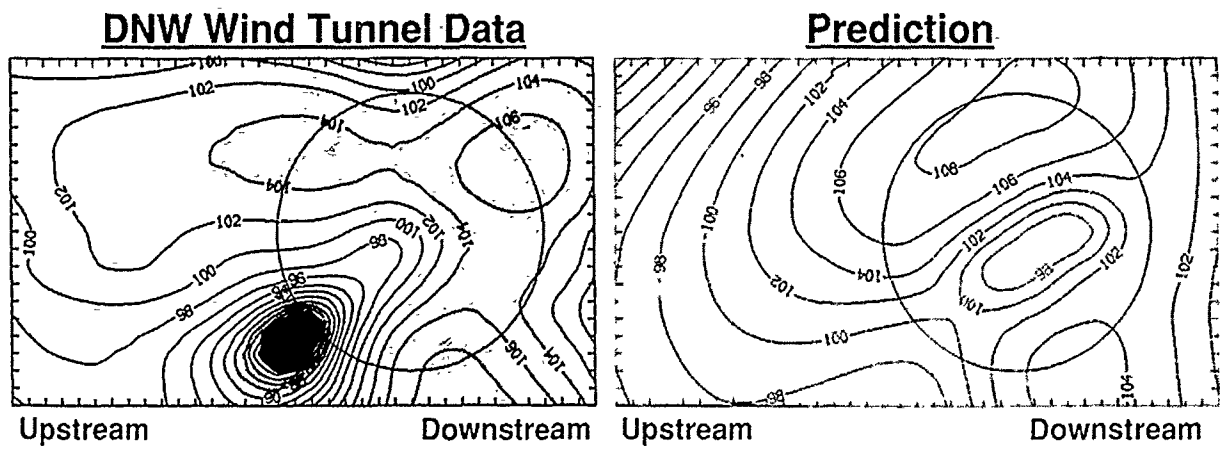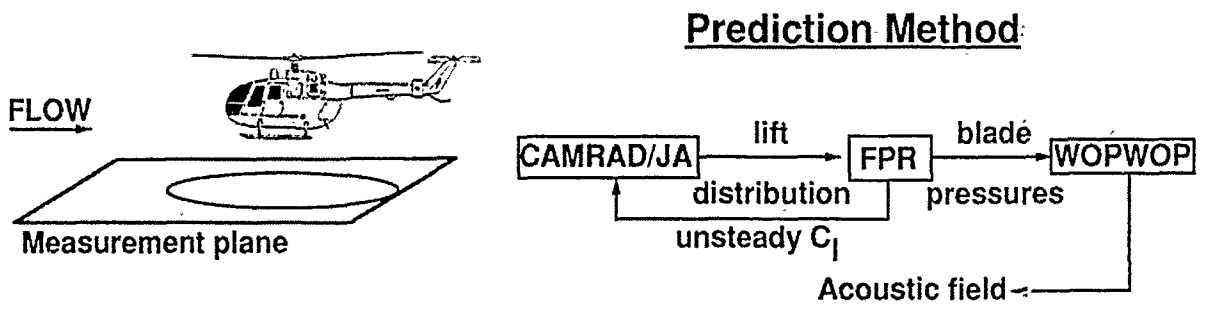
Figure 6-9. Directivity of Low-Frequency Rotor Noise

100

6-9 Directivity of Low-Frequency Rotor Noise

Objective. To define the directivity of low-frequency rotor noise over a horizontal plane and to evaluate current prediction methods by comparing predictions with experimental data taken over this plane.

Approach. Noise data from a joint DLR/NASA main rotor/tail rotor test were employed to define the directivity of low-frequency rotor noise and to validate a noise prediction method. The rotor was a four-bladed, 40% dynamically scaled model of the MBB BO-105 helicopter main rotor. The noise data were acquired on a horizontal plane approximately 1 rotor radius under the rotor as shown in the figure. The noise data were digitally bandpass filtered to obtain only the low-frequency components. Contours of equal sound pressure level (SPL) in decibels (dB) were computed from a rectangular grid of 72 measurement locations. The contours of measured SPL are shown in the figure. The measurement grid is 3 rotor radii in the streamwise direction and 2.5 rotor radii in the cross-stream direction. Predictions of the total loading noise were made at the same 72 locations using the process schematically shown in the figure. Similarly, SPL contours of the predicted data were computed and also are shown in the figure. The noise prediction method consists of three computer codes: CAMRAD/JA (Comprehensive Analytical Model of Rotorcraft Aerodynamics and Dynamics); FPR (Full Potential Rotor code); and WOPWOP (Farassat's acoustic formulation 1A). CAMRAD/JA is used to predict the rotor dynamics, aerodynamics, and performance and is coupled with FPR to directly compute the loading on the blade surface. The blade surface loading is then used by WOPWOP to compute the noise.

Accomplishments. Measured and predicted rotor noise has been compared for a number of operating conditions. The test condition presented here is for an advance ratio of 0.114 and a tip-path-plane angle of 3.11. The overall trends of the low-frequency rotor noise are predicted. The two high SPL regions shown in the measured data, one on the advancing side and the one on the retreating side, are predicted within 1 to 4 dB. However the low SPL region just upstream of the retreating side is not predicted well. This low region is seen in data at other test conditions and is not clearly understood at this time. One possible explanation is blockage due to the model fuselage, although it is possible that a more accurate blade pressure loading distribution will produce a similar trend in the predictions.

Significance. Current prediction methods for low-frequency rotor noise predict the overall trends well, but not the details. The low-frequency rotor noise is dominated by the loading noise and has a focused directivity pattern.

Status/Plans. The three-dimensional full potential aerodynamics code (FPR) is currently being modified by R. Strawn of AFDD, NASA Ames. The pitch rate computed by CAMRAD/JA will be included as an input to FPR. High pitch rate changes (greater than 10^0) have been shown to significantly alter the blade loading distribution computed by FPR. FPR predictions of the blade loads are to be compared with experimentally measured blade loads. In addition, the noise computed from the predicted loads will be compared with the noise computed from the measured loads.

Michael A. Marcolini
Aeroacoustics Branch
Langley Research Center
(804) 864-3629

Casey L. Burley
Lockheed ESC
(804) 864-3631
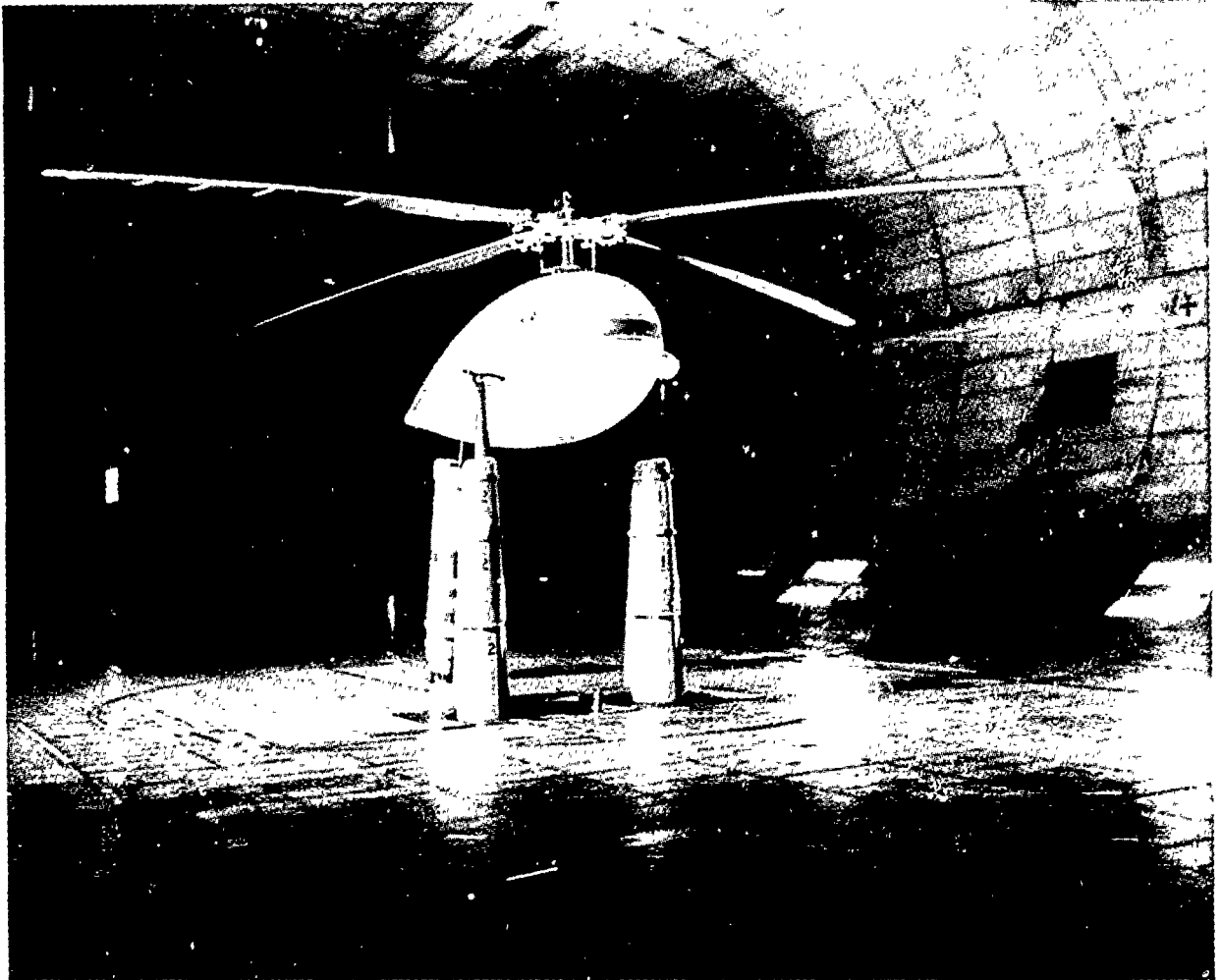
Figure 6-10. Full-Scale Rotor/Fuselage Interaction Test

6-10 Full-Scale Rotor/Fuselage Interaction Test

Objective. To provide quantitative full-scale data of the aerodynamic and acoustic interactions between a helicopter main rotor and simple fuselage. Additional objectives included (1) the acquisition of blade acceleration data to aid in the development of the Individual Blade Control (IBC) concept and (2) the acquisition of wall pressure data for use in the development of a wind tunnel wall correction method.

Approach. Data were acquired in the 40-foot by 80-foot wind tunnel using the full-scale Bell 412 rotor system mounted on the Model 576 Test Stand. Fuselage loads were measured independently of rotor loads with test stand mounted load cells. Combined rotor/fuselage loads were measured with the wind tunnel balance system. Blade acceleration data were acquired while exciting the rotor system using dynamic actuators located in the nonrotating system.

Accomplishments. A complete data set of rotor/fuselage loads and performance were acquired in the 40-foot by 80-foot wind tunnel up to advance ratios of 0.3 and thrust coefficients/solidity of 0.09. IBC data were acquired in hover and forward flight for both rotor flapping and lead-lag motion. Baseline acoustic data were acquired for a future main rotor/tail rotor aerodynamics and acoustics test program.

Significance. This data set is the first full-scale data acquired to specifically evaluate rotor/fuselage aerodynamic interactions. No corrections are necessary to performance due to Reynolds number or to acoustics due to tip Mach number effects. The data set also includes (1) the first-ever open-loop Individual Blade Control data with all four blades in-strumented and (2) the first set of acoustic data for a full-scale helicopter rotor in the acoustically treated 40-foot by 80-foot wind tunnel.

Status/Plans. Data reduction and analysis will be performed together with correlation with small-scale experiments and theory. The next phase of the Interactional Aerodynamics program will include main rotor/tail rotor testing with a Lynx tail rotor.

Tom Norman, Gloria Yamauchi, Dave Signor
Rotorcraft Aeromechanics Branch
Ames Research Center
FTS 464-6653 or FTS 464-6719

Rotor-Wake-Fuselage Aerodynamic Analysis

An Incompressible Potential Method for Unsteady Aerodynamic
Analysis of Realistic Rotorcraft Configurations

John D. Berry
Rotorcraft Aerodynamics Group
Subsonic Aerodynamics Branch, Langley Research Center
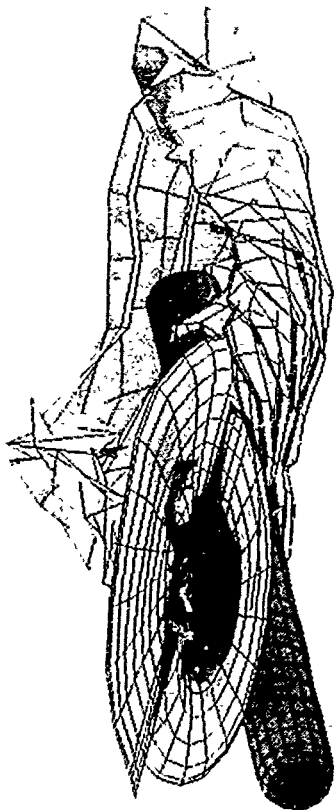
Georgia Tech Rotor-Airframe Experiment Panel Configuration
Color Indicates Singularity Strength

Inflow Velocity Comparison
12.7 mm above rotor

Average Inflow Velocity
12.7 mm above rotor
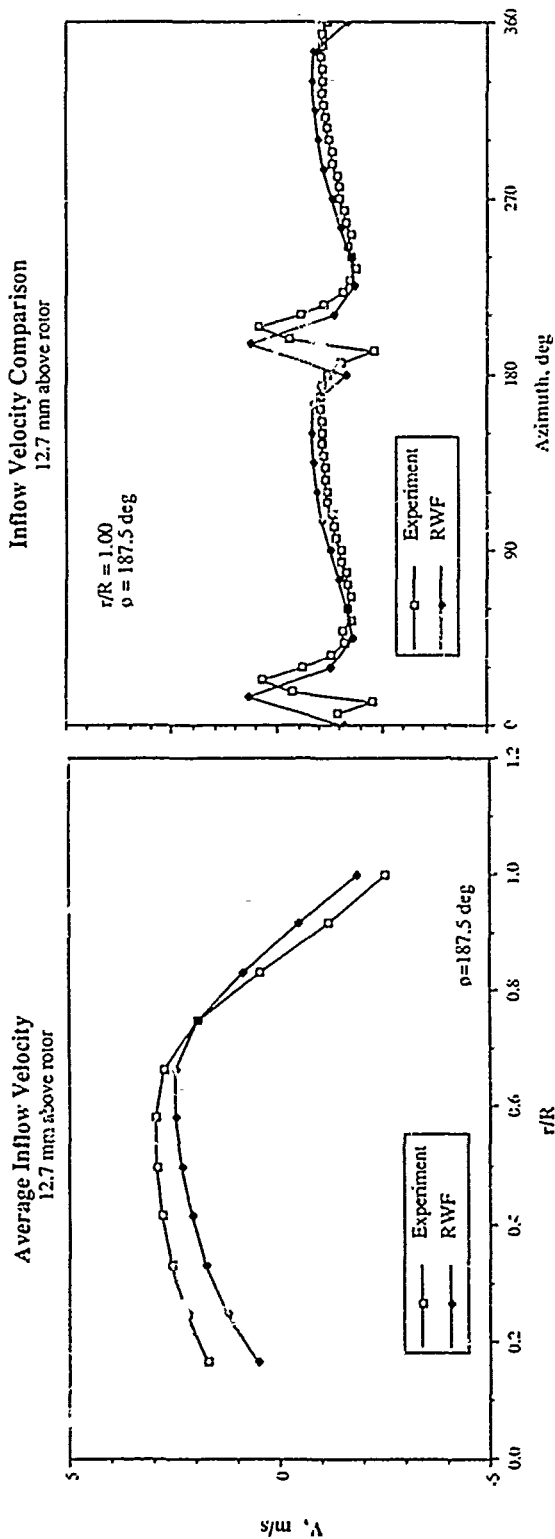
Figure 6-11. Rotor-Wake-Fuselage Aerodynamic Analysis

104

6-11 Rotor-Wake-Fuselage Aerodynamic Analysis

Objective. Realistic rotorcraft configurations represent the most challenging aerodynamic environment for analysis. Methods for computation of the unsteady flow fields associated with these rotorcraft configurations are needed.

Approach. The analysis that has been developed is based on incompressible potential flow. The unsteady flow is solved using a time-marching method. Three types of flow disturbances are modeled using panel techniques: the fuselage, the rotor blades, and the sheets of wake shed by the rotor blades. The geometry of the wake is computed at each time-step using the local convection velocities due to all of the flow disturbances.

Accomplishments. The method has been coded and shows excellent correlation with detailed laser velocimeter measurements made close to the plane of a lifting rotor. The influence of the fuselage on the velocity field above the lifting rotor has been computed at three advance ratios. The computed influence of the fuselage in the presence of a fully interactive wake has been compared with the influence due to the fuselage in isolation.

Significance. Current fuselage aerodynamic techniques are based on the technique of linear superposition. The effects of an isolated fuselage are linearly applied to the effects of an isolated rotor. The strongly nonlinear effects of the wake shed by the rotor on the fuselage and the resulting changes in the fuselage influence back on the rotor have never been assessed. The comparison of the fuselage influence in the presence of the fully interactive wake with the influence of an isolated fuselage helps assess the accuracy and potential problems associated with the superposition technique for fuselage aerodynamics.

Status/Plans. The code, as it currently exists, will be made available to U.S. users during summer 1990. Plans for further development of the code and a "production" version are considered in the same time frame.

John D. Berry
Rotorcraft Aerodynamics Group
Langley Research Center
(804) 864-5090

High Speed Autorotation Case
Ti:) Mach Nt.n.ber = 0.922, Advance Ratio = 0.429
$$C_T/\sigma = .0729$$
Sectio:: Lift - 0 to 64 Harmonics
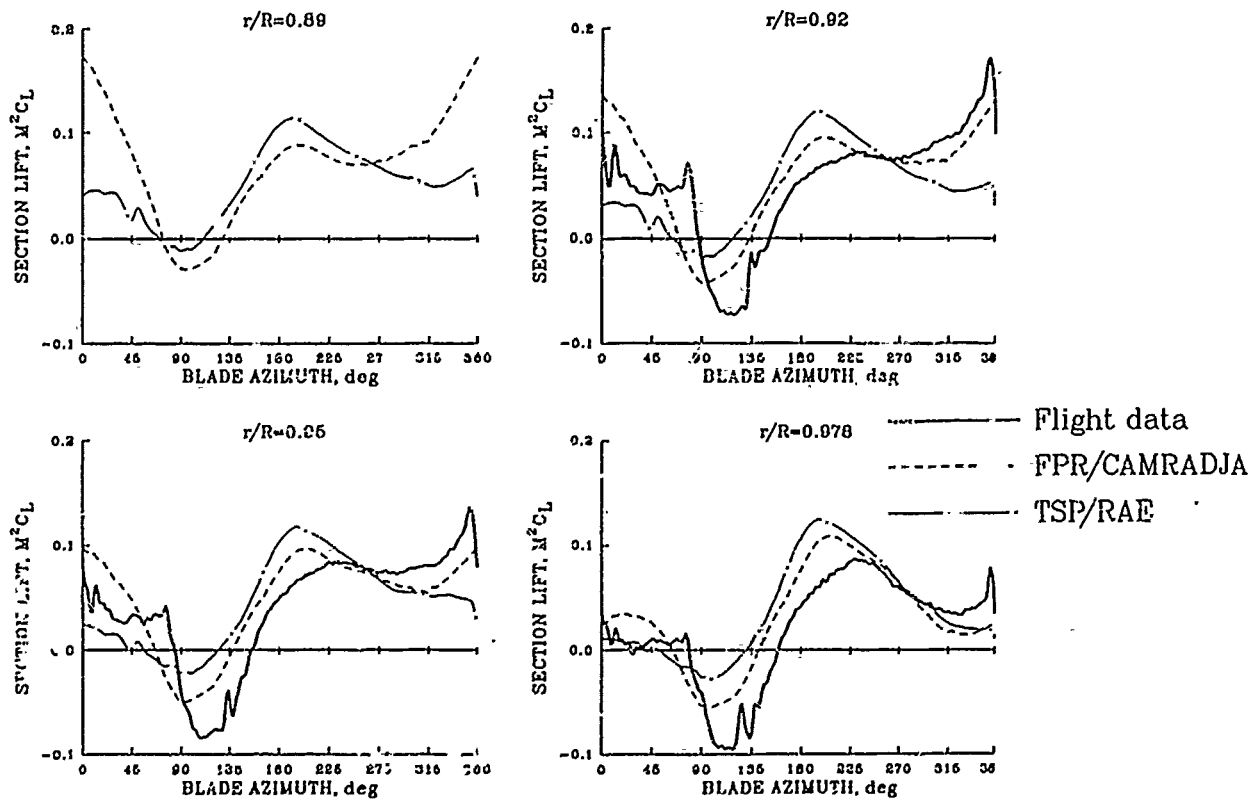
Figure 6-12. Puma Airloads Correlation
High Speed Autorotation Case

6-12 Correlation of Flight Measured Rotor Airloads with Analysis

Objective. To assess the airload prediction capabilities of different CFD methods for rotorcraft analyses by computing rotor airloads for the SA 330 Puma helicopter using a coupled CFD/lifting line method. The results, along with calculations done at RAE and ONERA were compared with flight measurements at the Puma Correlation Workshop.

Approach. The U.S. Army Full-Potential Rotor Code (FPR) was iteratively coupled with the Comprehensive Analytical Model of Rotorcraft Aerodynamics and Dynamics/Johnson Aeronautics (CAMRAD/JA) rotorcraft performance code. The coupling scheme, developed by the Army, uses inflow angles from CAMRAD/JA that represent the wake and blade dynamics effects. These are input as boundary conditions into FPR, which computes airloads that are fed into CAMRAD/JA to obtain a new rotor wake and blade dynamic response. The process is repeated until convergence. The final solution is the predicted airloads on the rotor system. The rotor stations for the calculation are selected to coincide with Puma flight test conditions. Airload prediction capability is assessed considering the airloads along with structural dynamic characteristics, both predicted and measured.

Accomplishments. Aerodynamic predictions were made for a high-speed case on a Puma helicopter with four swept-tip blades using CFD methods. The computed airloads were presented at the Puma Correlation Workshop held May 29-June 1 at Ames Research Center. They were compared with the Transonic Small Potential/Royal Aerospace Establishment code calculations done at RAE along with measured flight test data. An evaluation of the strengths of the different CFD/lifting line methods was made by comparing different aerodynamic parameters at different stations on the rotor disk. A summary report of the correlation work was prepared at the end of the workshop.

Significance. Rotorcraft CFD analyses have not yet reached the level of confidence obtained in fixed-wing CFD applications. This is due to the more complex aerodynamic environment present in the rotor system. The only method of determining the validity of the numerical calculations is through correlation work. This, in turn, will result in the development of better CFD codes in the near future, which will be helpful in the design of improved rotor systems. The capability utilized during the predictions for the Puma are crucial to the UH-60 airloads program being undertaken by NASA-Ames. The methodology has also been successfully applied to the AH-1G airloads predictions.

Status/Plans. Calculation will be done for an additional case with an improved coupling scheme. These results along with calculations done at RAE and ONERA will be included in a future NASA/Army publication. The same methodology is currently being applied to the correlation of measured airloads from the UH-60 DNW wind tunnel test in preparation for Phase II airloads testing with the full-scale UH-60.

Francisco J. Hernandez
Rotorcraft Technology Branch
Roger Strawn
Army Aeroflightdynamics Directorate
Ames Research Center
(415) 604-3150/4510

Design requirements

Minimum hover horsepower

$Hp_{req'd} \leq Hp_{avail}$ ⎫ For 3 flight
No airfoil stall   ⎬ conditions
Blade must be trimmed ⎭

Design variables

Point of taper initiation r/R
Blade root chord c_r
Taper ratio c_r/c_t
Maximum twist τ_{max}
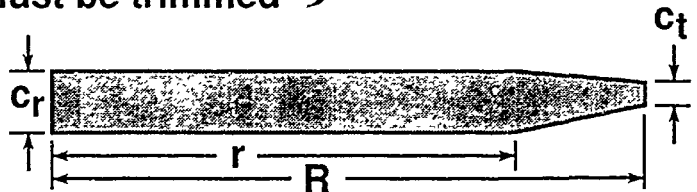
	Initial	Final
r/R	0.8	0.472
c_r	5.4 in	5.0 in
c_r/c_t	3	5
τ_{max}	-16°	-15.5°
Hover Hp	11.27	10.57
Forward flight Hp	8.95	8.0
Maneuver Hp	12.0	9.87

Figure 6-13. Performance Optimization for Model Rotor Blade

6-13 Performance Optimization of Helicopter Rotor Blades

Objective. To integrate various disciplines in the rotor blade design process. The present work deals with the performance aspect of rotor blade design.

Approach. The aerodynamic performance of rotor blades was optimized in both hover and forward flight by selecting the point of taper initiation, root chord, taper ratio, and maximum twist, which minimizes hover horsepower. The procedure uses HOVT (a strip theory momentum analysis) to compute hover horsepower and the comprehensive helicopter analysis program CAMRAD for forward flight and maneuver. The optimization algorithm consists of the general purpose optimization program CONMIN and approximate analyses. Sensitivity analysis consisting of derivatives of the objective function and gradients are carried out by finite differences. Satisfactory aerodynamic performance is defined by the following requirements, which must hold for any part of the mission scenario: the required horsepower must be less than the available horsepower, airfoil section stall along the rotor blade must be avoided, and the helicopter must be trimmed.

Accomplishments. The coupling of HOVT, CAMRAD, and CONMIN has been accomplished. The procedure has been applied to a test problem that is a wind tunnel model of the UH60-A Growth Black Hawk rotor blade. The model consists of 38 structural segments and 14 aerodynamic segments. Results shown in the accompanying figure indicate the optimized design has moved the point of taper initiation significantly in-board and reduced the root chord by 31%. A very significant decrease in the hover horsepower was obtained and the horsepower for the other flight conditions decreased as well. For example, the optimized design has an improvement of 7% in hover horsepower, 12% in forward flight, and 22% in maneuver horsepower.

Status/Plans. The effects of wake models and the effects of planform changes will be studied on the elastic stiffness of the rotor blade. Acoustics requirements (approximated by constraints on the tip Mach number and airfoil thickness) will also be added.

Joanne L. Walsh
Interdisciplinary Research Office
Langley Research Center
(804) 864-2806
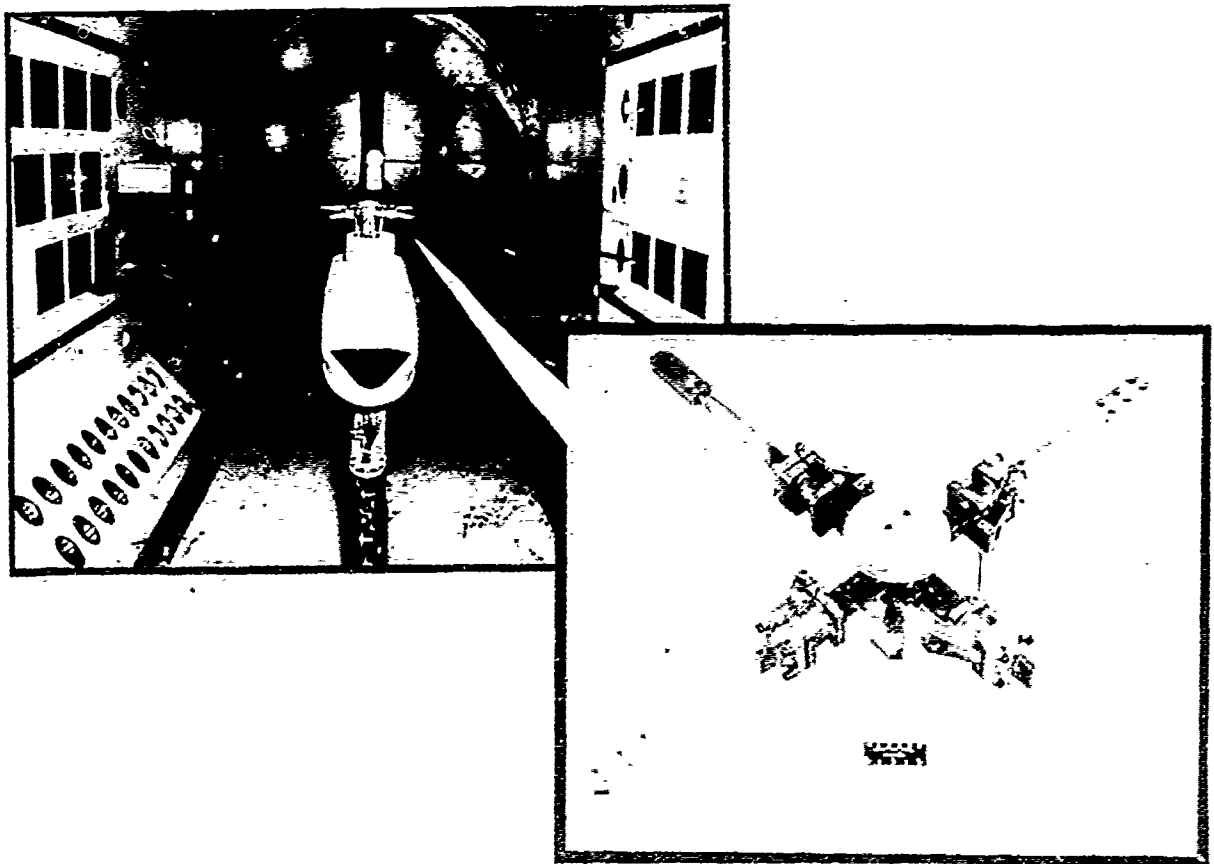
Figure 6-14. Aeromechanical Stability Data Base for Parametric Hingeless Rotor Expanded

110

6-14 Aeromechanical Stability Data Base for Parametric Hingeless Rotor Expanded

Objective. One goal of the Aeroelastic Research Experimental System (ARES) effort in the Langley Transonic Dynamics Tunnel (TDT) is to develop the capability to successfully test hingeless and bearingless rotor configurations. An important part of this capability is the development of an experimental technique for accurate measurement of the aeromechanical stability of the coupled rotor-body system. To investigate the aeromechanical instability phenomenon, a research effort was started in the TDT several years ago. The objectives of the research are to generate a data base for analytical correlation and to ensure safe testing of hingeless and bearingless rotors in the TDT.

Approach. The initial phase of the research program involved two wind tunnel tests of the ARES first generation hingeless rotor (AHRO). The current test utilized the ARES second generation hingeless rotor (AHRO-II), which has improved fatigue life characteristics and a higher lead-lag frequency than the original AHRO. Initial run-up of the AHRO-II mounted on the ARES model was conducted in the Helicopter Hover Facility (HHF). Testing in hover and forward flight was performed in the TDT. The moving-block technique was utilized to measure rotor in-plane damping for determination of aeromechanical stability. Damping measurements were made for a range of parameters including rotor speed, collective pitch, and blade droop. Initial attempts were made to measure damping in an autorotative condition.

Accomplishments. Testing in hover was conducted at different values of collective pitch over a range of rotor speeds. Testing in forward flight was performed over a range of advance ratios up to 0.35. The data obtained show a trend of increasing damping with collective pitch. It was found that in-plane damping decreases with increasing rotor speed. An unstable region exists in hover and forward flight. Similar results were obtained for configurations incorporating changes to blade droop.

Significance. This test has expanded the aeromechanical stability data base for the parametric hingeless rotor. Consistent and repeatable measurements of the rotor in-plane damping were obtained. The experimental data will be used for future correlation with analytical codes. The test has continued to show that safe testing can be accomplished even near and into the instability region.

Status/Plans. Tests will be conducted with AHRO-II mounted on a modified ARES, which has a static gimbal to allow for variation in roll and pitch frequencies. Future plans also call for correlating the experimental data with analytical methods and publishing the results in a formal report.

Jeffrey D. Singleton, William T. Yeager, Jr.
Configuration Aeroelasticity Branch
Langley Research Center
(804) 864-1266
M-Nabil H. Hamouda
Lockheed Engineering & Sciences Company

Chapter 7

Figi. .er/Attack Aircraft

The objective of the Fighter/Attack Aircraft Program is to provide the required technologies for fighter/attack aircraft to achieve efficient, sustained supersonic cruise and maneuver performance; efficient store carriage and deployment at supersonic speeds, increased agility at subsonic speeds and acceptable handling qualities at extreme angles-of-attack; and short takeoff and vertical landing (STOVL) operation.

Improved prediction methods and/or experimental techniques are now available for high-lift aerodynamics, propulsion integration, weapon carriage, supersonic store cavity and separation aeroacoustics, integrated flight controls, and systems design for fighter/attack aircraft. Wind tunnel and piloted simulation studies have demonstrated the potential effectiveness of multiaxis thrust vectoring for propulsive control at extreme angles-of-attack. In addition, powered lift systems consistent with the operation of advanced STOVL aircraft have been identified and configuration studies have been conducted to assess the impact of integrating these systems with supersonic airframe designs.

The Fighter/Attack Aircraft Program is focused on (1) CFD modeling and validation of cavity effects and near-field trajectory simulation for weapons launch during maneuver and modeling of 3-D flow fields for vehicle. at high angles-of-attack with separated flow; (2) development of innovative propulsive and aerodynamic control systems concepts to provide increased vehicle control at angles-of-attack near and beyond maximum lift; (3) improved understanding of control requirements for control concepts throughout the relevant flight envelope, (4) large-scale, ground-based testing of a STOVL fighter concept using ejector lift/vectored thrust to define critical transition aerodynamics, (5) studies of STOVL ground effects including inlet reingestion and ground erosion, and (6) integration studies to quantify the impact of emerging technologies and define the critical research areas for supersonic STOVL.

Program Manager: George Unger
                     OAET/RF
                     Washington, DC 20546
                     (202) 453-5420

113
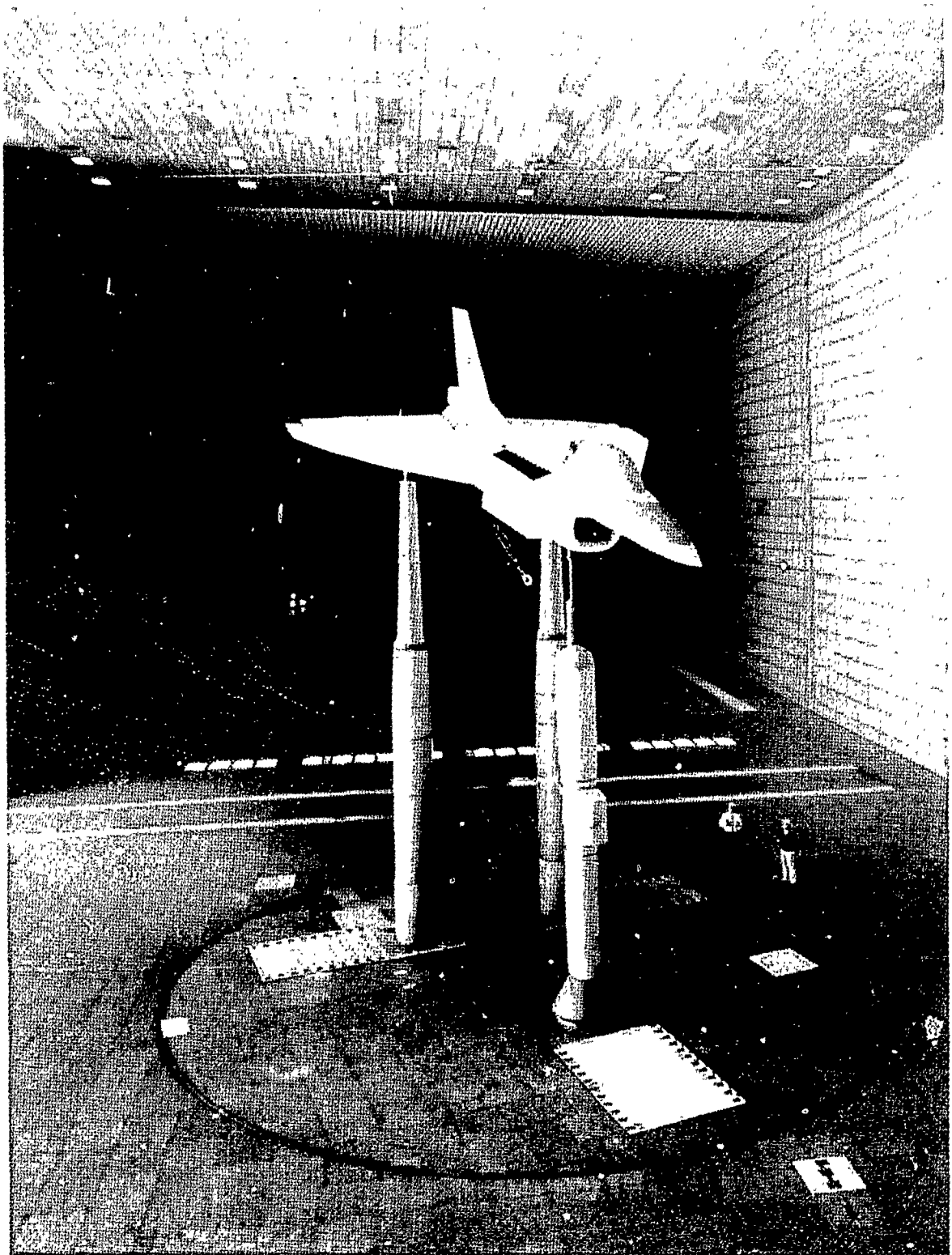
Figure 7-1. STOVL E-7A Testing

114

7-1 STOVL E-7A Testing

Objective. Tests of the full-scale wind tunnel model of General Dynamics STOVL E-7A fighter concept were intended to evaluate the overall aerodynamics of a candidate STOVL configuration employing an ejector-lift/vectored-thrust propulsion system. Particular emphasis was placed on determining the acceleration performance of the vehicle in the low-speed end of transition from jet-borne to wing-borne flight. An assessment of the longitudinal stability of the design was also a high priority due to the potentially large changes in vehicle pitching moments because of thrust vectoring during transition. The tests were also intended to measure the thrust augmentation of a lifting ejector system when integrated into a realistic aircraft configuration.

Approach. A high-performance lifting ejector designed by Boeing Canada, deHavilland Division, was incorporated into the E-7A configuration developed by General Dynamics, Ft. Worth Division. A Rolls Royce Spey 801-SF jet engine was installed to furnish gas to the propulsion system at actual flight pressures and temperatures. The split flow propulsion system delivered bypass air to the ejector system or to a fixed aft nozzle. Core air flow was directed to a vectorable ventral nozzle. The engine provided approximately half of the thrust required for a flight vehicle. Because of this, the model was tested at wind tunnel dynamic pressures, which were about half of actual flight conditions, in order to properly model the jet-to-free-stream velocity ratios. A suite of over 1,000 surface pressures measured jet-induced pressure perturbations on the model.

Accomplishments. Overall vehicle forces and moments generated by the E-7A model were measured over a speed range of 20 to 100 knots in the Ames 80- by 120-foot wind tunnel. The thrust vector angle of the ventral nozzle was adjusted to four different settings during the test program ranging from 90° from the horizontal to the cruise-flight setting of 6°. Three different ejector diffuser configurations were tested to evaluate effects of ejector stowage prior to up-and-away flight. Lateral/directional stability data was also acquired during the test program.

Significance. Despite the significant ram drag associated with operation of a lifting ejector system, the E-7A concept demonstrated very satisfactory acceleration capability (0.15 g) over the entire transition speed range. The installed thrust augmentation of the ejector system in hover approached the design requirement of 1.6. The full-scale wind tunnel investigations of the E-7A indicate that the concept appears to be a viable candidate for the next generation of STOVL fighter aircraft. The capability of making useful lateral/directional stability measurements on STOVL vehicles in the 80- by 120-foot wind tunnel was also demonstrated.

Status/Plans. The E-7A model is currently being prepared for hover performance and ground environment testing this summer at Ames Outdoor Aerodynamic Research Facility.

Brian E. Smith
Fixed-Wing Aerodynamics Branch
Ames Research Center
(415) 604-6669
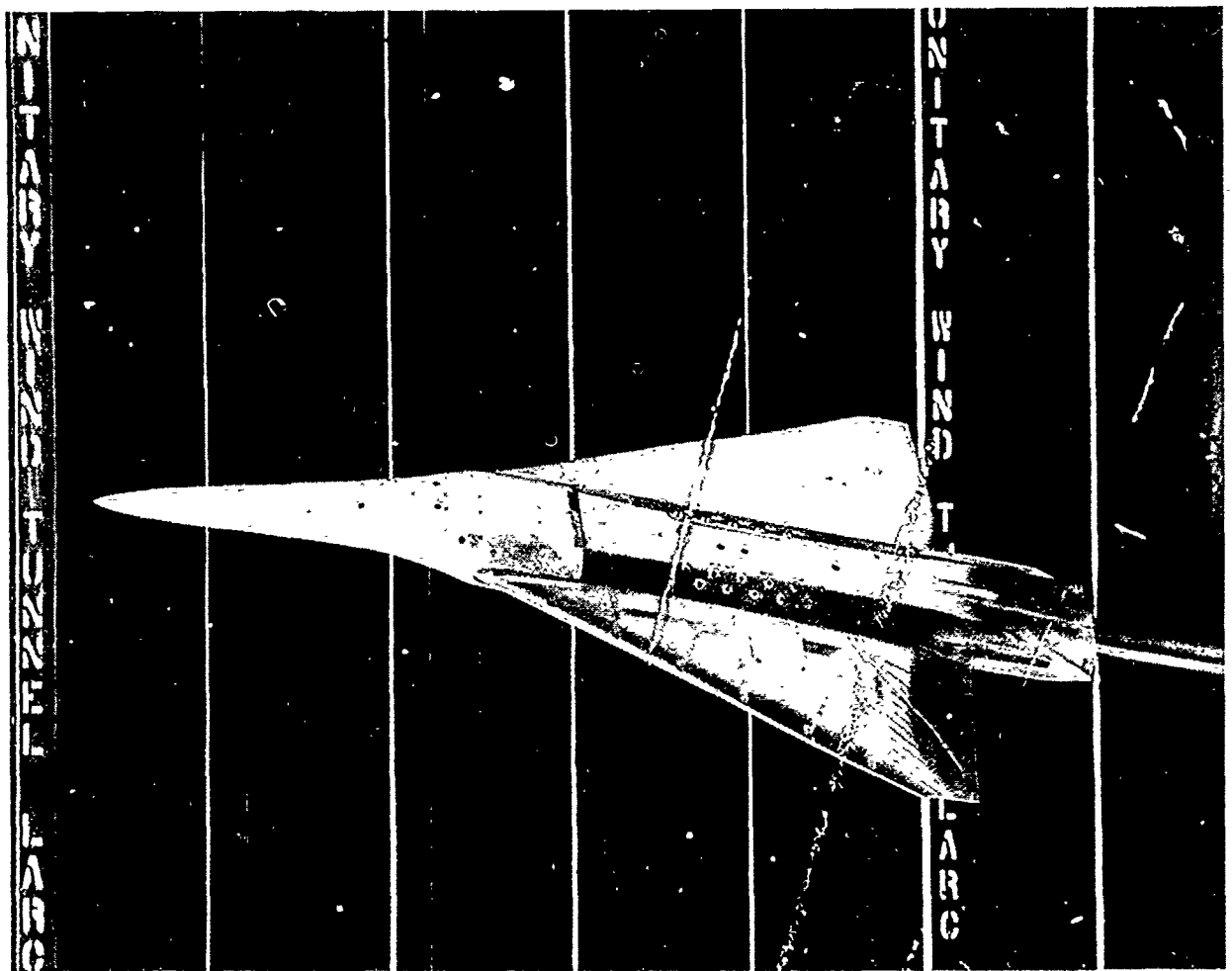
Figure 7-2. Code Calibration Study on a Generic Fighter Configuration

116

7-2 Code Calibration Study on a Generic Fighter Configuration

Objective. To evaluate full-potential, Euler, and Parabolized Navier Stokes (PNS) codes on a generic fighter configuration at supersonic speeds.

Approach. A cooperative wind tunnel study was performed with McAir using three wings: flat, cruise, and maneuver camber. Computational analysis was performed with a full potential code (NCOREL), a Euler code (GEM3D), and a PNS code (CFL3DE).

Accomplishments. Research results of this program show that:

o Data comparison for both cruise and maneuver wings indicate that the full-potential computations are overly optimistic in performance predictions.

o Data comparison for both cruise and maneuver wings indicate that the Euler surface pressure predictions do not agree well for the forward leeside wing stations, although forces and moments are accurately predicted.

o Flow visualization data indicate that both cruise and maneuver wings experience viscous effects which cannot be modeled by full-potential or Euler methods.

o Data comparison for both cruise and maneuver wings indicate that the PNS code is more accurate in predicting leeside surface pressures. However, uncertainty of the boundary layer behavior can lead to small errors in these predictions.

Significance. The results indicate the level of code necessary to accurately resolve overall forces and moments or detailed surface pressure distributions.

Status/Plans. The study is complete and documented in a George Washington University master's thesis.

Davy Haynes, Mitchell Stevens
Supersonic/Hypersonic Aerodynamics Branch
Langley Research Center
(804) 864-5584

117

DYNAMIC STALL RESEARCH

BASIC RESEARCH	APPLIED RESEARCH
• Develop understanding of dynamic effects on aerodynamics at high-α, especially vortex bursting	• Determine magnitude and persistence of dynamic effects on realistic configurations
• Investigate effects of wing planform shape	• Assess impact on maneuver capability
• Explore methods to enhance dynamic characteristics using active control concepts	• Correlate with flight test results

Figure 7-3. Dynamic Stall Research

118

7-3 Dynamic Stall Research

Objective. Numerous studies have documented significant aerodynamic force overshoots caused by dynamic stall on two-dimensional airfoils undergoing large-amplitude pitching motions. The objective of this research is to increase understanding of the complex aerodynamics involved during large-amplitude motions on more realistic three-dimensional configurations and to assess potential impact of the dynamic effects on aircraft maneuverability and controllability.

Approach. Wind tunnel tests were conducted in the Langley 12-foot low-speed tunnel using a computer-controlled, large-amplitude pitch apparatus. Data were obtained on simple delta-wing models to better understand fundamental dynamic stall mechanisms. Subsequently, tests of a 0.10 scale model of an F-18 were conducted to investigate effects on a realistic configuration and to evaluate impact of dynamic stall effects on maneuver capability. The amplitudes and rates associated with the tested motions are representative of the capability of current and projected fighter aircraft. In addition to wind tunnel tests, preliminary flight tests have been conducted to compare wind tunnel data with flight results using the NASA High Angle-of-Attack Research Vehicle (HARV).

Accomplishments. To date, the ongoing investigation has focused on ramp motions at various rates starting and ending at different angles-of-attack. The results show that lags in vortex flow formation and breakdown during large amplitude pitching motions at high angles-of-attack can produce significant lift, drag, and pitching moment increments over the static values. These complex dynamic effects were found to be strongly influenced by pitch rate and the initial and final values of angle-of-attack. Preliminary results, however,

show only modest performance impact due to the short persistence of the dynamic effects. Flight test data obtained with the HARV show good agreement with the wind tunnel derived results.

Significance. Future fighter aircraft will likely use technologies such as thrust vectoring controls that will provide a very high degree of agility and maneuverability. This capability will allow aggressive maneuvering in the high angle-of-attack flight regimen and thus emphasize the importance of dynamic effects such as dynamic stall. A broader understanding of the mechanisms involved in this flight regimen is vital to development of methods for improving the high angle-of-attack stall/post-stall combat maneuverability of advanced fighter aircraft.

Status/Plans. Follow-on investigations, including studies of arbitrary motions, scale effects, lateral-directional characteristics, and control effectiveness are planned. In addition, mathematical models of these dynamic effects will be developed and studied on the Langley Differential Maneuvering Simulator. The investigation will also assess the impact of unsteady flow phenomena on aircraft flight dynamics and combat effectiveness. Flight validation of maneuvering capability, flow behavior, and vortex control techniques are planned to be ultimately obtained on the NASA HARV.

Jay M. Brandon
Flight Dynamics Branch
Langley Research Center
(804) 864-1142
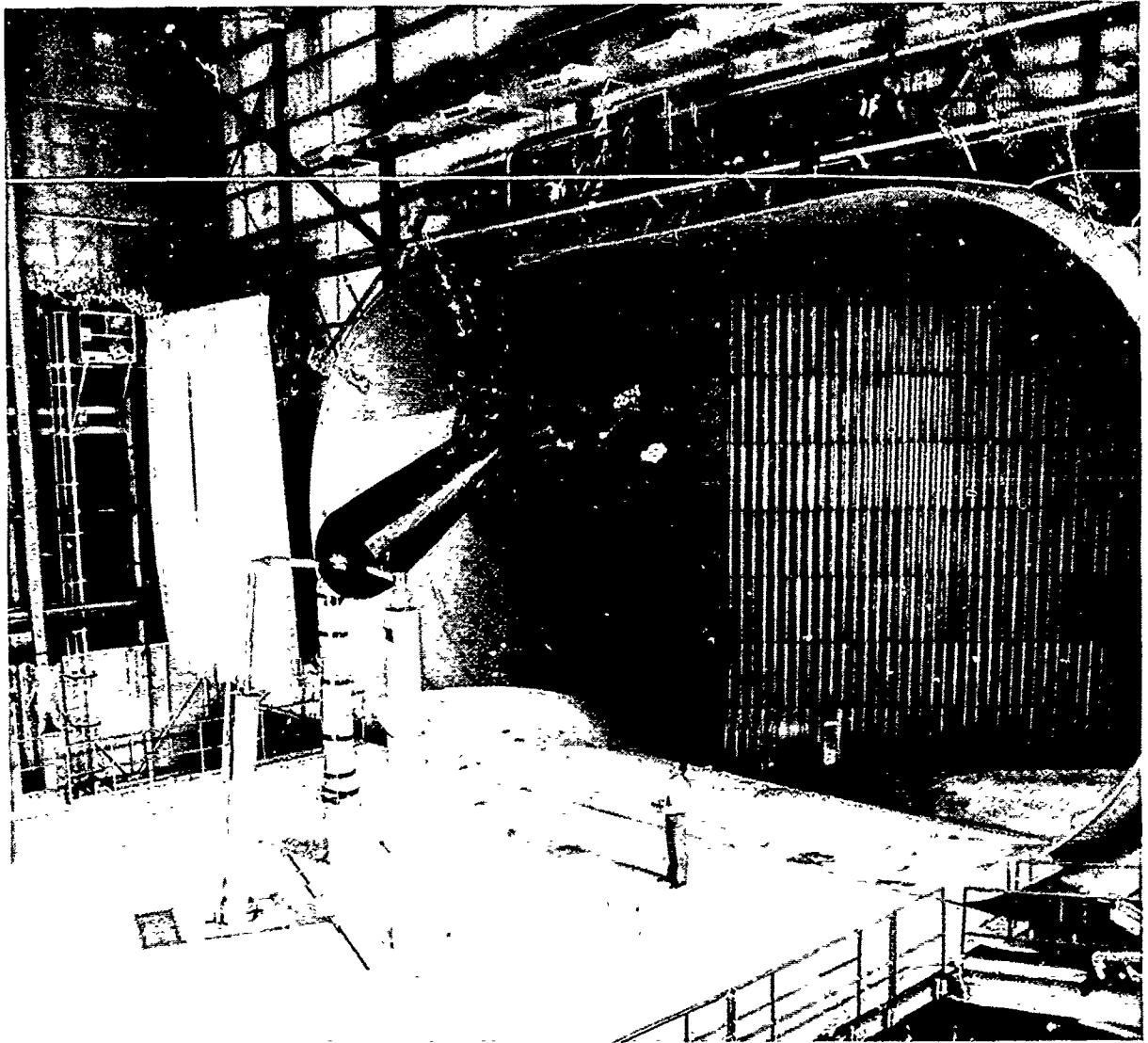
Figure 7-4. Full-Scale Wind Tunnel Investigation of the F-18 HARV Forebody

7-4 Full-Scale Wind Tunnel Investigation of the F-18 HARV Forebody

Objective. To provide large-scale model data on basic forebody aerodynamics and deflectable forebody strake yaw control effectiveness in support of the NASA F-18 High-Angle-of-Attack Research Vehicle (HARV) flight test program.

Approach. A static wind tunnel investigation was conducted on a full-scale isolated F-18 forebody model in the Langley 30 by 60 foot tunnel. The investigation was a cooperative program between NASA Langley Research Center and NASA Ames Research Center, Dryden Flight Research Facility. Tests were included to measure the three-dimensional vortex flow on the forebody and to study deflectable strake effectiveness at high Reynolds number. Effectiveness of the forebody strake was optimized by investigating the effect of strake deflection and radial location. Force, moment, and surface pressure measurements were obtained over an angle-of-attack range from -8° to 80° and a sideslip range from -20° to 20°. Surface flow visualization consisted of tuft and oil flow studies to provide a method of identifying regions of separated flow, including primary and secondary separation lines. Forebody vortical flow at high angles-of-attack was studied with a laser vapor screen technique. The model was also equipped with a Flush Air Data System, which consisted of an array of surface pressure ports near the forebody apex. The test Reynolds number was 2.78 million based on the forebody maximum diameter.

Accomplishments. Forebody pressure distributions showed the strong suction peaks on either side of the forebody and the location of the forebody vortex footprints on the upper surface. Oil surface-flow patterns showed flow streamlines and location of both primary and secondary vortex separation lines. These flow characteristics agreed very well with the surface-flow patterns from flight tests. The results with strakes confirmed sub-scale model data and showed that the strakes provided significant forebody yawing moments at high angles-of-attack, with the maximum control effectiveness occuring near $\alpha = 70°$. The strake created a strong isolated vortex away from the forebody, which prevented reattachment of the separated flow on that side. In contrast, the flow on the side of the forebody without the strake remained attached much farther up on the body. The resulting pressure distribution showed much higher suction pressures on the strake-off side, thus resulting in the large side-forces and yawing moments.

Significance. The large-scale model results on strake effectiveness validated previous subscale model data and provided design guidelines for actuated conformal strakes for flight test demonstration. The pressure and flow visualization results allowed a better understanding of the three-dimensional vortex flow on the F-18 forebody and provided a data base for correlation with flight results and with CFD calculations.

Status/Plans. A detailed analysis of the test data is currently under way for use in CFD code validation and for correlation with flight results. A second tunnel entry is planned to complete the overall program objectives, including an investigation of the final actuated forebody strake geometry which will be implemented on the F-18 HARV.

F. L. Jordan, G. H. Shah, L. J. Glaab, D. G. Murri, L. P. Yip
Flight Dynamics Branch
Langley Research Center
(804)864-1153

Suction ports
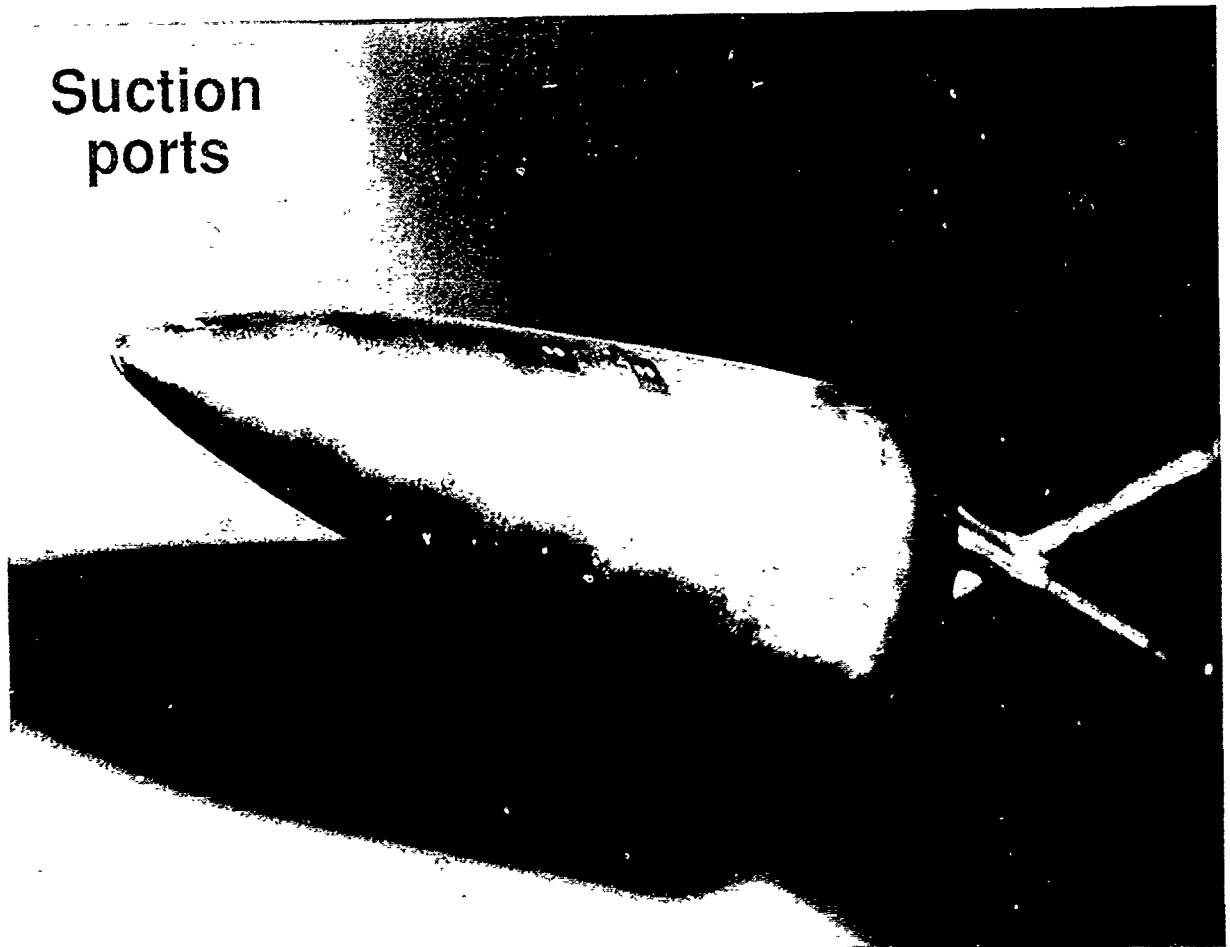
Figure 7-5. Forebody Suction Model

122

7-5 Effects of Forebody Suction on Directional Control Characteristics of a Slender Forebody at High Angles-of-Attack

Objective. To evaluate the use of suction near the apex of a slender forebody as a method of directional control at high angles-of-attack.

Approach. Preliminary work in this area was performed by the Royal Aerospace Establishment. A cooperative program was established under The Technical Cooperation Program to coordinate research activities. The evaluation of effectiveness of suction control methods is based primarily on the level of side force and/or yawing moments that can be generated as a function of angle-of-attack and suction momentum coefficient. These levels can be compared with conventional rudder effectiveness and other advanced control concepts, such as deflectable nose strakes or blowing.

Accomplishments. The present research has concentrated on exploratory studies in the Langley 12-foot low-speed tunnel using a 0.16-scale F-18 forebody. A number of suction port locations were evaluated using force and moment data, surface oil-flow studies, and laser light-sheet flow visualization techniques. The results show that significant yawing moments can be generated at very low momentum coefficient levels at angles-of-attack greater than 55°. However, the preliminary results indicate that for this forebody geometry suction is not as effective as blowing or deflectable strakes. The flow visualization studies indicate that the suction mechanism involves the prolonged attachment of flow in proximity to the active suction port, thus increasing the aerodynamic suction force on that side of the forebody as compared to the nonsuction side.

Significance. The results show that apex suction can strongly influence the forebody vortex system and thus potentially provide significant yaw control moments at high angles-of-attack. However, for the F-18 geometry, the levels of yawing moment and angle-of-attack range where the suction is effective are limited.

Status/Plans. Further tests are planned using a different forebody geometry of higher fineness ratio and circular cross-section capable of incorporating a blunt or pointed apex. In addition, other suction geometries such as slots will be investigated.

E. Richard White
Flight Dynamics Branch
Langley Research Center
(804) 864-1147
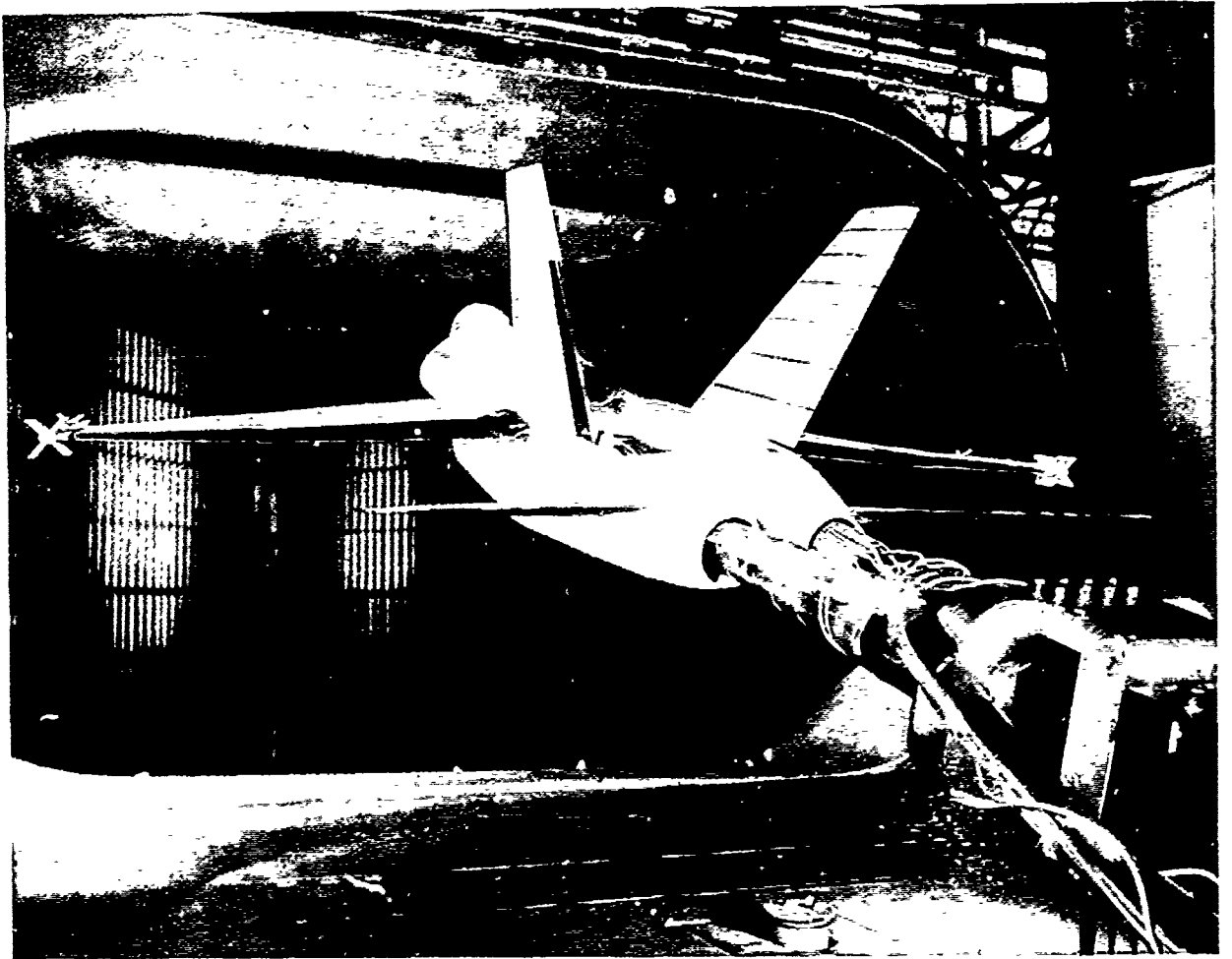
Figure 7-6. Tail Buffet Research

7-6 Tail Buffet Research

Objective. The use of high-energy vortex flow fields to enhance maneuvering capability has become a widely applied design approach for modern high-performance airplanes. Recent operational experience has shown that these vortex flow fields can induce severe levels of buffeting on the vertical tail and substantially reduce the fatigue life of the structure. The objective of this research is to study the effects of vortical flow fields on tail buffeting and explore methods of reducing buffet levels while maintaining favorable vortex flow effects on the high-angle-of-attack aerodynamic characteristics.

Approach. A cooperative program was established between NASA, the Navy, and McDonnell Aircraft Corporation. Low-speed wind tunnel tests were conducted on a 0.16-scale F-18 model equipped with dynamically scaled, extensively instrumented vertical tails to provide aerodynamic loading and unsteady surface pressure information. Changes to the configuration aimed at modifying the vortical flow field were tested to investigate the effect on both buffeting response levels on the tails and the overall aerodynamic characteristics of the configuration. Flow visualization was also conducted to develop a better understanding of the flow field interactions between the vortex system and vertical tails.

Accomplishments. Testing in the Langley 30 by 60 foot tunnel provided a large data base of dynamic response characteristics of the vertical tails (aerodynamic loads, accelerations, and unsteady surface pressures) and steady-state total force and moment data for several configurations. Correlation of measured tail buffet levels with results from previous, limited industry testing of the baseline F-18 configuration was extremely good and provided confidence in the current data. The study showed that changes in wing leading-edge extension (LEX) geometry can reduce tail buffet levels appreciably by repositioning and/or weakening the vortex system, but can also have a large impact on the overall lift and stability characteristics. Thus, careful design is required to obtain desired characteristics in both areas. Several LEX modifications were found to provide large reductions in buffeting, while having only modest effects on the aerodynamic characteristics.

Significance. The results of this test show that avoidance of severe tail buffeting can be achieved by proper configuration design to control the position and strength of the vortices. However, care must be taken to avoid adverse impact on the overall vehicle lift and stability characteristics. Successful correlation with previous data using scaling parameters suggest that the same approach may be used to develop wind-tunnel-to-flight scaling methods. The results also indicate that the subject test technique can be effectively used for preliminary concept evaluation and design trade-off studies.

Status/Plans. Follow-on investigations of various innovative concepts to alleviate tail buffeting are planned. Studies to provide accurate modeling of buffet excitation parameters will also be conducted to allow tail buffet concerns to be addressed early in the design cycle of future aircraft. Results of current and future wind tunnel tests will be correlated with airplane flight test data for development and validation of scaling methods.

Gautam Shah, Sue Grafton, Jay Brandon
Flight Dynamics Branch
Langley Research Center
(804) 864-1163
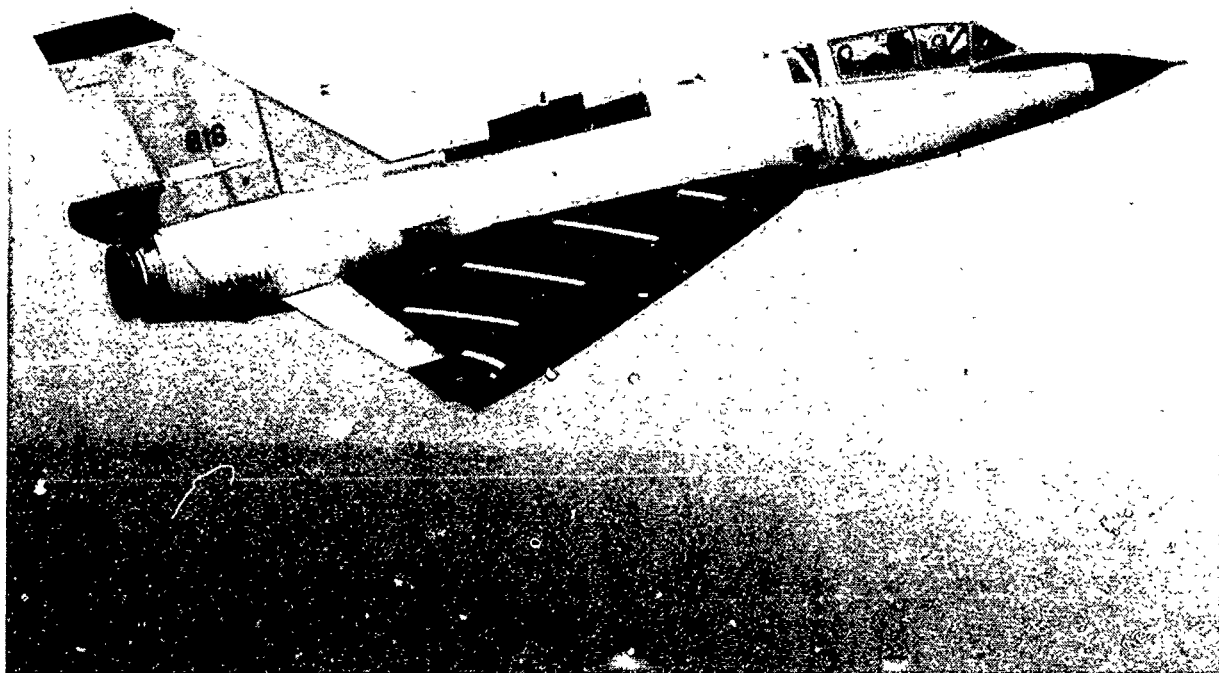
Figure 7-7. F-106 Vortex Flap Flight Experiment

7-7 F-106 Vortex Flap Flight Experiment

Objective. To demonstrate the feasibility of the vortex flap concept in a free-flight environment to characterize the wing flow field and to provide a data base for sharp leading-edge wings which can be used for calibration of design and analysis tools.

Approach. An F-106B aircraft has been modified by the addition of wedge-shaped leading-edge flaps to the existing wing. The wing flow field will be characterized with surface pressure measurements and flow visualization data obtained through use of flow cones and a light sheet/flow seeding system. A limited evaluation of the handling qualities and performance of the modified aircraft relative to the baseline aircraft will be conducted.

Accomplishments. Envelope expansion and research flights for the modified aircraft with vortex flap at 40° deflection has been completed. Aircraft performance data, detailed wing surface pressure measurements, and surface flow visualization (flow cones) were obtained at subsonic and transonic test conditions. Light-sheet and flow-seeding systems were installed to visualize the off-body flow and provided significant additional details of the wing flow field characteristics at subsonic test conditions. The accompanying figure shows the F-106 aircraft in flight with the vortex flap deflected 40° and the light sheet housing installed on the dorsal fairing forward of the vertical tail.

Significance. The vortex flap concept has potential application for enhancement of the maneuvering performance of military fighter aircraft and the landing and takeoff performance of civilian aircraft having high wing sweeps.

Status/Plans. Testing of the aircraft with the vortex flap at 30° deflection is expected to begin in July 1990, with flight test activities ending by December 1990.

James B. Hallissy, W. Elliott Schoonover, Jr., John E. Lamar
Transonic Aerodynamics Branch
Langley Research Center
(804) 864-2865

Chapter 8

Hypersonic Aerodynamics

The Generic Hypersonic Aerodynamics program focuses on key and enabling technologies in hypersonics, with the aim of establishing a robust hypersonic data base and methodology necessary to meet the design and development challenges of future NASA/DoD aerospace vehicles. The program stresses fundamental understanding and prediction of the controlling physical and chemical processes with emphasis on research and technology development of slender air-breathing hypersonic vehicles that use highly integrated airframe/propulsion concepts. The program provides a sustained NASA in-house effort with major involvement from academia and the aerospace industry. It utilizes unique NASA experimental facilities and computational assets to advance critical technologies. A major objective of the program is to structure cost-effective partnerships with industry such that research results can be transferred rapidly and efficiently into the design and development of aerospace vehicles. University participation involves sponsored research and a refocusing and rededication of the aeronautics/ astronautics curriculum to hypersonics.

Program Manager: Steve Wander
OAET/RF
Washington, DC 20546
(202) 453-2820

M. = 16.0
Re. = 1.0 x 10' /m
T. = 240 K
ı = 0'

Temperature Contours

Perfect Gas | Finite-Rate Air

Centerline Profiles

Body

Cowl

Temperature K
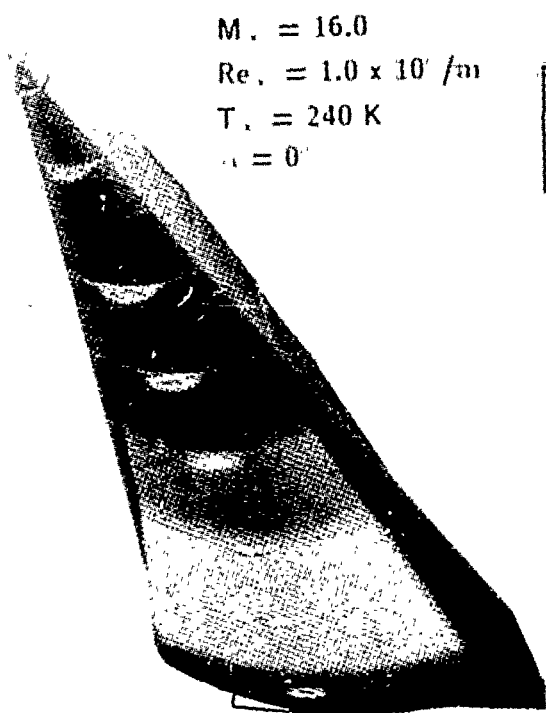
Atomic Oxygen Contours
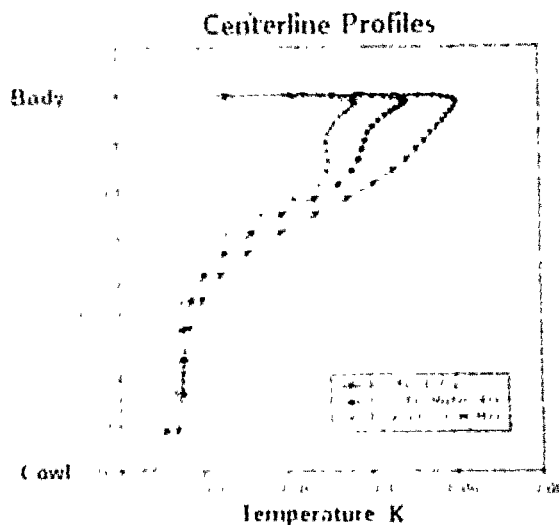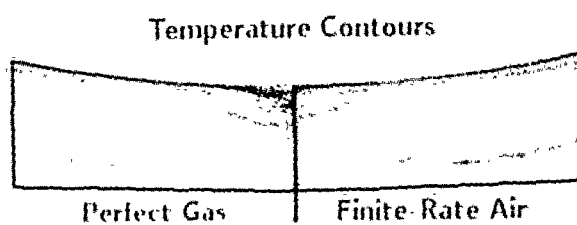
NASA Ames Research Center

Figure 8-1. McDonnell Douglas Generic Option II with Inlet Face

130

8-1 Evaluation of Forebody Flow-Field Sensitivity to Real Gas Effects

Objective. To examine the impact of real gas effects on the computed flow field of a blunt forebody operating at NASP-like cruise conditions.

Approach. The flow over the McDonnell Douglas Generic Option 36-inch blended-wing-body was computed for Mach 16 flow at an altitude of 125,000 ft. The upwind parabolized Navier-Stokes solver (UPS) was employed with each of three available gas models: (1) perfect gas, $\gamma = 1.4$, (2) equilibrium air, and (3) finite-rate air. Initial conditions for the space-marching calculations were provided by the time-dependent compressible Navier-Stokes solver (CNS), which possesses the same real gas capabilities as the UPS code.

Accomplishments. Solutions were obtained using each of the three available gas models for the conditions given in the preceding paragraph. The mass flux resulting from each of the three calculations was integrated over a hypothetical inlet face located at $x/L = 0.75$ for comparison. Although centerline temperature profiles indicate significant nonequilibrium effects, because the flow at the cowl lip is essentially free-stream in each case, there is little variation (approximately 1.5%) in integrated mass flux.

Significance. In addition to demonstrating the new capability to interface the UPS and CNS codes for finite-rate chemistry calculations of blunt bodies, these results give an indication of the level of importance of nonequilibrium effects at NASP-like cruise conditions. Because of the relatively small bluntness of the forebody (the inlet was located 200 nose radii from the nosetip), real gas effects did not strongly influence the inlet face mass flux. Increased bluntness would be expected to produce a stronger dependence on gas modeling.

Status/Plans. Studies are currently being conducted with sphere-cones to investigate the combined effects of gas model, bluntness, and free-stream conditions, in addition to numerical effects such as grid density, on computed results.

Scott Lawrence , Jolen Flores
Applied Computational Fluids Branch
Ames Research Center
(415) 604-4050

Conditions: $M_\infty = 14.4$
$Re_L = 10^6$
$P_\infty = 0.0932$atm
$T_\infty = 298°$K
$\alpha = 6.35°$

Experimental Facility: Ames Ballistic Range

Flow Solvers: Three-Dimensional Navier-Stokes
with Finite Rate Chemistry
(TUFF and STUFF)

EXPERIMENT

REAL GAS COMPUTATION
O Concentration Contours
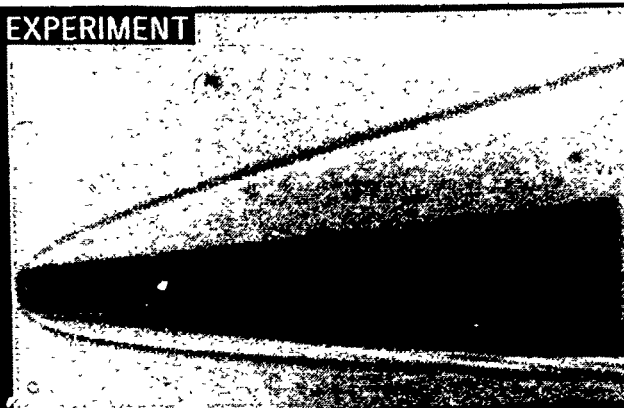
REAL GAS COMPUTATION
Pressure Contours
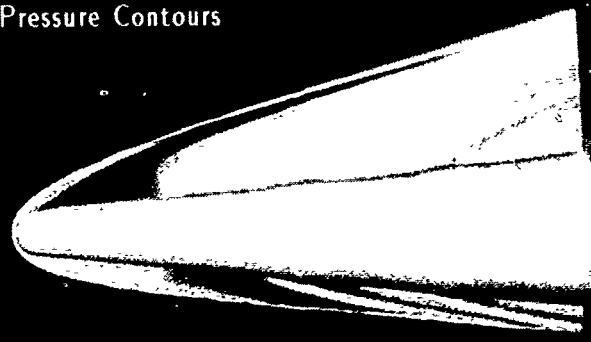
Figure 8-2. Blunt 5° Cone with Shock Generators

132

8-2 Development and Validation of Air Chemistry Effects for Hypersonic Computations

Objective. To incorporate real gas effects into the computation of hypersonic flows and to validate this capability.

Approach. Two new algorithms were developed to predict the flow of viscous, hypersonic, chemically reacting gasses over three dimensional bodies. These time- and space-marching codes are both finite-volume, upwind-differenced codes and have perfect, equilibrium, and nonequilibrium options. Strong coupling is used between the gas models and the fluid-dynamic equations. Transition and turbulent effects were accounted for by including zero and two-equation models.

Accomplishments. These codes have been validated on various types of geometries under hypersonic flow conditions. Comparisons were made with experiments, existing computational fluid dynamics (CFD) results, and exact solutions. One such validation was a blunt, 5° cone with shock generators. A coincident experiment was conducted in the Ames Ballistic Range to determine the aerodynamic forces acting on this geometry at high velocities. Agreement with the experimental results was very good. The effect of a real gas on the aerodynamic coefficients was also investigated by employing various gas models in the computations.

Significance. This research shows the degree to which the aerodynamic forces are influenced by real gas effects and provides researchers with a validated code for further computations. Currently, there are 11 industry and government installations using these programs.

Status/Plans. This effort has been completed and has resulted in three publications. Research is currently under way to enhance the codes by implementing a fully conservative zonal capability. The real gas modules are currently being ported to other CFD codes.

Gregory A. Molvik
Applied Computational Fluids Branch
Ames Research Center
(415) 604-4483
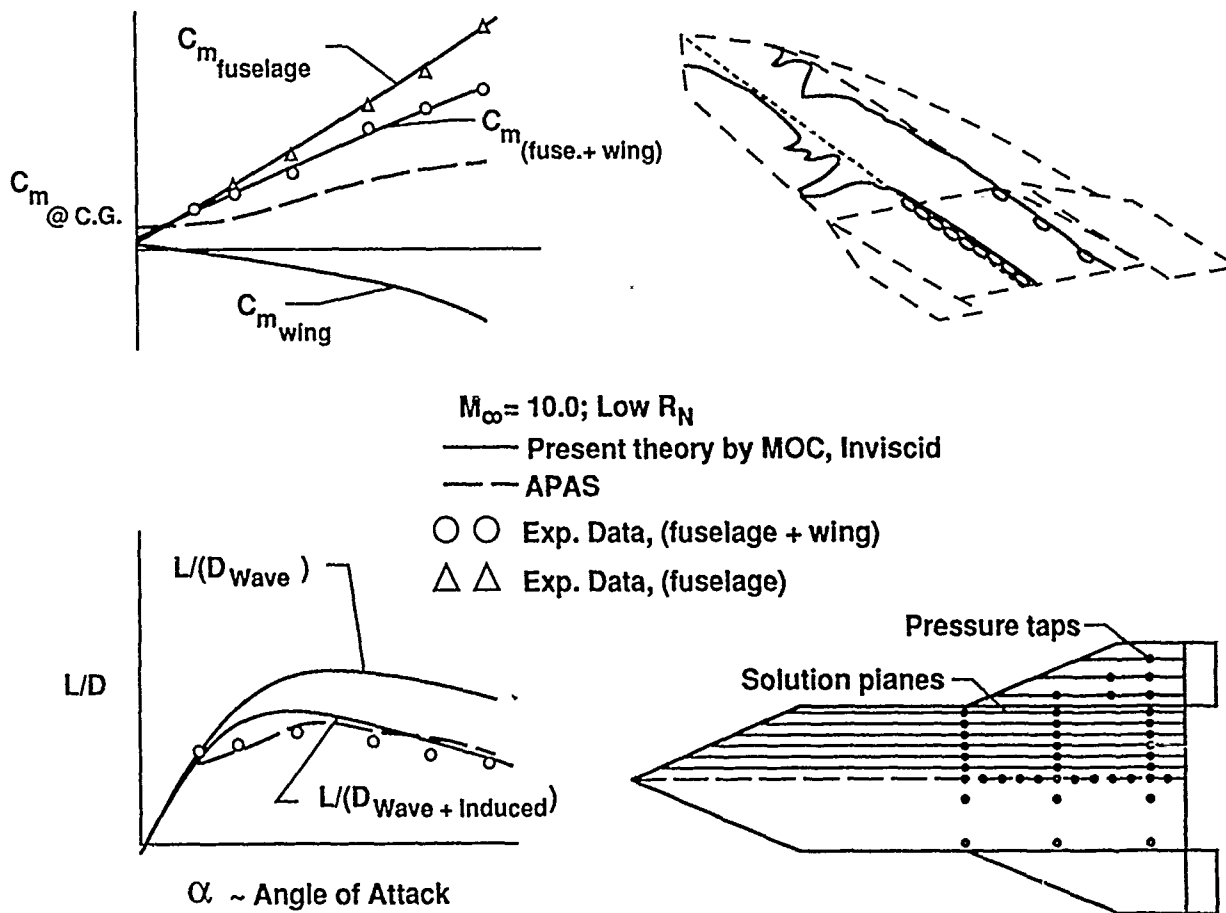
Figure 8-3. A Practical Engineering Method for Predicting Hypersonic
Configuration Aerodynamics

134

8-3 A Practical Engineering Method for Predicting Hypersonic Configuration Aerodynamics

Objective. To improve the current capability of being able to rapidly predict local pressure and thermal loads on hypersonic conceptual designs for structural analysis and stability and control analysis.

Approach. An engineering technique based on the method of characteristics (MOC) was chosen as a starting point for this study. Although this particular technique was originally developed for applications to supersonic wings and conical shapes, it has shown very good agreement with experimental and flight data up to Mach 4. The method will be adapted to complete hypersonic configurations and results compared with experimental data, Navier-Stokes (NS) calculations, and engineering methods currently in use.

Accomplishments. The MOC engineering technique has been modified for wing-fuselage combinations with finite swept sharp and blunt leading edges to yield configuration total inviscid forces and moments at hypersonic speeds. Comparisons with test results and Aerodynamic Preliminary Analysis System predictions of classified work done by Pel Phillips, Christopher Cruz, and Joel Everhart and with General Aerodynamic Simulation Program Navier-Stokes calculations show excellent agreement at M = 10. Local pressure distributions (inviscid) agree well with the experimental data and NS calculations.

Significance. The significance of the MOC engineering technique is to be able to predict quickly hypersonic configuration loads that are suitable for structural, thermal and stability, and control analyses.

Status/Plans. This technique is being documented as Version 0.0 and will be distributed on a limited basis for checkout. Future work will include adding boundary layer effects and validating at low and full-scale Reynold's numbers. Configuration dependency of the method will also be investigated, and the method to calculate inlet mass flow and powered effects on aerodynamic characteristics will be extended.

Suresh H. Goradia (Vigyan),
Sharon H. Stack, Charles R. McClinton,
Gregory L. Mekkes (AS&M)
Numerical Applications Office
Langley Research Center
(804) 864-3742
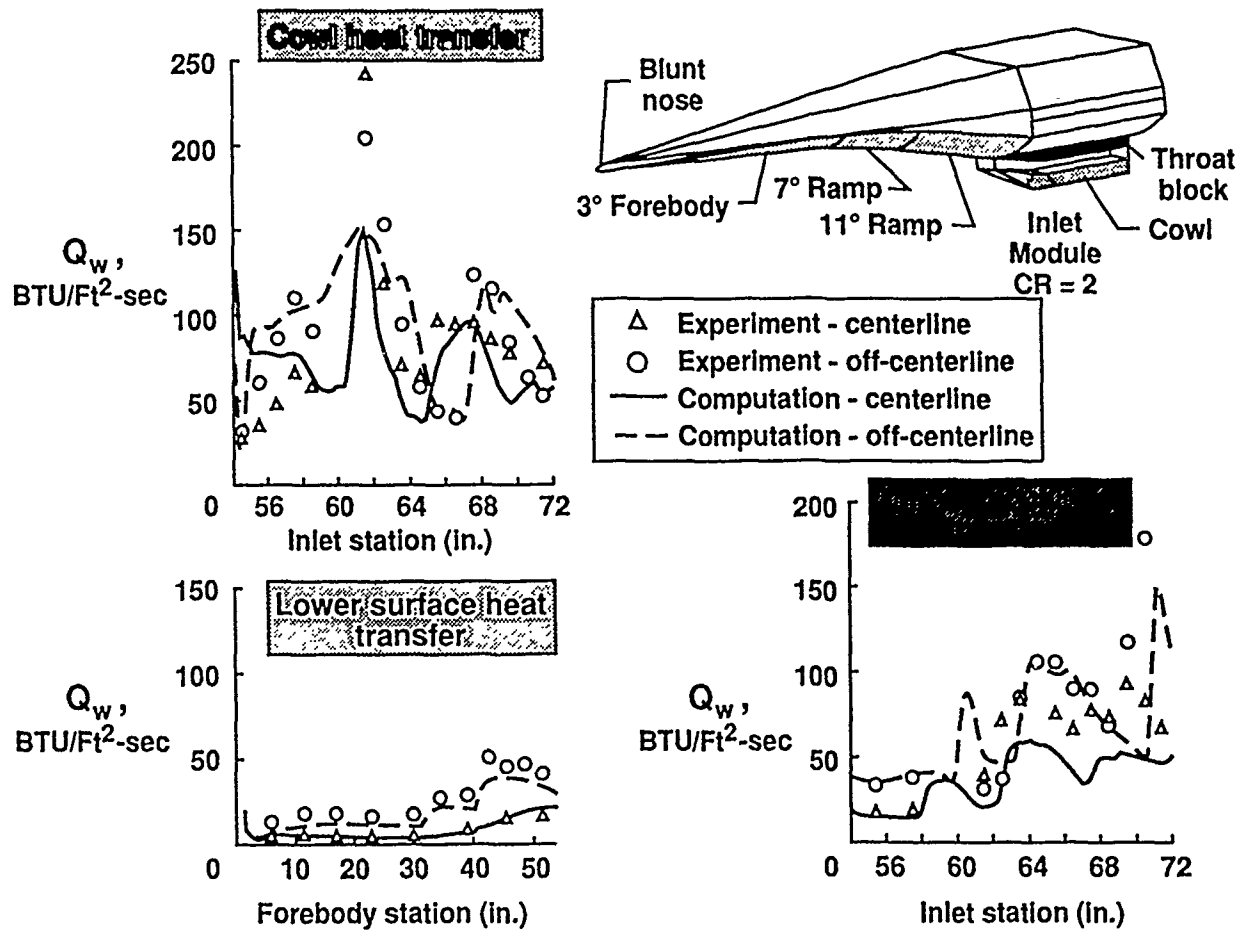
Figure 8-4. Navier-Stokes Calculations for a High-Speed Inlet

136

8-4 Navier-Stokes Calculations for a High-Speed Inlet

Objective. To calibrate current computational fluid dynamics (CFD) computer codes for hypersonic forebody/inlet flows using experimental data from the Generic Option #2 program.

Approach. Numerical simulation of three-dimensional hypersonic flow past a forebody/inlet configuration is performed using a state-of-the-art family of upwind methodology CFD computer codes, CFL3DE and CFL3D. Numerical results, including surface pressure and heat transfer along the forebody and inside the inlet, are compared with experimental data for the same configuration and freestream conditions.

Accomplishments. The forebody/inlet calculation has been completed. The computed forebody pressures and heat transfer exhibit reasonably good agreement with the experimental data as does the computed results in the inlet. In some regions of the inlet, the agreement is quite good considering the complex nature of the flow. In other regions, the agreement is poor indicating deficiencies in the numerical modeling.

Significance. The results demonstrate the ability of this family of CFD computer codes to predict forebody pressures and heat transfer rates with reasonably good accuracy. The results in the inlet are encouraging, but also indicate areas of needed improvement in the numerical modeling of internal flows. In particular, the turbulence modeling needs to be improved.

Status/Plans. Comparisons of the computed results and experimental data will be sent to the Generic Option #2 report authors for their comments and to learn of any update in the experimental data. After their response, the results will be documented in a NASP publication. Also, new turbulence models, better suited to internal flows, will be incorporated into this family of CFD computer codes.

Arthur D. Dilley, George F. Switzer,
William M. Eppard
Langley Research Center
(804) 864-2288

$\alpha = 12°$, $\dot{w} = 5$ lbs/sec, $h/b = 0.08$, $q_\infty = 30$ psf
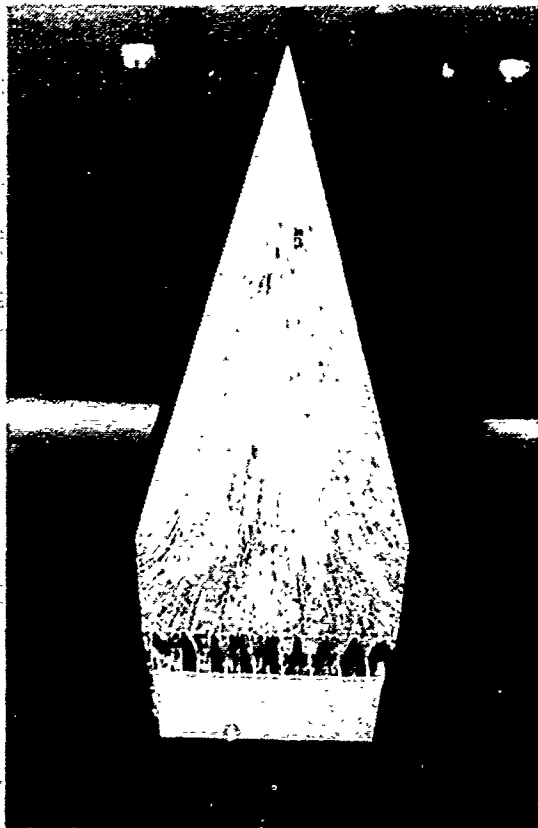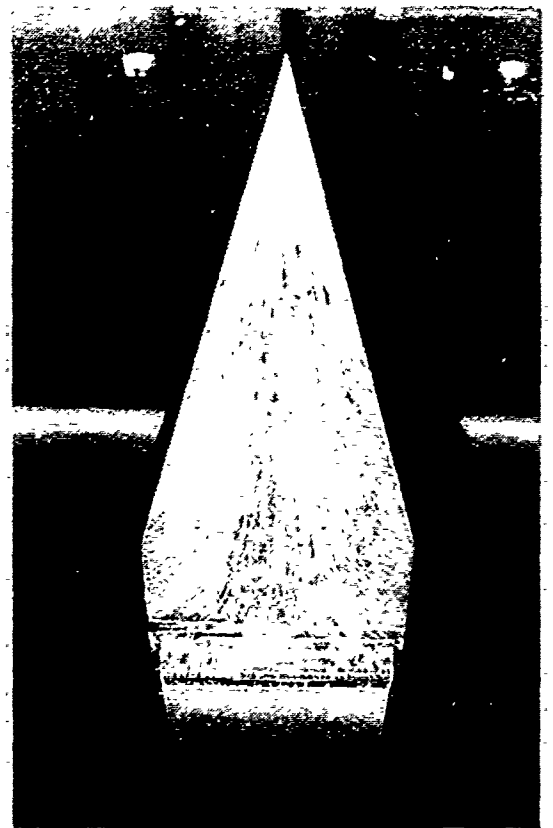
Flow through   **Faired inlet**

Figure 8-5. Effects of an Inlet Fairing

8-5 Low-Speed Propulsion/Airframe Integration

Objective. To establish and demonstrate test techniques for assessing low-speed performance, stability and control, and ground effects of hypersonic configurations.

Approach. Experimental investigations will be conducted in the 14-foot by 22-foot subsonic tunnel using generic powered hypersonic configurations. Force and moment data and both on and off surface flow visualization will be obtained and used to analyze configuration characteristics both in and out of ground effect. This analysis will also be used to verify testing techniques employing power simulation to give installed performance.

Accomplishments. Generic Ground Effects Model (GEM): Wind tunnel tests of powered model in ground effect were conducted to provide the first extensive set of data showing interaction of exhaust flow, airframe, and ground plane. Results show significant ground effects that are detrimental to takeoff performance. While there are certainly configuration effects to be included in a final analysis, it appears that powered hypersonic configurations will suffer lift losses in ground effect.

The tests confirmed that proper engine simulation should include both the exhaust flow as well as the inlet flow for highly integrated hypersonic configurations. Results show that the forebody flow field and force and moment data are significantly different with and without a flowing inlet.

Test Techniques Demonstrator Model (TTD): The low-speed powered model was delivered and is scheduled for initial testing in August 1990.

Significance. The GEM model has provided the first significant data set indicating the potential detrimental ground effects that may severely limit takeoff performance and give evidence of the need for proper inlet as well as exhaust modeling. As a consequence of this effort, the three NASP airframe contractors include ground effects testing as essential to risk reduction plans.

Status/Plans. All GEM results have been published in NASP Symposium Papers and NASA Technical Papers. TTD scheduled for initial testing in August 1990.

John W. Paulson, Jr., Gregory M. Gatlin
Applied Aerodynamics Division
Langley Research Division
(804) 864-5071
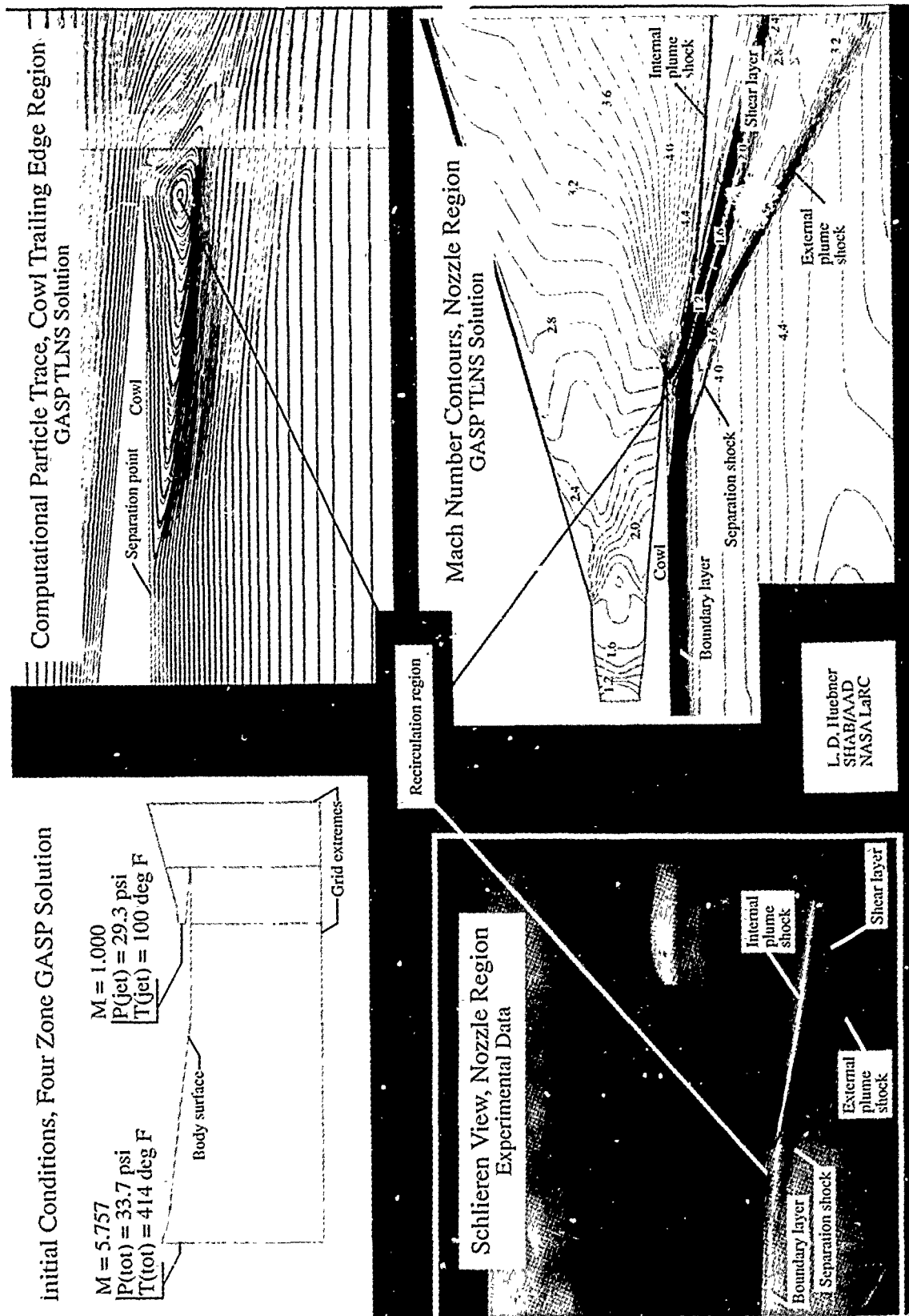
Figure 8-6. Nozzle Flow Field Prediction for a Hypersonic Airbreathing Vehicle

8-6 Hypersonic Propulsion Airframe Integration Research

Objective. To computationally analyze the flow field for hypersonic forebody/inlet and nozzle/afterbody regions as part of the overall National Aero-Space Plane Technology Maturation Plan (NASP-TMP) effort in the area of propulsion/airframe integration (PAI).

Approach. An Euler/Navier-Stokes (NS) computational fluid dynamics (CFD) code was used to compute the three-dimensional flow about a hypersonic forebody-alone, full body, forebody with blocked inlet, forebody with inlet fairing, and the two-dimensional flow about a powered hypersonic vehicle. CFD solutions were compared with surface and pitot pressure data, as well as schlieren and oil-flow photographs.

Accomplishments. Pitot pressure measurements made at the inlet plane of the forebody-alone showed very good agreement with pitot pressures calculated from parabolized NS (PNS) solutions. At four different conditions, the computational predictions accurately predicted boundary-layer thickness and the extent of the classic boundary-layer accumulation on the center line. PNS solutions of a NASP-type full body at Mach 20 in helium also showed good agreement of center line surface pressures. Thin-layer NS (TLNS) solutions of the forebody with blocked inlet and with faired inlet were performed with expectations of predicting massive flow separation on the forebody undersurface. Comparison of computational surface particle traces with oil-flow photographs showed excellent agreement of the extent of separation, flow patterns within the separated region, and the location of flow reattachment on the blocked- and faired-inlet surfaces. Finally, a two-dimensional study was conducted that analyzes flow-field features associated with a simulated powered hypersonic vehicle. Euler and PNS solutions were performed at four test conditions. Under one condition, an additional shock was seen underneath the cowl trailing edge and was attributed to the boundary-layer separation caused by localized recirculation. Salient features of this complex flow were predicted by using the code as a TLNS solver .

Significance. The ability of computational methods to accurately predict flow phenomena associated with NASP PAI is critical to the design of this vehicle. The accurate comparison of CFD results with wind tunnel data provides confidence and the first step in the code's ability to predict the flow about NASP-type vehicles at full-scale flight conditions.

Status/Plans. Computations on the simulated powered configuration will be expanded to three dimensions and will be executed with a turbulence model. This effort will eventually result in a tip-to-tail three-dimensional, NS solution capability on the entire NASP configuration.

Lawrence D. Huebner
Supersonic/Hypersonic Aerodynamics Branch
Langley Research Center
(804) 864-5583
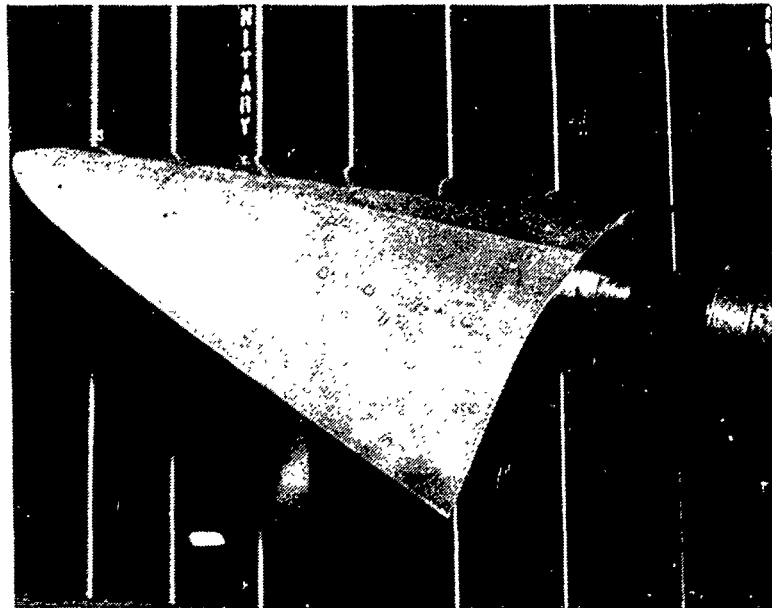
MACH 4 WAVERIDER IN UPWT
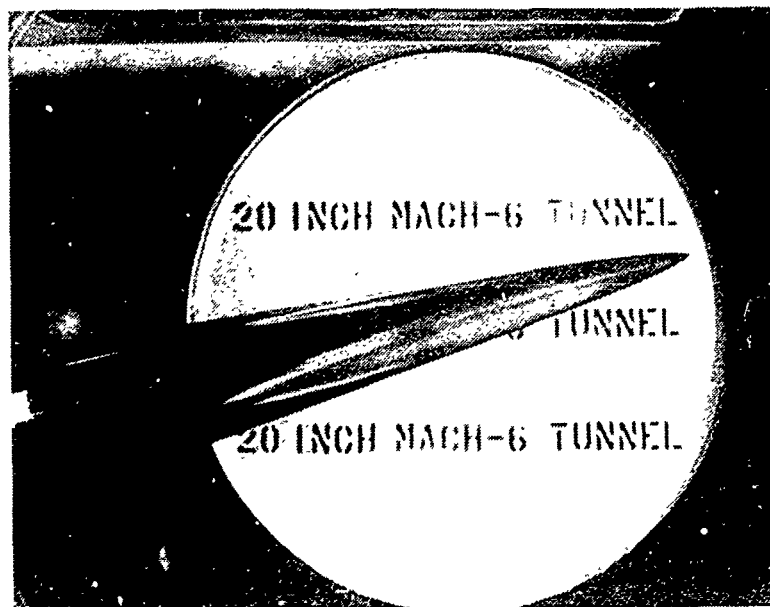
**MACH 6 WAVERIDER
IN 20-INCH MACH 6 FACILITY**

Figure 8-7. Analysis of Optimized Hypersonic Viscous Waveriders

142

8-7 Analysis of Optimized Hypersonic Viscous Waveriders

Objective. To evaluate two waverider configurations developed from a hypersonic cone-derived viscous waverider optimization code.

Approach. Two viscous waverider configurations were designed, assuming fully turbulent flow conditions at Mach 4 and Mach 6, respectively, using a hypersonic cone-derived viscous waverider optimization code developed by the University of Maryland. Also, a reference model was designed with a flat upper surface and with the same planform and cross-sectional area distribution as the Mach 4 configuration.

Accomplishments. The Mach 4 waverider model and the reference model were tested in the Unitary Plan Wind Tunnel, and the Mach 6 waverider model was tested in the 20-inch Mach 6 facility. Force and moment, surface pressure, and flow visualization (i.e., schlieren, shadowgraph, vapor-screen, and oil-flow photographs) data were obtained for all three models. Theoretical analyses using full-potential and Euler solvers were conducted on these shapes.

Significance. Results from theoretical analyses agree well with experimental data for the Mach 4 waverider, verifying the performance potential of the waverider.

Status/Plans. Tests of the waverider configurations at Mach numbers from 1.5 to 6.0 are complete; the data for the reference model and the Mach 6 waverider model are being analyzed and will be compared with theoretical analyses. An invited talk on the results of this study will be presented at the First International Hypersonic Waverider Symposium at the University of Maryland campus in October 1990. Navier-Stokes analysis will begin in the fall 1990.

Steven X. S. Bauer
Supersonic/Hypersonic Aerodynamics Branch
Langley Research Center
(804) 864-5946

Chapter 9

Aeroacoustics Research and Technology

Aeroacoustics is concerned with the fundamental understanding, prediction and control of noise and acoustic loads produced by the motion of fluids and bodies moving through the atmosphere. To achieve this objective, research is being conducted in three main areas:

- Computational Aeroacoustics--establish CFD methodology as a discipline for acoustics technology development focusing on computational models of high-speed flow noise and shock/vortex interactions
- Supersonic Jets/Loads--understand/predict/reduce noise and acoustic loads generated by high-speed aircraft and in particular, establish innovative concepts for supersonic jet noise suppression and develop a detailed acoustics loads data base on airframe structures
- Long Range Propagation--model atmospheric propagation effects supported by fundamental verification/validation experiments.

Program Manager: Steve Wander
                        OAET/RF
                        Washington, DC 20546
                        (202) 453-2820
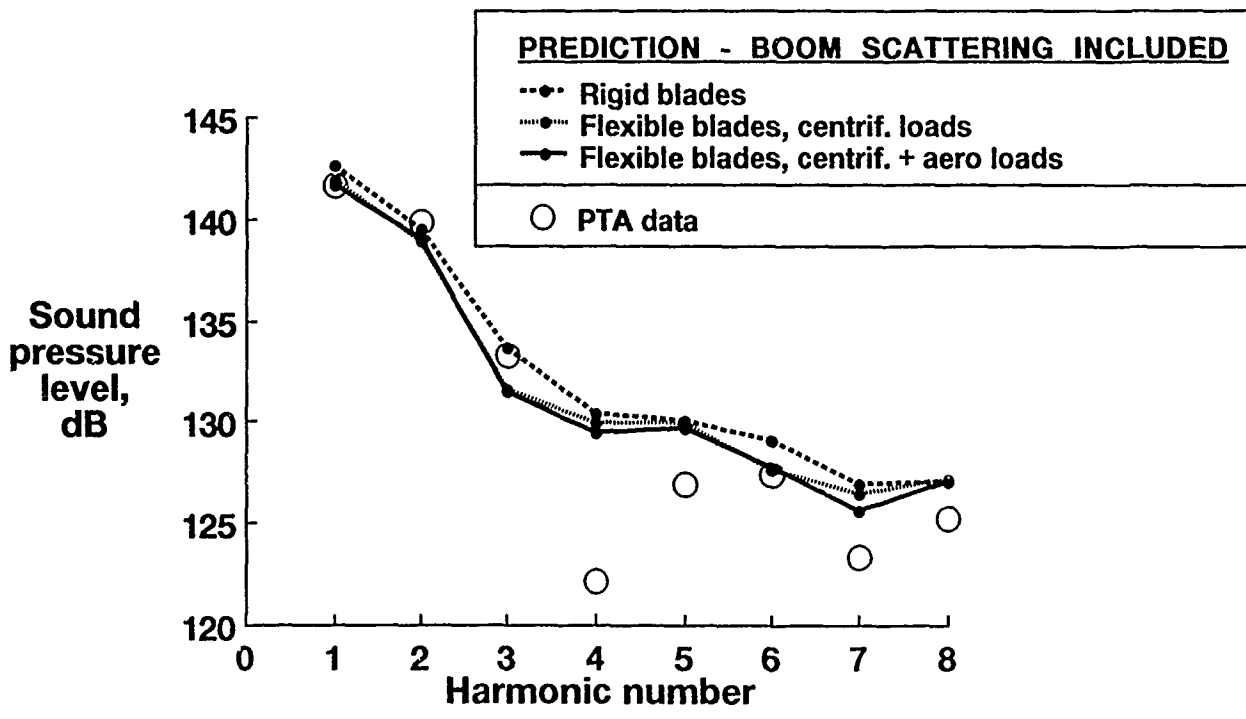
Figure 9-1. PTA Aircraft Boom Microphone 3 Spectra
(Cruise Condition: $M_{A/C} = 0.81$, $M_{H\,TIP} = 1.15$, BPF = 226 Hz)

146

# 9-1 The Effect of Blade Deformation on Aerodynamics and Noise of Advanced Technology Propellers

Objective. To study the effect of blade deformation by centrifugal forces and loads on the aerodynamics and noise of advanced technology propellers.

Approach. The deflection and blade aerodynamics are interrelated and could only be calculated by an iterative process. An aeroelastic code (NASTRAN) first calculates blade deflections due to centrifugal forces, and a CFD code then calculates blade loads. The blade loads are then used in NASTRAN to calculate total blade deflection due to blade loads and centrifugal forces. The new blade shape is once more used as input to the CFD code and the iteration is continued. The resulting blade shape and loads are then used as input to the propeller noise prediction code by Dunn, Farassat, and Padula (DFP-ATP) to give the acoustic time history and spectrum at any given observer position. Two formulations for moving sources are used in this code for subsonic (formulation 1-A) and transonic/supersonic sources (formulation 3) with automatic switch to either of the formulations, as necessary. The resultant output can be compared to free-field measurements or used as input to the boundary layer noise propagation code MRS-BLP.

Accomplishments. The complete aeroelastic, aerodynamic, and noise calculations were performed for a full-scale advanced technology propeller (SR-7L) with diameter 2.74 m (9 ft.) operating at flight Mach number of 0.813 and helical tip Mach number of 1.15 at an altitude of 10.7 km (35,000 ft.) In particular, the measured power of the propeller was known and was used in the aeroelastic-aerodynamic iteration. The results show that the blade camber shape and twist are influenced by elastic deformation, and the outboard region of the blade is primarily affected. The centrifugal effect is more important than blade loads in blade deformation. Blade deformation affects propeller power and blade surface

pressure significantly. Again the surface pressure of the outboard region of the blade is affected more by the blade deformation. The accompanying figure shows the effects of the blade deformation on the spectrum of the noise of the PTA propeller for boom microphone 3 (1.12 propeller diameter from axis and 0.5 radius behind disc). In this figure, the boom-scattering correction is included in the predictions, and the propeller power is the same for all cases. It is seen that the inclusion of blade deformation affects the predicted noise. The deformation by centrifugal forces accounts for most of the changes in the noise spectrum. Up to 2.5 dB change is observed in some harmonics, and the agreement between measured and predicted noise spectra is improved by inclusion of blade deformation.

Significance. Blade deflection has significant effects on propeller aerodynamics and noise. This effort has once more demonstrated the multidisciplinary nature of propeller noise prediction. An automated aeroelastic-aerodynamic iteration scheme has been developed to use in the noise prediction of advanced technology propellers. This scheme is also valuable for other rotating blade systems such as the new high bypass turbofan engines.

Status/Plans. Further propeller noise predictions and comparison with measured data at different operating conditions of PTA aircraft are planned. The predictions will include both the boom and fuselage microphones.

F. Farassat
Applied Acoustics Branch
Langley Research Center
(804) 864-5279
M. H. Dunn, P. L. Spence,
Lockheed Engineering & Sciences Company
(804) 766-9600

NOISE SOURCE
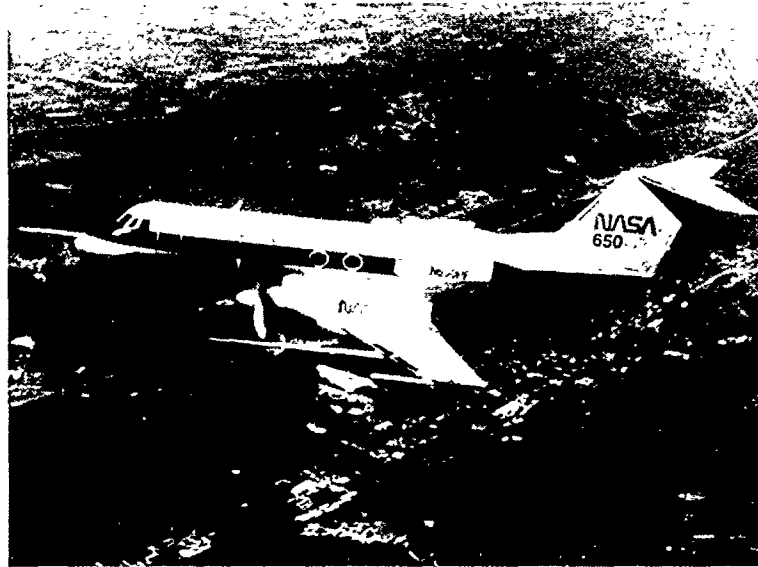
PREDICTION ERROR
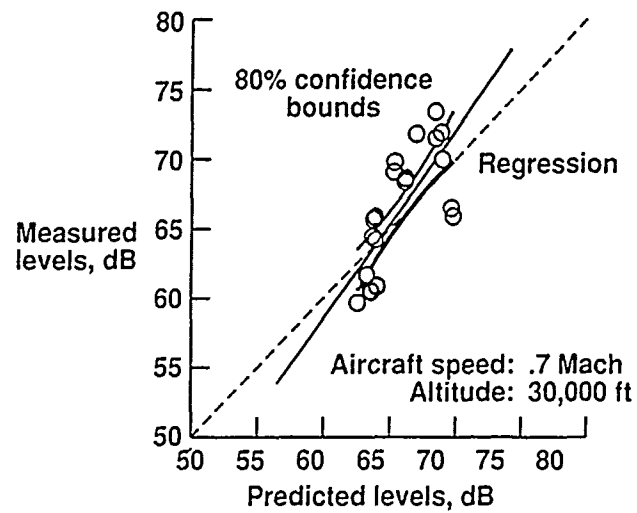
Figure 9-2. PTA En Route Noise Test

148

9-2 En Route Noise Test

Objective. To predict the noise received on the ground from an advanced turboprop operating at cruise conditions.

Approach. A flight experiment, referred to as the En Route Noise test, was conducted in cooperation with NASA LeRC and the FAA to investigate the propagation of advanced turboprop noise. The experiment conducted at White Sands Missile Range consisted of flying LeRC's Propfan Test Assessment (PTA) airplane over a microphone array. Extensive weather measurements, including free-release radiosonde weather balloons, were made during the flight test. Radar tracking of the PTA airplane was used to measure its position as a function of time. Ninety flyovers of the PTA airplane were measured at altitudes of 15,000 to 30,000 ft and at Mach numbers ranging from 0.540 to 0.77 M. The microphone array was an 8-element linear array with an inter-element spacing of 400 ft.

Accomplishments. Shown in the figure is a photograph of the PTA airplane. Visible in the photograph is the installation of the eight-bladed, single-propeller advanced turboprop mounted on the port wing in a tractor configuration. For the majority of the test the advanced turboprop was operated with a rotational tip speed of 800 ft/sec. The plot in the figure is a comparison between predicted and measured peak ground level Overall Sound Pressure Levels for the eighteen 30,000 ft, 0.7 M runs. The measured results are an ensemble average from eight ground-level microphones. The dashed line in the plot represents perfect agreement between measured and predicted noise levels. The longest solid line is a regression analysis, best fit line through the data points. The shorter solid lines represent 80% confidence bounds about the regression line. The predicted noise levels were made with a two-dimensional ray-tracing propagation model. The source noise directivity used as input in the propagation prediction were predicted using Langley's Aircraft Noise Prediction Program (ANOPP). Measured advanced turboprop operating parameters, including boom microphone noise levels, and a measured weather profile up to 40,000 ft were also used as input to the ray-tracing model.

Significance. The agreement between predicted and measured advanced turboprop flyover noise is good. The perfect agreement line falls within the 80% bounds of the regression line. Because of propagation-induced variability, past comparisons between predicted and single microphone measurements showed less agreement. The application of ensemble-averaging techniques to the En Route Noise issue has demonstrated that ray-tracing propagation models are adequate to predict daily average received noise levels from advanced turboprops operating at cruise conditions.

Status/Plans. In the future, sophisticated propagation models, like a three-dimensional ray tracing and the fast field program, will be used to investigate day-to-day (long term) variability in average peak overall sound pressure levels. The short term (within a flyover) variability will also be investigated.

William L. Willshire, Jr.
Applied Acoustics Branch
Langley Research Center
(804) 864-5270

HOT GAS MODEL IN LEWIS 9 x 15 WIND TUNNEL

CANARD TRANSDUCER

NASA

FREESTREAM MICROPHONE

EFFECT OF THRUST ON NOISE

TEMP = 500°F

Sound pressure level, dB

CANARD

FREESTREAM

Thrust level, per cent
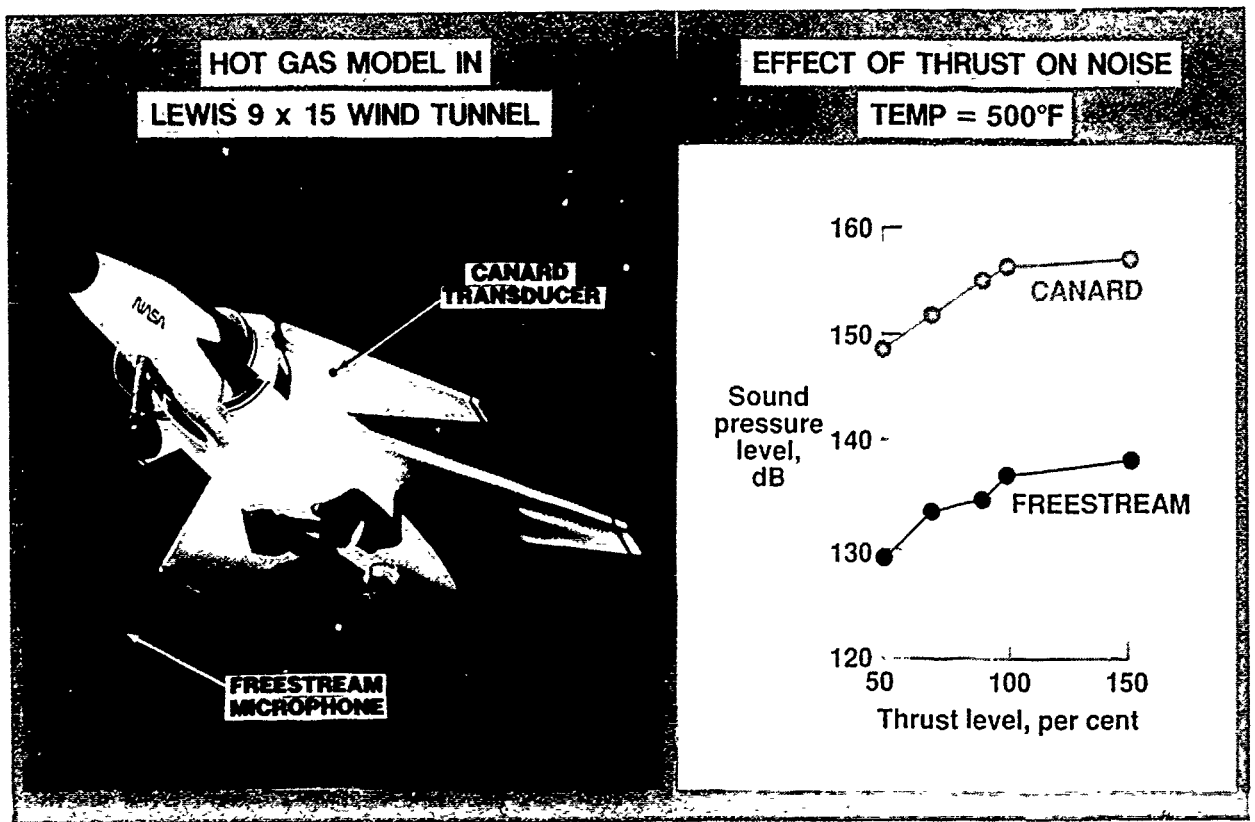
Figure 9-3. Joint Lewis/Langley ASTOVL Acoustic Loads Test

150

9-3 Joint Lewis/Langley ASTOVL Acoustic Loads Test

Objective. To characterize the acoustics and dynamic structural loading of an advanced short takeoff/vertical landing (ASTOVL) aircraft operating in ground effect and at elevated jet exit temperatures. This research is part of a Lewis/Langley cooperative program, complementary to in-house research aimed at improving the understanding of jet impingement acoustics, particularly for multiple, heated jets.

Approach. A 9.2% scale model of an ASTOVL aircraft was tested in the Lewis 9 x 15 Wind Tunnel. The model was built to evaluate the hot gas ingestion (HGI) characteristics of the design up to temperatures of 1000°F, and nozzle pressure ratios (NPR) of 4. The accompanying figure shows the installed model. Water injected upstream of the nozzles allows the jet plumes to be visualized. Acoustic data were obtained from a linear array of five freestream microphones, located parallel to the model centerline. Model dynamic loads were measured with eight watercooled dynamic pressure transducers located on the underside of the canard, wing, and aft fuselage. The placement of the inboard canard transducer is illustrated in the figure.

Accomplishments. Data were taken for over 700 combinations of model geometry and test conditions. The data shown illustrate the effect of nozzle height on the overall sound pressure level as measured on the canard and in the freestream, while the jets were operating at the design condition. As shown by the data, levels up to 160 dB were observed on the model, and up to 140 dB in the freestream. At other conditions, levels as high as 180 dB, as well as discrete tones 160 dB in amplitude were measured. Tones were generated at a wide variety of operating conditions (model height, nozzle pressure ratios, jet tempera-

tures) and geometries. Both free-jet tones and impingement tones were observed, and their frequencies were found to obey certain scaling laws.

Significance. Acoustic loads on ASTOVL configurations are of a sufficiently high level to potentially cause structural failure. No satisfactory model exists that can predict the acoustics of multiple heated, nonaxisymmetric jets operating in ground effect in an off-design condition. The acquired measurements provide data that will be valuable in understanding both the fundamental physics of jet impingement and the configuration issues involved in ASTOVL aircraft acoustics.

Status/Plans. This test served as Phase II of Lewis' HGI work with this design. Additional acoustic work is planned for Phase III, including the placement of transducers on the underside of the fuselage between the nozzles. This will allow for the investigation of the dynamics of fountain impingement on the model, and the propagation of noise from the fountain to the far field.

L. Kerry Mitchell
Aeroacoustics Branch
Langley Research Center
(804) 864-3625

151
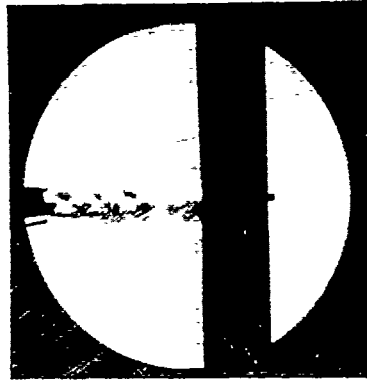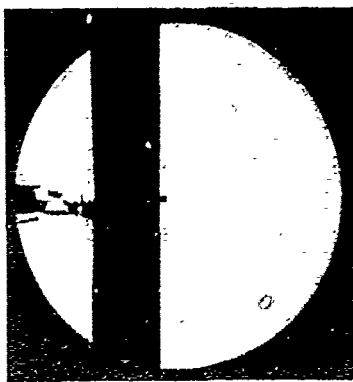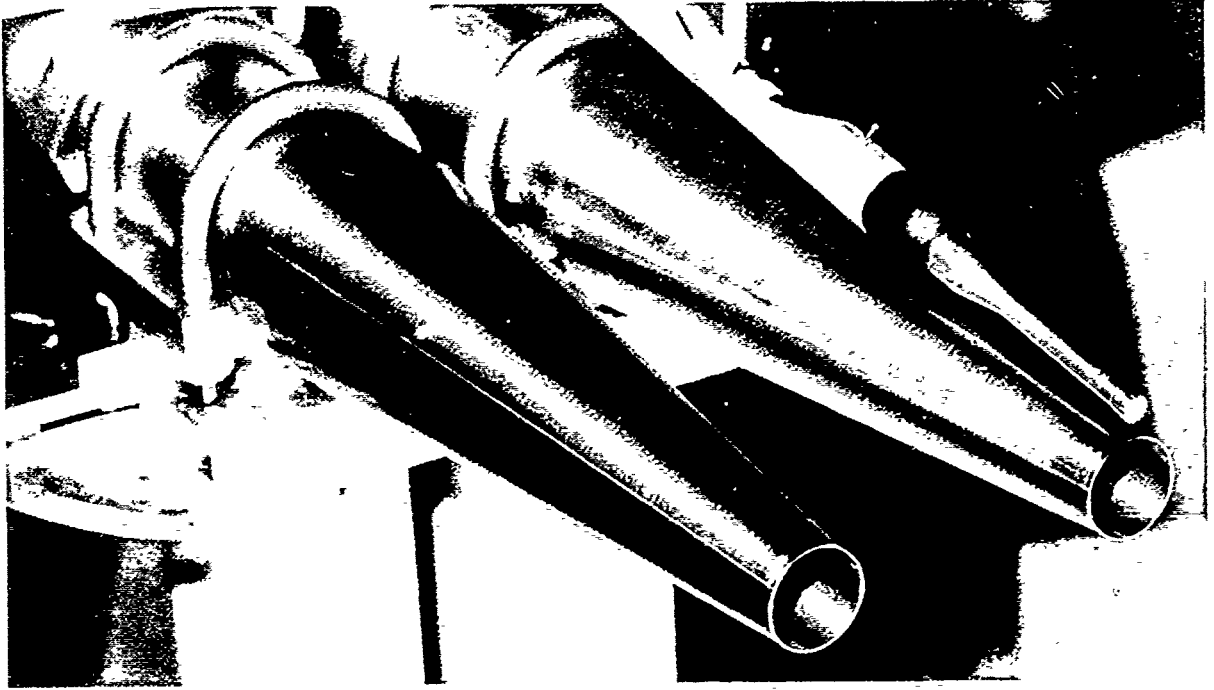
Figure 9-4. Acoustic Loads Generated By Ground Impingement of Twin Supersonic Jets

152

9-4 Acoustic Loads Generated by Ground Impingement of Twin Supersonic Jets

Objective. To determine the acoustic loads due to twin supersonic nozzles of various exit geometries on a STOVL aircraft operating in takeoff and hover.

Approach. Twin convergent and convergent-divergent circular, rectangular, and D-shaped nozzles were tested over wide ranges of nozzle pressure ratios and nozzle to ground surface distances. Pressure fluctuations resulting from jet oscillations and jet-ground interactions were obtained from microphones positioned upstream of the exit plane of the nozzles. Complementary measurements of plume pressure distributions and phase locked optics were used to correlate the acoustic loads.

Accomplishments. Preliminary analysis of the data shows loads of similar magnitude being generated by all the various exit geometry nozzles. This is true even for the convergent-divergent nozzles at their design pressure when the nozzle exit-to-ground separation distance is small, since the jet impingement process dominates the noise generation. This jet impingement noise reaches a maximum at an intermediate nozzle pressure ratio (jet Mach number approximately 1.4). The strong jet oscillations associated with the generation of impingement tones is highly dependent on separation distance as seen in the accompanying schlieren photographs.

Significance. The ranges of nozzle pressure ratios and nozzle-to- ground separation distances of the most severe acoustic loading and jet instability arising from twin supersonic jet impingement has been determined for various nozzle exit geometries. This will aid in designing for acoustic fatigue of STOVL aircraft and vectored thrust hardware of jets operating at supersonic pressure ratios.

Status/Plans. The experiments have been completed and analysis of the data is in progress.

Thomas D. Norum
Aeroacoustics Branch
Langley Research Center
(804) 864-3620

Chapter 10

High Speed Research

The High Speed Research Program seeks to provide the technology answers for an environmentally safe design of a supersonic transport. In aerodynamics the technologies focus on efficiencies needed to provide a low noise configuration, both in climb out and cruise. The specific objectives of the Program are to provide enabling technologies for supersonic transports to achieve in a practical configuration: acceptable overland sonic booms, efficient second stage climb-out for low noise, and supersonic laminar flow control for peak cruise efficiency. The laminar flow control will significantly reduce the aircraft gross weight, hence the noise signatures. The sonic boom element will be evaluated in FY 1992 to determine whether the promise of low boom is great enough to continue research.

There is a great body of data from the previous supersonic cruise research program that ended in the early 1980s. However, prediction methods, optimization techniques, and experimental testing have improved for complex configurations. In addition, new ideas for high lift devices and subsonic laminar flow control are now candidates for investigation for supersonic configurations. These developments have given hope that supersonic aircraft efficiencies can be improved to help the environmental and economic realities of the coming age. Based upon systems studies these efficiencies translate into goals for lift-to-drag ratios of 10 in climb, 15 in transonic cruise, and 10 in supersonic cruise.

The High Speed Research Program is focused on (1) CFD modeling and validation of aeroacoustic analysis including measurement techniques and atmospheric modeling, (2) development of innovative high lift devices to provide increased lift-to-drag ratios on climb out; (3) design, wind tunnel test and analysis of low sonic boom configurations; (4) large-scale flight evaluation of supersonic laminar flow control including design codes for transition prediction, and the practical installation of suction systems.
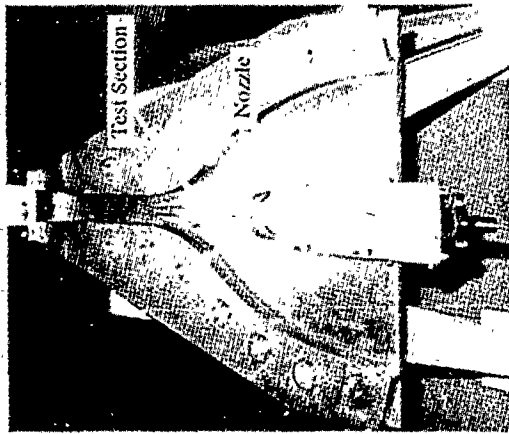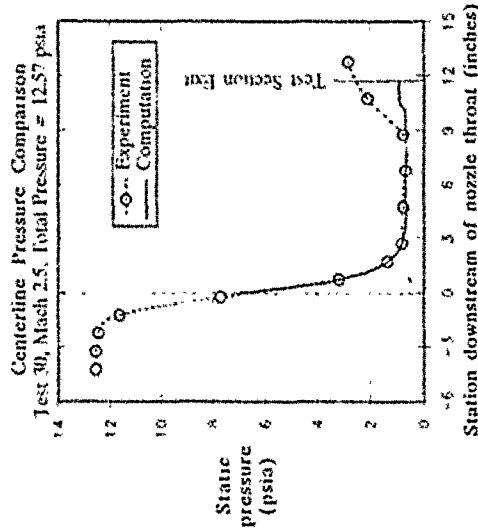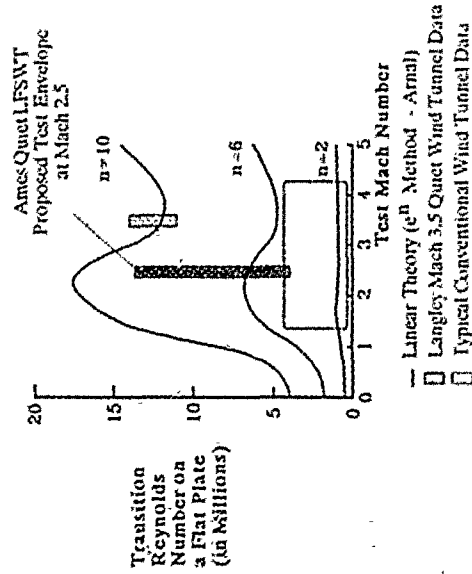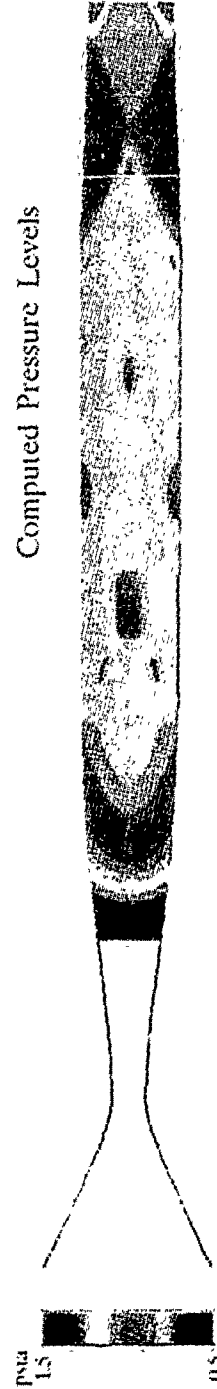
Program Manager: George Unger
                     OAET/RF
                     Washington, DC 20546
                     (202) 453-5420

Figure 10-1. Quiet Supersonic Wind Tunnel Project

156

10-1 Development of a Quiet Laminar Flow Supersonic Wind Tunnel for the MACH 2.5 Regime

Objective. To validate design principles for a new generation of low-cost laminar flow supersonic wind tunnels (LFSWT) using "quiet" technology. The LFSWT is essential for studies of boundary layer transition receptivity at high speed civil transport (HSCT) Mach numbers.

Approach. Prior to construction of a full size (~16 x 8 inch test section) LFSWT, a 1/8 scale Proof of Concept (PoC) model was built. The PoC was needed to establish that the Fluid Mechanics Laboratory (FML) indraft compressor could support the desired test envelope of M = 2.5 @ Re = 1-5 million/foot. The low compression ratio (~1.7) of the compressor led to the use of a unique tunnel injector design proposed by Riise. Computational Fluid Dynamics (CFD) support is providing additional nozzle and tunnel drive system design results. Additionally, innovative techniques for low-cost quiet nozzle and test section development are being investigated. In keeping with the low-budget concept, a minimal number of full-time personnel are involved; the small size of the wind tunnel will keep the project below funding requirements for "Construction of Facilities."

Accomplishments. The PoC was designed, fabricated, and successfully operated at M = 2.5 within 9 months. We have established that improvements to the tunnel drive system are needed if we are to achieve natural laminar flow on the nozzle walls of the LFSWT. A Navier-Stokes code is being applied to complement experimental studies of the tunnel drive system and nozzle/test section flows. A substantial amount of information on nozzle design has been gathered and is published in a bibliography (NASA CR-4294, May 1990).

Significance. LFSWT development will provide NASA with a unique M = 2.5 quiet testing environment. This low-budget project has demonstrated that we can operate supersonic wind tunnels with nonspecialized compressors. The small scale of the LFSWT will enhance supersonic nozzle and transition research progress within NASA.

Status/Plans. We are currently investigating methods for PoC test envelope expansion. Flow visualization of the test section, injector, and mixing region, using a novel focusing schlieren system, will be implemented soon. Based on the outcome of these studies, we plan to start final design and fabrication of the full-scale LFSWT. During the construction phase of the LFSWT, the PoC will be used for nozzle studies and instrumentation research.

Jim Laub, Stephen Wolf, Lyn King
Fluid Dynamics Research Branch
Ames Research Center
(415) 604-4136

Wing Upper Surface

Region	Geom	Cp
A	Pos. Slope	+
B	Pos. Slope	-
C	Neg. Slope	-
D	Neg. Slope	+

Expansion Region

Compression Region

- - - Airfoil Maximum Thickness Line

Standard Geometry

Near-Conical Geometry

Performance Characteristics

- Baseline
- - - Near-conical
-·-·- Natural
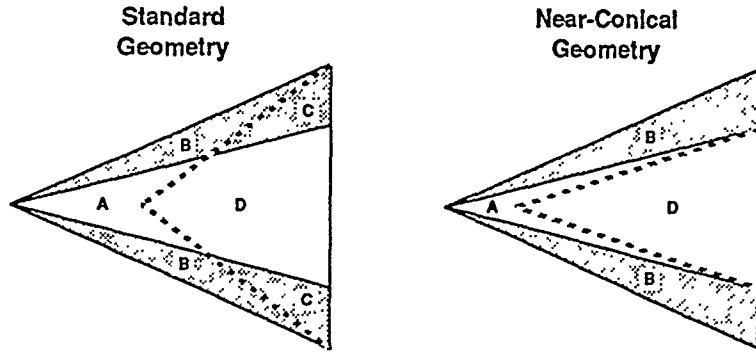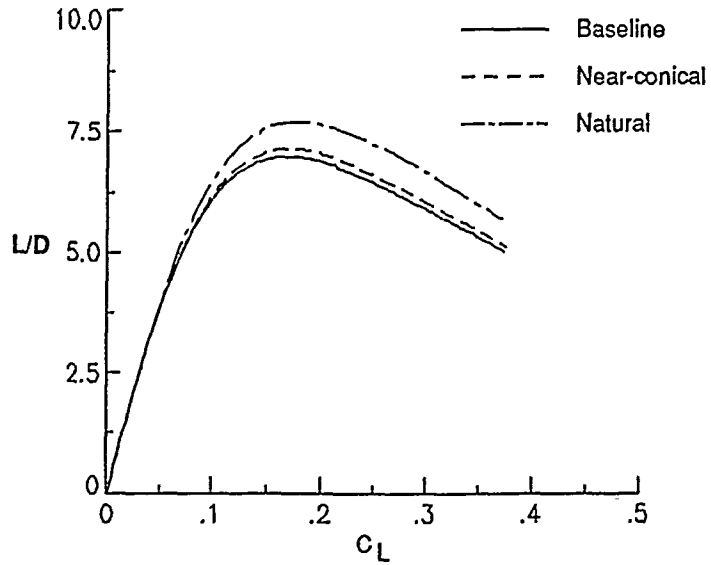
Figure 10-2. Natural Flow Wing Design

10-2 Natural Flow Wing Design Study

Objective. To design a series of wings with reduced drag by shaping the surface geometry to make better use of the naturally occurring conical flow on the upper surface and the positive pressure coefficient loading on the lower surface of the wing.

Approach. Three 65°-swept delta wings with a design Mach number of 1.62 were chosen for the study by examining a large amount of existing data. The wings were designed using NACA modified 4-digit airfoils. Theoretical evaluation of these wings was done using a full-potential solver (SIMP, Supersonic Implicit Marching Potential) and a Euler solver (EMTAC, Euler Marching Technique for Accurate Computation). Wing designs were rated by the level of drag reduction that could be achieved at both cruise and maneuver lift conditions (i.e., $C_L = 0.1$ and $C_L = 0.3$, respectively).

Accomplishments. With respect to a typical baseline wing, an 18% increase in lift/drag has been predicted at both cruise and maneuver lift conditions for the natural flow wing.

Significance. Results from the theoretical analysis show a marked improvement in performance over conventional delta wings throughout cruise and maneuvering conditions.

Status/Plans. Three 65°-swept delta wings are in the process of construction for testing in the Unitary Plan Wind Tunnel (i.e., a baseline wing with typical airfoil thickness distribution, a near-conical wing, and a natural-flow wing).

Steven X. S. Bauer
Supersonic/Hypersonic Aerodynamics Branch
Richard M. Wood
Subsonic Aerodynamics Branch
Langley Research Center
(804) 864-5946

EFFECT OF TRANSITION LOCATION
Grit Drag Removed

$M = 3.0, C_L = 0$

- o $X_t = .4"$
- □ No grit
- △ $R_{\infty, t} = 3.5 \times 10^6 / \text{ft}$ ⎫ $\left(\frac{X}{C}\right)_t = .5$
- ▲ $R_{\infty, t} = 2.0 \times 10^6 / \text{ft}$ ⎭
- —— Theory - Turbulent
- — — Theory - 50% Laminar

$C_{D,o}$

$R_\infty \times 10^6 / \text{ft}$

BOUNDARY LAYER CONDITIONS

1.2"

$X_t = .4"$

$\left(\frac{X}{C}\right)_t = .5$

12.575"
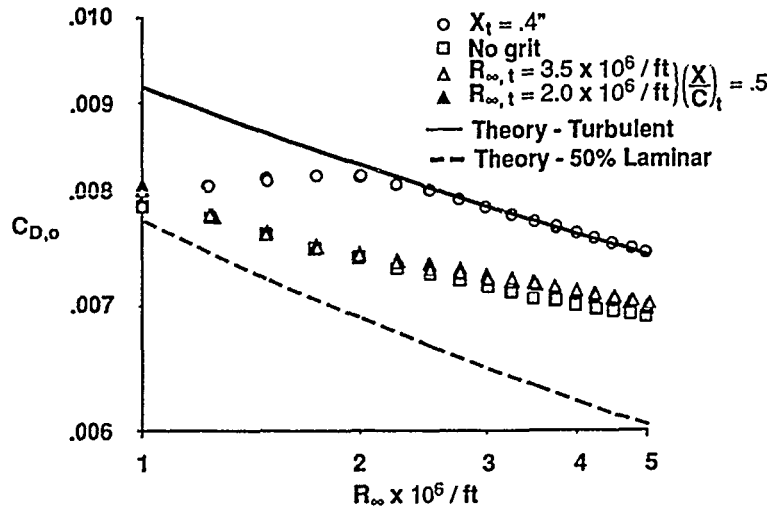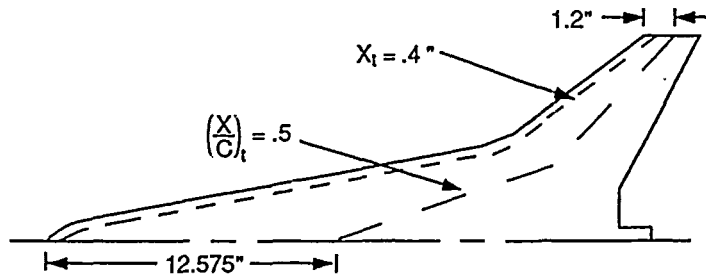
- Free transition (no transition grit)
- Turbulent flow ($X_t = .4"$)
- 50 percent laminar ($\left(\frac{X}{C}\right)_t = .5$)
  - $R_{\infty, t} = 2.0 \times 10^6 / \text{ft}$
  - $R_{\infty, t} = 3.5 \times 10^6 / \text{ft}$

Figure 10-3. HSCT Laminar Flow Study

160

10-3 Experimental Laminar Flow Drag Characteristics of a High Speed Civil Transport (HSCT) Configuration

Objective. To determine experimentally the difference in drag between an HSCT configuration with 50% laminar flow and one with fully turbulent flow.

Approach. Wind tunnel studies were performed on a current HSCT configuration in which both fully turbulent and 50% laminar (based on local chord) boundary layer conditions were simulated through the use of artificial transition.

Accomplishments. The HSCT was tested in the Langley Unitary Plan Wind Tunnel at Mach 3.0, the design cruise point, and over a Reynolds number range of 0.75 x 10^6 to 5.0 x 10^6 per foot. Data were obtained for three different boundary layer transition grit conditions. The fully turbulent case utilizes empirically sized grit to artificially transition the boundary layer very near the wing leading edge. The 50% laminar case utilized Braslow's method to size the grit necessary to cause transition at the 50% local chord location. In addition, free transition (no grit) tests were also performed. The measured reduction in zero lift drag between the fully turbulent and the 50% laminar case was significantly less than that estimated from reference temperature skin friction theory. Liquid crystal studies were performed to determine the Reynolds number at which natural transition occurred upstream of the 50% chord location, however the results were inconclusive. Based on previous studies it is believed that laminar flow existed up to 50% chord for Reynolds numbers of at least 2.0 x 10^6 per foot.

Significance. The large differences between the experimental and theoretically determined laminar flow drag reductions must be understood in order to reliably apply laminar flow technology to HSCT configurations.

Status/Plans. Studies will be prepared utilizing various methods (sublimating chemical, infrared, surface pitot) to verify the location of boundary layer transition. Also analysis using higher order boundary layer methods will be performed to refine the skin friction drag estimates.

Jeffrey D. Flamm, Peter F. Covell, Gloria Hernandez
Supersonic/Hypersonic Aerodynamics Branch
Langley Research Center
(804) 864-5955
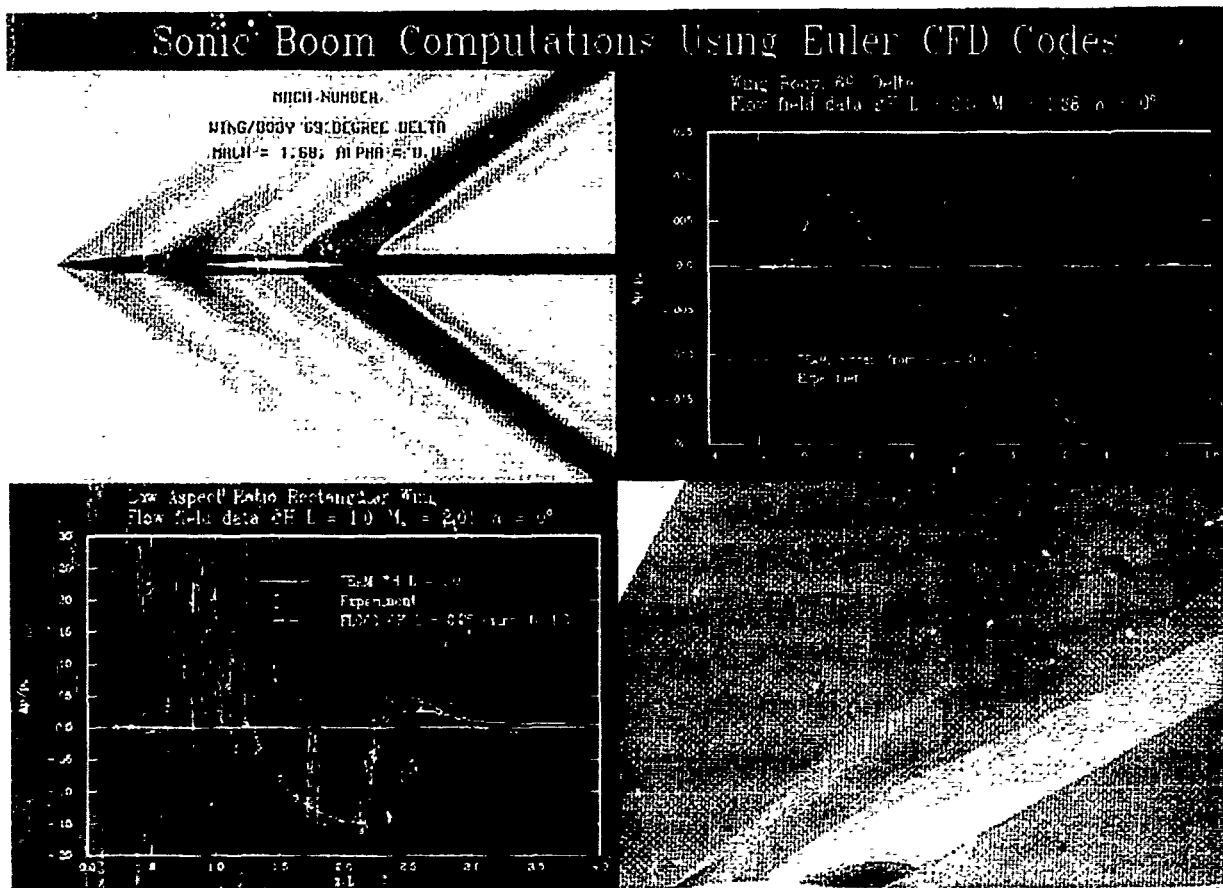
Figure 10-4. Sonic Boom Computations Using Euler CFD Codes

162

10-4 Sonic Boom Computations Using Euler CFD Codes

Objective. To evaluate Euler CFD codes for predicting near-field pressure signatures and use CFD computations as input to extrapolation codes. The near-field pressure signatures will be evaluated by comparing with experimental data on the following configurations: cone-cylinder, low aspect ratio rectangular wing and parabolic cross-sections, wing/body 69° delta, and Langley wind tunnel models.

Approach. Multiple block grids were developed that are clustered both near the surface and several body lengths into the flow field. The computations from the Euler CFD codes FLO60 and TEAM are used to obtain pressures in the centerline plane. The data are taken away from the surface when the shock waves are weak and isentropic flow can be assumed. The pressures are then extrapolated to the h/l (height divided by the model length) of the experimental data using the waveform parameter method.

Accomplishments. We obtained solutions on the rectangular wing using FLO60 with an internal H-H grid and without the sting being modeled. The solutions indicate that the grid should be 192 x 128 x 64. Grids that are more coarse give poor results, indicating weaker shocks than the experiment. The pressures were obtained at an h/l of 0.75 and extrapolated to the experimental h/l of 1.0, and agree well with experimental data. The effect of the sting was found to be insignificant. FLO60 requires large CPU time and memory when using the internal two-zone H-H grid. TEAM computations were obtained using a 10-zone grid on the rectangular wing, which reduced the amount of memory and CPU time. The computed shock strengths were sufficient to obtain a pressure signature at an h/l of 1.0. The pressure signatures are slightly worse than the extrapolated pressures obtained from FLO60.

The wing/body 69° delta was modeled using a 32-zone grid, and the pressure signatures were taken at an h/l of 0.5 and extrapolated to the experimental h/l of 3.6. The pressure signatures agree fairly well with experiment.

Significance. CFD has typically been used to predict forces, moments, and pressures on the body, and grid systems have been developed to emphasize this region of interest. The use of CFD to predict pressure signatures relatively far from the body is a new application for CFD. The Euler codes may be used to design a low sonic boom configuration.

Status/Plans. The study is continuing. The cone-cylinder and Langley wind tunnel models will be evaluated using multiple block grids and TEAM.

Susan Cliff-Hovey
Advanced Aerodynamic Concepts Branch
Ames Research Center
(415) 604-5656
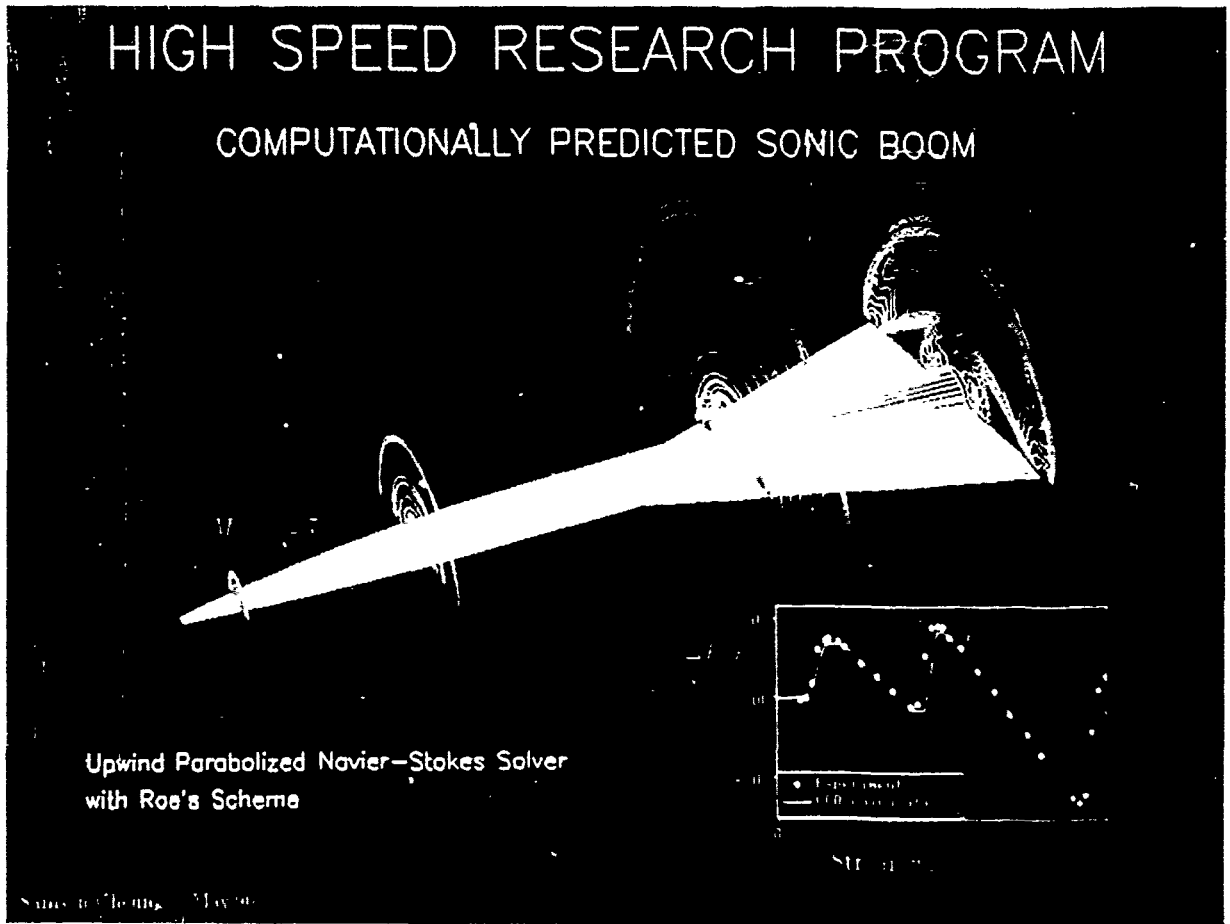
Figure 10-5. Computationally Predicted Sonic Boom

164

10-5 CFD Prediction of Sonic Boom Near-Field Waveforms

Objective. To demonstrate that computational fluid dynamics can produce efficient near-field-flow solutions for input to sonic boom extrapolation codes.

Approach. A computationally efficient CFD code (UPS) was obtained which had been previously validated for problems in the supersonic and hypersonic flight regimes. It was applied to sonic boom test cases that have experimental data in order to assess the accuracy of the CFD solution. A three-dimensional near-field solution (within one or two body lengths) was generated, and the near-field pressure signature extrapolated to the mid-field.

Accomplishments. The UPS code has been applied to three test cases of increasing complexity: a cone/cylinder, a low aspect-ratio wing, and a wing/fuselage. Early comparisons with the experimental data indicated the need for better shock resolution, and subsequent refined-grid calculations produced very good agreement. The most recent application has been to a wing/fuselage that exhibits most of the complexities present in_preliminary designs of supersonic transports. The figure shows the surface geometry and pressure field around the body at a freestream Mach number of 2.7 and zero incidence. This vehicle produces three distinct shock waves due to the bow, wing, and tail. These shocks propagate into the mid-field to produce the sonic boom waveform shown in the inset. As seen in the inset, the correlation with the measured sonic boom signature is very good.

Significance. This calculation demonstrates that CFD can provide flow solutions accurate enough to predict sonic boom waveforms generated by realistic transport configurations. Previous techniques based on linear theory have not been accurate enough to use for tailored waveform designs. The present method is efficient enough that configurations can be optimized numerically for minimum sonic boom early in the design process.

Status/Plans. Validation studies are complete, and the results will be presented at an upcoming AIAA conference. The CFD capability will be used to perform sonic boom analysis of optimized geometries and study the influence of nacelles and exhaust plumes on the sonic boom.

Samson Cheung, Tom Edwards,
Scott Lawrence
Applied Computational Fluids Branch
Ames Research Center
(415) 604-4465

80% thrust, 60% Lift increase
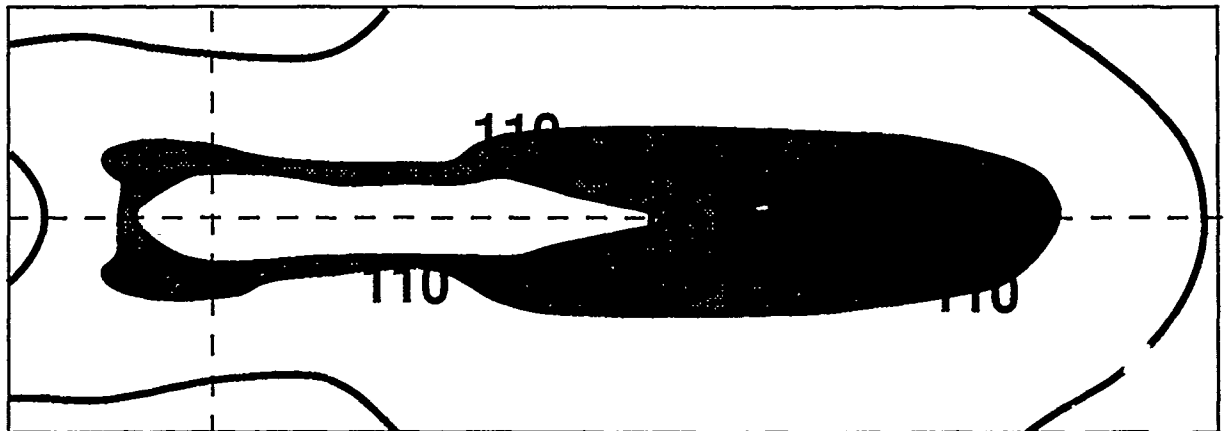
100% thrust, standard lift configuration
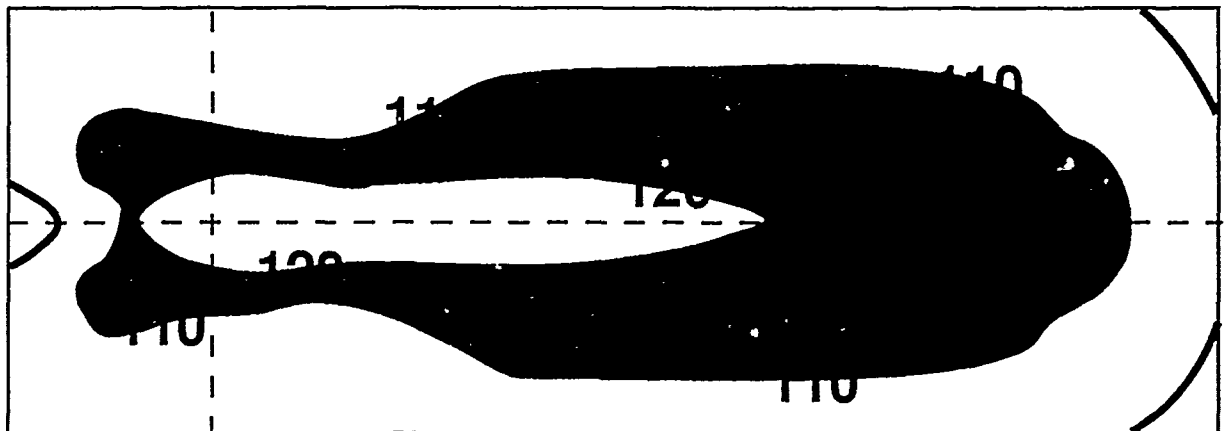
● FAA noise measuring points
microphone height = 4 feet

Figure 10-6. ANOPP System Noise Predictions for HSCT
Effective Noise Level Contours (EPNdB)

10-6 ANOPP System Noise Predictions for HSCT

Objective. To use ANOPP to evaluate the effects of reduced jet thrust on community noise levels. Reduced jet thrust levels at takeoff increases the required ground roll before lift-off. To compensate for the increased ground roll, several levels of increased lift were included in the study.

Approach. Predictions were made using the ANOPP dual stream coannular jet noise module for the AST-205-1 aircraft powered by GE21/J11B14A scaled engines. A power setting of 100% thrust and a standard lift configuration was used as a baseline for this study. Power settings varied from 100% to 80% maximum thrust, while lift was increased in increments of 15%, to a maximum of 60%. A constant climb angle of 8° and a constant rate of climb of 3° per second were used. Effective Perceived Noise Level (EPNL) values were calculated at the FAA noise measuring points as described in Part 36, Section C36.3 of the FAA's Code of Federal Regulations. Noise levels were also calculated on a 1-by 6-mile grid consisting of observer positions. Each observer is located 4 feet above the ground. Noise contours were generated from these observer positions.

Accomplishments. Contours of the 100% thrust, standard lift configuration, and the 80% thrust 60% increased lift cases are shown in the accompanying figure. The 110 and 120 EPNdB levels are shown. By reducing the thrust level from 100% to 80% maximum thrust, a 4 EPNdB decrease in the critical sideline EPNL level can be achieved. By using a 60% lift increase, the ground roll can be shortened to be within 16% of the standard lift configuration. As can be seen when comparing the two contours presented in the figure, reducing thrust and increasing lift alters the shapes of the contours. In general, as thrust is decreased and lift is increased, the contours shorten in length and become more compact.

Significance. The use of the ANOPP prediction code shows that reduced thrust takeoff procedures can be beneficial. Sideline noise levels are of greatest concern during takeoff. Since the FAA sideline noise measurement point location depends on the point of lift-off, only a slight benefit can be derived from increasing the amount of lift while keeping thrust at a maximum. The key to reducing jet noise lies in thrust reduction.

Status/Plans. It has been shown that reduced thrust, used in conjunction with increased lift to compensate for ground run distance, can reduce EPNLs at the sideline and centerline FAA noise measurement locations. Better jet noise prediction modules being designed for ANOPP will allow the noise impact from an HSCT aircraft on community noise to be evaluated.

Robert A. Golub
Applied Acoustics Branch, ACOD
Langley Research Center
(804) 864-5281
Mark R. Wilson
Lockheed Engineering and Sciences Company
Langley Research Center
(804) 766-9715

167
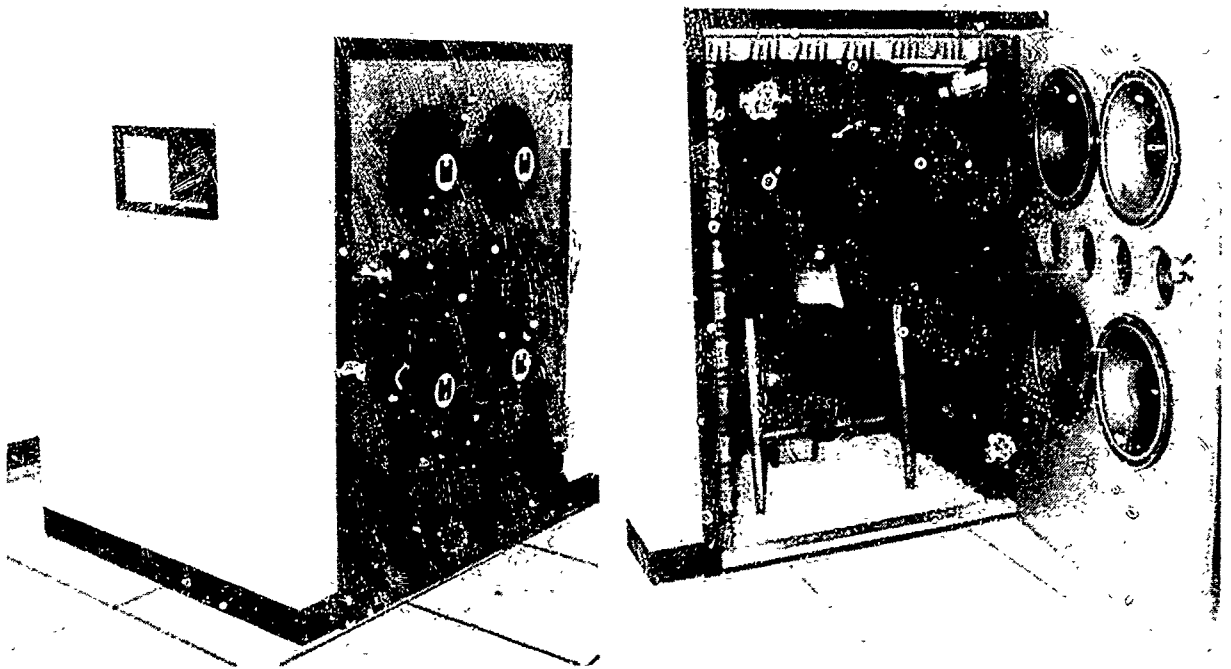
Figure 10-7. Sonic Boom Simulator

168

10-7 Sonic Boom Simulator

Objective. To examine human response to sonic booms that might be produced by a new generation supersonic transport. As part of a program to determine criteria for acceptable overland supersonic flight, this research addresses the design and construction of a sonic boom simulator.

Approach. The acoustic energy contained in sonic booms is predominantly at low frequencies, and cannot be reproduced using conventional loudspeaker arrangements. A solution is to have loudspeakers radiate into an enclosed volume containing the test subject. Effective simulation requires that the enclosure have rigid walls and be airtight. The accompanying photograph illustrates the array of loudspeakers mounted in the door of the concrete enclosure, which is lined with sound absorbing foam. The enclosure has internal dimensions of 60 x 38 x 42 inches and is equipped with four 15-inch woofers and four 7-inch midrange loudspeakers. The sonic boom pressure signatures are computer generated in order to attain precise control of the amplitude and phase of the signal and to overcome some of the inadequacies of the sound reproduction system.

Accomplishments. Construction of the simulator is complete and it has met all the requirements for testing with human subjects. These requirements include the provision of closed circuit television, two-way audio communication, and a limiter circuit to prevent noise levels from exceeding a peak sound pressure level of 140 dB and an RMS level of 95 dB(A). The simulator can achieve peak levels of approximately 139 dB (equivalent to overpressure of 4 psf) and has a low frequency limit of less than 0.5 Hz. The high frequency limit is above 5 kHz, enabling the generation of sonic booms with short rise times.

Significance. The sonic boom simulator is the only such facility in existence. The computer-generation of the sonic boom signatures will enable comparisons to be made between conventional N-wave sonic booms and those shapes of booms that are predicted to occur for new aircraft designs. The results of these comparisons will be used to guide the design of "low boom" configurations.

Status/Plans. A series of tests using human subjects is planned. The principal objectives are to examine human responses to a range of shapes of sonic booms and to compare these results with predictions from a sonic boom loudness model. The incorporation of the acoustic transmission characteristics of buildings will enable simulation of sonic booms as heard indoors.

Kevin P. Shepherd
Structural Acoustics Branch
Langley Research Center
(804) 864-3583
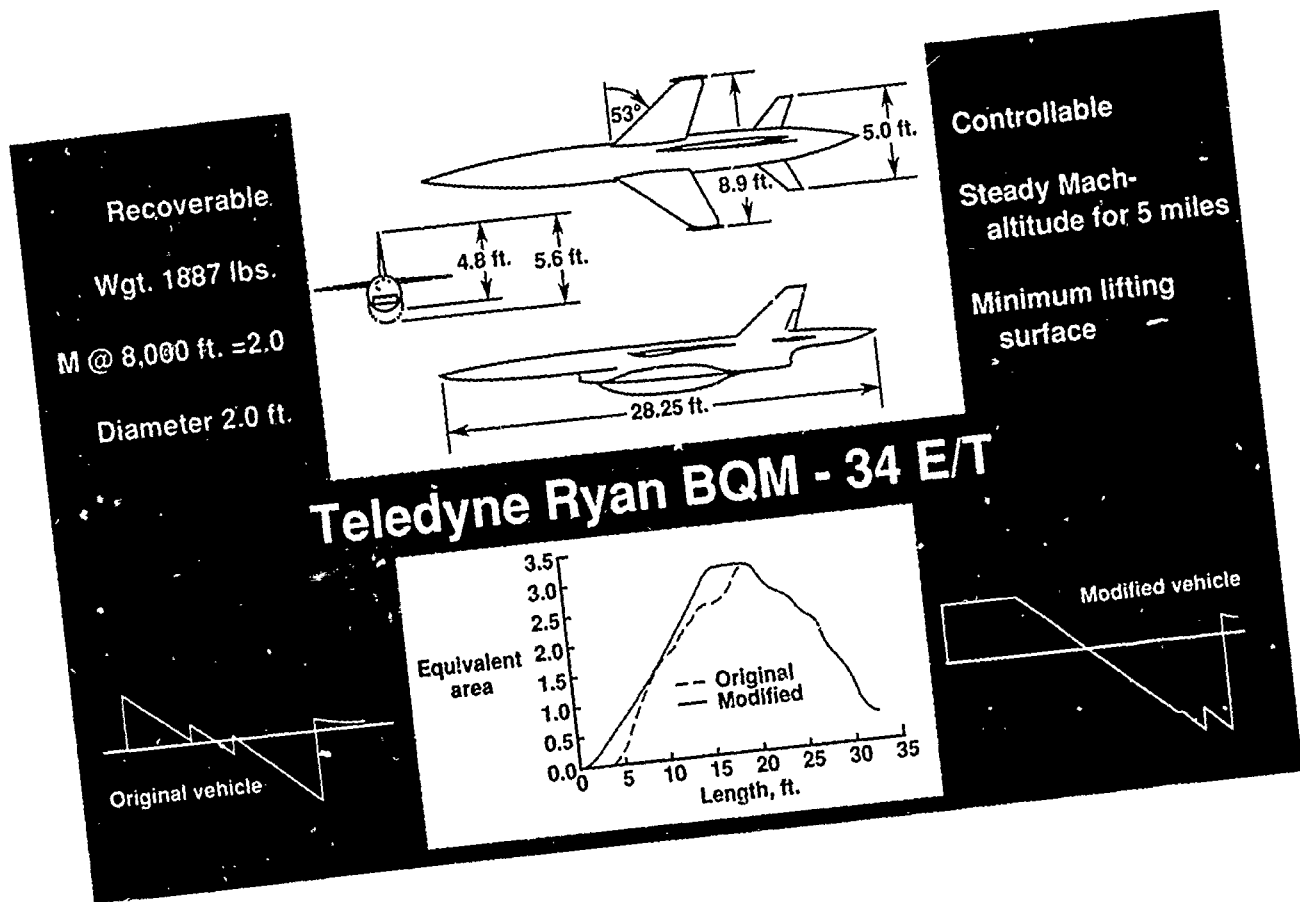
Figure 10-8. Sonic Boom Flight Tests Using Remotely Piloted Vehicles (RPVs)

10-8 Sonic Boom Flight Tests Using Remotely Piloted Vehicles (RPV)

Objective. To demonstrate propagation through the real atmosphere of a mid-field shaped sonic boom pressure signature generated by volume only.

Approach. A feasibility study was conducted using an RPV, a missile, or a ground sled to evaluate the propagation of a shaped sonic boom signature through the real atmosphere. Vehicle selection was based on Mach number; altitude of flight; launch capability; period of steady flight; size; and modifiability, recoverability, and availability of vehicle. Because of the above factors and its minimal lifting surface, the BQM 34 E/T Vehicle was chosen as the most appropriate vehicle for initial sonic boom flight tests.

The amount of volume increase necessary to convert the forebody of the BQM 34 E/T Target Missile into a flat-top shape will be determined theoretically. The aerodynamics of the modified vehicle will be evaluated theoretically, in flight simulation by Teledyne Ryan, and with wind tunnel tests. Two target vehicles and supporting equipment are scheduled to be acquired from the Navy and the Air Force.

The flight test program will begin in 1992. The vehicles will be launched to cruise at Mach 1.5 at 8,000 feet for 5 miles of steady cruise. Both the baseline vehicle and the modified vehicle will be flown and its signature measured in calm conditions and in late afternoon turbulent conditions.

Accomplishments. Details of an RPV feasibility study are being completed. For flight tests within 3 years, the Firebee BQM 34 E/T has been selected as the most attractive vehicle. Estimates on the modifications necessary on the vehicle have been made and preliminary estimates of the effects of these modifications also have been calculated (see figure). Plans to acquire two Firebee vehicles in preparation for such tests are under way.

Significance. These tests would demonstrate for the first time that a shaped signature could sustain itself while propagating through the atmosphere. It would also give initial indications of the effect of turbulence on a shaped flat-top signature.

Status/Plans. Activities to plan and evaluate preliminary designs in the wind tunnel continue in preparation for flight tests in 1992.

Christine M. Darden
Vehicle Integration Branch
Langley Research Center
(804) 864-5258

Shallow-angle nozzle with isentropic internal flow
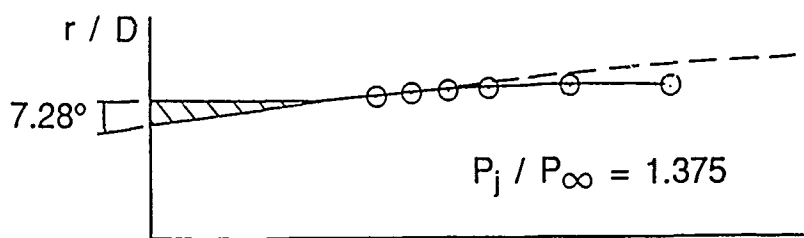
Wider-angle nozzle with internal flow containing shocks
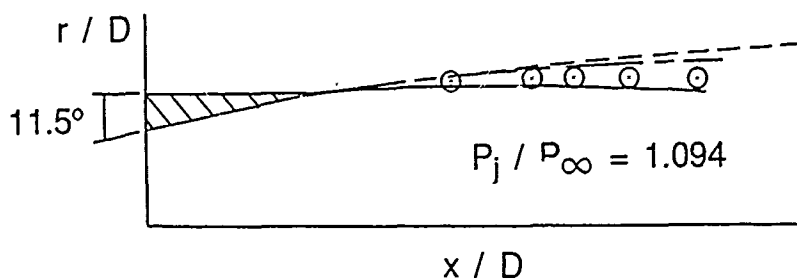
(All calculations assume isentropic nozzle flow)

Figure 10-9. Plume Shape Calculation

172

10-9 Calculation of Jet Plume Effect on Sonic Boom Signature

Objective. To find a method to accurately compute jet plume shapes and assess the influence of the jet plume on the ground level sonic boom signature of representative high speed transport configurations.

Approach. Previous attemps using a small perturbation method (NASA TN D-279) and a method of characteristics with conical nozzle flow (NASA TN D-5553) both failed to yield satisfactory predictions of empirically determined plume shapes. In the current work, a Euler shock-fitting marching code was used to predict the plume shape. Conventional methods were then used to compute the signature.

Accomplishments. The present method yields precise predictions of plume shapes for isentropic nozzle flow. For nonisentropic nozzle flow, the accuracy is significantly better than previous techniques. Influence of the plume on sonic boom signatures has been computed for some generic configurations (see figure).

Significance. The influence of the plume shape on the signature can be predicted without wind tunnel tests and without boundary layer or mixing-region calculations. For small jet pressure ratios ($1 < P_j/P_\infty < 3$)– ratio of jet pressure to free stream pressure, this influence may be favorable, reducing the strength of the rear shock. For larger pressure ratios the plume influence invades the forward positive part of the signature where the effect is always unfavorable.

Status/Plans. Calculations of the internal nozzle flow for nonisentropic nozzles are being prepared. These are expected to lead to plume calculation accuracy comparable to that for the isentropic case. Plume effects on the signature will be calculated for current supersonic transport configurations. Plume effects on aerodynamic drag will be assessed.

Raymond L. Barger, N. Duane Melson, Manuel D. Salas
Langley Research Center
(804) 864-2315
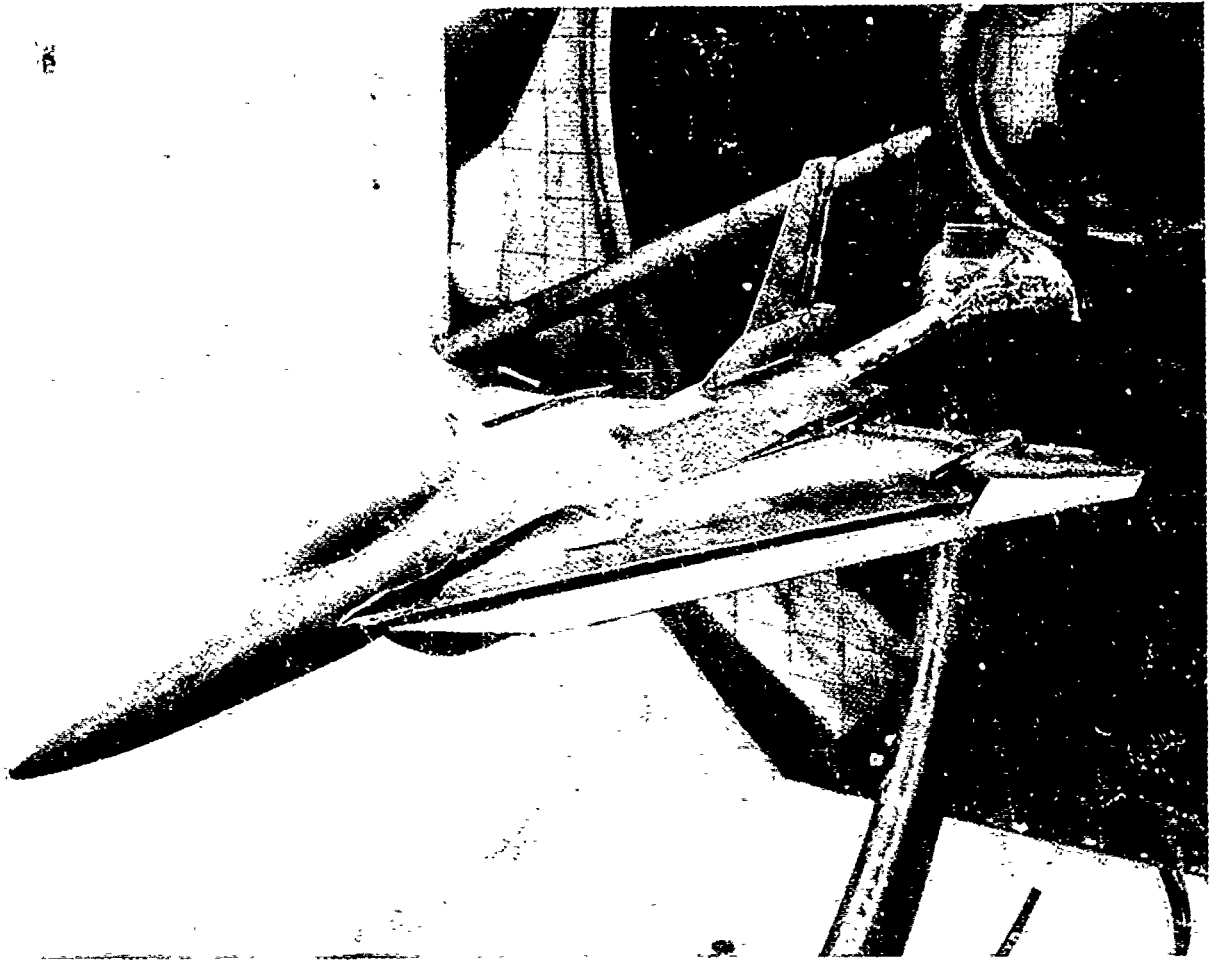
Figure 10-10. Longitudinal Stability of a Highly Swept-Wing Configuration Having Application to HSCT Designs

174

10-10 Longitudinal Stability of a Highly Swept-Wing Configuration Having Application to HSCT Designs

Objective. To modify the wing apex of the F-16XL to a geometry consistent with current High Speed Civil Speed Transport (HSCT) designs and develop means to alleviate the low-speed pitch-up instability that is inherent for this class of highly swept cranked wings.

Approach. Exploratory static force tests and flow visualization studies were conducted in the 12-foot low-speed tunnel with a 0.10-scale model of a modified F-16XL. The model modifications are intended to return the wing to the original, supersonically efficient planform having a constant in-board wing sweep of 70° and a 50° swept outboard panel. This original wing planform was modified to an "S" shaped apex to alleviate a pitch-up problem, however the "S" shaped apex also degraded the supersonic performance. The supersonic performance degradation associated with the F-16XL "S" shaped apex would probably be unacceptable for HSCT application; accordingly, tests were conducted in the 12-foot tunnel to explore alternate leading-edge treatments to alleviate the pitch-up without compromising high-speed performance

Accomplishments. Wing leading-edge flaps were incorporated with the supersonically efficient 70°/50° wing. A simply deflected apex flap was found to alleviate the low-speed pitch-up problem to the same extent as the "S" shaped wing apex modification. If the wing leading-edge is further modified to include a vortex flap on the outboard wing panel, the pitch-up characteristic can be totally eliminated.

Significance. A modified F-16XL aircraft with a 70°/50° wing planform would be representative of current HSCT wing designs.

This aircraft could then be used for full-scale flight correlation and validation of analytical and experimental prediction methods. Once validated, these methods could be used with confidence to predict the aerodynamic and acoustic characteristics of HSCT configurations. Of course, the F-16XL wing could only be modified to the desired 70°/50° planform if a satisfactory solution to the low-speed pitch-up problem can be developed. Although very preliminary, the results of this test are promising and indicate that wing-leading edge treatments that alleviate the low-speed pitch-up problem without compromising supersonic performance can be developed.

Status/Plans. Further testing of these pitch-up alleviatiaon concepts are planned. A larger scale model of the F-16XL will be modified and tests conducted in the 30-by 60-foot tunnel.

Paul L. Coe, Jr.
Flight Dynamics Branch, FAD
Langley Research Center
(804) 864-1150

PRESSURE COEFFICIENT

F16XL WING: EULER SOLUTION, Cp CONTOURS

Mach Number=2.0, Alpha=4 deg., CFL3DE (top half), EMTAC (bottom half)
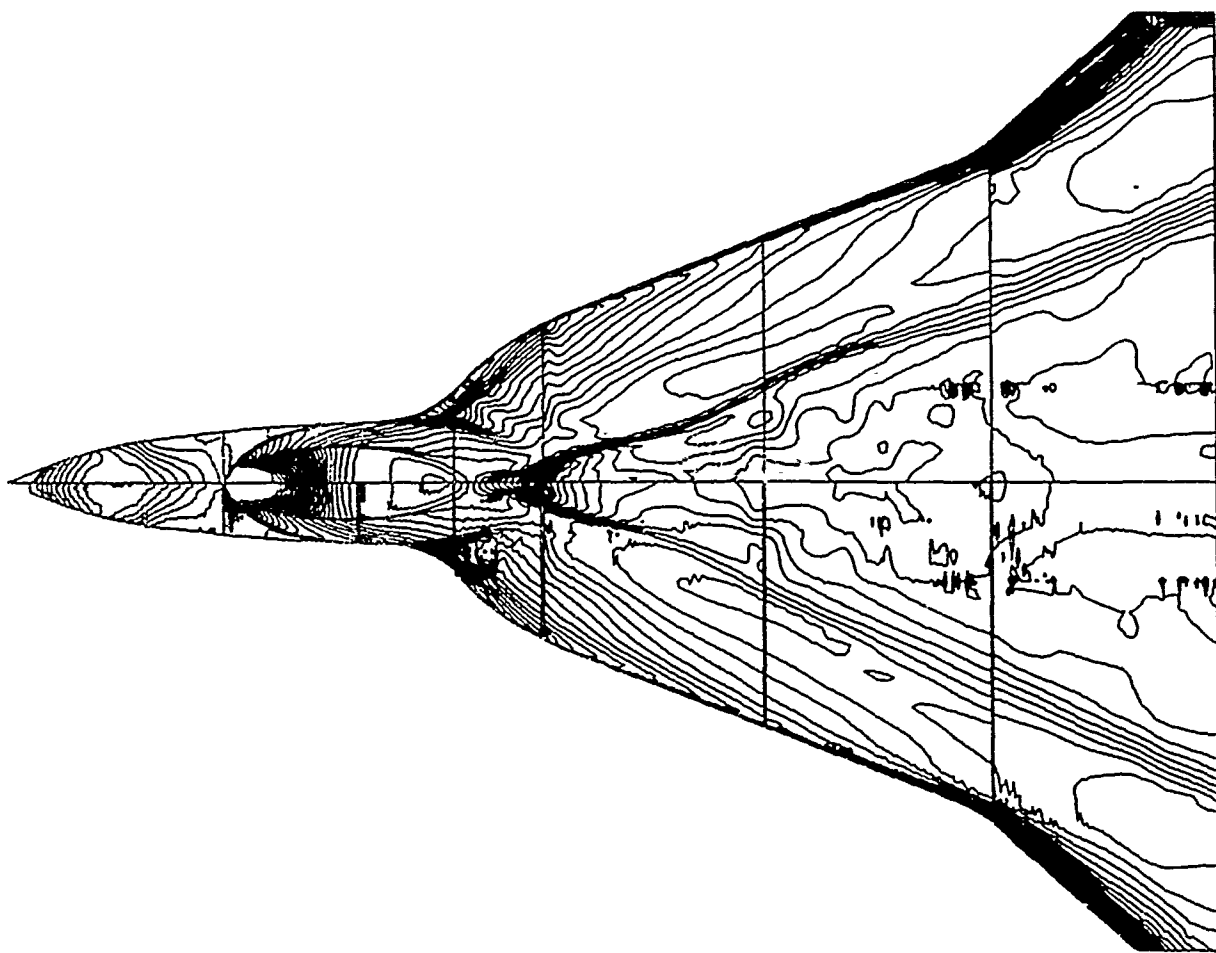
Figure 10-11. Inviscid Flow Calculation Over F-16XL Configurations

10-11 Inviscid Flow Calculation Over F-16XL Configurations

Objective. To conduct inviscid flow calculations over F-16XL geometry for providing surface pressure field for 3-D boundary layer analysis.

Approach. The F-16XL base geometry (with no laminar glove) at M_∞ and $\alpha = 4°$ is used as a preliminary study case here. Euler calculations were performed using two codes, the Langley code CFL3DE and the Rockwell code EMTAC (Fisher/Vemuru, LRC Project Office). The calculation uses 40,000 points on the surface and 20 to 30 points in the normal direction, totaling approximately one million grid points. Computation is performed in seven grid blocks using the upwind-differenced Euler marching scheme and with solution patching at the grid interfaces.

Accomplishments. The accompanying figure shows a comparison of upper surface pressure coefficient distribution obtained from the two Euler calculations. The swept shock originating from the tail-end of the canopy will be an important factor in the design of the laminar glove. The pressure field shown in the figure has been interpolated to a chordwise-oriented grid and will be used for 3-D boundary layer computation.

Significance. Good comparison between the two Euler codes points to the accuracy of the results. The location of the canopy shock will be a factor in glove design. Future calculations with different geometries and conditions can now be routinely accomplished.

Status/Plans. Comparison will be made with measured pressure distributions for a few sets of flight conditions. Three-dimensional boundary-layer calculations are planned based on Euler results and calculation of Re and boundary layer stability characteristics. Correlation of the above with Navier-Stokes calculations using CFL3D is planned.

Venkit Iyer
Vigyan
Theoretical Flow Physics Branch
Langley Research Center
(804) 864-2319

Figure 10-12. Unstructured Euler Flow Solutions Using Hexahedral Cell Refinement

10-12 Unstructured Euler Flow Solutions Using Hexahedral Cell Refinement

Objective. To develop a simple computational grid refinement technique for the detailed study of aerodynamic flows such as vortices and shock waves.

Approach. A well-established, structured Euler code (FL057) was used as the basis for the developr ent of a topologically independent, unstructured, hexahedral-based Euler code (TIGER). The unstructured nature of the program allows for user-specified local grid refinement in areas of large flow gradients. Cells may be repeatedly split into eight smaller cells in order to provide increased resolution in areas where large flow-field variations exist. Because this refinement is done locally, specific regions of the flow field can be analyzed with higher grid resolution, while unnecessary refinement in other regions of the flow field is avoided.

Accomplishments. The flow analysis program is capable of displaying data using color mapping and contour lines on user-specified, unstructured flow field planes. Computer implementation was critical in order to avoid large CPU-time and memory penalties. The resultant code runs at a rate equivalent to conventional structured Euler and Navier-Stokes solvers and uses simple, straightforward programming techniques to take advantage of the vector-processing capabilities of the Cray Y-MP. An interactive graphical analysis tool was developed in conjunction with the flow solver for visualization of the unstructured flow data, checking the boundary condition specifications, and for performing the grid refinement in user-specified regions.

Significance. The computational analysis of aerospace vehicles requires the ability to capture fine details of the flow field. An unstructured methodology allows for localized grid refinement appropriate for each freestream condition, thereby concentrating grid points only in regions of greatest interest. This dramatically increases computational efficiency, because the refinement is not required to extend throughout the entire flow field. The use of hexahedral-based grids also allows current conventional grid generation techniques to be used to generate the starting grid, and eliminates many of the difficulties associated with the generation of unstructured tetrahedral grids and the visualization of tetrahedral-based flow-field data.

Status/Plans. The TIGER program has been used to successfully compute solutions with refinement for a variety of configurations over a wide range of Mach numbers and angles-of attack, including a generic fighter, the F-16 and ONERA M6 wings, a cone-cylinder, and a variety of two-dimensional airfoils. Four different grid topologies were used with no substantial difficulties. Current research is focused on the determination of appropriate refinement criteria for vortex and shock-dominated flow fields. Future applications will include the detailed analysis of HSCT and advanced fighter configurations.

John E. Melton, Scott D. Thomas
Applied Aerodynamics Branch
Ames Research Center
(415) 604-6208

Chapter 11

Aerothermodynamics Research and Technology

The design and development of future aerospace vehicles present some formidable aerothermodynamic performance prediction challenges. To meet these challenges, the Aerothermodynamics Research and Technology base program is pursuing the following objectives.

- development and application of advanced computational methods and numerical techniques covering the entire spectrum of continuum, transitional, and rarefied flows,
- development of accurate and detailed real-gas chemistry and high speed turbulent flow models and the efficient integration of these models with standard computational flow codes;
- establishment of a high quality ground and flight experimental data base for code validation/verification;
- direct correlation and comparison of numerical computations with available ground and flight data;
- establishment of a detailed aerothermal loads data base and development of a fully integrated analysis technique;
- enhancement of engineering design codes and advanced configuration analysis capability to support future vehicle/mission requirements.

Program Manager: Steve Wander
OAET/RF
Washington, DC 20546
(202)453-2820

Vibrational Temperature Contours

Figure 11-1. Direct Particle Simulation of Hypersonic Flows

182

11-1 Direct Particle Simulation

Objective. To extend the capabilities of a new discrete particle simulation method for rarefied hypersonic flows in the thermochemical nonequilibrium to realistic, three-dimensional geometries and to apply the method to simulate the flow field about the Aeroassisted Flight Experiment vehicle.

Approach. Direct particle simulation methods model the flow as a large collection of discrete particles that interact with each other through mutual collisions. The approach is to model the physics of these interactions on a probabilistic basis while paying particular attention to the efficiency of the algorithm and its mapping to modern computer architectures.

Accomplishments. Substantial work has been done on the structure of the algorithm to take advantage of the vector and parallel computer architectures now available. The accompanying graphic depicts the vibrational temperature field of the three-dimensional flow about the Aeroassisted Flight Experiment at 100 km and Mach 25.4 The number of particles used to represent the flow was 4.24 million. This calculation required 5.0 hours of Cray-2 CPU-time and 760 megabytes of memory.

Significance. The national interest in hypersonic flight requires a computational predictive capability for the aerodynamic and thermal environment to be found around vehicles such as the proposed aerospace plane or ASTV. Because of difficulties in applying the continuum equations to the very low density hypersonic flight regimes that they will encounter, it is appropriate to consider the application of direct particle simulation methods. The numerical efficiency of the current approach enables direct particle simulations on a much larger scale than previously possible, providing a more viable means for the solution of practical hypersonic rarefied flow problems.

Status/Plans. The algorithm is now capable of the simulation of flows in multispecies gases in thermodynamic nonequilibrium. The algorithm has been constructed to take advantage of vector and parallel machine architectures and shows a considerable speed advantage over competing methods. Work in progress at the moment includes the incorporation of a finite-rate chemistry model and the generalization of the algorithm to allow implementation of the same code on considerably disparate computing platforms.

William J. Feiereisen
Aerothermodynamics Branch
Ames Research Center
(415) 604-4225
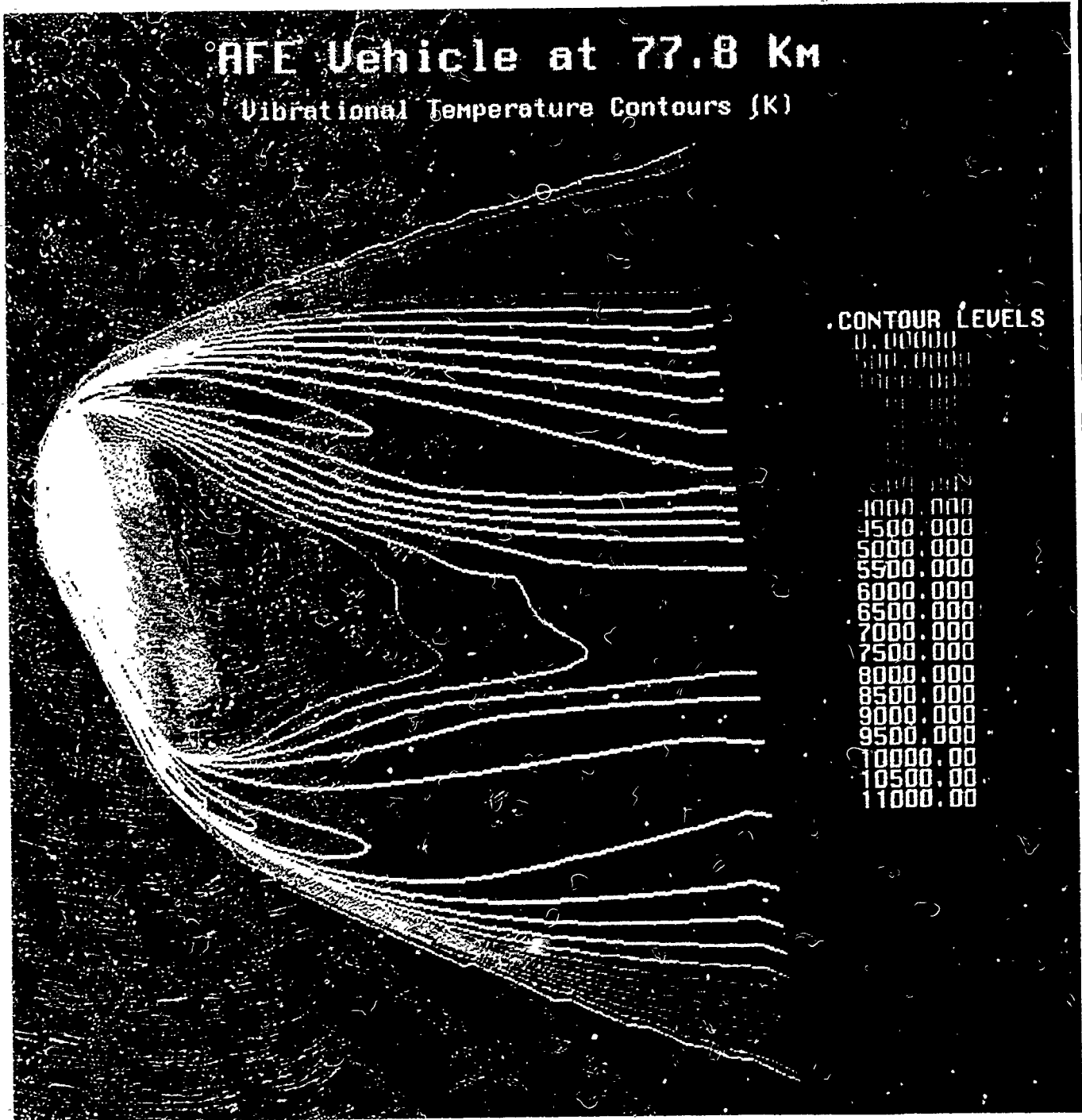
Figure 11-2. Three-Dimensional AFE Flow Simulations

184

11-2 Three-Dimensional AFE Flow Simulations

Objective. To numerically compute flow around the Aeroassist Flight Experiment (AFE) vehicle at one of its flight trajectory points and use the results to design the AFE Base Flow Radiometer Experiment.

Approach. The three-dimensional thermo-chemical nonequilibrium Navier-Stokes equations with finite-rate chemical reactions were solved using upwind-differencing fully coupled flow codes around the AFE geometry.

Accomplishments. An explicit code has been developed to compute 3-D thermo-chemical nonequilibrium flows. It has been producing AFE flow-field solutions for over a year. The code employs a two-temperature physical model and includes 11 species and 30 chemical reactions. Comparisons against ballistic range and computational data have been used to partially validate the code. A full flow-field calculation, including the most detailed computation of the base flow to date, has been completed at the 77.8-km trajectory point. The explicit code's efficiency is comparable to that of implicit ones being used elsewhere. A solution over an 85 x 23 x 85 grid consumes about 65 hours of Cray-2 CPU time.

The accompanying figure shows vibrational temperature contours computed with the explicit code over the AFE at its 77.8 km trajectory point where the freestream density is 2.779×10^{-5} kg/m^3 and the velocity is 8914 m/s.

Significance. The AFE project will test the validity of using aerobraking as a fuel-saving technique for atmospheric entry and will provide data for real-gas code validation. The altitude and velocities of the planned AFE trajectory dictate that design of the experiments carried aboard will depend significantly on numerical simulations made prior to the flight. In turn, the AFE flight data will be used to validate the computer codes, which then can be used in the design of actual Aeroassist Space Transfer Vehicles.

Status/Plans. The codes will continue to be enhanced and used to study aspects of the AFE flow field, particularly in the base region.

Grant Palmer
Aerothermodynamics Branch
Ames Research Center
(415) 604-4226
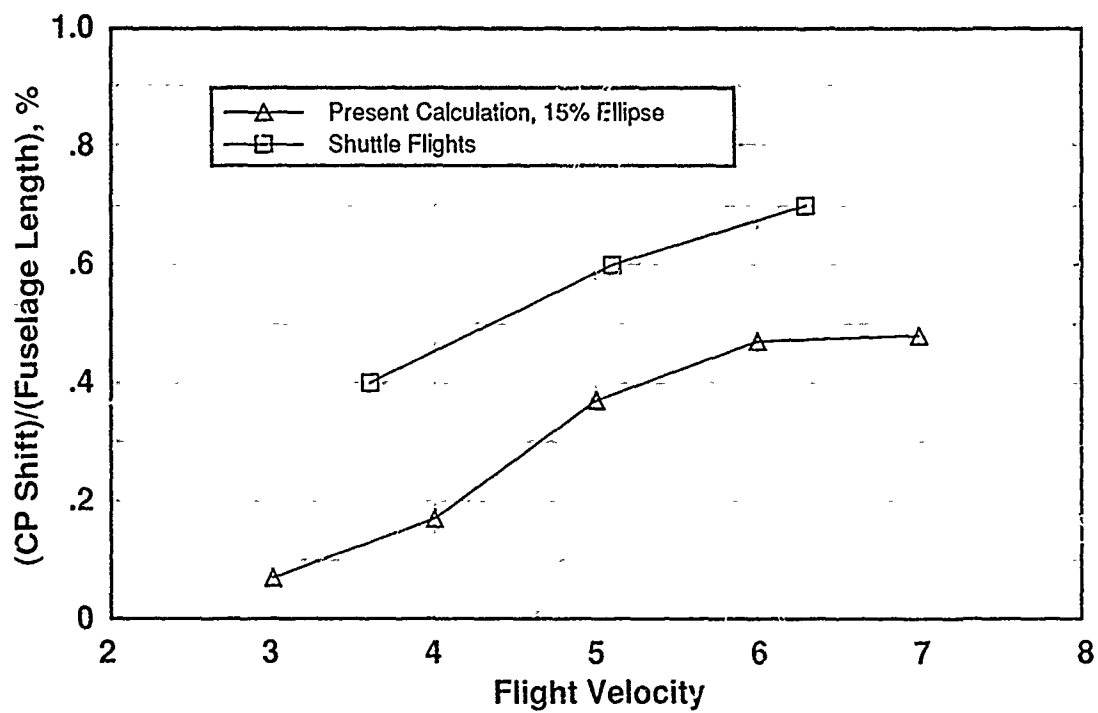
Figure 11-3. Real-Gas Effects on Airfoil Aerodynamic Coefficients

11-3 Real-Gas Effects on Airfoil Aerodynamic Characteristics

**Obje ;tive.** To theoretically determine the aerodynamic characteristics of the airfoils at hypersonic flight speeds accounting for the nonequilibrium thermochemical phenomena occurring at high temperatures.

Approach. Two-dimensional Navier-Stokes code incorporating the two-temperature thermochemical nonequilibrium phenomena, named CENS2H, was run to solve for the flow fie. 's around airfoils. Lift and drag coefficients and center of pressure were calculated for these ai. 'oils and plotted. The calculated results were compared with the Space Shuttle flight data.

Accomplishments. Several important conclusions are drawn from this study: (1) One-temperature and two-temperature thermochemical models yield nearly the same lift and drag coefficients, and discernibly different centers of pressure. (2) The ideal gas model with a $\gamma(= Cp/Cv)$ different from 1.4 can reproduce the lift and drag coefficients of the two-temperature model when the γ value is appropriately chosen, but the accompanying center of pressure is considerably different from the two-temperature model. (3) According to the two-temperature model, lift and drag coefficients become systematically smaller than the $\gamma 1.4$ gas values as the flight velocity is increased. (4) An approximate binary scaling relationship (between the airfoil size and free stream density) exists for the lift and drag coefficients. (5) The body thickness and angle-of-attack have little effect on the relative changes in lift and drag coefficients as a result of the real-gas effects, but they have a large effect on the center of pressure location. (6) The center of pressure shift predicted by the constant γ model shows no consistent trend, etc.

Significance. Aerodynamic characteristics of hypersonic vehicles such as the Apollo Command Module or Space Shuttle vehicle are known to be systematically different from those observed experimentally in ground-based wind tunnels. This study explains the reason for the differences. From the charts derived in this work, one can estimate the extent of the differences.

Status/Plans. The CENS2H code will be modified to solve three-dimensional problems.

C. Park
Aerothermodynamics Branch
Ames Research Center
S. Yoon
MCAT Institute
(415) 604-5394
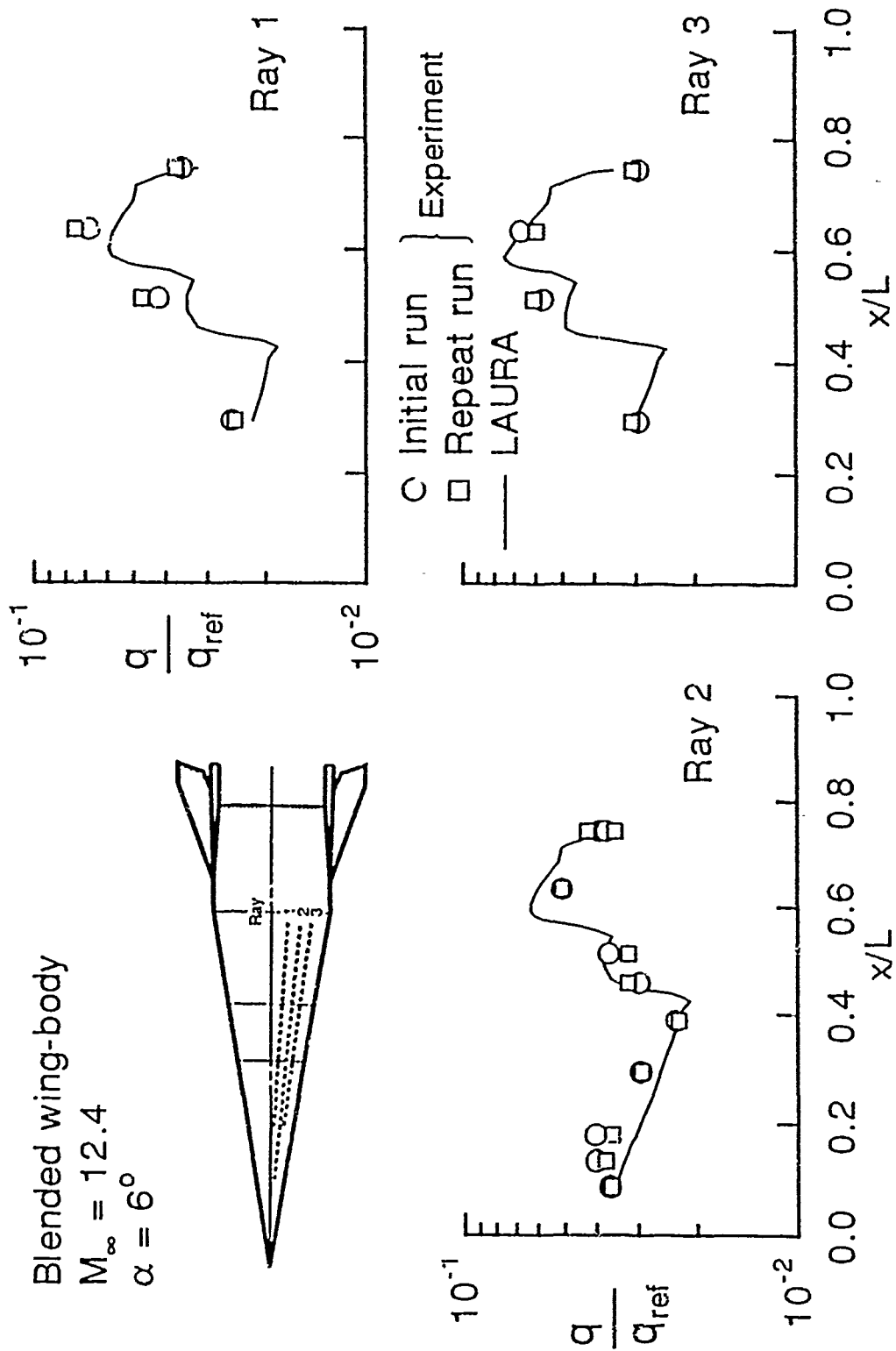
Figure 11-4. Off-Centerline Heat Transfer

11-4 Application of the LAURA Code for Slender-Vehicle Aerothermodynamics

Objective. To demonstrate the application of the Langley Aerothermodynamic Upwind Relaxation Algorithm (LAURA) code to compute the flow over slender hypersonic vehicles and to evaluate the capability for predicting aerodynamic heating.

Approach. To evaluate the LAURA code, comparison of predictions with experimental data will enable an assessment of the code for slender-vehicle applications and will contribute to the verification process. A generic blended wing-body configuration of the National Aero-Space Plane (NASP) has been designed and tested by McDonnell Douglas in the Calspan shock tunnel. These tests yielded pressure, heat transfer, and force measurements on a generic vehicle and provide a data base for validation of the computational technique.

Accomplishments. Two cases from the experimental tests were selected for study. The flow-field grids and a numerical definition of the body surface were generated for the model geometry. Computations were performed on the Langley Cray-2 computer, and the predicted results have been compared with the experimental data. Good-to-excellent agreement between prediction and measurement was found for windward surface pressure and heat transfer as shown in the accompanying figure. Some discrepancies in the comparisons were noted on the leeside of the vehicle, which have been attributed to insufficient grid resolution of a region of vortical flow.

Significance. The results of this research show that the LAURA code is capable of flow-field calculation and accurate heat transfer predictions over slender NASP-like vehicles.

Status/Plans. The results have been documented in AIAA Paper 90-1714. Additional comparisons with flow-field survey data are being performed, and calculations with turbulence modeling are planned.

Richard A. Thompson, Peter A. Gnoffo
Aerothermodynamics Branch
Langley Research Center
(804) 864-4367

STAGNATION STREAMLINE TEMPERATURES
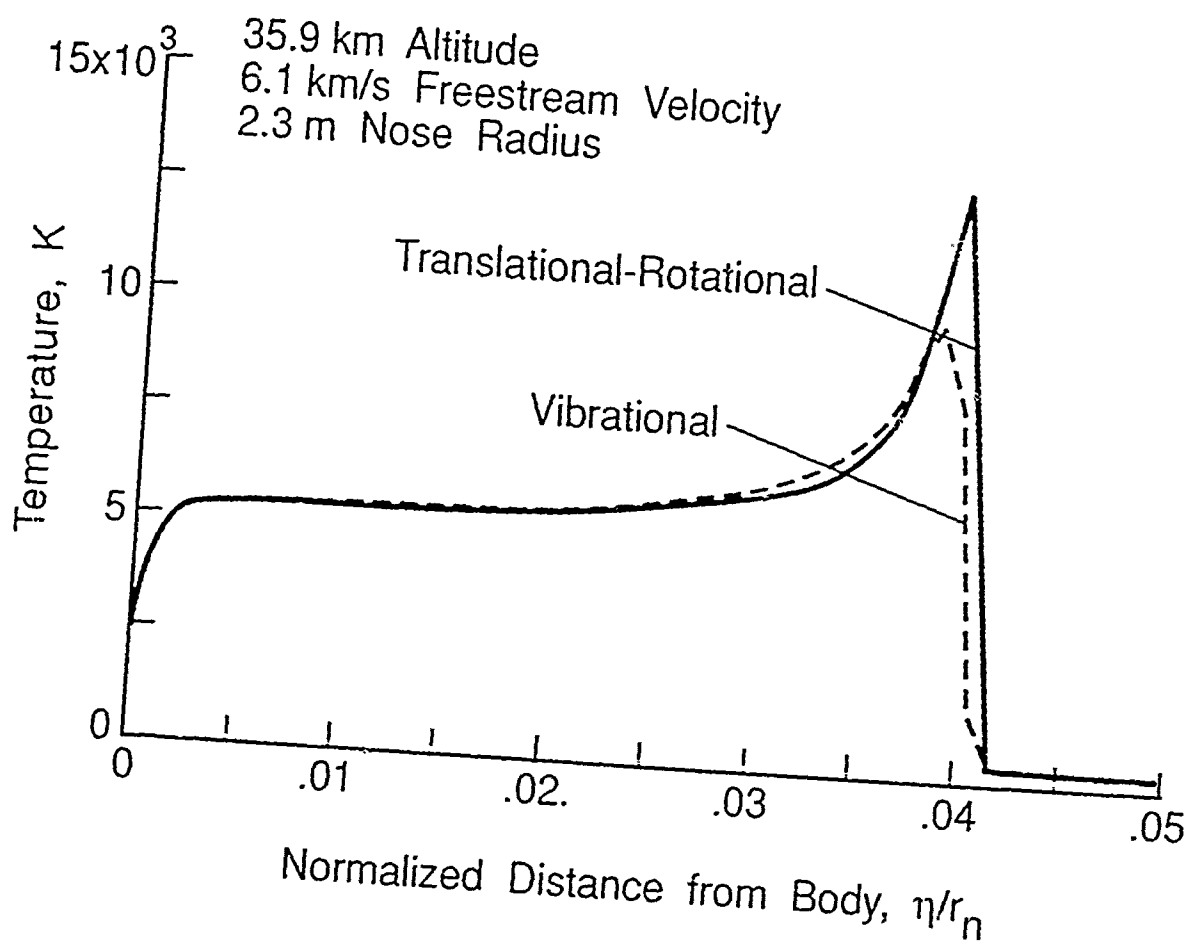
Figure 11-5. Mars Aerobraking Entry
Stagnation Streamline Temperatures

11-5 Thermochemical Nonequilibrium for Mars Aerobraking Entry

Objective. To develop a computational technique to study the aerothermodynamics of Mars aerobraking entry and determine the degree of thermochemical nonequilibrium present in these flows.

Approach. An eight-species chemical kinetics model for the CO_2-N_2 mixture found in the Mars atmosphere was implemented in an existing thermochemical nonequilibrium, Navier-Stokes computational technique. The flow about an ellipsoidally blunted 60° cone was studied at two points, 6.1-km/sec velocity at 36-km altitude and 7.4-km/sec velocity at 50-km altitude, on a proposed Mars aerobraking trajectory. Two nose radii, 2.3 m and 23 m, were used for each trajectory point.

Accomplishments. The results obtained show that thermal equilibrium prevails in all cases computed, except in a small region of the shock. For the low-speed case (6.1 km/sec), the flow is nearly chemically equilibrated; however, at the higher speed (7.4 km/sec), the flow exhibits significant chemical nonequilibrium. Convective heat transfer rates were computed.

Significance. The numerical method developed may be used to study Mars atmospheric entry flows. Surface pressure distributions and convective heat transfer rates can be obtained for use in the design of Mars aerobrakes and entry vehicles. Requirements for modeling the thermochemical state of these flows can be determined.

Status/Plans. Further extensions of the thermochemical model are planned to allow higher energy entry conditions to be simulated. The effects of thermal radiation on the flow will be considered. The results were published in AIAA Paper 90-1695.

Kenneth Sutton
Aerothermodynamics Branch
Langley Research Center
(804) 864-4406

Graham V. Candler
Dept. of Mechanical and Aerospace Engineering
North Carolina State University
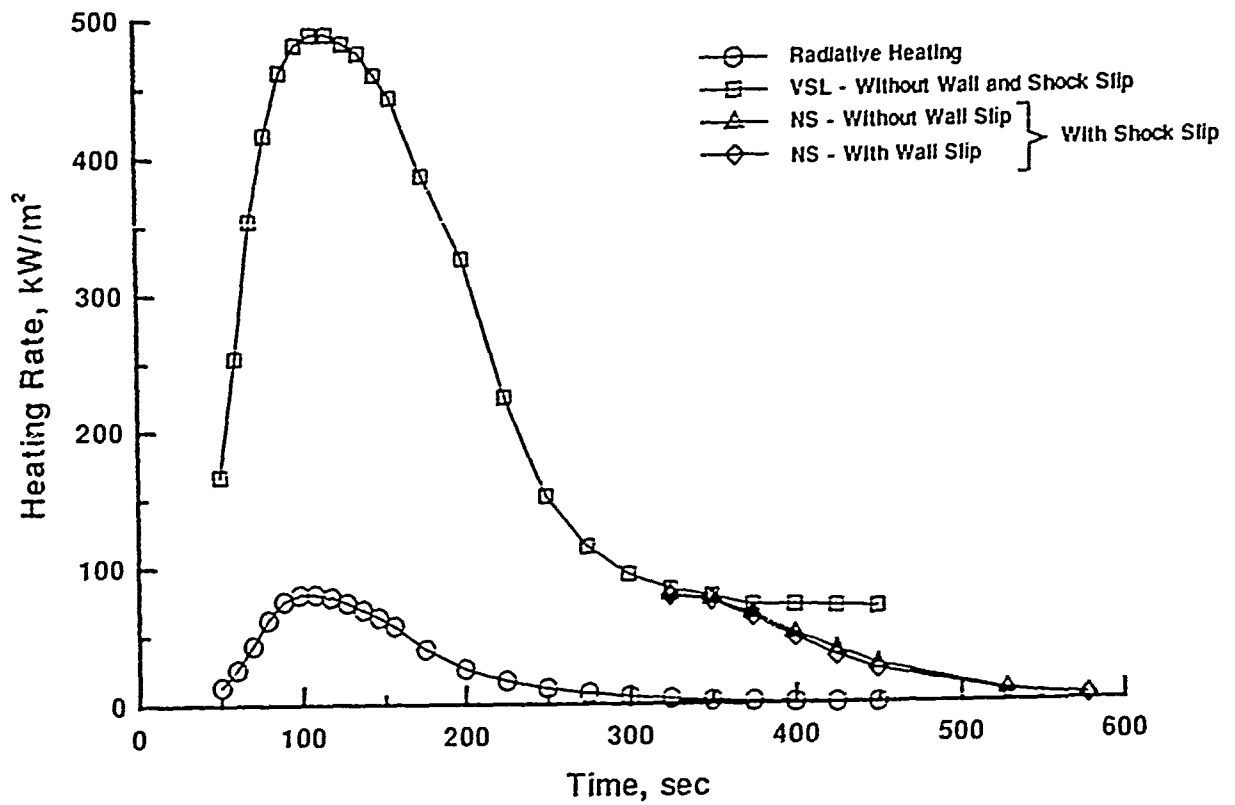
Figure 11-6. Stagnation-Point Heating on Aeroassist Flight Experiment Vehicle

11-6 Stagnation-Point Heating Calculations on Aeroassist Flight Experiment Vehicle

**Objective.** To provide flight, nonequilibrium stagnation-point heating rates that can be used to define the aerothermodynamic environment of the Aeroassist Flight Experiment (AFE) vehicle.

Approach. To reduce computational time, a nonequilibrium viscous shock layer (VSL) code has been used to compute the convective stagnation-point heating rate over a sphere. The radius of the sphere was chosen to produce results that matched Navier-Stokes (NS) calculations for the convective stagnation point heating rate over the actual vehicle geometry in flight. Similarly, the radiative heating was calculated using a correlation that has been shown to match more exact nonequilibrium radiative heating calculations to within approximately 10% for the AFE flight conditions. This approach allowed the calculation of accurate stagnation point heating rates over an entire trajectory in a fraction of the time required for more detailed codes.

Accomplishments. Calculations have been performed at several points on a typical AFE trajectory, as shown in the accompanying figure. Peak total heating occurs at approximately 117 sec (76 km) and produces a radiative equilibrium temperature of 1785 K, which is near the upper limit of the surface tile. Peak radiative heating occurs slightly earlier and is only approximately 15% of the total heating. For times greater than 325 sec, where the altitude is above 90 km, the heating rates calculated by the VSL code level off. For these conditions, the atmospheric density is very low and the VSL code is no longer completely valid. For these high altitudes, heating rates have also been calculated using a stagnation line Navier-Stokes code, which can be applied at high altitudes. The heating rates obtained using this code match the VSL results at the lower altitudes and decrease with increasing altitude (time) as would be expected. Similar effects would be expected on the entry leg of the trajectory at high altitudes (< 50 sec), but these calculations are not included.

Significance. These results represent the most complete and accurate set of continuum stagnation-point heating rates that have been obtained over the high heating portion of the AFE trajectory. They are currently being used in conjunction with nonequilibrium boundary layer calculations to define the aerothermodynamic environment needed for heat shield design.

Status/Plans. The study has been completed and the results accepted for publication in the AIAA *Journal of Spacecraft and Rockets.*

Roop N. Gupta
Scientific Research Technology
Jim J. Jones
Analytical Mechanics Associates

H. Harris Hamilton
Aerothermodynamics Branch
Langley Research Center
(804) 864-4365

1° CORRIDOR WIDTH REQUIREMENT, 5-G DECELERATION LIMIT, AND ENTRY INTO A 1 SOL PARKING ORBIT

Minimum required L/D

High α

Moderate α

High α

V_{atm}, km/sec
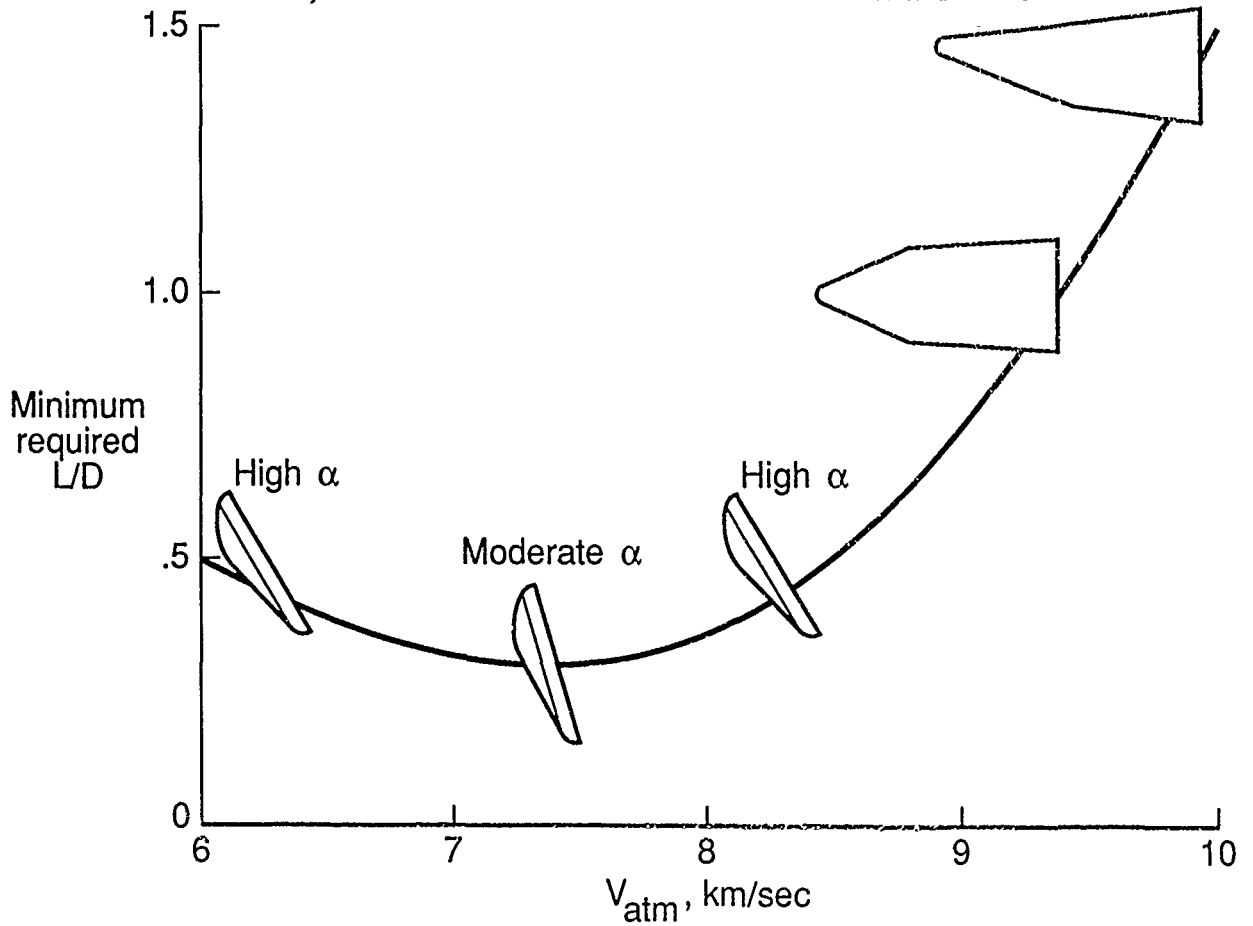
Figure 11-7. Minimum Aerobrake L/D for Mars Aerocapture

194

11-7 Aerodynamic Requirements of a Manned Mars Aerobraking Transfer Vehicle

Objective. To identify the aerodynamic requirements for a manned Mars aerobrake configuration.

Approach. By assessing aerodynamic performance, vehicle packaging, and mission flexibility issues, the significance of the aerobrake lift-to-drag (L/D) ratio was determined. The emphasis was placed on identifying the minimum aerobrake L/D that could successfully accomplish the aerocapture maneuver.

Accomplishments. Based on a typical set of mission constraints, the required Mars aerobrake L/D was shown to be a function of the Mars atmospheric entry velocity (which typically varies from 6 to 10 km/sec) and the degree of interplanetary mission flexibility inherent in the analysis. For example, a minimum aerobrake L/D of 1.5 is required for a manned Mars vehicle to successfully aerocapture at entry velocities from 6.0 to 10.0 km/sec. This L/D selection induces significant vehicle packaging concerns but provides a large amount of interplanetary mission flexibility. On the other hand, an aerobrake L/D of 0.3 is feasible, but only over an extremely limited range of entry velocities (7.2-7.3 km/sec). An aerobrake L/D of 0.3 incurs minimal vehicle packaging concerns, but is limited from a mission opportunity standpoint. A compromise is reached between the conflicting interplanetary and atmospheric trajectory requirements by limiting the Mars entry velocity to values between 6.0 and 8.5 km/sec and selecting an aerobrake L/D of 0.5. In this manner, a minor restriction on mission flexibility is induced while alleviating vehicle packaging concerns. Based on this research, a manned Mars aerobrake L/D in the range of 0.3-0.5 and a Mars entry velocity in the range of 6.0-8.5 km/sec are recommended.

Significance. The results of this research show the significance of the trade off between aerobrake L/D (aerodynamic performance and vehicle packaging) and entry velocity (mission opportunity and flexibility).

Status/Plans. The results of this study have been documented in AIAA Paper 90-2817. Further refinement of this analysis is currently being performed based on the trade-off between the number of interplanetary mission opportunities and aerobrake packaging constraints.

Robert D. Braun, Richard W. Powell
Vehicle Analysis Branch
Langley Research Center
(804) 864-4507

Increasing Temperature
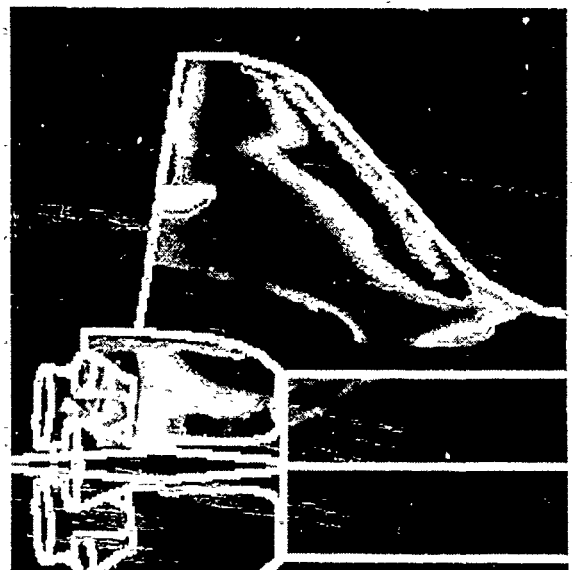
Camera View   Projection to Planview

Figure 11-8. Shuttle Infrared Leeside Temperature Sensing (SILTS) Experiment STS-28 and STS-32 Flight Results

196

11-8 Shuttle Infrared Leeside Temperature Sensing (SILTS) Experiment STS-28 and STS-32 Flight Results

Objective. To provide high spatial resolution measurements of the orbiter's leeside temperature during entry.

Approach. A scanning infrared radiometer (camera) is mounted in an experiment pod atop the vertical tail of the Shuttle Columbia. The radiometer is mounted in such a way that it may view the leeside surfaces through either of two infrared-transparent windows—one which provides a view of the orbiter fuselage and one which provides a view of the left wing. The infrared detector senses the level of infrared radiation emanating from the surfaces being viewed. Post-flight processing of the detector output data then provides for determination of the surface temperature levels.

Accomplishments. The SILTS experiment obtained high quality data over the orbiter's left wing during entry on Shuttle missions STS-28 and STS-32. These data have been processed to provide over 150 infrared images, obtained during 22 minutes of experiment operation, on each flight. The basic SILTS imagery has been cast in a time-variable presentation format (movie), which enables observation of the variability of the wing leeside thermal environment throughout the hypersonic portion of entry. A process for correcting the raw data to account for radiation emanating from the viewport window has been developed and applied. The SILTS-inferred surface temperature data have been validated by comparison with measurement from in-situ surface thermocouples.

Significance. The STS-28 and STS-32 experiment results provide the first accurate measurements of the leeside surface temperature of an entry vehicle in flight with high spatial resolution. Data from these and subsequent flights will provide a benchmark set of flight data with which to assess the applicability of state-of-the-art computational fluid dynamic (CFD) codes for simulation of the leeside flow field of a lifting vehicle during entry from low Earth orbit.

Status/Plans. Results of this study were presented in AIAA paper 90-1741. The SILTS experiment will be aboard STS-35 in August 1990. On that flight, the experiment will be configured to view the orbiter fuselage. Two additional flights are planned to occur on STS-40 and STS-42. A CFD study and a ground-based experimental study, using thermographic phosphor and infrared emission techniques, are under way to compare with flight results and to assess ground-to-flight extrapolation capability.

David A Throckmorton, E. Vincent Zoby
Aerothermodynamics Branch
Langley Research Center
(804) 864-4406

Mach 6 Air $\alpha = 25°$

—— Thermographic phosphor
● Phase change paint

$Re/ft = 2 \times 10^6$

$Re/ft = 8 \times 10^6$

Turbulent theory,
Miniver code

Laminar theory, Miniver code

h/h$_0$

x/l
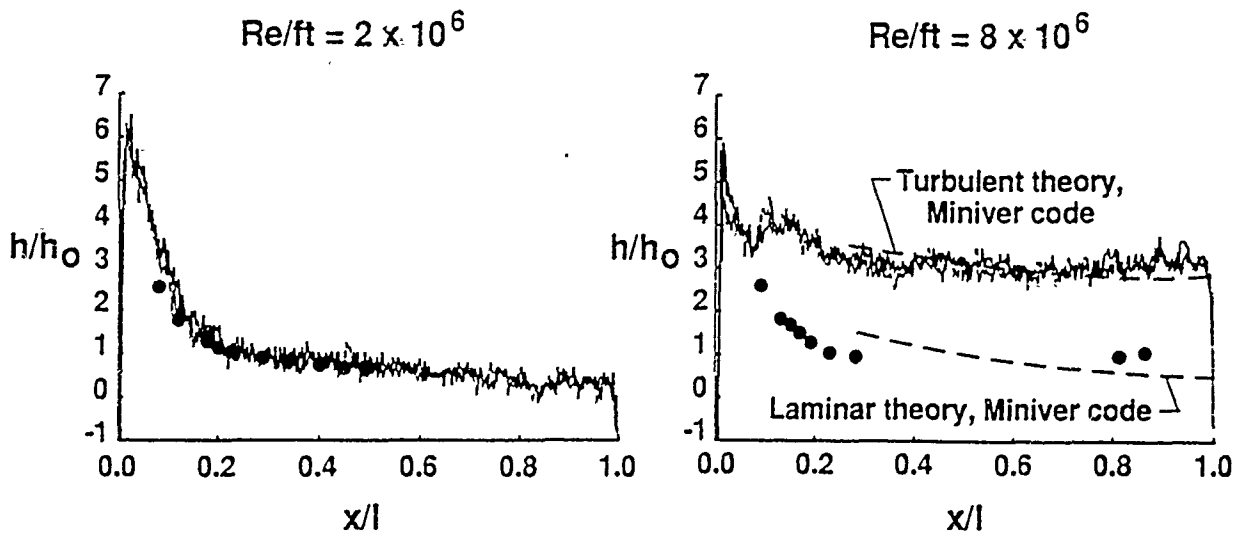
Figures 11-9. Comparison of Heating Coefficients on the PLS Obtained with Thermographic Phosphor and Phase Change Paint Techniques

198

11-9 Experimental Aerothermodynamic Characteristics for Proposed Personnel Launch System Lifting-Body Concept

Objective. To determine aerothermodynamic characteristics of a proposed Personnel Launch System (PLS) lifting body over a wide range of flow conditions. Determine the effects of angle-of-attack, Reynolds number, and Mach number on windward and leeward surface heating.

Approach. Wind tunnel tests were conducted in the Langley 31-inch Mach 10, 20-inch Mach 6, and hypersonic CF4 tunnels to assess heating characteristics of the PLS, and qualitative/quantitative thermal mapping tests were performed using the phase-change paint and two-color thermographic phosphor techniques. Surface streamline patterns were obtained with the oil flow technique to aid in the interpretation of the heating results and to identify regions of separated and reattached flow.

Accomplishments. As expected, the tip-fin leading edges, canopy and nose of the PLS experienced the highest heating. Windward centerline heating increased with increasing angle-of-attack, whereas no significant effects of compressibility were measured. Transition from a laminar to a turbulent boundary layer resulted in a factor of 3 to 4 increase in windward centerline heating at the highest Reynolds number in Mach 6 air. The leeward flow field was very three-dimensional and was dominated by crossflow separation and vortex reattachment.

Significance. The aerothermodynamic data generated from this study are an essential portion of the information needed to define, evaluate, and select a PLS vehicle. The information is being incorporated into the design of high-fidelity, highly instrumented models from which a benchmark data base for CFD code calibration will be established. The ap-

plication of the two-color thermographic phosphor technique to determine convective heating in a quantitative manner has been successfully demonstrated on the PLS. The results indicate the influence of the state of the boundary layer on windward centerline heating.

Status/Plans. Experimental data were obtained, analyzed, and presented in AIAA publication 90-1744. We plan to complete design and initiate fabrication and testing of high-fidelity models for CFD code calibration.

Thomas J. Horvath
Experimental Hypersonics Branch
Langley Research Center
(804) 864-5221

PLS ENTRY
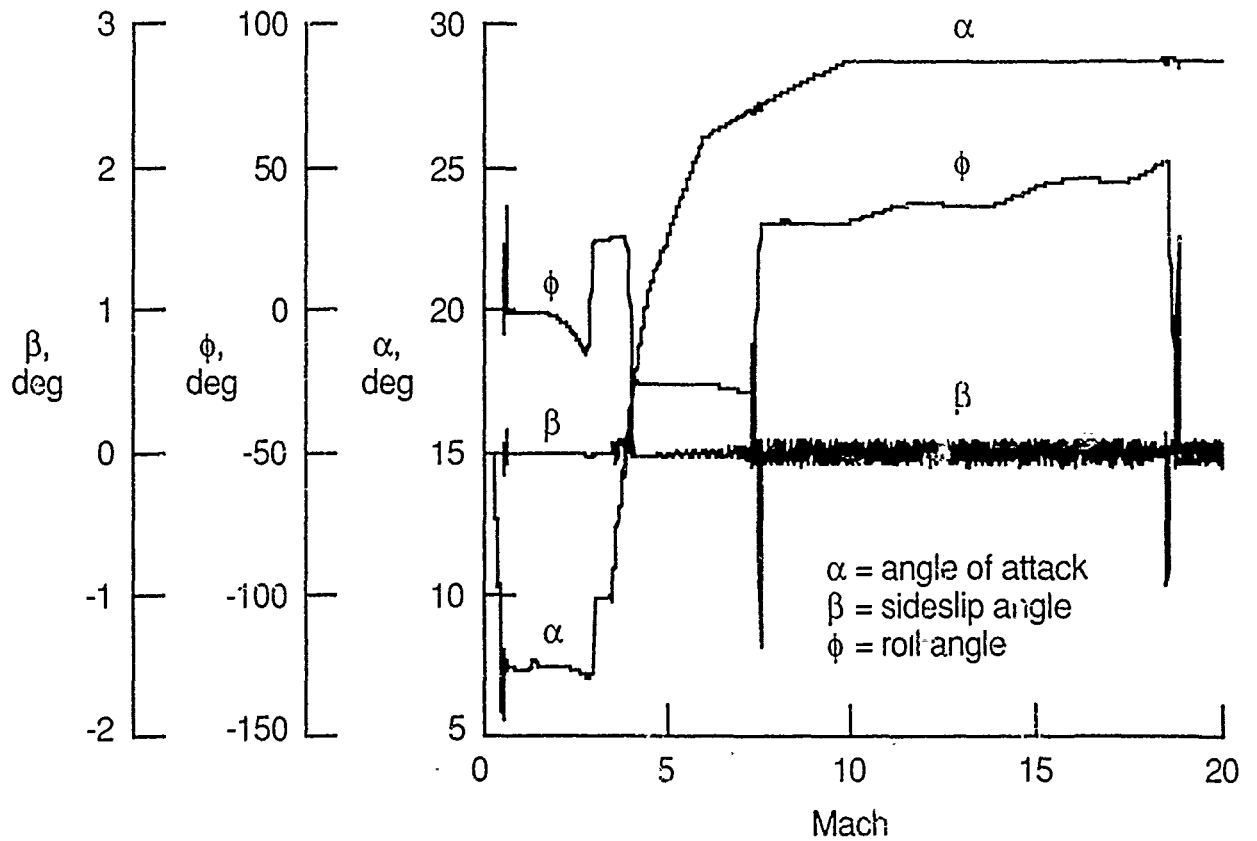
Figure 11-10. Personnel Launch System Entry

200

11-10 Lifting Body Personnel Launch System (PLS) Flying Characteristics

Objective. To demonstrate entry and landing characteristics of a lifting body for a personnel launch vehicle application.

Approach. The demonstration was divided into multiple phases. The first phase involved 3-DOF analysis. After completion of this phase, a guidance and control system was developed and incorporated into a 6-DOF simulation. Off-nominal atmospheric density and wind profiles were generated to determine the robustness of the lifting-body configuration.

Accomplishments. The results of the 6-DOF study are as follows: (1) Maximum deceleration encountered during entry is less than 2.5 g. (2) Precision landings are possible within ±400 feet downrange and ±5 feet laterally. (3) Touchdown vertical velocities are less than 5 feet per second. (4) Entries with no lateral center of gravity offset consume less than 40 lb of reaction control system (RCS) propellant. Those with lateral center gravity (YCG) offsets of 0.5 inches consume approximately 200 lb of propellant.

Significance. This research has demonstrated that the lifting body is a viable candidate for the personnel launch vehicle.

Status/Plans. Based on these results, the study is being extended to do the following: (1) Examine configuration modifications, particularly planform loading of the vehicle for reducing the maximum dynamic pressure.

(2) Expand the aerodynamic data base to include hypersonic yaw control data from the fins, which will reduce the increased RCS fuel consumption required. Include turbulence and gusts in the 6-DOF analysis to design the control actuators and include alternative speed brake approaches.

Richard W. Powell
Vehicle Analysis Branch
Langley Research Center
(804) 864-4506

Chapter 12

Aerobraking

The long-term objective of the Aerobraking Program is to develop and validate key aerobraking technologies for lightweight space-based orbital transfer vehicles. The use of aerobraking will provide significant reductions in mass delivered to low-Earth orbit (LEO) for both robotic and piloted missions to Mars as well as Lunar and cis-Lunar mission scenarios. The program will focus on improving Computational Fluid Dynamics codes for accurate prediction of complex aerodynamic and aeroheating environments; development and validation of fault-tolerant, adaptive guidance, navigation, and control technologies; and the evaluation and development of advanced thermal protection system (TPS) materials, designs, and structures. Overall vehicle configuration analysis and optimization and system trade studies for Lunar and Mars aerobraking vehicles will be developed and supported by appropriate ground testing. The definition and conduct of flight test(s), including the Aeroassist Flight Experiment (AFE) and other such validation experiments, will provide verification of all key aerobraking technologies.

Program Manager: Steve Wander
                   OAET/RF
   Washington, DC 20546
                   (202) 453-2820
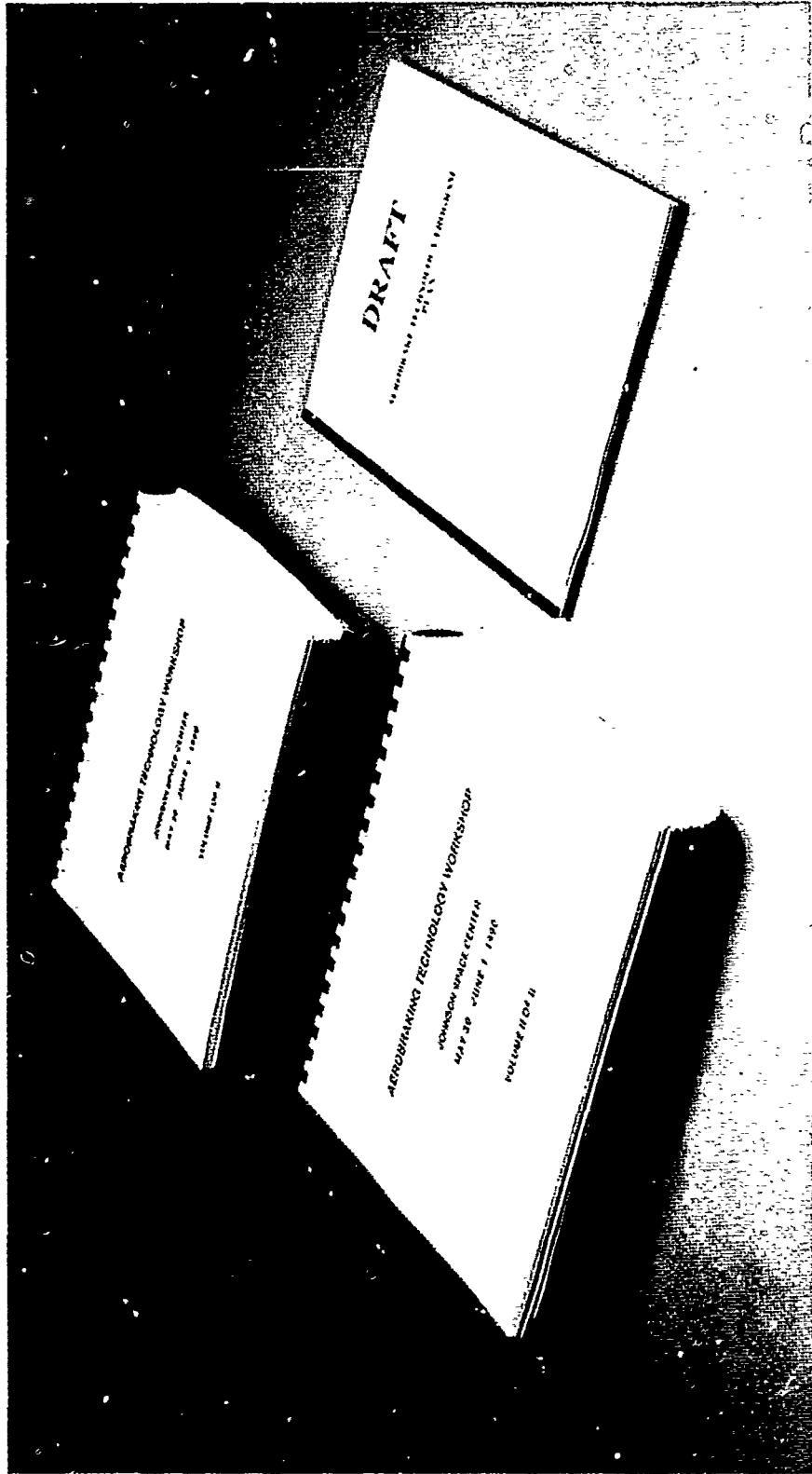
Figure 12-1. Some Products of OAET Aerobrake Program

12-1 Space Exploration Initiative Aerobraking

Objective. To fulfill lead center role for OAET Space Exploration Initiative Aerobrake Technology Project

Approach. A cooperative project with participation from Ames, Langley, JSC, and JPL was established to conduct system studies and to mature appropriate technologies to meet the objectives of the agency's new Space Exploration Initiative. This project grew out of the Pathfinder High Energy Aerobraking activity (primarily directed toward Human Missions to Mars) and included Aerobraking for the Lunar Base, Mars Precursor Mission, and the eventual Human Missions to Mars.

Accomplishments. System studies were conducted and efforts were expended to develop Aerobrake technologies at the four field centers. Considerable effort was devoted to supporting the 90-day study with a full-time participant from Ames (Dave Cooper) assigned to Greg Reck's OAET technology team and part-time participation in the MSFC transportation studies . The second Aerobrake workshop was organized and chaired by Ames and held at JSC with strong contributions from the NASA field centers, industry (McDonnell-Douglas, Rockwell, Boeing, and Martin-Marietta), and academia. This workshop summarized the prior years' activities. Additionally, a draft Aerobrake Technology Plan was submitted on the required deadline date of June 1, 1990.

Significance. The importance of aerobraking was reaffirmed, key technologies required for its implementation were identified, progress toward developing these technologies was made, and a det .iled plan for future activities was drafted: The results from this year's work far exceeded those that would be expected from the small amount of OAET funding ($1.5M) supporting the project.

Status/Plans. The lead center role for Aerobrake Technology Project has been transferred to Langley. Ames will support this activity and will lead in the Aerothermodynamics and Thermal Protection Systems Technology elements of the project.

J. Arnold, Dave Cooper
Thermosciences Division
Ames Research Center
(415) 604-5265

V

62°

45°

(51° in
crossplane)
Eccentr. = 1.235
Eff. $r_n \approx 0.95$ m

70°

L/D = 0.5
at $\alpha \approx 0°$

L/D = 0.3
at $\alpha \approx 25°$

L/D = 0.2
at $\alpha \approx 14°$

Scale

1 m
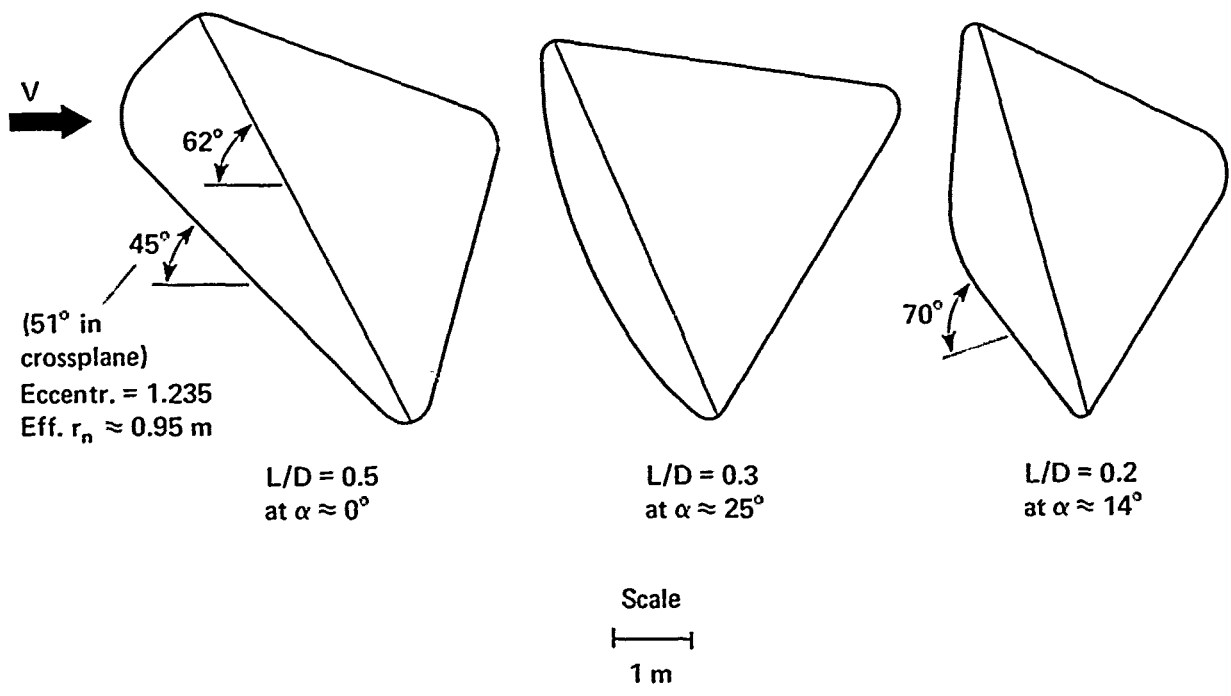
Figure 12-2. Entry Configurations Studied

206

12-2 Earth Atmospheric Entry Studies for Manned Mars Missions

Objective. To determine vehicle environments for manned aerobraking vehicles returning from early Mars missions.

Approach. An entry speed range from 12 to 16 km/sec was considered. Special emphasis was placed on the mission abort condition, which has an entry speed of 14 km/sec. Furthermore, lifting capsules were studied, since early missions will have a 4 to 6 person crew where current guidelines set an upper g-load limit due to deceleration at 5g.

Accomplishments. Vehicles with maximum lift-to-drag (L/D) from 0.2 to 0.5 (see figure) and m/C_DA of 300 and 500 kg/m^2 were studied. For the design entry speed of 14 km/sec and a 5-g limit, an L/D of 0.5 was needed for a 1° entry angle corridor. The Apollo shape's L/D of 0.3 is too low. The raked cone with a 1-m nose radius minimizes heating and control problems, since maximum C_L (at overshoot) and maximum L/D (at undershoot) are both near $\alpha=0$. Peak, cold-wall, stagnation point heating rates ranged from 0.9 to 1.3 kW/cm^2, and total heat load was about 100 kJ/cm^2 for $m/C_DA=300$ kg/m^2. Boundary layer transition at high speeds, although unlikely, could triple forebody heating rates and heat loads. Ablative heat shields are required.

Significance. We established entry vehicle L/D requirements that determine configuration, and calculated heating rates and heat loads that are needed to study various ablators and to find the lightest heat shields.

Status/Plans. The results were presented at the AIAA Thermophysics meeting in Seattle, June 1990. However, additional parametric studies are planned.

M. Tauber, G. Palmer
Aerothermodynamics Branch
Ames Research Center
L. Yang
Sterling Software
(415) 604-6086
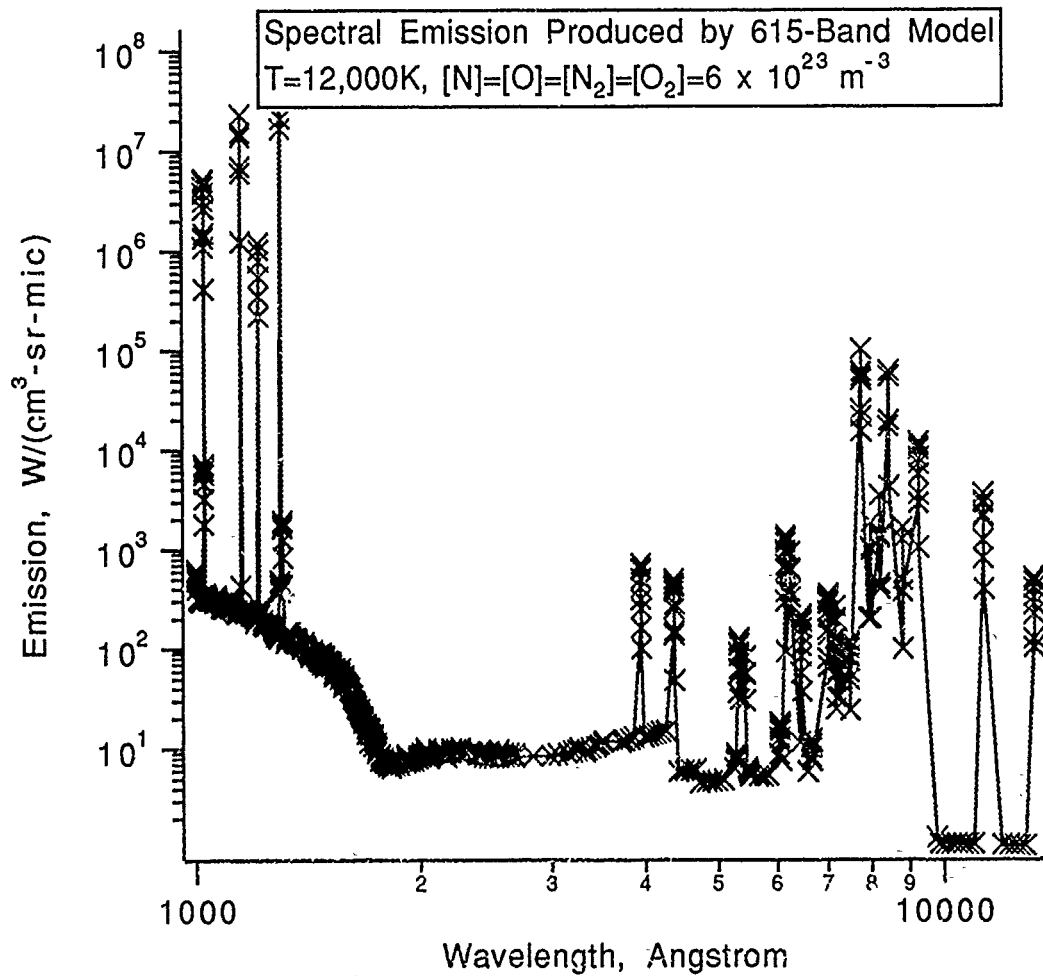
Figure 12-3. Computational Technique for Strongly Radiating Flow

208

12-3 Computational Technique for Strongly Radiating Flow

Objective. To find an appropriate method for computing a flow field in which radiation is so strong that it affects the flow appreciably.

Approach. An existing computer code based on the equilibrium assumption (RASLE) and an existing two-temperature nonequilibrium code (SPRAP) were operated for a typical Mars-return Earth-entry condition to determine the general features of the radiating shock layer. From this it was concluded that a nonequilibrium approach must be taken. A radiation model that employs only 615 wavelength points was shown to yield radiation spectra approximately equal to those of the detailed spectra using 5 million wavelength points. A computing algorithm that implicitly solves the radiative transport fully coupled with fluid motion was developed and was applied to solve a one-dimensional flow in a nozzle. The algorithm solved the integro-differential equation in one dimension by inverting a solidly loaded matrix equation.

Accomplishments. A 615-band model was shown, at least tentatively, to be useful in representing the detailed spectra for the Mars-return Earth-entry conditions. The implicit technique for solving the radiation coupled flow, based on the inversion of the solidly loaded matrix equation, was shown to converge. The computing times for such calculations are about a factor of 20 to 100 times longer than for the nonradiating cases.

Significance. There has never been a rational computing procedure for the strongly radiating flow, because (1) the governing equations for such a flow are a system of nonlinear integro-differential equations rather than differential equations found in all fluid mechanical problems, and (2) any proce-

dure that attempts to solve the integro-differential equations must carry out prohibitively expensive radiative transport calculations. Thus, up to the present, such solutions were unobtainable. The present work shows that both these problems may be overcome, at least for two-dimensional problems.

Status/Plans. A Gauss-Seidel relaxation procedure is being examined to replace the fully loaded inverted matrix equation in order to reduce the computing times.

C. Park, F. S. Milos
Aerothermodynamics Branch
Ames Research Center
(415) 604-5636
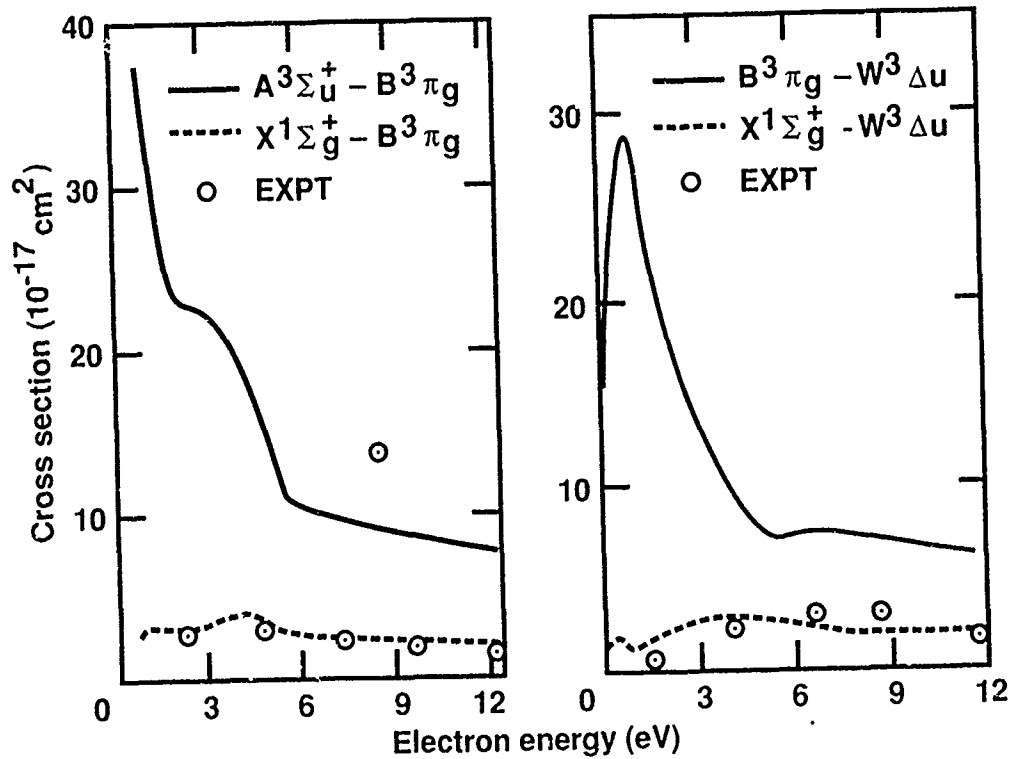
Figure 12-4. Electron Collision Cross-Sections

210

12-4 Electron Collision Cross-Sections

Objective. To develop an accurate and comprehensive theoretical method for determining electron molecule collision cross-sections.

Approach. The Schwinger multichannel (SMC) formulation was used to calculate the collisional excitation cross-sections for transitions between the ground state and selected excited states and also between excited states. The molecular energy levels were determined from computational chemistry solutions of the quantum mechanical Schrodinger equation.

Accomplishments. Electron excitational cross-sections between electronic states of N_2 have been calculated. The accompanying figure displays the results for transitions between the ground state ($X^1\Sigma^+_g$) and two excited states ($B^3\Pi_g$ and $W^3\Delta_u$). Also included on the figures are the results of excited state transitions ($A^3\Sigma^+_u$- $B^3\Pi_g$) and ($B^3\Pi_g$ and $W^3\Delta_u$). The theoretical results for both ground to excited state transitions agree well with the experimental data. Experimental data for the excited state transitions are nonexistent.

Significance. The flow field around an Aeroassisted Space Transfer Vehicle (ASTV) at high altitudes is characterized by nonequilibrium conditions in which the molecular vibrational, electronic, and rotational-translational temperatures are different, reaching values perhaps as high as 50,000 K. Under the ionizing conditions anticipated for ASTV shock layers, electron-molecule collisions are effective methods of transferring energy in the excitation ionization and dissociation processes in the flow field. Since experimental data are nonexistent for the excited state transitions, current nonequilibrium flow-field calculations assume that the excited-excited state cross-sections are equal to the ground-excited state cross-sections resulting in some final state. The calculations described herein show that this assumption is invalid and provides reliable data to fill the void.

Status/Plans. Electron excitational cross-sections will be calculated for additional states of N_2. Similar calculations will be performed on additional molecules such as CO and O_2.

David M. Cooper
Computational Chemistry Branch
Ames Research Center
(415) 604-6213
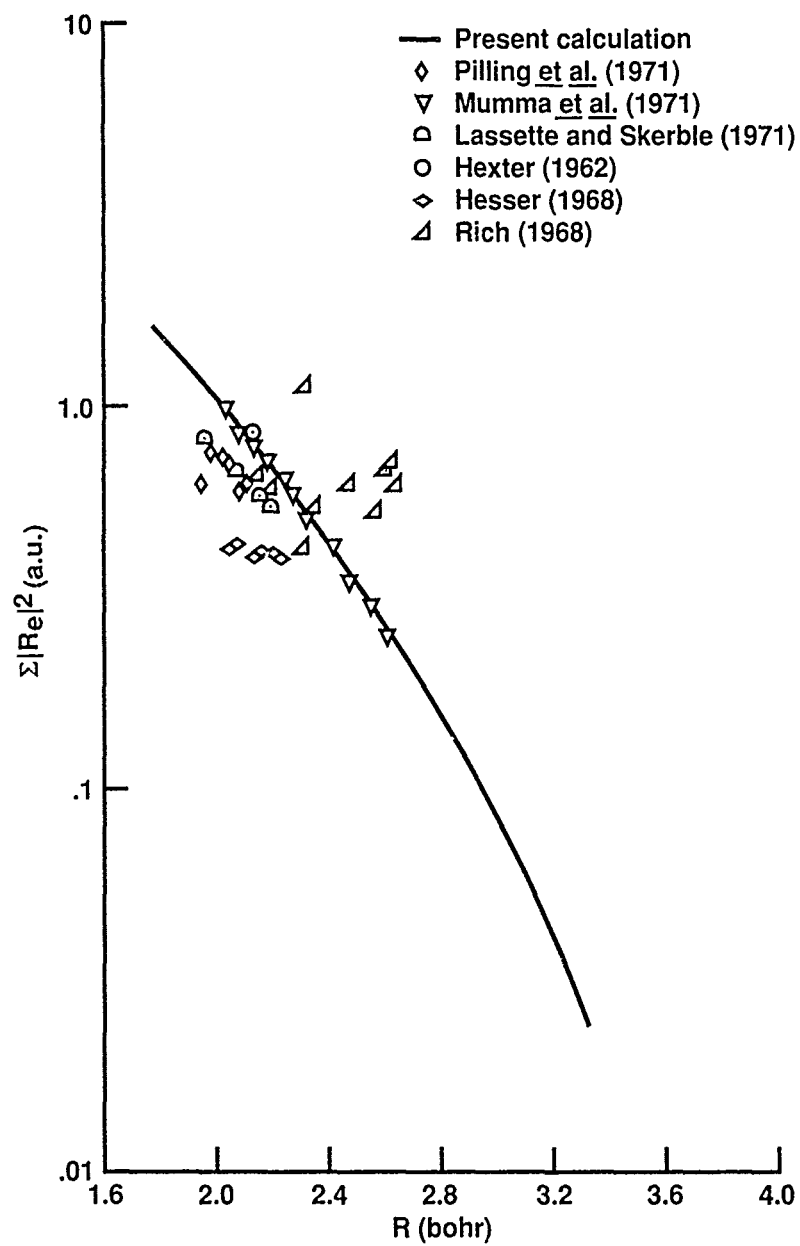
Figure 12-5. Electronic Transition Moment for CO Fourth
Positive System

212

12-5 Radiative Intensity Factors

Objective. To determine reliably the radiative intensity factors (transition moments, lifetimes, Einstein A-coefficients) for the strongly radiating systems in air, Martian atmospheric gases, and ablation product species.

Approach. State-of-the-art computational chemistry methods were used to calculate the potential energy curves and the radiative intensity factors for transitions between the electronic states.

Accomplishments. The radiative intensity factors (electron transition probabilities that control the absolute strength of radiation from transitions in molecules) for all strongly radiating transitions in N_2, O_2, NO, N_2^+, and O_2^+ have been completed. In addition, the electronic transition moment for the CO Fourth Positive System, which is the strongest radiating system in CO (and shock-heated Martian atmospheric gases), has been calculated.

Significance. To predict the radiative heating of a vehicle accurately as it enters a planetary atmosphere or one that travels at high speeds in a dense atmosphere, the radiative intensity factors for atoms, molecules, and ions must be known. The present results will allow the CFD/Aerothermodynamic codes (assuming they realistically model the flowfield chemistry and physics) to determine accurately the radiative heating rates encountered by vehicles traveling at hypersonic speeds.

Status/Plans. Radiative intensity factors will be determined or verified for planetary and ablation product species.

David M. Cooper
Computational Chemistry Branch
Ames Research Center
(415) 604-6213

Velocity directions - modified Malemute
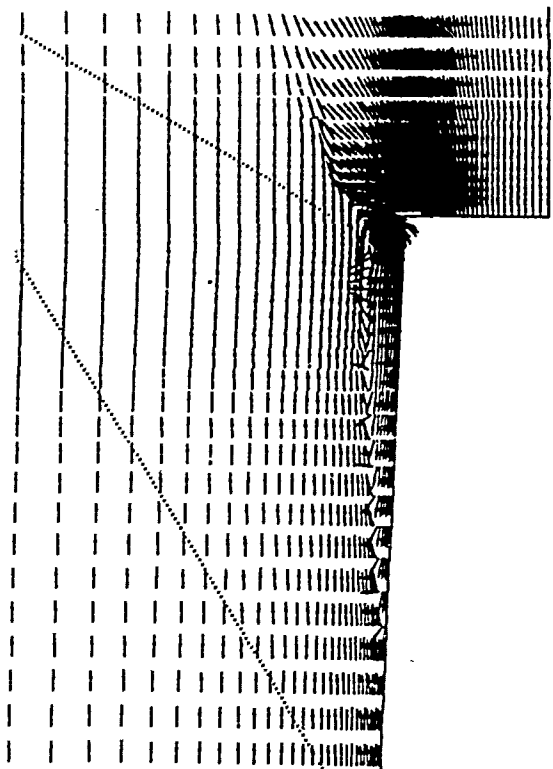
Velocity directions - original Malemute

Surface heat transfer predictions

Without ablative effects
With ablation effects

Plume induced separation and fin interaction

plume induced separation on leeside due to high plume pressure with respect to local leeside pressure.

Plume Region

Pw/Pl is around 15 for 40 Km conditions and higher windside pressure does not permit large separation

Expansion on the leeside

Fin Shock on the windward side

Figure 12-6. Computational Analysis of Plume-Induced Separation

214

12-6 Computational Analysis of Plume-Induced Separation

Objective. The Malemute rocket that carried the boost-phase signature experiments was predicted to be statically and dynamically unstable because of plume-induced separation, and design modifications were made to improve the stability. The objective was to perform computational experiments of the propulsive-plume flow including the Malemute hardbody and analyze the solution for plume-induced separation and evaluate the modified geometry for improved stability.

Approach. An ideal gas, upwind, full Navier-Stokes code was used to predict the complete supersonic flow around the original Malemute rocket and the modified axisymmetric version at four different flight trajectory points.

Accomplishments. The numerical simulations clearly showed plume-induced separation at high altitudes and the resultant instability because of fin ineffectiveness. The extent of separation and the peak heating due to separation were predicted. Special heat shields were suggested and added to these regions. The analysis of numerical solutions allowed a thorough evaluation of the aft body modifications with respect to plume-induced separation. The modified aft body was able to limit the plume-induced separation to a very small region, and thus increased stability was achieved. The vehicle was launched successfully (though MICOM recommended even the modified geometry to be unstable). The increased confidence from the numerical simulations and the augmentations of heat-shield and nonablative coatings at appropriate regions are believed to be major reasons for the successful flight.

Significance. For the first time, plume-induced separation and the primary cause of instability due to high altitude plumes were demonstrated clearly. This particular study was successfully carried out in a timely fashion and at a very critical phase of the boost-phase signature flight experiment program.

Status/Plans. Most of the results are in the process of being documented as a NASA publication. The study has been completed and relevant results will be published in an upcoming AIAA meeting.

Ethiraj Venkatapathy
Computational Aerothermodynamics Branch
Ames Research Center
(415) 604-4282

Report Documentation Page

1. Report No.	2. Government Accession No.	3. Recipient's Catalog No.
NASA TM-4312		

4. Title and Subtitle		5. Report Date
NASA Aerodynamics Program Annual Report 1990		August 1991
		6. Performing Organization Code
		RF

7. Author(s)	8. Performing Organization Report No.
Louis J. Williams, Kristin A. Hessenius, Michael Dudley, Pamela F. Richardson, George Unger, and Steve Wander	
	10. Work Unit No.

9. Performing Organization Name and Address	11. Contract or Grant No.
NASA Office of Aeronautics, Exploration and Technology Aerodynamics Division (OAET/RF)	NASW 4430
	13. Type of Report and Period Covered
12. Sponsoring Agency Name and Address	Technical Memorandum
National Aeronautics and Space Administration Washington, DC 20546	14. Sponsoring Agency Code

15. Supplementary Notes

This report is an annual accomplishments review for the Aerodynamics Division (Code RF). The information contained herein covers FY 1990.

16. Abstract

This report is the annual accomplishments review for the Aerodynamics Division (Code RF) during FY 1990. The program includes both fundamental and applied research directed at the full spectrum of aerospace vehicles, from rotorcraft to planetary entry probes. This report contains a comprehensive review of the following aerodynamics elements: computational methods and applications, CFD validation, transition and turbulence physics, numerical aerodynamic simulation, test techniques and instrumentation, configuration aerodynamics, aeroacoustics, aerothermodynamics, hypersonics, subsonics, fighter/attack aircraft and rotorcraft.

17. Key Words (Suggested by Author(s))			18. Distribution Statement
aerodynamics	subsonic	waverider	Unclassified - Unlimited
aeroacoustics	supersonic	flowfield	
aerothermodynamics	NAS	crossflow	Subject Category 47
hypersonics	NASP		
rotorcraft	Navier-Stokes		

19. Security Classif. (of this report)	20. Security Classif. (of this page)	21. No. of pages	22. Price
Unclassified	Unclassified	228	A20

NASA FORM 1626 OCT 86